

2

**AD-A263 588**



CENTER FOR ADVANCED PROPULSION SYSTEMS

FINAL REPORT

G. BORMAN, M. CORRADINI, P. FARRELL, D. FOSTER,  
J. MARTIN, R. REITZ, C. RUTLAND

FEBRUARY 1993

U.S. ARMY RESEARCH OFFICE

DAAL03-86-K-0174

UNIVERSITY OF WISCONSIN - MADISON

APPROVED FOR PUBLIC RELEASE;

DISTRIBUTION UNLIMITED

**DTIC**  
**ELECTE**  
**MAY 05 1993**  
**S B D**

93 5 04 14 8

**93-09607**



207ff

REPORT DOCUMENTATION PAGE			Form Approved OMB No. 0704-0188	
<small>Public reporting burden for this collection of information is estimated to average 1 hour per response, including the time for reviewing instructions, searching existing data sources, gathering and maintaining the data needed, and completing and reviewing the collection of information. Send comments regarding this burden estimate or any other aspect of this collection of information, including suggestions for reducing this burden, to Washington Headquarters Services, Directorate for Information Operations and Reports, 1215 Jefferson Davis Highway, Suite 1204, Arlington, VA 22202-4302, and to the Office of Management and Budget, Paperwork Reduction Project (0704-0188), Washington, DC 20503</small>				
1. AGENCY USE ONLY (Leave blank)	2. REPORT DATE February 1993	3. REPORT TYPE AND DATES COVERED Final 1 Oct 86 - 2 Jan 93		
4. TITLE AND SUBTITLE Final Report Center for Advanced Propulsion			5. FUNDING NUMBERS DAA03-86-K-0174	
6. AUTHOR(S) G. Borman, M. Corradini, P. Farrell, D. Foster, J. Martin, R. Reitz, C. Rutland				
7. PERFORMING ORGANIZATION NAME(S) AND ADDRESS(ES) Engine Research Center University of Wisconsin - Madison 1500 Johnson Drive Madison, WI 53706			8. PERFORMING ORGANIZATION REPORT NUMBER	
9. SPONSORING/MONITORING AGENCY NAME(S) AND ADDRESS(ES) U. S. Army Research Office P. O. Box 12211 Research Triangle Park, NC 27709-2211			10. SPONSORING/MONITORING AGENCY REPORT NUMBER ARO 24623.129-EG-VIR	
11. SUPPLEMENTARY NOTES The view, opinions and/or findings contained in this report are those of the author(s) and should not be construed as an official Department of the Army position, policy, or decision, unless so designated by other documentation.				
12a. DISTRIBUTION / AVAILABILITY STATEMENT Approved for public release; distribution unlimited.			12b. DISTRIBUTION CODE	
13. ABSTRACT (Maximum 200 words)  This final report covers a six year period of research conducted by the Engine Research Center. The objectives of the ERC are: 1) to train students in special areas of diesel research of interest to the Army and its industrial suppliers, 2) provide a source of consultation for the Army, 3) provide knowledge and research tools for solution of long range problems of interest to the Army, 4) provide solution methods for problems of immediate interest to the Army, 5) to identify and explore new technologies which have potential value to the Army. A brief account is given of how these objectives were addressed. Subjects covered are; faculty, facilities, publications, and research results. The research topic areas discussed are: engine modeling; combustion, emissions and fuels; heat transfer; fluid mechanics; diesel sprays; lubrication, mechanical design and materials.				
14. SUBJECT TERMS Diesel engine, engine modeling, combustion, emissions, fuels, heat transfer, fluid mechanics, diesel sprays and lubrication.			15. NUMBER OF PAGES 205	
			16. PRICE CODE	
17. SECURITY CLASSIFICATION OF REPORT UNCLASSIFIED	18. SECURITY CLASSIFICATION OF THIS PAGE UNCLASSIFIED	19. SECURITY CLASSIFICATION OF ABSTRACT UNCLASSIFIED	20. LIMITATION OF ABSTRACT UL	

THE VIEW, OPINIONS, AND/OR FINDINGS CONTAINED IN THIS REPORT ARE THOSE OF THE AUTHOR(S) AND SHOULD NOT BE CONSTRUED AS AN OFFICIAL DEPARTMENT OF THE ARMY POSITION, POLICY, OR DECISION, UNLESS SO DESIGNATED BY OTHER DOCUMENTATION.

## TABLE OF CONTENTS

SECTION		PAGE
1.0	SUMMARY	1
2.0	INTRODUCTION	12
3.0	ERC CONTRIBUTIONS TO THE ARMY AND INDUSTRY	16
4.0	FACILITIES	20
5.0	FACULTY	23
6.0	STAFF AND VISITORS	31
7.0	DISCUSSION OF RESEARCH	32
7.1	Engine Modeling	33
7.2	Combustion, Emissions and Fuels	46
7.3	Heat Transfer	74
7.4	Fluid Mechanics	98
7.5	Diesel Sprays	118
7.6	Lubrication, Mechanical Design and Materials	137
8.0	LIST OF REFERENCES	171
9.0	APPENDIX A- ERC PUBLICATIONS	181
10.0	APPENDIX B - LIST OF THESES	191
11.0	APPENDIX C - INVENTIONS AND PERSONNEL	195

DTIC QUALITY INSPECTED 5

<b>Accession For</b>	
NTIS GRA&I	<input checked="" type="checkbox"/>
DTIC TAB	<input type="checkbox"/>
Unannounced	<input type="checkbox"/>
Justification	
By	
Distribution/	
<b>Availability Codes</b>	
Dist	Avail and/or Special
A-1	

## LIST OF FIGURES

Figure		Page
7.1.1	Comparison between measured and predicted cylinder pressure (left) and wall heat flux (right) for premixed-charge SI engine combustion using heat transfer model with (modified case) and without (original) the effect of compressibility and unsteadiness. Engine speed 1500 rev/min.	36
7.1.2	Comparison between computed (dashed line) and measured (solid line) cylinder pressures (left) and wall heat flux (right) for compression ignited, homogeneous charge engine combustion (engine speed 1200 rev/min, compression ratio 10.5, swirl ratio 1.8, equivalence ratio 0.4).	36
7.1.3	Predicted pressure histories obtained by incorporating the multistep Shell ignition model (Case 2) and the standard one-step Arrhenius kinetics model (Case 1).	39
7.1.4	Intake flow computation using the unstructured grid version of KIVA-3 for stationary valves.	40
7.1.5	Calculated cylinder pressures with and without ignition at 100 rpm and initial air temperatures of 241 K and 298 K.	44
7.2.1	Schematic of laser range finding system.	49
7.2.2	Particulate emissions and premix burn for engine condition D, low intake pressure, high intake temperature. Error bars represent one standard deviation.	55
7.2.3	Combustion system schematic.	56
7.2.4	Soot mass concentration vs temperature at a mass flow rate of 1.25 g/s.	57
7.2.5	Experimental setup schematic.	58
7.2.6	Soot yield for cross-flow vs. co-flow geometries.	59
7.2.7	Correlation of soot yield to mixing index, $V_a V_j$ .	59
7.2.8	Optical Window Cutaway View (part 1 of 2).	61

7.2.8	Optical window relative position to the combustion chamber(part 2 of 2).	61
7.2.9	The instrumentation system.	62
7.2.10	Flame temperature and soot concentration factor KL at three angular positions for window A (24, 25, 26-3).	63
7.2.11	Flame temperature and soot concentration factor KL at three angular positions for window B (24, 25, 26-3).	64
7.2.12	Flame temperature and soot concentration factor KL at three angular positions for window C (24, 25, 26-3).	65
7.2.13	Probe	67
7.2.14	Mass deposition for runs 3-6.	68
7.2.15	Cyclic variation of soot volume fraction in the exhaust stream.	69
7.2.16	LHR and Baseline AHRR (1300 rpm, 25% Load).	72
7.3.1	Cross-Section Instrument Position in Head and Its Position in Relation to the Piston. Location of the Radiation Instrument in the Modified Head (Top View).	77
7.3.2	Layout of cylinder head bottom view.	79
7.3.3	Instrumentation plug with heat flux probe.	80
7.3.4	(Yamada et al. 1989). Logarithmic fit to temperature data obtained by speckle method.	81
7.3.5	Cylinder schematic - top view.	82
7.3.6	Variation of the instantaneous heat flux for the seven RTD sensors.	83
7.3.7	Comparison of ensemble average heat flux for the shrouded valve producing tumble flow and swirl flow.	84
7.3.8	Comparison of the heat flux intensities for the shrouded valve producing tumble flow and swirl flow.	85

7.3.9	Comparison of integral length scales for the shrouded valve producing tumble flow and swirl flow.	85
7.3.10	Ensemble average heat flux from four RTD sensors under SIHC conditions.	87
7.3.11	100 cycle ensemble average heat flux trace under SIHC conditions showing details during the gas exchange processes. The peak value of 1.4 MW/m <sup>2</sup> is not shown on the graph.	88
7.3.12	Total surface heat flux for all locations at Load 3; equivalence ratio 0.49, imep = 603 kPa, rpm = 1200. (Runs 3, 4, and 7).	89
7.3.13	Flame temperatures at different equivalence ratios at 1500 rpm (Runs 3, 4, and 7).	90
7.3.14	Extinction coefficient, KL, at different equivalence ratios at 1500 rpm (Runs 3, 4 and 7).	91
7.3.15	Total emissivities at different equivalence ratios at 1500 rpm (Runs 3, 4, and 7).	91
7.3.16	Radiation fluxes at different equivalence ratios at 1500 rpm (Runs 3, 4, and 7).	92
7.3.17	Comparison of radiation flux for run 4 with total flux (10).	93
7.3.18	Total heat flux at low and high wall temperatures with variations in quenching distances.	97
7.4.1	Photographs of a pin protruding 1 mm from the cylinder head surface. Top photograph taken at BDC, lower at TDC, engine operated at 750 rpm, low swirl.	100
7.4.2	Photographs of a pin protruding 0.5 mm from the surface of the cylinder head. Top taken at BDC, lower at TDC, engine operated at 1500 rpm, high swirl.	101
7.4.3	Comparison of side-scatter PIV, near-forward scatter PIV and LDV results for a laminar pipe flow.	102
7.4.4	PIV optical image processing system incorporating LCTV as a spatial light modulator.	103

7.4.5a	Surface plot of the OFT of a Young's fringe pattern shown.	104
7.4.5b	Surface plot of the FFT of a Young's fringe pattern.	104
7.4.6	Velocity vectors scales by mean piston speed ( $U_p$ ) from the 1500 rpm case.	105
7.4.7	Velocity vectors for the 1500 rpm high swirl case at 360 degrees, and 390 degrees.	106
7.4.8	PIC vector plot at TDC produced by pancake shape cylinder geometry. Engine crankcase has a boost port. Engine speed: 500 rpm.	107
7.4.9	Swirl component of velocity for the high swirl case at 1500 rpm (solid line) and the low swirl case at 1500 rpm (dashed line). BDC of compression is 180°, 360° is TDC.	108
7.4.10	Axial component of velocity for both swirl levels measured 2 mm from the at 1500 rpm. Positive velocity is in a direction away from the surface. The solid line represents the low swirl case, and the interrupted line high swirl. BDC of compression is 180 degrees, 360 is TDC.	109
7.4.11	Swirl component of turbulence intensity 4 mm from the cylinder head. Solid line represents data from 1500 rpm high swirl, dashed line represents 1500 rpm low swirl case. BDC of compression is at 180 degrees, 360 is TDC.	110
7.4.12	Axial component of turbulence intensity measured 2 mm from surface for 750 rpm cases. Solid line represents high swirl data, interrupted line represents low swirl data. BDC of compression is at 180 degrees, 360 is TDC.	110
7.4.13	PIV vector plot at TDC produced by pancake-shaped cylinder geometry. Engine crankcase does not have a boost port. Engine speed: 500 rpm.	111
7.4.14	PIV vector plot at TDC produced by bomb-in-head engine geometry. Engine crankcase has a boost port. Engine speed: 500 rpm.	112
7.4.15	Field of view of the measurement plane.	113
7.4.16	Valve lift versus cam shaft angle profile.	115

7.4.17a	Instantaneous velocity; dynamic intake valve flow, 300 rpm cam speed, 35° cam angle (valve opening, 7.6 mm).	115
7.4.17b	Instantaneous velocity; dynamic intake valve flow, 300 rpm cam speed, 60° cam angle (valve at maximum lift, 15.2 mm).	116
7.4.17c	Instantaneous velocity; dynamic intake valve flow, 300 rpm cam speed, 88° cam angle (valve closing, 7.6 mm).	116
7.4.17d	Instantaneous velocity; dynamic intake valve flow, 300 rpm cam speed, 130° cam angle (valve closed).	117
7.4.18	Instantaneous velocity; dynamic intake valve flow, 300 rpm cam speed, 35° cam angle (valve opening, 7.6 mm), case 2.	117
7.5.1	A comparison of the strain gage transducer's injection rate shapes from the Bosch and Zeuch rate of injection meters at 140 MPa and 500 Hz.	119
7.5.2	Crank angle resolved SMD, mean velocities, RMS velocities, and correlation along spray axis. Each data point was ensemble averaged from 50 injections with 0.5 degree resolution. Injection at 800 rpm, 19.5 mg per injection, $P_c = 1$ atm.	120
7.5.3	Comparison of SMD measured by digital imaging, PDPA, and estimated by breakup model for two chamber pressures.	122
7.5.4	Exciplex images for a single main injection. Images are ensemble averaged for 8 individual images. Times are from the start of injection, with swirl clockwise.	126
7.5.5	Drop locations in the plane mid-axis of the spray using the atomization model (top) and an initial 5 $\mu$ m drop radius (bottom) without breakup or coalescence.	128
7.5.6	Comparison of experimental spray outline vs. the modified models prediction for the medium rail pressure case (6.1 MPa).	134
7.5.7	Comparisons of the experimental impinged spray penetration vs. the modified models predictions at the three rail pressures as a function of time.	135

7.6.1	Capacitance probe construction.	139
7.6.2	Installation of probes, top view.	139
7.6.3	Schematic of the laser system for LIF lubrication film measurements.	140
7.6.4	Compression stroke oil film thickness, intake valve side.	142
7.6.5	Compression stroke oil film thickness, thrust side.	143
7.6.6	Schematic of laser range-finding system.	143
7.6.7	Piston-tilt measurements. Conditions 750 rpm, supercharged.	144
7.6.8	Surface temperature and heat flux TC1.	145
7.6.9	Surface heat flux for TC2 and TC3.	145
7.6.10	Schematic of the Cameron Plint West Tester.	146
7.6.11	Ring profile superimposed on oil film measurement.	147
7.6.12	Measurements showing hydrodynamic behavior, Cameron-Plint Tester.	148
7.6.13	Maximum oil film thicknesses at 23°C.	149
7.6.14	Maximum oil film thicknesses at 100°C.	149
7.6.15	Maximum oil film thicknesses at 200°C.	150
7.6.16	Viscosities of new and used oils.	152
7.6.17	Elasticity of new and used oils.	154
7.6.18	Consistency index vs. temperature for two lubricating oils. Data taken from Lee et al. 1988.	155
7.6.19	Power-law exponent vs. temperature for two lubricating oils. Data taken from Lee et al. 1988.	156
7.6.20	Dimensionless pressure vs. dimensionless position along film for a slider bearing with parabolic shape. The pressure is assumed to vanish at the ends of the film.	157

7.6.21	Minimum oil film thickness vs. crank angle for two oils.	157
7.6.22	Hypocycloid Motion.	159
7.6.23	Basic Hypocycloid Gearing.	159
7.6.24	Modified Hypocycloid Gearing.	160
7.6.25	Modified Hypocycloid Engine	161
7.6.26	Modified Hypocycloid Engine Motoring Losses.	163
7.6.27	Window mounting arrangement in modified head of Briggs Stratton engine.	165
7.6.28	At left isotherms for 0.75mm ZrO <sub>2</sub> 3000 RPM 0.94 Equivalence ratio, template behind sample. At right, same as left except insulation behind template raises the temperature.	166
7.6.29	Infrared thermal imaging layout.	166
7.6.30	Layout of platinum film stripe of window inner (cylinder side) and outer (room side) surfaces. Stripes on aluminum piston were unpolished areas and are shown as shaded diagonals.	170

## LIST OF TABLES

Table		Page
4.0.1	Engines	20
4.0.2	General Purpose Equipment	21
4.0.3	Computer Facilities	21
4.0.4	Special Equipment	22
7.1.1	Status of KIVA Submodels	34
7.1.2	Error Estimates for Peak Cylinder Pressure as a Function of Azimuthal Mesh Spacing.	41
7.2.1	Fuel Blends	51
7.2.2	Test Fuel Properties and Composition.	52
7.2.3.	Summary of the Heat Transfer and Indicated Specific Fuel Consumption of the Ceramic Coated and Base Engine	71
7.3.1	Engine Specifications	79
7.3.2	Engine Specifications	82
7.3.3	Inadequacy of Law-of-Wall Model	95
7.5.1	Tabulated Engine Test Results.	125
7.6.1	Single Cylinder Cummins L-10 Diesel Engine Specifications.	151

## 1.0 SUMMARY

When the contract which is the subject of this report was granted in 1986, the then Internal Combustion Engines Lab name was changed to the Engine Research Center (ERC), in keeping with the contract, which established the lab as the Center of Excellence for Advanced Propulsion for the U.S. Army. The awarding of the contract was, in part, recognition of the lab's 40 years of research contributions and its over three decades of service to the army, particularly TACOM.

It is interesting to note that the lab was initiated in 1947 by a grant of \$50,000 and lab space in a WW II barracks called T-25. The award to then Assistant Professors Phillip Myers and Otto Uyehara was largely based on their pioneering work using the two-color optical method to measure particulate temperature in the cylinder of a firing diesel engine.

The 1986 contract from ARO which forms the basis of this report covered operating expenses (salaries, supplies, travel, etc.). However, separate ARO grants supplied equipment and special Army Fellowships. These later two aspects of the ARO center funding are covered in separate final reports. The facilities are, however, also reviewed here for completeness, and the research results of the fellows are included in the general discussion, because their research costs were supported from the subject contract.

### OBJECTIVES

The ERC has five major objectives.

- The first objective of the ERC is to train students in the special research areas of importance to the Army and to its industrial suppliers.
- The second objective of the ERC is to provide a source of consultation for use by the Army and by industry.
- The third objective of the ERC is to provide knowledge and research tools for use in the solution of long range problems of special interest to the Army.
- The fourth objective of the ERC is to provide solutions to problems of Army interest by pulling together models and experimental data.
- The fifth objective of the ERC is to identify new technologies which may become important to the Army and to exercise such technologies in a research environment.

How each of these objectives has been met is discussed below. This is then followed by a brief summary of specific research accomplishments and how they benefit the army.

### Student Training

The training of students in technologies of importance to the Army and its industrial suppliers is the most natural consequence of university research provided that the thesis topics are properly selected and the students remain in the U.S. after graduation. The ERC has thus put great emphasis on project selection and on recruitment of U.S. citizens as students. As a result 88% of the MS and 75% of the PhD students graduated are now working in this country. All of the 16 Army PhD Fellows were, of course, U.S. citizens, but in a global economy this does not insure they will end

up working in the U.S.; just as many foreign born students elect to stay and to become U.S. citizens. Although graduate training is emphasized, many undergraduates work in the ERC as paid helpers and thus receive important training in engineering practice.

A list of graduates who were trained by the ERC during the period of this contract is given in Appendix B, along with theses titles.

### Consultation

Although graduates provide a direct and immediate means of technology transfer to their employer, they do not serve as a continuing resource of the ERC - the faculty does. Faculty provide information as a resource either by direct consultation or by serving on panels or study groups. Both formal and informal consultations have taken place.

Much of the informal consultations take place through telephone calls. It is estimated that such calls occur at a rate of three to four per day and have covered evaluations of inventions and new concepts, helping with the use of computer codes such as KIVA, discussion about cooperative projects, transfer of information about recent research methods and results, etc.

Of course short visits back and forth between Army facilities (especially TACOM) and the ERC have also been frequent. Formal consulting by Professor Myers with TACOM and by the ERC faculty with more than a dozen industries has continued throughout the period.

Panel participation by ERC staff has included the Army's "STAR" study, the NAS study on "Mobile Electric Power Technologies for the Army of the Future," the DOE study on the "State of the Art and Projected Technology of Low Heat Rejection Engines," the NAS study on CAFE goals, and the Army Committee on producing obscuration smoke.

In all of these various roles, it was the comprehensive nature of center research and the wide scope of subjects covered by the faculty expertise that made the ERC a unique source of information and technical judgment.

### Instrumentation for Problem Solution

Because university research is typically concerned with long range problems, its major influence comes to play through increased understanding and by supplying tools for development and shorter term problem solution. Modeling plays a major role, because it stores knowledge in an orderly and assessable form. The modeling work of the 60's produced cycle analysis programs which are now an integral part of the engine design process. Modeling work of the 70's produced emissions models and more detailed models for combustion and heat transfer. Modeling of the 1980's produced the computational fluid dynamics (CFD) codes which promise to become useful predictive tools in the 1990's. The U.W.-Madison has historically played a strong role in these efforts, much of it in the past sponsored by TACOM.

Through the period of this report, much of the ERC modeling work has concentrated on improved submodels for the CFD code KIVA. To provide the knowledge required for such improvements, experiments, both in engines and laboratory rigs, have been performed to better understand droplet vaporization, spray

breakup, spray dynamics, convective heat transfer, radiation, in-cylinder mixing, soot formation, deposits, in-cylinder flows, fuel property effects and lubrication.

While much can be learned from modeling, engine development remains remarkably empirical, requiring many experiments to obtain the final design. Thus it is very important that tools be provided in the form of experimental techniques and instruments which can be used to shorten the design process and produce a superior product. The ERC research has thus emphasized development of new instruments and application of diagnostic methods [mostly laser based] to state-of-the-art diesel engines. The challenge in each case has been to apply the instrumentation without seriously changing the engine performance.

The methods are discussed in terms of resulting data later, but the instrumentation includes: a two-color method which works at high load and steady state operation, an optical measurement of in-situ particulate size and number density, methodology for assessing soot deposit growth, a new instrument for measurement of in-cylinder radiation heat flux, a laser instrument for determining piston height and tilt motions, an instrument for non-intrusive imaging of fuel sprays during engine operation, a speckle method for determining thermal gradients in-situ, a forward scattering method for particle image velocimetry (PIV) measurements of in-cylinder flows which allows use of high rep-rate lasers, application of resistance films to ceramic surfaces for in-cylinder heat flux measurements in low heat rejection (LHR) engines, a new design for an engine heat flux measurement which determines both the unsteady and the steady state flux component, development of an optical processor for PIV data which makes analysis of PIV data from engines more practical, application of PIV to inflows with moving valves, development of methods for spray analysis including drop size, drop velocity and spray images, application of TACOM developed IR imaging to engine piston temperature measurement, measurements of linear oil films including a new single fiber application of the laser induced fluorescent (LIF) method.

### Combining Models and Data

A very important consequence of center funding, as opposed to many separate individual investigator contracts, is the ability to coordinate modeling data needs and modeling validation with the modeling effort itself. Having done this, it should be then be possible to use the models and data to solve some of the more fundamental Army problems. Examples of this are the application of KIVA and cycle analysis to cold starting and the analysis of a new injection geometry as a means of spark igniting low cetane fuels in a diesel. In each case a combination of projects was pulled together to obtain the result. For example, in the low cetane case, a TACOM funded experimental study at the ERC had shown the difficulty of spark igniting low cetane fuels in a conventionally fueled diesel. A combination of testing in the cold, high pressure bomb and KIVA calculations using spray impingement models developed at the ERC showed that single hole spray impingement on a central target could produce a cloud of fuel droplets. Subsequent tests showed that such a cloud could be spark ignited with rapid flame spreading. This combination of spray imaging, CFD calculations and engine testing was possible because of the wide range of abilities available in a center.

### New Technologies

Engines are a mature technology and thus radical new changes are not anticipated. However, the attainment of higher power density, improved fuel economy and lower emissions is very difficult. Thus the new technologies used in engines are apt to be applied to the design process more than to the design itself. Thus in the investigation of liner cavitation at the ERC, new computer codes were developed to suggest designs to prevent cavitation, but the new designs themselves require no additional new technologies. The ERC has, however, developed or tested such new technologies as electronic high pressure injection with controlled injection rates, two fuel injection, an improved hypocycloid piston drive mechanism, augmented mixing for reduced late burning and improved soot oxidation, and the new spark ignited diesel configuration mentioned previously. More often however the new technologies have been those used in the instrumentation development already discussed.

It should be recognized that the ability to respond rapidly to new technologies is an important attribute of a center. An example of this is the response of the ERC to the 1992 DOE-Texaco initiative to develop a fuel additive for reduction of NO<sub>x</sub> emissions. The ERC was able to rapidly start testing on a low emissions engine, and to also start tests that reveal more fundamental information about the processes going on in the engine cylinder.

### FACULTY AND FACILITIES

The ERC faculty has both grown and changed over the past six years covered by this report. Professor J. Ellzey\* left during the early years of the ERC, Professor Reitz and Rutland subsequently joined the ERC in 1989. At present, six faculty devote their entire research activities to ERC subjects. Gary Borman, the present ERC Director, devotes his research efforts to engine combustion and emissions, heat transfer, and lubrication. Patrick Farrell, has worked on fluid mechanics, heat transfer and sprays with major emphasis on development of new optical diagnostic techniques. David Foster, specializes in chemical kinetics of emissions with special emphasis on soot formation and fuels and in-situ engine measurements. Jay Martin works on fluid mechanics, heat transfer, sprays and combustion with a special interest in engine diagnostics. Rolf Reitz spends most of his efforts on upgrading models for KIVA, but also conducts experiments on sprays and their effects on engine combustion. Chris Rutland is primarily interested in combustion and fluid flow modeling with a special expertise in fundamental computations of reactive fluid mechanics.

In addition to these faculty, the ERC has benefited from the efforts of Reid Cooper on materials, Mike Corradini on spray measurements and modeling, Roxanne Engelstad on finite element analysis, Frank Fronczak on mechanisms and hydraulics Millard Johnson on lubrication modeling, and Arthur Lodge on rheology. Special mention must be made of Phillip Myers, Professor Emeritus, who has acted as the ERC contact to the Army and has given his advice on many technical issues.

During the duration of the contract the ERC has had many visiting researchers who have stayed for periods of one to two years. Special mention is given to William L.

---

\*Now at U.T. - Austin

Brown, Jr., who spent the years 1987-88 and 1991-92 at the ERC on leave from Caterpillar.

It is a special advantage of a center to have a nucleus of faculty devoted to a single subject area. This concentration attracts other visitors as well as excellent students. It allows funding of a supporting staff, which helps to improve productivity.

The facilities of the ERC provide a unique blend of state-of-the-art engines, optical diagnostics and computational capabilities. Each of the six modern heavy duty single cylinder diesel engines has full instrumentation and modifications for special diagnostics. In addition, the lab has an Isuzu ceramic diesel, a small see-through engine, a CFR engine, a glass two-stroke, and three small utility engines. A full listing of the other special instruments and facilities is given in Section 4 of this report.

## RESEARCH RESULTS

Because of the large amount of research covered by this report, the main body of the report, which follows, is a highly abbreviated discussion of the research. Thus this summary simply lists some of the major results for each topic area. The reader should examine the pertinent portions of Section 7 to obtain more detail and to be guided to ERC publications of special interest.

### Engine Modeling

The majority of the modeling efforts have been directed to improvement of submodels and to implementing them in the CFD code KIVA. Although the models for diesel combustion and emissions still require considerable work, a great deal of progress has been made and even in their current state they can be used for aiding the design process.

The following achievements are of particular interest.

- A better understanding of cold starting as related to in-cylinder events has been achieved through use of KIVA.
- An improved model for heat transfer which can be efficiently applied in KIVA computations has been developed and evaluated.
- Improved engine flow and analysis tools have been applied to both two and four stroke engines.
- Improved models for spray breakup, spray impingements, fuel vaporization and fuel-air mixing have been implemented in KIVA.

The improvements made in KIVA are listed in Table 7.1.1 of the main body; this table is repeated here for convenience (see following page).

A substantial portion of the improvements listed, are the result of funding from DOE/NASA combined with experimental work funded by the subject contract, and for the heat transfer work additional funding from TACOM. The computer work could not have been accomplished without support from the San Diego Super Computer Center and generous support from Cray Research.

Table 7.1.1 Status of KIVA Submodels

	Original KIVA	Updated submodels
Wall impingement	none	rebound-slide model
Blow-by	none	Namazian model
Wall heat transfer	law-of-the-wall	compressible, unsteady
Spray atomization & drop drag	Taylor Analogy Breakup	surface-wave-growth & distorting drops
Spray vaporization	single component	multicomponent
Ignition	none	Shell model
Combustion	Arrhenius	laminar-turbulent char time
Intake flow	assumed initial flow	compute intake flow
NO <sub>x</sub>	Zeldo'vich	-
Unburned HC	Arrhenius	laminar-turbulent char time
Soot	none	KIVA-coal
Radiation	none	Rayleigh-limit, band model

#### Engine Combustion, Emissions and Fuels

Most of the research on these topics was carried out on the ERC diesels with the exception of a few combustion rigs used for soot formation and combustion studies. The results have created an excellent data base for future model validation work as well as a better understanding of the processes involved. The following achievements are of particular significance.

- Two-color method pyrometry was used to obtain a data base of flame temperature and soot concentration in the Cummins NH diesel under fully warmed-up conditions.
- Measurements of soot deposit rate were made in the Cummins NH using a temperature controlled window.
- A laser system was developed and used to assess imep errors due to inaccurate piston position calculations and piston tilt.
- The effects of volatility of various fuel components, such as aromatics, were found not to significantly influence combustion or emissions in either a high swirl or low swirl engine.
- The effects of fuel aromatic content and type were investigated to determine effects on combustion and emissions. Unlike previous ERC work with N.A. engines, the turbocharged engine showed a higher sooting tendency for single than for double ring aromatics. This result may indicate at higher engine temperatures the aromatic structures are unstable and thus lower temperature burner data cannot be used to predict fuel composition effects on sooting.
- It was found that augmented mixing of combustion by a jet after peak pressure could significantly reduce particulates in an already low emission state-of-the-art engine.

- In situ measurements of mean particle size and number density of soot in an operating diesel were obtained by a combination of two-color radiation, scattering, and extinction data.
- From the in-cylinder diesel soot measurements it was found that initial particle diameters were 15 nm and grew to 35-55 nm. A rapid decrease in particle size with a simultaneous increase in number density was observed during expansion. Although not proven, it is believed that this phenomena was the result of rapid oxidation.
- Soot measurements in a jet-stirred combustor yielded data on nucleation rates and surface growth rates for a range of equivalence ratios and temperatures. The data show remarkable consistency with measurements made in a variety of other laboratory flames. This supports their use in diesel modeling of growth and oxidation rates.

### Heat Transfer

In 1987 when this contract was awarded by ARO, the lab was already working on a TACOM contract dealing with heat transfer. Thus the work reported here is inevitably intermixed with the TACOM work. The companion equipment-grant from ARO greatly aided both contracts and the parallel projects certainly each benefited by the joint activity.

The heat transfer work falls into three categories; diagnostic methods development, experimental results, and model development for use in CFD codes such as KIVA. The major achievements for each category are listed below.

The diagnostic methods developed are:

- Development and application of a multiple sensor probe which gives both instantaneous surface flux and steady state flux and can be applied in engines where the steady heat transfer in the solid is three dimensional.
- Development of resistance film technology for miniature multiple sensors and for application to ceramic surfaces in engines. This technology greatly reduces noise to signal ratio, thus allowing measurements even during gas exchange.
- Development of a radiation sensor which measures the instantaneous flux coming from all directions to the spot on the surface. Prior sensors always measured a narrow cone angle of radiation.
- Development of techniques for near-wall measurement of thermal gradients in engines using a speckle method.

The experimental results were obtained for; motored engines, a fired diesel, a homogeneous charge compression ignition engine (so called "flameless" combustion), and a homogeneous charge spark ignited engine. The data on the fired diesel includes the same engine with and without a plasma spray coating.

Significant results obtained are:

- Motored data from a see-through piston engine in which heat flux, laser doppler velocimetry (LDV) data and speckle holographic data were taken on the same engine. These data gave a data base for model validation.
- Data for heat flux at each of seven sensors located on the head and in a line 7mm long. These data were obtained for motoring, spark ignition and homogeneous charge compression ignition. They allow calculation of a heat

flux based length scale which revealed many details connecting the engine cylinder flows and the boundary layer. The data were also used for model validation.

- Data on a Cummins NH single cylinder diesel with and without coatings showed the combustion changes are significant factors which change the heat balance and can result in unfavorable effects from coatings.
- Heat flux measurements on the ceramic head of a small diesel showed the importance of turbulence and combustion on the heat flux distribution over the surface.
- Radiation data to a spot on the head were obtained for a fully warmed-up NH diesel engine under turbocharged conditions and for various loads. For full load the peak radiation flux was about 33% of the total flux and the time averaged radiation was about 15% of the time-averaged total heat transfer. These data show the much lower significance of radiation in a modern low emissions diesel.

The modeling effort objective was to obtain and validate an improved heat transfer model for KIVA. Several new models were developed each of which reduced the number of assumptions contained in the existent law-of-wall model.

The final model of Yang and Martin was validated by Reitz using SI data and showed excellent results. A similar validation for diesel data cannot be made until other aspects of the KIVA model are improved.

The improved model was used to estimate the effects of wall temperature on heat flux due to reactions in the boundary layer. It was predicted that significant increases in flux can be caused by this effect if the quench distance is very small. The ERC data on boundary layer thickness and flux scale indicates that very thin boundary layers can often occur.

### Gas-Phase Fluid Mechanics

Fluid measurements were taken for both near-wall flows and for cylinder flows including scavenging flows. Achievements and results are:

- Methods were developed that allow accurate positioning and spatial resolution for LDV measurements in the near-wall regions of an engine cylinder. An important result here was qualification of index of refraction gradient shifting of the data.
- A near-axis scatter method was developed for PIV which allowed use of a copper vapor laser and thus could give multiple images in time (10 or 20 KHz).
- A method of optical interrogation of PIV images was developed which avoids use of lengthy super computer processing.
- Near-wall velocity measurements showed little evidence of low momentum flow for either 2 or 4 strokes.
- Bulk flow and moving valve jet flow measurements using PIV showed very complex flows with a wide range of characteristics and has provided a data base for CFD validation although the issue of cyclic variations remains a problem.

## Diesel Sprays

The spray work covered all aspects, including; fundamental measurement, modeling, and engine testing. Emphasis was placed on using modern high pressure and even prototype diesel injectors and thus results include a large range in injection pressures and the effects of rate-shaping. Methods developed and results obtained are:

- Comparisons were made of two types of rate-of-injection meters. These meters were then used extensively as part of the data base for injector systems.
- A Phase Doppler Particle Analyzer (PDPA) was used to characterize a diesel spray for both spatial and temporal variations. It was shown that both axial and radial distributions of droplet size and velocity varied significantly with time after injection. Data taken at various ambient pressures in a room temperature bomb showed wave patterns. The frequency and existence of these patterns was not correlated with chamber pressure, but such patterns were observed even for spraying into a vacuum, indicating that details of the fluid motion in the injector could be an important factor.
- An imaging method which gives an overall Sauter Mean Diameter (SMD) for the entire spray was developed. The results show that the SMD decreased with time during injection approaching an asymptote. Axial variation showed a minimum at the interior. Good agreement was obtained when compared with PDPA data for the same Lucas injector and same conditions.
- Droplet breakup for droplets of less than 200  $\mu\text{m}$  diameter in air flow streams up to 250 m/s was investigated experimentally. Both photograph and PDPA measurements were used. Breakup regimes were identified and drag coefficients obtained. It was shown that breakup and distortion greatly affect trajectory modeling.
- A detailed experimental study of droplet impingement on heated surfaces was conducted. Droplet breakup, bouncing and surface heat transfer were quantified over a range of velocities (2.4 - 7 m/s), diameters (100 - 300  $\mu\text{m}$ ) and surface temperatures (56 - 400 c). A model was developed which correlates the data.
- A study of pilot injection using an electronic unit injector on a Detroit Diesel 53 engine has been performed in which both engine performance data and spray visualization data were obtained. The visualization utilizes a fiber optic bundle and is thus not intrusive, requiring only minor engine modification. The work shows decreased NO emissions can be obtained using pilot injection in this engine without increasing smoke.
- A heated, engine-fed bomb with airswirl was used to obtain data using an electronic fuel injector (UCORS). Exciplex fluorescence and photographic imaging were used to study liquid and vapor distributions. Pilot injection was shown to have significant impact on rate of combustion.
- A study of injector hole flows was conducted using a scaled up flow rig. Inlet hole geometry with a sharp edge generates more local turbulence than a rounded inlet and have minimum near wall RMS velocities for an L/D of 4.5. Rounded holes tend to pass the upstream (sac volume) turbulence through the hole. The maximum value of these data will be obtained when spray breakup models can be coupled to internal nozzle flow calculations.

- A large amount of spray penetration data were obtained for high pressure injection into a cold pressurized bomb. These data were used for validation studies of non-vaporizing jet breakup models.
- A series of modeling studies were performed for both non-vaporizing and vaporizing sprays using the Reitz breakup model in KIVA. These studies revealed problems in grid resolution and subgrid vapor distribution modeling and have led to improved models.

### Lubrication and Design

Although the ERC research has been primarily concerned with combustion chamber aspects for diesels a few projects were conducted dealing with mechanical aspects of the engine. The following achievements highlight these activities:

- Relatively non intrusive methods were developed and used to measure oil film thickness on the liner of an operating engine. These methods used single fiber laser induced fluorescence and capacitive probes. The data also include some temperature and heat flux measurements.
- The oil film data have been compared to results from a computer model which includes effects of temperature on oil viscosity. These comparisons show the importance of oil starvation on boundary conditions.
- A model for power-law lubricants in piston-liner lubrication has been developed.
- The lubrication model has been used to clarify the effects of viscosity variation with temperature, liner vibration and viscous heating all of which were shown to be handled without major changes in the model assumptions.
- Lube oil viscosity for both used and unused oil has been measured at realistic levels of shear and temperature.
- An improved analysis for design of liner vibration has been developed. This model includes the important effects of coolant on the vibration and suggests ways to design for reduced cavitation.
- An improved version of the hypocycloidal drive mechanism has been designed, fabricated and tested for a small four stroke engine. The design shows promise for reduced piston vibration, noise and piston tilt.
- A new technique for evaluating and quantifying the high temperature mechanical response of interfaces in fiber-matrix ceramic composites has been developed. A comparison of the model to results obtained for a silicate-SiC reinforced composite system illustrates the ability of assessing the interfacial mechanical response based upon the steady-state creep rate of the composite.
- In cooperation with TACOM, and using a TACOM developed IR imaging system, the ERC has developed an engine test rig which can be used to evaluate material samples attached to the top surface of an engine piston. The instrumentation allows measurement of the temperature distribution at both the top and bottom surfaces of the disk shaped sample.

### Closure of Summary

This brief summary has given a listing of some of the research discussed in more detail in this report and in the publications listed in Appendix A. Study of these results shows that in many cases numerous individual projects have been used in conjunction, either to complete an understanding, to evaluate a model or to conduct an applied analysis. Such synergism is the result of having a center with its composite of faculty expertise and facilities resources. It is felt that the ARO Center of Excellence contract and grants have allowed a unique facility to be created for use of the Army and U.S. industry. The principal investigators are grateful to the Army for the privilege of serving in this manner and wish to thank all those involved, particularly Dr. David Mann of ARO and Dr. Walter Bryzik of TACOM.



## 2.0 INTRODUCTION

When the contract which is the subject of this report was granted in 1986, the then Internal Combustion Engines Lab name was changed to the Engine Research Center (ERC), in keeping with the contract, which established the lab as the Center of Excellence for Advanced Propulsion for the U.S. Army. The awarding of the contract was, in part, recognition of the lab's 40 years of research contributions and its over three decades of service to the army, particularly TACOM.

It is interesting to note that the lab was initiated by a grant of \$50,000 and lab space in a WW II barracks called T-25. The award to then Assistant Professors Phillip Myers and Otto Uyehara was largely based on their pioneering work using the two-color optical method to measure particulate temperature in the cylinder of a firing diesel engine.

Although the "T" in T-25 stood for temporary, it served as the primary I.C.E. Lab space until 1969 when the Lab was moved to its present location in the Engineering Research Building (ERB). By that time over 200 MS and 75 PhD students had graduated from the Lab and the faculty had grown to include Gary Borman and Henry Newhall in addition to Myers and Uyehara. Henry Newhall eventually joined Chevron Research and Otto Uyehara retired in 1982. David Foster joined the staff in 1979. By 1986, the faculty also included Patrick Farrell and Jay Martin. At this point the laboratory became the ERC and the expanded opportunities helped to attract Rolf Reitz and Chris Rutland. The expansion of activities also caused the Center to seek help from faculty in other areas such as Professors Cooper, Corradini, Engelstad, Fronczak, Johnson and Lodge. At present the six core faculty (Borman, Farrell, Foster, Martin, Reitz, and Rutland) form a group which covers both the experimental and modeling aspects of engine combustion system research. The faculty and their areas of interest are presented in section 5 of this report.

The 1986 contract from ARO which forms the basis of this report covered operating expenses (salaries, supplies, travel, etc.). However, separate ARO grants supplied equipment and special Army Fellowships. These later two aspects of the ARO center funding are covered in separate final reports. The facilities are, however, also reviewed here for completeness, and the research results of the fellows are included in the general discussion, because their research costs were supported from the subject contract.

Although the ARO Center contract formed the core of ERC funding during the five years and ten months of the contract, many other sources of support have contributed to the ERC activities. Some of these were contracts in place in 1986. Other new contracts were initiated during the contract period. Additional sources included industrial fellowships, industrial gifts-in-kind, and support of visiting researchers. Where these sources were supplemented by significant ARO supported facilities and/or staff time paid by ARO, the results from them have been intermingled with strictly ARO supported research. For projects clearly fully funded by separate sources the work is not included here, although it may be referenced.

Four important sources need to be singled out. First, DOE has supplied substantial funds, technically monitored by NASA Lewis, to support the modeling efforts of Professors Reitz and Rutland. Second, substantial supercomputer time has

been provided by Cray Research and the Super Computer Center at San Diego. Much of the systems modeling work reported here was thus supported in the majority from these three sources. The fourth source was TACOM contract DAAE07-84-CR063 which was already in place in 1986 and continued until 1990. This contract supported significant portions of the work done on heat transfer and cycle analysis.

It is important, during reading of this final report to understand the ERC objectives and the special needs of the Army. Thus the next two sections of this introduction discuss these aspects of the ERC.

## OBJECTIVES

The first objective of the ERC is to train students in the special research areas of interest to the Army and to its industrial suppliers. Because the Army purchases commercial equipment when possible, many of these students also serve the commercial engine industry. Special emphasis has thus been placed on graduate students who will remain in the U.S. to work. As a result, 87.5% of the MS and 75% of the PhD students produced during the period of this report are currently working in the U.S. Although emphasis has been placed on graduate education, a large number of undergraduates have also participated in the ERC as hourly helpers. For many, it has been their primary opportunity to experience work on real engineering systems and to engage in engineering practice.

The second objective of the ERC is to provide a source of consultation for use by the Army and by industry. Although graduating students provide a direct technology transfer to their employer, they do not provide a continuity of such experience. The faculty, however, do provide such continuity and thus serve as a composite source of the prior experience.

The third objective of the ERC is to provide knowledge and research tools for use in the solution of long range problems of special interest to the Army. In many cases the development of such tools for research has an important continuing impact in industry. For example, the work on diesel cycle analysis sponsored by TACOM at U.W. in the early 1960's has become a routine tool used in engine development by industry. It is expected that the CFD code KIVA, a more recent subject of ERC research, will play a similar role in the years to come. Such models, like the accumulated knowledge of the faculty, serve as a composite of information gathered from the experimental programs. Their effective use, however, requires people trained to understand both their power and their limitations.

The fourth objective of the ERC is to provide solutions to problems of Army interest by pulling together models and experimental data. Because ERC research is limited to basic approaches, the types of problems investigated are typically fundamental rather than those encountered in the later stages of development. An example is the TACOM supported ERC work on spark ignited diesels which suggested practical approaches, but stopped short of developing a practical working system.

The fifth objective of the ERC is to identify new technologies which may become important to the Army and to exercise such technologies in a research environment. In many cases, technologies have been developed outside of engines, but considerable effort is needed to apply them to engines. In other cases, the technologies require evaluation by special techniques available only in a sophisticated research laboratory.

## RESEARCH AREAS

The primary power plants for the U.S. Army are diesel engines. Smaller engines that now use gasoline are to be replaced by power plants which can utilize JP8 as a fuel. Because of this need for diesel technology, the ERC has concentrated its research on diesel problems, with emphasis on heavy duty engines.

Many of the Army's objectives are shared with those of commercial engine manufacturers. In particular, the Army has been asked to use commercial power plants for tactical vehicles and in combat vehicles whenever possible. However, in the case of combat vehicles the Army's objectives are unique, with quite different design restraints from those of commercial vehicles. For example, engines for combat need not meet emissions standards. In all cases, the army has more severe operating requirements, such as cold starting below -25°F, and the possible need to use available fuels of unspecified quality. An objective of the ERC has thus been to identify the most important Army needs and to conduct research directed toward helping to build engines that satisfy these needs. The following segment briefly discusses some of these needs in a research context.

A very significant goal for the Army is to reduce the weight and volume of the powertrain for a given output power. This system includes the engine, heat exchangers for both coolant and lube oil, the transmission and the fuel tank. This goal could be achieved by designing more effective heat exchangers, reducing engine heat rejection, increasing engine power density, improving fuel economy, decreasing friction, and improving strength to weight ratio of the materials used. The benefits of this goal are typically much higher for the Army, particularly in combat equipment, than for commercial applications. Thus approaches, such as low heat rejection engines, require Army funded research and development.

Research to reduce coolant system volume could either identify techniques to produce more compact heat exchangers or to reduce the need for engine cooling by cylinder insulation technology. Direct attempts to insulate have not only produced materials problems, but have also shown unanticipated changes in combustion and heat transfer.

Because the Army needs to operate its equipment globally, severe ranges in environmental conditions are possible. In particular, diesel engines suffer from starting difficulty at low temperature. Starting aids to be practical for Army use should be compact and reliable and should not require a special logistic tail. The cold starting problem is a systems problem involving degradation under cold conditions of many of the system parameters ranging from the battery to the fuel system. An important part of the research is to better understand the combustion system parameters in order to identify and evaluate techniques for improved starting.

As previously mentioned, the Army vehicle may be forced to use locally available fuels and lubricants. Thus engines which can operate with a wide range of fuels and lubricants are desirable. Special engine designs for combat vehicles may be achieved by using new technologies; however, tactical vehicles/engines which use available commercial designs are apt to be increasingly sensitive to fuel and lubricant quality. This is because commercial systems designed to meet stringent emission standards will use special reformulated fuels and low oil consumption designs.

Identifying these potential problems and finding solutions requires research done in parallel with the evolving designs for low emissions. Emissions research is thus needed in order to find methods of reduction that are as compatible as possible with Army needs.

Because the design of engines is so complex, involving many conflicting demands, tools that can provide a guide to design are very desirable. Such tools can be provided by detailed system models and by diagnostic instrumentation. The models offer the additional potential of evaluating new design concepts before they are reduced to hardware. However, current cycle analysis lacks the details of fluid mechanics and combustion required to accomplish such evaluations. Thus CFD models such as KIVA must be improved and evaluated.

Many of the improvements needed for CFD codes require improved understanding of engine phenomena. Examples of poorly understood phenomena are spray breakup, heat transfer to the piston bowl, the influence of combustion chamber geometry on combustion, the combustion mechanisms, soot formation and oxidation, and the detailed mechanisms of lubrication of the piston-liner. Fundamental understanding of these phenomena may not only improve the models, but may lead to new design concepts.

While better understanding of the general phenomena is important, as discussed above, many Army needs are unusual and require understanding of special systems such as high temperature lubrication, heat transfer for very high temperature surfaces, and very high imep combustion.

#### CENTER ADVANTAGES

The engine research needs of the Army require many approaches - both experimental and computational. Center funding allowed a group of faculty to approach these problems as a team, helped to attract excellent students, and provided the special facilities required to carry out complex diagnostic experiments. It is unlikely that any group of individual contracts/grants could have produced the resulting capabilities of the ERC as it exists today.

In the following, ERC contributions to the Army and to industry are discussed, followed in turn by a discussion of ERC facilities and faculty. Finally, the research results for each subject area are discussed briefly. A more complete discussion of these results can be obtained by reading the papers referenced or even more details can be obtained from the theses themselves. A list of ERC publications for 1987 to present is given in Appendix A, a list of theses is given in Appendix B.

### 3.0 ERC CONTRIBUTIONS TO THE ARMY AND INDUSTRY

Details of Center research activities are presented later in this report. Consequently, this section will primarily present illustrative examples of ERC contributions to the Army and Industry. As indicated in the previous section, many of the Army's objectives are shared with those of commercial engine manufacturers. However, basic technical data can assist both groups. Consequently, the Army-Industry classifications used below are not mutually exclusive and there is much overlap.

#### TECHNICAL DATA

Engine design and development times range from four to five years for commercial engines to ten years or more for the high-power-density engines such as AIPS which are used in combat vehicles. Any approach that can reduce this time saves both money and time. The following examples of ERC research illustrate the development and potential use of basic technical data as an aid in shortening this time.

- Quantitative information on engine-related factors affecting cold (-65°F) starting of diesel engines.
- A computational approach to the 3-D modeling of engine intake flow which affects combustion, power output and engine power density.
- Measurement of cylinder oil film thickness in normally cooled engines as a start to studying the problem of lubrication of uncooled or minimally cooled engine cylinders
- An improved cylinder heat transfer model used by the Army in CFD engine modeling and new instrumentation for heat flux measurement
- New diagnostics and models applied to advanced, state-of-the-art high pressure injector sprays
- Development of a particle image velocimetry system using high rep rate lasers and optical processing of the data
- Development of in-cylinder imaging methods that can be utilized with only minor engine modification

Similar examples of ERC activities which were focused more on development and potential use of basic technical data for industry problems are:

- An engine mechanism which eliminates the problem of engine balance and piston side thrust and could lead to quieter, simply balanced engines.
- A new finite element analysis of liner vibration for use in designing liners and preventing cavitation damage.
- A new injection geometry approach to spark ignited diesel designed shown to work well for low cetane fuels.
- An investigation of the effects of injector tip hole geometry on the flow characteristics.

#### TECHNOLOGY TRANSFER

Technology transfer occurs in many ways and is a two-way process wherein both parties benefit.

Employment of graduates is the optimum way to transfer advanced technology since they know both the problem and the advanced technology. If the graduate is employed by Industry the transfer to the Army is through industries' products rather than directly from the individual. However, both are beneficial to the Army. During the period 1987-92 the ERC had 58 total graduate students; more detailed information is given in Appendix B of this report. An indication of Industry recognition of this technology transfer is the long-time, continuing scholarship support from industries such as General Motors, AMOCO, Mercury Marine, Chevron and Outboard Marine.

Open publications are another obvious means of transferring technology. Their general availability provides for transfer to a wide audience. Additional transfer of technology occurs when there is a presentation of the paper, particularly during the question and answer period and via "corridor" discussions after the presentation. ERC has published 110 articles in archived journals during the period 1987-92; more detailed information is given in Section 8 of this report.

Visits, presentations, and informal consultations are another mechanism for technology transfer. Two-way technology transfers as ERC staff visits Army and Industry Laboratories and, in turn, when Army and Industry personnel visit the Center. In both cases, formal presentations may or may not be made. Informal consultations normally occur during these visits. In addition, a surprising amount of technology transfer occurs via the telephone.

It is obviously impractical to keep track of all telephone conversations but a reasonable estimate is three to four calls every day. Discussions would cover such diverse topics as: technical evaluation of a proposal to an Army facility from an outside inventor; use of a computer program developed at the Center and in use by Army personnel; results of a recent experiment at the Center; plans for cooperative experiments; application of diagnostic techniques recently developed at the Center; plans for workshops and visits, etc.

It is equally impractical to recognize all visits by Center personnel. Many visits were made to TACOM. Other Army Laboratory visits included Fort Belvoir, the Army Fuels and Lubricants Laboratory at Southwest Research and Watertown Arsenal as well as NIST. Visits to industry included all of the major engine manufacturers in the U.S., as well as engine manufacturers and engine research laboratories in Germany, Austria, England, Italy, France, and Japan.

There is a continuous stream of visitors to the Center but it should be noted that the duration of the stay of visitors varied from hours to years. For example, William L. Brown, Jr., one of the top engine research persons at Caterpillar, spent 23 months at Wisconsin between two separate times, 1987 and 1991. His stay was obviously mutually beneficial. Several, more junior, persons from Japan were in residence for extended periods. Visitors from Army facilities, particularly TACOM but also Fort Belvoir, came frequently for one or two day visits as well as for workshops. Industrial visitors, many of which held high administrative positions, were too numerous to list.

Another method of technology transfer is workshops. Army workshops were held at Wisconsin in September 1988, June 1990, and June 1992. Center staff attended workshops held outside of Madison. Center staff also participated in pertinent workshops not sponsored by the Army, such as the DOE Working Group on Diesel Engines.

## COOPERATIVE PROJECTS

There were cooperative research projects with both the Army and Industry. These cooperative endeavors were selected and carried out when there was a problem that could best be solved by combining unique facilities available at each organizations. A good example would be the cooperative research project carried out with Dr. Steve Shephard of TACOM. Piston top temperatures are desired for many reasons but particularly for stress analysis resulting from the temperature distribution in the piston. Knowledge of temperature contours are essential to estimating stresses. Putting one or two thermocouples in a piston is routine, but getting the signal out from the large number necessary to define the isotherms required for stress analysis is a formidable task.

Through discussions between TACOM and ERC it became clear that the special infrared imaging system developed by Dr. Shephard of TACOM might be utilized to measure top surface piston temperatures including ceramic coated surfaces. A special engine was fabricated by the ERC to allow long wave length infrared imaging of the piston through a specially developed window. Briggs and Stratton Corporation supplied the engine and technical advice. The first set of data showed good results, but there was interference from combustion gases. A second set of experiments run in the spring of 1992 focused on this problem and measurement of the cylinder side surface temperature of the window. Although the focus of the work was oriented to Army interests in ceramics, the results on flame motion are of direct interest to small engine manufacturers.

On the Industry side, a PhD Army Fellow, Dan Richardson, as a part of his thesis, developed a fiber optic probe which could be used to send laser light to the oil film at the piston-liner interface with the intensity of the light returning from the fluorescing oil film being a measure of oil film thickness. During his thesis work he ran tests on a TACOM/LABECO engine at the ERC and used special apparatus at Cummins to run out-of-engine tests. He is now employed at Cummins where he is continuing his work on lubrication. Meanwhile, Cummins has donated a modern, single-cylinder engine to the ERC which has been instrumented for further work on lubrication.

Cummins also participated in an Industry-dual Universities cooperative research project. The needed engine was available at Purdue so they supplied facilities, including a technician. ERC supplied researchers, instrumentation, and data acquisition while Cummins supplied a variety of injectors and tips. Data were obtained on smoke and  $\text{NO}_x$  in an insulated engine when load, speed and injection timing were varied.

Jay Martin, who wanted to study the effect of pilot injection on emissions, cooperated with Detroit Diesel in developing and adapting their electronic injector and controls to accomplish the desired injections.

In another Industry cooperation effort, Center student Jeff Naber, spent the summer working with Dr. Rolf Reitz then at GMRL. The paper resulting from this work won the SAE Horning Memorial Award.

Another unique cooperation with Industry occurred as a result of Professor Reitz's work on characterization of sprays. S. C. Johnson & Sons who produces products using aerosol sprays funded fundamental research on sprays.

One other aspect of cooperative research should be mentioned, i.e., the contribution of equipment and supplies by industry. This is an important indicator of their interest and support. Cummins supplied two different, single-cylinder, research engines while Caterpillar supplied another. The market value of each of these engines is in the \$75,000 to \$100,000 range. Equally important, is the invaluable support also supplied in the form of parts, understanding of the peculiarities of the engine, etc.

Also the contribution of special test fuels not available in the market place by Amoco, Texaco and Chevron was invaluable and permitted the Center to sort out the effect of fuel characteristics, particularly on combustion and emissions.

#### JUDGMENTAL DECISIONS

Both the Army and Industry are continuously making judgmental decisions. These judgments range from relatively mundane matters to long range policy matters. In these decisions it is often helpful to listen to outside judgments offered by persons knowledgeable about both the technology and the specific problem. These mundane judgments are often rendered over the telephone as previously mentioned. Consequently, this section will deal only with major judgmental decisions. However, Center staff serves in two different ways in making these major decisions; as individual consultants and as a member of a group of studying the problem.

One example of the Army's desire for assistance in making group judgments was the recent STAR study. Professor Borman served as a member of that study committee. Another example was the Army-sponsored NAS study on the "Mobile Electric Power Technologies for the Army of the Future". Professor Myers served on that Committee. Professor Myers also served on the DOE sponsored study that was of considerable interest to the Army "State of the Art and Projected Technology of Low Heat Rejection Engines." Professor Myers also served on an Army Committee studying the problems of producing obscuration smoke and participated in the Technology Base Investment Strategy Conference. Of considerable interest to Industry was the recent NAS CAFE report entitled "Automotive Fuel Economy - How Far Should We Go?" in which Professor Myers participated.

Formal consultation is a two-way technology transfer, a learning of problems, and assistance in making judgmental decisions. Professor Myers has been a consultant to TACOM for more than 30 years. Professor Borman has been consultant to General Motors for more than 20 years. During the term of this grant, Professor Reitz has served as a consultant to Caterpillar, S. C. Johnson & Sons, Southwest Research Institute, and Advanced Fuel Research. Professor Martin as served as a consultant to Hansen Engine, John Deere, and Barrack Technologies. Professor Foster has served as a consultant to Texaco and Eaton. Professor Farrell has served as a consultant to Honeywell. Professor Rutland has served as a consultant to Astronautics. Clearly the Center Staff has transferred technology to the Army and to Industry, learned of their problems, and assisted them in making judgmental decisions.

## 4.0 FACILITIES

A listing of ERC facilities is given in Tables 4.0.1, 4.0.2, 4.0.3, and 4.0.4. A larger amount of the equipment was obtained from Grant which was awarded in parallel with the subject contract; a report on this equipment is given in the final report for that grant (Borman et al., 1992).

It should be noted that in all cases some modifications have been made to each of the nine larger engines. Engines III and VII are greatly modified and thus are not useful for obtaining emissions or performance data. In fact, engine VII is only a vehicle for pumping gas in-and-out of the spray chamber attached to it. The CFR engine (VI) is a research engine and is not representative of modern production engines. The other five engines are representative of modern production engines. In two cases the injection system and/or geometry have been upgraded; this is particularly true of engine I which now has a high pressure injection system and is quiescent, with a wide piston bowl. Engine II has been modified to accept a Nippondenso U2 prototype high pressure injector. Each of the nine engines has some optical access, but for the five "normal" engines the modifications do not seriously affect performance.

The listing of special equipment is conspicuous for the number of lasers and laser based instruments. These form the heart of many of the research project described in this report.

The ERC is housed in the first three floors of the Engineering Research Building. The basement engine cells currently contain nine engine test stands. Each engine is connected to an electric dynamometer with speed control, and all setups include conventional oil and water temperature controls, air and fuel flow measurements, and a shaft encoder. The engines currently in use follow.

Table 4.0.1 Engines

I	TACOM/LABECO; single-cylinder diesel with special head for instrumentation, simulated turbocharging, and mini-dilution tunnel.
II	CAT-OIL TEST I; with special head and injector, simulated turbocharging and dilution tunnel.
III	Triptane See-Through; small engine with optical ports through piston into clearance volume, annular sapphire ring for observation into the clearance volume, and a special head with a large instrumentation port for mounting surface thermocouples or further optical access.
IV	DDA 53; single-cylinder two-cycle diesel with simulated turbocharging and EFL, spark plug in head, auxiliary port injection, and pilot injection.
V	Cummins NH single cylinder with simulated turbocharging, special instrumentation ports in head, special load control system, and minidilution tunnel.
VI	CFR; single-cylinder with variable compression ratio optical ports and heated homogeneous charge for autoigniting combustion.
VII	CAT-OIL TEST II; single-cylinder open chamber modified for optical access spray chamber.

VIII	Isuzu Ceramic Diesel; single-cylinder direct-injected with silicon nitride and no cooling. Instrumented for temperature measurements.
IX	Cummins L-10; one active cylinder, direct-injected with electronic fuel injection, simulated turbo-charging, and instrumentation for liner oil-film measurements.

In addition, there are three small engines, one of which is connected to a variable speed drive and the other two to water brake dynamometers. These engines are:

X	Mercury Glass Two-Stroke; single-cylinder ported two-stroke with almost complete optical access to the combustion chamber.
XI	Briggs and Stratton; single-cylinder with specially-modified head and piston for piston surface temperature measurements using infrared imaging and evaluation of candidate ceramic materials.
XII	Kubota; single-cylinder with instrumentation for determining emissions and performance characteristics.

Table 4.0.2 General Purpose Equipment

XIII	Twelve channels of high-speed data acquisition (externally clocked 80286 and 80386 machines)
XIV	Low-speed data acquisition systems.
XV	Tektronix 11401, 2430, 2210 digital oscilloscopes.
XVI	Tektronix FG 504 function generator, other scopes, DMM, etc.
XVII	Gas chromatography instruments, and exhaust emissions analysis instruments for CO, CO <sub>2</sub> , NO, NO <sub>x</sub> UHC, H <sub>2</sub> O gas analysis and soot mass.
XVIII	Borescope
XIX	Pyrometer and high-temperature black body for optical calibration.
XX	Cameras and darkroom facilities.
XXI	PCs dedicated for experiment control.
XXII	Complete full-size and range machine shop, including vertical milling machine and engine lathe, band saw, welding equipment, and complete tooling.

Table 4.0.3 Computer Facilities

XXIII	A Micro Vax II minicomputer with Telnet access to Cray supercomputers at U.S. Army, TACOM and at Cray Research in Mendota Heights, Minnesota.
XIV	Several PC-type workstations with CAD, graphics, wordprocessors, etc.
XXV	Five Silicon Graphics Workstations for interactive sessions with the Cray computers that include extensive graphics animation.
XXVI	An Ardent Titan Supercomputer/Workstation capable of very high speed computations, typical of those necessary for multidimensional simulations such as KIVA, and advanced display features.

Table 4.0.4 Special Equipment

XXVII	High-speed movie camera.
XXVIII	Ten Watt copper-vapor laser for use in high-speed photography and PIV.
XXIV	Three laser Doppler velocimeter two-component systems with traversing systems.
XXX	Excimer laser for laser-induced fluorescence.
XXXI	Three video camera/frame grabber systems for digital image analysis.
XXXII	Two Nd: YAG lasers, dye laser for Raman spectroscopy.
XXXIII	Two HeCad lasers for fluorescence studies of engine oil film thickness.
XXXIV	Coherent fiberoptic bundle for visualization and spatially-resolved measurements in ordinary diesel engines.
XXXV	Many smaller lasers for scattering and extinction measurements, particle image velocimetry, speckle interferometry.
XXXVI	0.5 and 1 m spectrometers.
XXXVII	Phase/Doppler Particle Analyzer.
XXXVIII	Radiant heat transfer instrument.
XXXIX	Surface thermocouples for dynamic heat transfer.
XL	High temperature, controlled atmosphere deformation machine.
XLI	High shear rate Lodge stressmeter.
XLII	Flow bench for measuring valve and port flow characteristics.
XLIII	A shock tube and special radiation source to simulate conditions in the engine cylinder at the time of injection.
XLVI	Pump test stand for testing high flow rate injection systems.
XLV	Gated image-intensified CID camera for in-cylinder imaging.
XLVI	Hybrid optical-numerical and all-optical PIV processors.
XLVII	Berglund-Liu type monodisperse droplet generators.
XLVIII	Zuech and Bosch-type rate-of-injection meters.
IL	Jet-stirred reactor for soot oxidation studies.
L	High-pressure bomb for spray studies.
LI	Elevated pressure flow tube for soot formation/oxidation studies.
LII	High-pressure continuous flow spray facility.
LIII	Long-distance microscope photographic lens.

## 5.0 FACULTY

The faculty of a center must work together, each bringing on expertise from a given area, but also a broad understanding so that the group can interact with a minimum of tutorial discussion. Each of the faculty also contributes to an area of teaching so that the graduate students obtain a well rounded background. Formal teaching is supplemented by seminars and group or individual discussions with graduate students. Students at the ERC are encouraged to consult with any of the faculty members as needed.

The following discusses the relationship between the core faculty and then goes on to discuss how other faculty have been utilized for particular interdisciplinary problems. A brief resume is then given for each investigator.

### THE CORE FACULTY

The ERC core faculty consists of Professors Borman, Farrell, Foster, Martin, Reitz and Rutland. Each of these faculty devote all of their research efforts to engine topics. Professor P.S. Myers serves as a special consultant, making available his forty-five years of experience in research, consulting and teaching.

Professor Borman has served as director of the center since the start in 1986. He has wide experience in engine topics covering both modeling and experiments. He typically bridges areas of expertise suggesting general objectives and priorities. He teaches the general graduate course in combustion (ME 769) and collaborates with Professor Ragland in teaching a first course in applied combustion (ME 569). His own research during the contract period has involved heat transfer, combustion diagnostics, lubrication and fuel effects.

Professor Foster's research has focused on chemical kinetics and he teaches a graduate course in this subject (ME 774). A natural extension of kinetics has been research on fuels, gaseous emissions and soot. Because of his wide interest in engines, he also teaches the general engines course (ME 469).

Associate Professor Farrell comes to the engines area from a background in fluid mechanics and optical diagnostics, although he has worked with engines in a practical way for many years as an avocation. His research has included droplet vaporization, and optical diagnostics applied to engine flows, heat transfer and sprays. He teaches graduate courses in turbulence (ME 775) and boundary layers (ME 773) and a special course in applied optics (ME 601).

Associate Professor Martin had experience in diagnostics at Sandia Livermore and engines at GMRL before joining the ERC. His interests in instrumentation have been applied to both spark ignition and diesel engines and cover a wide range of topics including flame propagation, engine flows, heat transfer and sprays. He teaches a graduate course in instrumentation methods (ME 770).

Associate Professor Reitz had considerable experience in spray and engine modeling at both Princeton and GMRL before joining the ERC. He has led the ERC's focus on CFD modeling and upgrading of the CFD code KIVA. He has also started a number of experimental programs aimed at providing understanding of droplet phenomena in sprays and validating the KIVA results using engine data. He teaches a first year graduate course in compressible flow (ME 572) and Fluids (ME 563).

Assistant Professor Rutland worked on fundamental modeling of flames for his PhD at Stanford. Since joining the ERC he has worked on fluid mixing, inflow modeling and diesel combustion models. His more basic modeling approaches complement the more applied work of Reitz, although they often work in collaboration. Since joining the ERC he has started a popular graduate course in CFD modeling (ME 573).

All of the ERC core faculty have been involved with both models and experiments dealing with engines. Key approaches are the use of optical diagnostics to understand engine phenomena and validate models. The modeling efforts in turn have been directed to practical engine applications. The diagnostics have been applied to engines whenever possible. Technical collaborations have thus been common, such as Borman and Reitz on cold starting; Borman, Farrell and Reitz on droplet vaporization; Borman and Foster on emissions and fuels; Borman and Martin on heat transfer; Farrell and Martin on PIV, sprays, and heat transfer; Farrell and Rutland on intake flows; Foster, Martin and Reitz on scavenging flows; Farrell, Foster and Martin on spray analysis, Reitz and Martin on high pressure injection, and Reitz and Rutland on KIVA improvements.

Although the core faculty of the ERC provides a strong synergism for research related to engine combustion and emissions, interdisciplinary topics dealing with mechanisms, materials and lubrication have required reaching out to other faculty. Even in the area of sprays, already covered by the core faculty, it has been desirable to add the expertise on two-phase flow offered by Professor Corradini. Professors Cooper, Johnson, Lodge and Fronczak were recruited from the start to add their expertise to the areas mentioned above. Professor Engelstad's involvement actually arose due to a graduate student who came from the engine industry with considerable expertise in finite element analysis. Application of his experience to engine liner vibrations under the guidance of Engelstad was a serendipity which provided use of available faculty expertise.

## BRIEF FACULTY VITA

### **Gary L. Borman**

Professor; BS 1954, MS 1956, MS 1957, PhD 1964, UW-Madison

Engine combustion, particularly diesel engine combustion, is Professor Borman's primary research interest. Research subjects have included detailed cycle analysis, combustion modeling, droplet vaporization, engine heat transfer, and alternative fuels.

Current projects concern; heat transfer measurements in a low heat rejection ceramic diesel engine, spray characteristics for injection onto a pedestal, laser induced fluorescence measurements of the oil film on a engine liner, measurement of inter-ring gas pressure, and emissions from a small utility engine.



He teaches thermodynamics, heat transfer, thermal systems analysis, and combustion. He is a fellow of the Society of Automotive Engineers and a member of the National Academy of Engineering.

**Reid F. Cooper**

Associate Professor; BS 1977, The George Washington University; MS 1980, PhD 1983, Cornell University

Professor Cooper's research centers on the experimental investigation of the physical and associated defect structures in ceramic, glass-ceramic, and geologic materials at high temperatures. An overall goal of the research is to enhance the applicability of inorganic, non-metallic materials in structural applications. In current studies of transport properties and plastic deformation, he seeks to correlate macroscopic properties with microscopic physical and chemical mechanisms.

Professor Cooper's involvement with the ERC is in the evaluation of promising new high-temperature structural materials in simulated and real engine environments; emphasis of the experiments is on the high-temperature chemical stability and overall dimensional/mechanical reliability of the polyphase ceramic material. Current work has involved the all-ceramic composites of carbide fibers (such as SiC or graphite) embedded in an oxide or silicate matrix. Solid-state chemical reactions between two phases create improved, nonbrittle properties.

**Michael L. Corradini**

Professor; BS 1975, Marquette University; MS 1976, PhD 1979, Massachusetts Institute of Technology.

Fluid mechanics and heat transfer with a special emphasis in multiphase flow have been Professor Corradini's research interests in mechanical and nuclear engineering.

The main objective of his work is to better understand fuel injection from the study of the jet breakup process and the associated fuel oxidant mixing. Models developed for this phenomena are compared to each other and the data obtained in the tests (e.g., jet breakup length, drop diameters and velocities). In addition, Professor Corradini is involved in the modification and improvement of a multi-dimensional, multi-phase computer model, KIVA, for this purpose and in associated spray experiments.



**Roxann L. Engelstad**

Assistant Professor; BS 1977, MS 1979, PhD 1988, UW-Madison.

Professor Engelstad's areas of interest are structural dynamics, vibrations, solid mechanics, and mechanical design. Current research topics include the study of cylinder liner vibrations (from piston impact) which can lead to cavitation damage on the waterside of wet liners.

As a member of the Fusion Technology Institute, she is concerned with the mechanical design and structural response of fusion reactor chambers to impulsive pressure and shock loadings.

With the Center for X-ray Lithography, Professor Engelstad is investigating the mechanical response of x-ray lithography masks which are used in the development of advanced integrated circuits.

She is a member of the American Society of Mechanical Engineers, the American Nuclear Society, and the American Institute of Aeronautics and Astronautics, and a Presidential Young Investigator.



**Patrick V. Farrell**

Associate Professor; BS 1976, University of Michigan; MS 1978, University of California-Berkeley; PhD 1982, University of Michigan.

New optical methods for combustion diagnostics less sensitive to system vibration than others are among Professor Farrell's areas of study. He also examines turbulence in combustion systems conducting experimental and analytical studies of turbulent flow.

Professor Farrell's current projects include studies of fuel spray and droplet vaporization, engine heat transfer measurement methods, and full field velocity measurement methods.

He teaches courses in thermodynamics and fluid mechanics and is a member of the American Society of Mechanical Engineers, the Optical Society of America, and the Society of Automotive Engineers.



**David E. Foster**

Professor; BS 1973, MS 1975, UW-Madison; PhD 1979, Massachusetts Institute of Technology.

Professor Foster's research interests in the field of combustion are aimed at understanding the combustion and emission formation processes for developing more efficient, cleaner engines. Specifically, he works to perfect the application of optical diagnostics to engine and combustion systems using photography, and laser scattering, extinction, excitation and velocity techniques. In addition, he studies soot formation processes, knock kinetics, early flame development, combustion characteristics of alternate fuels, and modeling of particulates.

Professor Foster teaches thermodynamics, fluid mechanics, I.C. engines, and chemical kinetics of combustion. He has won departmental, engineering society, and university awards for his classroom teaching.

**Frank J. Fronczak**

Associate Professor; BS 1972, MS 1974, University of Illinois Urbana-Champaign; DE 1977, University of Kansas-Lawrence.

Professor Fronczak's research interests include machine design, product design for manufacturing, fluid power, and vibrations. Current research involves both analytical and experimental work in the fluid power area.

Professor Fronczak has prior experience in the aerospace industry at NASA/Langley Research Center where he investigated the dynamic characteristics of helicopter rotors. He maintains a strong interest in vibration problems and the design of a free-piston engine pump.

He is investigating the application of computer control to hydraulic accumulator energy storage vehicles and the design of a free-piston engine pump.

His experience in design is being applied in the ERC to the evaluation of engines incorporating a hypocycloid crankcase mechanism. Such engines can ideally be perfectly balanced and also produce no side thrust on the piston. Thus the potential for reduction in vibration may allow new high temperature techniques to be implemented.



**Millard W. Johnson**

Professor; BS 1952, MS 1953, UW-Madison; PhD 1957, Massachusetts Institute of Technology.

Professor Johnson is interested in the construction of continuum theories to model the behavior of materials and in developing methods for the solution of the governing equations. He is particularly interested in the formulation of theories for thin bodies, both solid and liquid. Recent work in the fluids area has concentrated on studying the effect of non-Newtonian behavior in fluids on piston ring lubrication and wear. To this end, models for thin films of different non-Newtonian fluids are being developed and entrance and exit effects are being studied.

Professor Johnson teaches courses in continuum mechanics and related areas in the Department of Engineering Mechanics and courses in linear algebra and differential equations in the Department of Mathematics. He is a member of the executive committee of the UW Rheology Research Center.



**Arthur S. Lodge**

Emeritus Professor; BA 1945, PhD 1948, University of Oxford.

Professor Lodge became an Emeritus Professor in the summer, 1991. His research interests include the development of molecular and continuum mechanical theories for polymeric liquids, together with the development of instruments for measuring their rheological properties in shear flow. His recent work has involved the development of a new instrument, called a Stressmeter, which has been used by Shell UK and General Motors to measure elastic and viscous properties of multigrade oils at high shear rates and at temperatures approaching those of journal bearing operation; preliminary results favor the possibility of developing low friction oils.

Professor Lodge has also worked in theoretical nuclear physics with the National Research Council of Canada (1945) and has been a member of the International Union of Pure and Applied Chemistry Macromolecular Division Working Party on Structure and Properties of Commercial Polymers (1973-1984). He is a member of the Society of Rheology (U.S.), the British Society of Rheology, and the National Academy of Engineering.



**Jay K. Martin**

Associate Professor; BA 1975, Indiana University; MS 1980, University of Tennessee; PhD 1984, University of Michigan.

Professor Martin's research interests include combustion, internal combustion engines, and diagnostic development for measurements in complex flow and combustion environments. His most recent studies involve KIVA predictions and particle image velocimetry in motored two-stroke engines.

Professor Martin has participated in research efforts at the Oak Ridge National Laboratory, the Combustion Research Facility of Sandia National Labs, and at the General Motors Research Laboratories. In addition, he has just returned from a collaboration effort with researchers at Hokkaido University and Nissan's Central Engineering Labs during a year long sabbatical in Japan.

**Phillip S. Myers**

Emeritus Professor; BA 1942, Kansas State University; MS 1944, PhD 1947, UW-Madison.

Thermodynamics, heat transfer, and fluid flow phenomena occurring in internal combustion engines are among Professor Myers' interests, as well as pollutants from engines, air pollution, and alternate fuels. His graduate students at UW-Madison have developed sophisticated diagnostic instruments to cope with these rapid time-varying phenomena, including measurements of instantaneous gas temperature, gas pressure, gas velocity, and rates of heat transfer in engine cylinders. The resulting data have been used to construct mathematical models of the thermodynamic behavior of engines.

Professor Myers is a member of the National Academy of Engineering, a past-president (1969) of the Society of Automotive Engineers, and a fellow member of both the American Society of Mechanical Engineers and the Society of Automotive Engineers. His numerous awards include the Pi Tau Sigma and the Benjamin Smith Reynolds teaching awards.



**Rolf D. Reitz**

Associate Professor; MS, University of Cape Town; MS 1974, SUNY-Stony Brook; PhD 1978, Princeton University.

Rolf Reitz joined the faculty as an associate professor in the fall of 1989. Previously, Professor Reitz worked as a research scientist at the Courant Institute of Mathematical Sciences in New York, as research staff at Princeton, and most recently, as a staff research engineer in the Fluid Mechanics Department at the General Motors Research Laboratories.

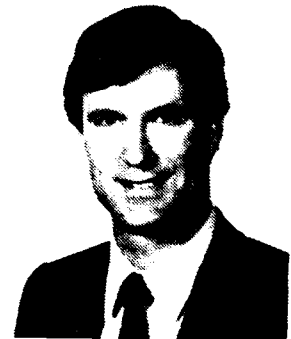
Professor Reitz is interested in developing models for internal combustion engines and sprays. Currently, he is testing a detailed computer model for predicting diesel engine combustion and is performing experiments to gather engine data to test the model predictions. He is also studying the mechanisms of air assisted-atomization of liquids using an experimental high pressure spray facility. Air-assisted atomization is currently being considered as an alternative fuel injection process for future low emission engines.

**Christopher J. Rutland**

Assistant Professor; BA 1975, Austin College; BS 1981, University of Texas-Austin; MS 1986, PhD 1989, Stanford University.

Chris Rutland joined the faculty as an assistant professor in the fall of 1989. His research interests include basic and applied research in turbulence and turbulent reacting flows, numerical simulation and modeling of internal combustion engines, the development of turbulence closure models using full simulation data, and spectral and finite difference methods in computational fluid dynamics. He is also performing basic research in both turbulence-flame interactions using full simulations and in the modeling of reacting flows using large eddy simulations and Reynolds-averaged models.

Professor Rutland is a member of Tau Beta Pi and Sigma Xi.



## 6.0 STAFF AND VISITORS

The guidance of graduate students by their major professors is the primary mode of operation at the ERC. Typically graduate students have been assisted by undergraduate helpers (paid hourly). This work experience has been a valuable part of the educational process for more than fifty students. In addition to such "hands-on" help, the students need training in the use of instruments, procedures, and shop practices. This has been provided by four staff engineers, David Bidner, Peter Jensen, Joe Krueger and Boleslav Sehmman.

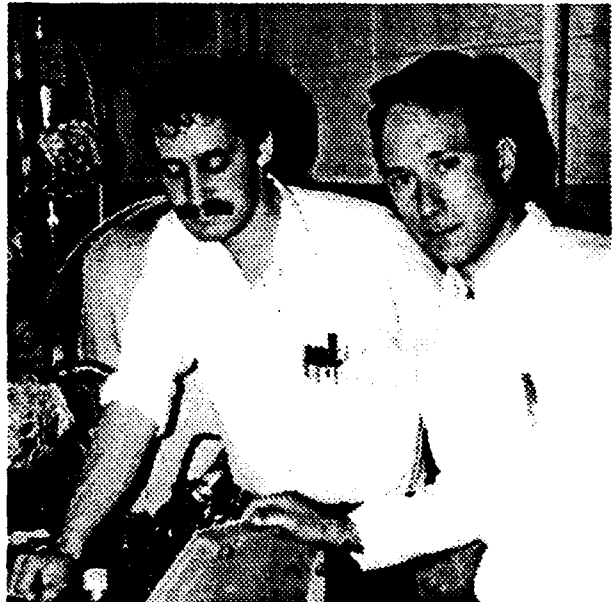
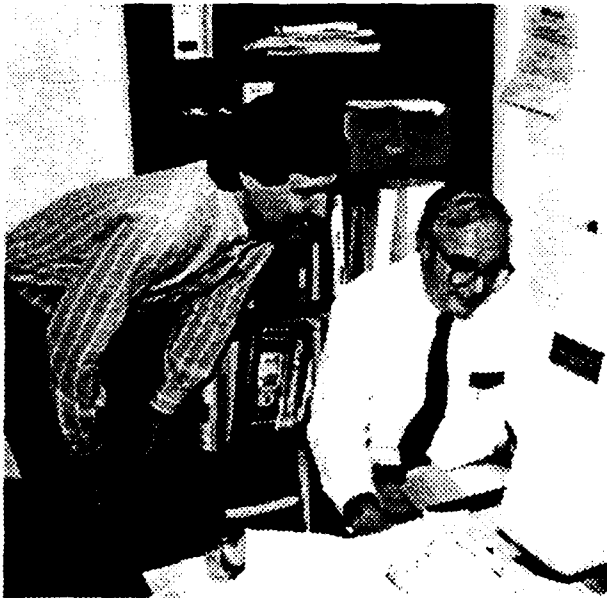
Administration of computer systems has been carried out by a project assistant hired from the computer science area. Over the period of the contract Victor Foo and then Jim Yu served in this capacity. General administration and office duties were carried out by Sally Radecke, Sharon Russ, and JoAnn Spring. Accounting, production of publications and other administrative functions were handled by hiring an MBA student as a project assistant. Serving in this capacity were Kevin Joachim, Steve Lingemann, Debra Hubbard and Glenn Walberg. Specific editing duties were handled by students who typically had previous editing or writing experience. Publications produced in this way were numerous ERC Newsletters and four Center brochures. The Newsletters served to tell about recent research and events while the brochures gave an overall picture of the center and its research. Students serving as editors were Gerald Hill, Steve Klabunde, Mark Plesac, Mark Voss and Michael Welk. Glenn Walberg has most recently served as an editor in addition to his accounting duties.

Visiting researchers at the ERC have fallen into two categories, those sent to the ERC by their own employer for a period of research and those who were hired by the ERC as limited term (post-doctoral) researchers. Those in the first category are: S. Ashikari (Komatsu), M. Fukuda (Tsuyama College), A. Fusco (CNR, Naples), Professor H. Hassan (AMTA, Egypt), M. Hayashida (Kubota), Professor M. Ishida (Nagasaki University), Professor S. Kim (KAIST, Korea), Professor E. El-Shenowy (Tanta University, Egypt), G. Valentino (CNR, Naples), S. Yamada (Kubota), M. Yukioka (Isuzu). In the second category are Professor R. Fiedler (U.W.-Platteville), J. Hodges (after completing his post-doc position at IFP), L. Lian (PhD, Clarkson University), Y. Zhu (PhD, Dalian University and Post-doc at Eindhiven University), and J. Zurlo (PhD, Carnegie-Mellon University, and post-doc at NIST). Dr. K. Huh worked under TACOM funding after completing a post-doc at Imperial College, London. A special visitor was William L. Brown, Jr., of Caterpillar, who spent a year at the ERC in 1986-87 while Professor Foster was on leave at Sandia, Livermore and then returned for a second year long visit in 1991-92, while Professor Martin was on leave in Japan. In both cases Caterpillar had approved the leave and provided partial funding.

Five student trainees were funded by the center under the aegis of IAESTE. Each worked for a period of about a year on a research project. The student trainees were Birch (Denmark), Paulsen (Norway), Matias (German), Sheldon (England) and Smaling (Holland). E. Quiros also received training in the ERC which served as partial fulfillment of his doctoral requirements at his home institution in the Philippines. His research with Professor Myers was partially funded by TACOM.

## 7.0 DISCUSSION OF RESEARCH

The following seven subsections each briefly describe an area of research with emphasis on the most important results. Because of the extensive nature of the work no attempt has been made to duplicate the results described in the many ERC publications listed among the references given at the end of this section.



## 7.1 Engine Modeling

### Introduction

The goal of this research is to apply advanced modeling techniques to study the influence of in-cylinder processes on engine efficiency and pollutant emissions. The research includes the development of a comprehensive analytical model of diesel combustion which will be available as a design tool for use by the industry.

The model can be used to evaluate combustion systems and to propose new systems, thus reducing engine development times and costs, since engine optimization using cut-and-try is time consuming and expensive. With a validated model it would be possible, for example, to predict the effects on engine operation of combustion chamber geometry changes (e.g., deep versus shallow piston bowls, reentrant versus straight wall bowls, and the influence of crevices), the effects of different inlet flow conditions (e.g., the influence of intake manifold design on engine flow swirl, tumble, and turbulence), and the effects of different fuel injection strategies (e.g., the influence of spray orientation, cone angle, number of nozzle holes, injection duration and velocity history). These parameters all influence diesel engine combustion efficiency, emissions, heat rejection and noise (rate of pressure rise) in complex, interacting and poorly understood ways.

The engine modeling effort has been based on the KIVA-2 (Amsden 1989) and KIVA-3 (Amsden 1992) codes. The codes solve the conservation equations for the transient dynamics of vaporizing fuel sprays interacting with flowing multi-component gases which are undergoing mixing, ignition, chemical reactions and heat transfer. Many of these processes occur on time and length scales that are too short to be resolved in practical computations. Thus, submodels are needed to describe the processes. The submodels require detailed validations before they can be used for engine performance predictions (Reitz, 1991a). For example, for modeling sprays, submodels are needed to describe drop drag, drop turbulence interaction, vaporization, atomization, breakup and coalescence, and spray/wall interaction. These spray processes influence the combustion and pollutant formation processes profoundly through their effect on the fuel-air distribution in the engine. Individual submodels are usually developed starting from simplified theoretical models or experiments that isolate a particular process. However, the accuracy of predictions made using combinations of submodels to describe the performance of the overall engine must be assessed by comparisons with detailed and informative engine experiments.

An important goal of the present research is to use the engine comparisons to identify areas where submodels need improvement, and to develop improved models where necessary. One important additional benefit of the application of these systems of submodels to engine computations is that the model can help identify key processes that would be difficult to identify in any other way, since direct measurement is typically not feasible. Progress is outlined below. Reviews of current attempts to assess the capabilities of models for diesel engine combustion simulations are also given in Reitz et al. (1990, 1991ab, 1992ab).

### Model Development

The computer model used for describing turbulent, multi-phase, 3-D engine flows with combustion is based on the KIVA code. A summary of achievements in assessing and improving the predictive performance of the code is presented below. The code has been modified to include state-of-the-art submodels for diesel engine flow and combustion as listed in Table 7.1.1 (Reitz, 1992b). The accuracy of the predictions is being assessed by comparisons with available measurements. To date, comparisons have been made with measured engine cylinder pressure and heat flux data for homogeneous charge, spark-ignited and compression-ignited engines, and also comparisons of cylinder pressure data for diesel engines. The model results are in good agreement with the experiments. Details of these activities are discussed individually below.

Wall impingement - The standard KIVA code does not contain a spray/wall interaction model and the model of Naber, 1988a has been included in KIVA. The performance of this model was also tested by Naber (1988b) under simulated diesel pressures and densities at ambient temperature in a bomb study. The study found that the spray rebound was under-estimated by the model. A simple correction was suggested in which drops were given a rebound velocity that was a function of the drop impingement velocity, and the drop sizes were also reduced to account for drop breakup during impingement. This model has been refined further to account for rebounding and sliding drops by Gonzalez (1991a). In this case, upon impact, drops rebound from the surface with an angle of rebound that is determined by curve-fitting experimental data on single drops obtained by Wachters and Westerling (1966).

	Original KIVA	Updated submodels
Wall impingement	none	rebound-slide model
Blow-by	none	Namazian model
Wall heat transfer	law-of-the-wall	compressible, unsteady
Spray atomization & drop drag	Taylor Analogy Breakup	surface-wave-growth & distorting drops
Spray vaporization	single component	multicomponent
Ignition	none	Shell model
Combustion	Arrhenius	laminar-turbulent char time
Intake flow	assumed initial flow	compute intake flow
NO <sub>x</sub>	Zeldo'vich	-
Unburned HC	Arrhenius	laminar-turbulent char time
Soot	none	KIVA-coal
Radiation	none	Rayleigh-limit, band model

Table 7.1.1 Status of KIVA Submodels

Drop rebound after impingement was found to influence computations of diesel engine cold-starting by Gonzalez (1991a). Under these conditions drop impingement velocities (or Weber numbers) are low and the model indicates that drop rebound is the

dominant mode. The implication of this finding on diesel engine cold-starting is discussed further in the next section.

Blow-by model - Flow through the piston-cylinder-ring crevice has been modeled using the phenomenological crevice-flow model of Namazian (1982). This model was also used successfully by Reitz (1989) to explain experimental trends of exhaust hydrocarbon emissions from spark-ignition engines. This crevice flow model has been coupled with KIVA in the present effort (Reitz, 1991b) to supply boundary conditions on the piston top in the crevice region. The effect of crevice flow was found by Reitz (1991b) to reduce significantly the effective in-cylinder charge mass during the main stages of combustion.

The crevice flow model makes the assumptions of uniform pressure, constant wall temperature and laminar flow within the ring pack. The flow is calculated by considering the continuity equations, supplemented by phenomenological expressions for the flow rates through each region of the ring pack. The motion of the rings within the grooves is accounted for by considering friction, inertia, pressure and oil resistance forces. Additional details about the model are given by Namazian (1982) and Richardson (1992).

Gonzalez (1991a) included the blowby model in computations of diesel engine cold-starting. The results showed that high blowby gas flow influences diesel cold-starting profoundly. This is also discussed further in the next section.

Wall heat transfer - An understanding of wall heat transfer mechanisms in engines is important because heat transfer influences engine efficiency, exhaust emissions and component thermal stresses. Heat transfer also influences engine operation limits such as lean combustion, knock and start-ability limits. Current multidimensional codes employ 'wall function' models to describe heat transfer. This is necessary because wall boundary layers are thin relative to practical computational grid sizes. The wall functions are based on steady-state, incompressible, turbulent-flow correlations such as those developed for turbulent pipe flow. However, use of these correlations is questionable in engine applications where the heat transfer process is inherently unsteady. Indeed, Borman (1987) has observed that instantaneous heat transfer predictions can assume unreasonable values if unsteadiness is not accounted for. Similarly, the validity of the incompressible-flow assumption is not assured in low Mach Number engine flows which have significant density variations due to piston compression and combustion.

The influence of unsteadiness and compressibility on engine heat transfer has been studied by Yang (1989, 1990) and Huh (1990). The approach adopted in those studies was to consider the one-dimensional, unsteady energy equation. This methodology has been included in KIVA by Reitz (1991b). To account for compressibility, a transformed distance is used instead of the physical distance from the wall in the turbulence, momentum and heat transfer boundary conditions. Unsteadiness is accounted for by using solutions to the one-dimensional energy equation solutions of Yang (1989). Reitz (1991b) found that the heat flux predictions from the modified KIVA are much improved, as can be seen in Fig. 7.1.1 which presents comparisons with the measurements of Alkidas (1980) for premixed-charge SI engine combustion.

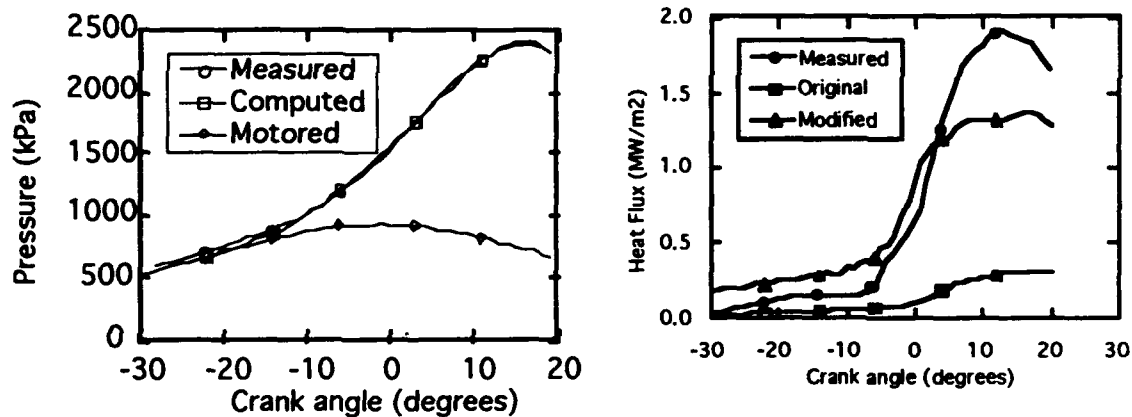


Figure 7.1.1 Comparison between measured and predicted cylinder pressure (left) and wall heat flux (right) for premixed-charge SI engine combustion using heat transfer model with (modified case) and without (original) the effect of compressibility and unsteadiness. Engine speed 1500 rev/min.

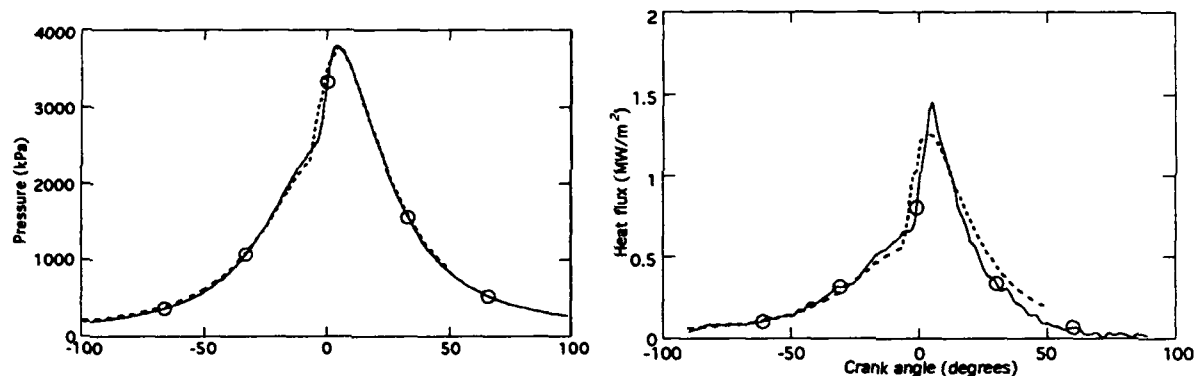


Figure 7.1.2 Comparison between computed (dashed line) and measured (solid line) cylinder pressures (left) and wall heat flux (right) for compression ignited, homogeneous charge engine combustion (engine speed 1200 rev/min, compression ratio 10.5, swirl ratio 1.8, equivalence ratio 0.4).

Similar conclusions about the importance of compressibility and unsteadiness effects on wall heat transfer were found in studies of combustion in a homogeneous-charge, compression-ignited engine. Figure 7.1.2 shows comparisons between the predicted heat flux results of Kong (1992ab) and the measurements of Boggs (1992). It is seen that the modified heat transfer model performs extremely well.

Spray atomization and drop drag - In the spray atomization submodel, drop parcels are injected with sizes equal to the nozzle exit diameter following Reitz (1987), and the subsequent breakup of the parcels and the resulting drops is computed using a stability analysis for liquid jets. This model was adopted because, in principle, it removes the need to specify an assumed initial droplet size distribution at the nozzle.

Breakup due to Kelvin-Helmholtz instabilities, Rayleigh-Taylor instabilities and boundary layer stripping mechanisms have also been considered by Bower (1988).

These models are improvements over KIVA's standard Taylor Analogy Breakup (TAB) model of O'Rourke (1987). The atomization model has been improved further by extending the stability analysis to consider ambient gas compressibility and evaporation from the liquid jet by Lian (1992ab). The analysis shows that surface evaporation causes surface waves to break slower, and to produce larger droplets. The effect of compressibility is to destabilize the jet. Interestingly, Lian (1992b) has shown that the two effects appear to counteract one another under engine conditions.

KIVA's spray models have been evaluated using the experimentally measured trajectories and drop sizes of single drops injected into a high relative velocity gas flow of Liu (1992ab). It was found that the drop drag coefficient and the drop breakup time model constant had to be adjusted in order to match the measurements (Mather, 1992). Based on these findings, a new drop drag submodel has been proposed by Liu (1993) in which the drop drag coefficient changes dynamically with the flow conditions. The model accounts for the effects of drop distortion and oscillation due to the relative motion between the drop and the gas. The model has been applied to diesel sprays and the results show that the spray tip penetration is relatively insensitive to the drag coefficient. However, the drop size distribution is found to be influenced significantly by drop drag.

Spray vaporization - Predicted spray drop size and penetration lengths have been found to agree well with experimental measurements for non-evaporating sprays by Reitz (1987) and Gonzalez (1991c) using the surface-wave-growth atomization model. In addition, diesel spray predictions made under cold-starting conditions by Gonzalez (1991a) were found to be in qualitative agreement with engine experiments. However, for high-pressure, high-temperature sprays, significant discrepancies between computations and experiments have been observed by Gonzalez (1992). For example, computed vapor penetration results were found to under-estimate the measurements of Kamimoto (1987). Considerable effort has been spent on identifying the causes of this discrepancy and making corresponding modifications to the models.

The effects of several factors have been considered, including the influence of numerical and physical parameters. The study has revealed the importance of accurate predictions of the vapor concentration surrounding the dense vaporizing spray drops. It was found that condensation of the vapor must also be accounted for, since the vapor concentration surrounding the spray drops is high and the large drops are relatively cold. Vaporizing spray results were found to be especially sensitive to the numerical grid size near the exit of the nozzle where the gradients in the flow are the largest, and a sub-grid-scale correction procedure was proposed for use with coarse grids by Gonzalez (1992).

Ignition and Combustion Models - Ignition delay is an important parameter in the operation of a diesel engine since it influences hydrocarbon and NO<sub>x</sub> emissions. It is also critical to the cold-starting problem. During the delay period, the injected fuel undergoes complex physical and chemical processes such as atomization, evaporation, mixing and preliminary chemical reaction. Ignition takes place after the preparation and reaction of the fuel-air mixture leads to fast exothermic reaction. Approaches to

describe autoignition phenomena in diesel engines in multi-dimensional models have been reviewed by Kong (1993).

The kinetics chemistry submodel used for ignition and combustion modeling in KIVA considers a single step Arrhenius mechanism for the stoichiometric reaction of the fuel. The pre-exponential factor, activation energy and component rate constants used by Gonzalez (1991abc, 1992) were those given by Bergeron (1989) for the ignition of isolated drops in a heated environment. Kong (1992ab) combined this model with the laminar and turbulent characteristic time combustion model of Abraham (1985), that was used successfully in the spark-ignited engine study of Reitz (1991b) (see results in Fig. 7.1.1), and by Kuo (1989, 1992) for premixed-charge and fuel injected two-stroke engines. In this way the combustion model has been extended to allow predictions of ignition. The homogeneous-charge, compression-ignition engine experiments of Boggs (1990) were used for the study since the homogeneous charge engine offers a well characterized environment for the study of ignition processes.

The characteristic time for reaction in the combustion model of Kong (1992ab) is assumed to be the sum of the laminar (high temperature) chemistry time, the turbulence mixing time, and an ignition (low temperature) chemistry time which has the Arrhenius form. It was found to be possible to match all of Boggs' engine experiments reasonably well with one set of ignition model constants. Typical results showing comparisons between measured and predicted cylinder pressures are given in Fig. 7.1.2, and the level of agreement is seen to be good.

It should be noted that this good level of agreement was not possible if the turbulent mixing timescale was not included in the combustion model. This finding implies that thermal mixing phenomena control the rate of combustion, even in an engine that is characterized by the absence of a propagating flame. The significance of this finding and its relationship to diesel combustion is discussed further by Kong (1992ab), and Section 7.2.

A more accurate prediction of ignition phenomena has been achieved by implementing the multistep Shell kinetics model of Halstead (1977). The model was found to be capable of predicting successfully the autoignition of homogeneous mixtures in a rapid compression machine and diesel spray ignition in a Cummins NH diesel engine by Kong (1993). In Fig. 7.1.3 the measured engine cylinder pressure data of Yan (1988) is compared with predictions made using the standard Arrhenius and the multistep Shell ignition models. The post-ignition combustion was simulated using the single-step Arrhenius model in both cases. The single-step kinetics model is seen to work reasonably well. However, it was found necessary to use slightly different model constants for the Arrhenius model results in Fig. 7.1.3 than those recommended by Bergeron (1989) and used by Gonzalez (1991a) in the cold-starting study.

The multistep ignition model is more predictive. The computations in Fig. 7.1.3 used parameters derived from out-of-engine, low temperature chemistry data. The multistep model is seen to give excellent results prior to the main stage of combustion. The discrepancy between the predictions of both models and the measured results during the main stage of combustion suggests the need to consider other effects such as turbulent mixing on post-ignition combustion. Also, the discrepancy has been found to be influenced by numerical errors, and by the details of the fuel injection (Lian, 1992c). This activity is currently in progress.

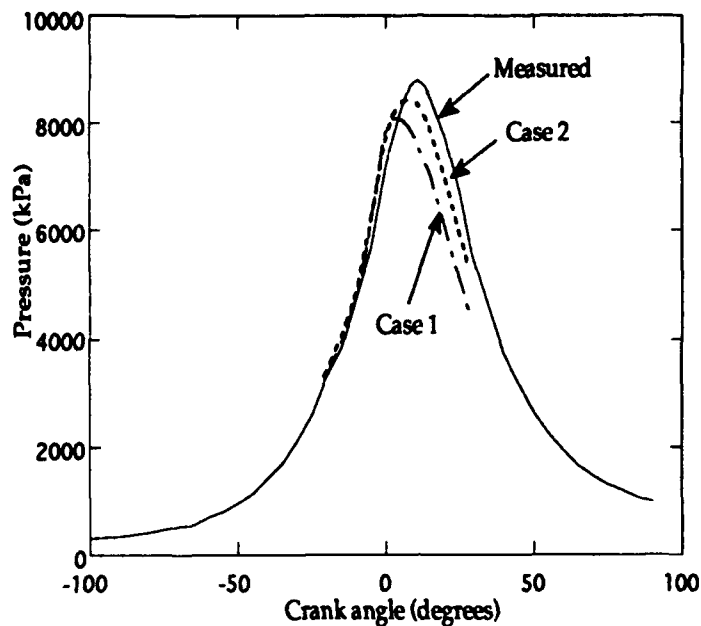


Figure 7.1.3 Predicted pressure histories obtained by incorporating the multistep Shell ignition model (Case 2) and the standard one-step Arrhenius kinetics model (Case 1).

**Intake flow** - A modification of KIVA-2 was presented by Epstein (1991) that allowed computations to be made in complex engine geometries by dividing the computational domain into separate blocks which exchange boundary condition information at their common interfaces. The scavenging flow in the cylinder, transfer pipes (ports), and exhaust pipe of a ported two-stroke engine with a moving piston was modeled in this way. Results were obtained for engine designs with different boost port angles and the calculated flow fields, and the resulting fuel distributions, were found to be markedly different with the different geometries.

Based on this work, diesel engine intake flow modeling is being conducted using a block structured grid version of KIVA, KIVA-3 (Amsden, 1992). An example calculation is given in Fig. 7.1.4 which shows pathlines of fluid particles entering through the two-valve intake manifold in a steady state computation (fixed valve openings). A constant pressure boundary condition was used at the top of the intake port, and the flow entering the cylinder is deflected by the valve head, establishing a large scale tumbling and swirl flow pattern. The grid generation is done with the Gridgen code of Steinbrenner (1990). As described by Pieper (1992), the intake flow predictions also agree well with measured mass flow rates through the valves.

Various approaches have been evaluated for implementing moving valves into the computation. The most promising method involves the "snapper" algorithm which is used to move the piston in KIVA-3 (Amsden, 1992). This algorithm maintains grid point connectivity by snapping grid points between neighboring cells as the grid moves. The snap occurs when the grid has moved a specified percentage of a cell distance. A method of extending the snapper algorithm to consider a moving valve has been

developed and work is in progress on testing the accuracy of multi-valve intake flow predictions using this technique (Pieper, 1992, 1993, Reitz, 1992a).

Work in Progress - Work is in progress on implementing submodels for NO<sub>x</sub>, unburned hydrocarbon and soot emissions, and drop evaporation under critical conditions. The characteristic time combustion model specifies the rate of conversion from reactants to products using a characteristic time which is controlled by the longer of the local turbulent mixing or laminar kinetics times. The model is formulated such that correct thermodynamic equilibrium is recovered in the burned gas (Reitz, 1991b). The correct burned-gas temperature is needed for accurate NO<sub>x</sub> predictions using the Zeldo'vich model (Heywood, 1976), which has been included in KIVA. The combustion model automatically predicts unburned hydrocarbon (HC) in regions of low gas temperature or high equivalence ratio where the characteristic chemistry time is large and the conversion of fuel to products is arrested.

The soot model based on the model of Gentry (1987) has been implemented in KIVA. This model was developed for coal slurry applications and is being tested for diesel combustion. The model also includes a black body soot radiation model. In the model the soot formation process starts by considering the formation of radical nuclei which grow to become soot particles by surface growth and agglomeration mechanisms following Surovkin (1976). The soot particles themselves are subject to oxidation processes following the Nagle and Strickland-Constable (1962) mechanism.

The fuel vaporization model in KIVA is also being extended to allow consideration of multicomponent fuels. The model is based on the isolated drop model of Jin (1985). Initial studies of drop evaporation close to critical point have been conducted by Curtis (1992).

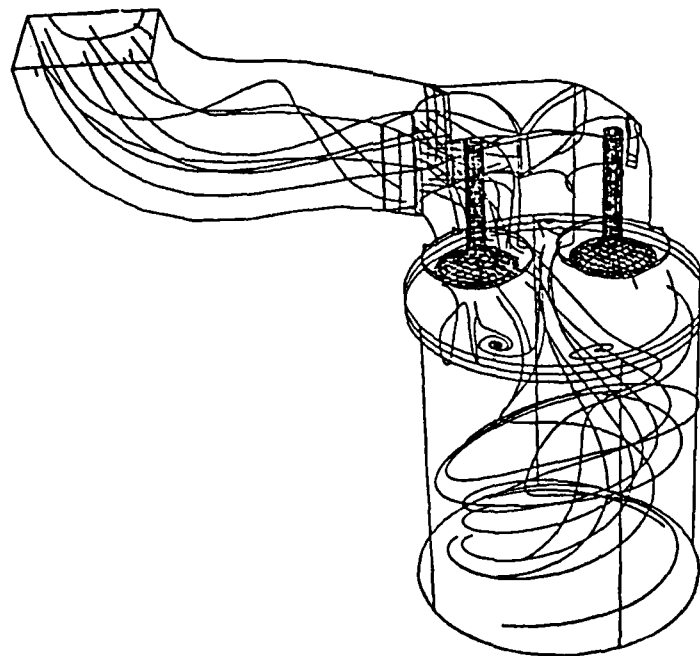


Figure 7.1.4 Intake flow computation using the unstructured grid version of KIVA-3 for stationary valves.

### Validation

As mentioned above, vaporizing spray and combustion computations have been found to be sensitive to numerical grid resolution. This is discussed in detail by Lian (1992c), Kikuta (1992) and Gonzalez (1992). To test the effect of grid resolution on engine combustion predictions, calculations were made using successively finer grids. The results show that the discrepancy between measured and predicted cylinder pressures is reduced significantly with a fine grid, since the spray penetration is predicted more accurately with fine grid resolution.

The magnitude of numerical errors has been estimated by Gonzalez (1992) who found that the results are most sensitive to the azimuthal mesh spacing. This is to be expected since the largest gradients in the flow are across the spray cross-section, as also pointed out by Kikuta (1992). Table 7.1.2 presents a summary of computational results of combustion in a Cummins NH engine using meshes with azimuthal mesh spacings of 7.5, 2.25, 1.8 and 1 degrees (i.e., equal spacing in the azimuthal direction). It can be seen that finer grid resolution gives higher peak cylinder pressures. The convergence is quite slow, and very fine mesh resolution is needed to get accurate results. The cpu time in Table 7.1.2 is the time spent during the combustion period from 18 crank angle degrees before top dead center to 8 degrees after top dead center. The results show that to maintain reasonable accuracy while avoiding excessive computer time, an azimuthal grid size of less than about 2° is a good compromise.

Table 7.1.2 Error estimates for peak cylinder pressure as a function of azimuthal mesh spacing

azimuthal mesh spacing (degrees)	max. pressure (kPa)	error (%)	cpu time (hour)
0°	7233 (est.)	-	-
1°	6875	4.95	14.5
1.8°	6589	8.89	6.5
2.25°	6249	13.6	3.5
7.5°	5619	22.4	0.3

## Impact of Research

Several areas important to the Army that have been addressed by this research:

- A new understanding of diesel engine cold-starting phenomena has been gained
- Improved thermal analysis procedures have been developed for predicting engine heat transfer
- Improved engine flow and combustion analysis tools have been developed
- The tools have been used to gain an improved understanding of factors that influence fuel preparation in engines.

These issues are discussed further below.

Engine performance will continue to be improved, incrementally, through the use of new technologies such as ultra-high injection pressure fuel sprays (this has been used effectively in diesel engines to reduce soot and NO<sub>x</sub> emission levels) and advanced materials (the use of ceramics makes it possible to influence engine heat transfer losses and to alter the details of the thermodynamic cycle through the use of lighter valves). However, comprehensive computer models are now available to help explore new engine concepts, and to speed up the traditional pace of change in the automotive and engine manufacturing industries.

The internal combustion engine represents one of the more challenging fluid mechanics problems because the flow is compressible, low Mach number, turbulent, unsteady, cyclic, and non-stationary, both spatially and temporally. The combustion characteristics are greatly influenced by the details of the fuel preparation process and the distribution of fuel in the engine which is, in turn, controlled by the in-cylinder fluid mechanics. In the diesel engine, fuel injection introduces the additional complexity of describing the physics of dense, vaporizing two-phase flows.

In the course of the present research multidimensional models have been applied to predict combustion in spark-ignited and compression ignited, premixed-charge and fuel-injected, SI, diesel and two-stroke engines. Results have been obtained which demonstrate the usefulness of the models for engine design and optimization. The computations reveal detailed information and understanding about processes that occur within the engine that can be exploited by designers of improved engines.

For example, the starting of diesel engines in low temperature environments represents a difficulty which has mostly been studied in terms of description of the phenomena and development of devices and techniques to solve the problem. Cold starting can be characterized as a situation where either the combustion event in the cylinder is present in one cycle and absent in subsequent cycles (in the so called borderline condition of starting) or not present at all in the limit case. The study of Gonzalez (1991a) used computational modeling to obtain an understanding of the cold

starting process, and to identify practical areas for possible improvement of the cold starting characteristics of direct injection diesel engines.

In that study, spray/wall interaction details were found to influence diesel engine cold-starting. Drop rebound that occurs at low impingement velocities was found to provide a mechanism for fuel (vapor) to penetrate back into the central regions of the chamber where the gas temperature would be high enough for ignition to occur. Without drop rebound the fuel was predicted to accumulate near the walls where the gas temperature is too low for ignition. It is noteworthy that significant quantities of liquid fuel were predicted to enter into the squish region between the piston and the head. This provides a mechanism by which fuel could reach the ring area and be carried over from one engine cycle to the next. Analyses of engine data under skip-firing, cold-starting conditions show that in the firing cycles, the heat release can be higher than that calculated from the energy input of the fuel injected that cycle (Henein, 1990). Thus, the modeling results provide a plausible explanation for the carry-over phenomenon that could be considered in the design of the piston bowl geometry.

The computations of cold-starting of Gonzalez (1991a) also included a blowby model. The results showed that high blowby gas flow cancels the effects of the squish flow, reduces the peak temperature of the cycle, and removes fuel from the combustion chamber. In addition, as described above, the fuel reaches the crevice region in low vaporizing environments, contributing to the amount of fuel in the chamber for successive cycles. A sensitivity study of the results also showed that blowby reductions produce improvements of start-ability only for borderline conditions.

Figure 7.1.5 shows the predictions of engine cylinder pressure with initial air temperatures of 298 K (ambient) and 241 K (cold-start) versus crank angle from intake valve closing until after top dead center. For the initial temperature of 298 K, ignition occurs with a short ignition delay and high rate of pressure rise as expected. For the low temperature case of 241 K, one data set without fuel input is shown as baseline. With fuel, there is a small pressure rise after top dead center, but the amount of energy released is not enough to continue increasing the pressure in the combustion chamber during the expansion stroke. This border-line cold-starting behavior, showing insufficient energy release in the combustion chamber to be called a normal combustion event, has been documented in the literature by several authors, and gives additional confidence to the model predictions.

An additional factor that influences cold-starting in diesel engines significantly is wall heat transfer. The accuracy of wall heat transfer models has been assessed for both compression ignition and SI engines by Huh (1991), Chang (1991), Kong (1992ab) and Reitz (1991b). The research demonstrates that accurate heat transfer predictions are possible, and that it is important to include the effects of compressibility and unsteadiness in multidimensional heat transfer models for engine thermal analysis.

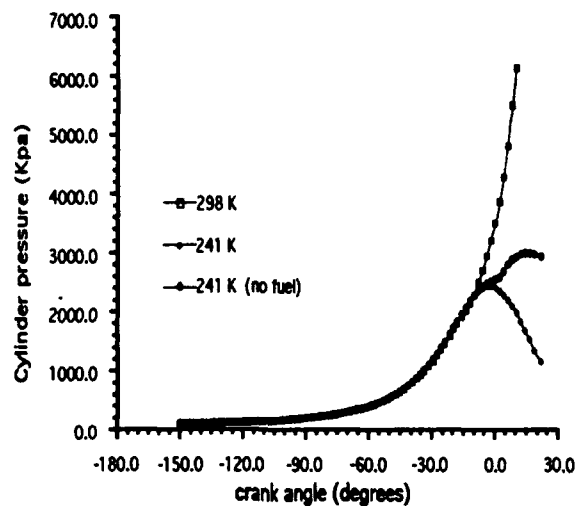


Figure 7.1.5 Calculated cylinder pressures with and without ignition at 100 rpm and initial air temperatures of 241 K and 298 K.

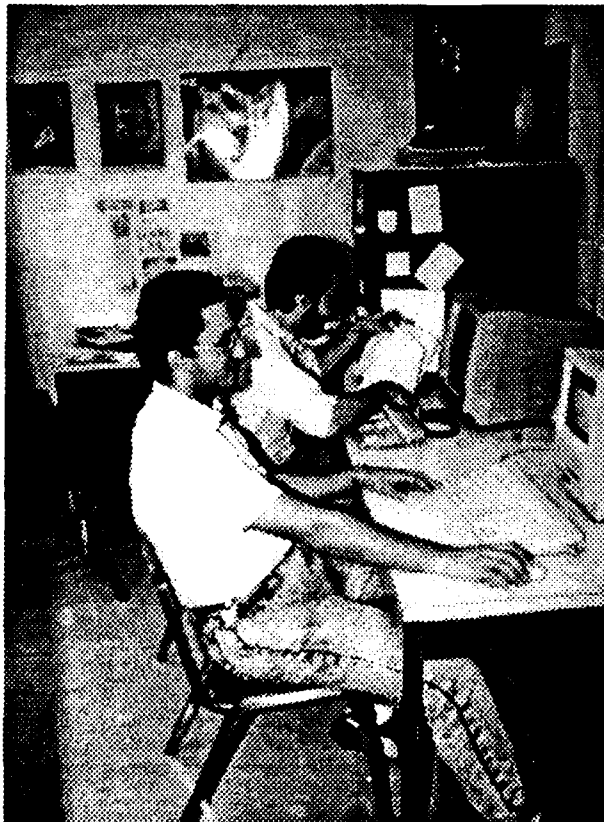
A similar ignition model to that used in the diesel engine cold-starting study of Gonzalez (1991a) was also used by Kong (1992ab) for modeling homogeneous-charge, compression-ignition engine combustion. It was found that it was possible to match the engine experiments of Boggs (1990) reasonably well with one set of combustion model constants. Combustion was found to be controlled by the chemical kinetic rates up to the time of ignition. After ignition, comparisons between the measured cylinder pressure data and predicted pressures showed that good levels of agreement were *not* possible unless the turbulent mixing time scale was included in the combustion model. This important result implies that turbulent mixing effects, control the rate of combustion after ignition, even in an engine that is characterized by homogeneous mixtures and the absence of a propagating flame. This implies that the effect of turbulent mixing on combustion must be considered in all engines, and combustion models that account for turbulence are being developed at present.

As noted above, the distribution of fuel in the combustion chamber is important for combustion. The fuel distribution is also influenced by the air motions in the cylinder. Epstein (1991) studied the effect of boost port angle on scavenging and fuel/air mixing in a two-stroke engine. The results indicated that the port intake flow velocity profiles vary with time, and are not uniform across the ports. This indicates that the uniform inlet flow assumption commonly used in computations may not be sufficiently accurate. Indeed, the sensitivity study of Kuo (1992) shows that the combustion characteristics of two-stroke engines are extremely sensitive to the details of the intake flow.

Epstein (1991) found that the boost port flow at high boost angles breaks up the toroidal vortices in the cylinder that are generated by the side ports and puts more fuel into the cylinder head dome, increasing the trapping efficiency. This type of information is useful for engine design, since it could be used to provides guidelines for

the optimal placement of a spark plug in that engine, for example. These results also demonstrate that multi-dimensional models can be a useful design tool for assessing the influence of engine design parameters on engine flow fields.

Other issues of relating to the use of comprehensive models to help engine design, such as in the design of piston ring packs, and the inclusion of the effects of liner vibration are given in other areas of this report.



## 7.2 Engine Combustion, Emissions and Fuels

### INTRODUCTION

There are multiple objectives of the combustion, emissions and fuels work carried out under the Engine Research Center funding. The ability to achieve high power density engines will be enhanced by further understanding of the fundamental aspects of combustion. Also as the commercial industry modifies their engines to meet more stringent emission standards problems may arise in using those engine for the army's tactical operation. For example if exhaust gas recirculation is required the oil change interval may be shortened which would create additional logistical problems; it is also possible the cold start characteristics could be adversely affected by emission driven engine design changes. Understanding of the emission problem truly represents a dual use mission for Army research money.

A concurrent objective to the combustion and emissions research is to provide data that will be used in comparisons with the ERC modeling effort. Doing both the modeling and experimentation in the same laboratory is a very efficient mode of operation. Regular interaction between the researchers involved guarantees that the necessary parameters are recorded and the pertinent data taken. The experiments and models evolve together, under the same roof. To meet these ends basic combustion studies were undertaken focusing on the compression ignition chemistry, turbulent diffusion flames in heterogeneous systems, soot chemistry, fuel spray cylinder charge interactions (also described in the section on fundamentals of sprays) and the influence of low heat rejection (LHR) systems on combustion.

### EXPERIMENTAL FACILITIES

The facilities at the Engine Research Center are well suited for the necessary fundamental studies. The ERC has a total of nine single cylinder engine test facilities. Of these nine, four have been specially designated for diesel combustion research. In each facility care was taken to preserve or reproduce as closely as possible current engine designs and operation. This is evident by the engine set ups:

A Cummins NH single cylinder engine with a mini-dilution tunnel in the exhaust system has been one of the primary engines used in diesel combustion studies at the ERC. Modifications have been made in which an exhaust valve has been replaced with an instrumentation port to facilitate two color optical pyrometry, soot particle size and number density measurements via scattering and extinction and thermophoretic deposition rate measurements. We also ran experiments in which the exhaust system was modified to facilitate a laser sheet extinction and LDV measurement which led to cycle resolved soot volume and mass flux assessments.

During the course of this research an old TACOM/LABECO engine was replaced with a single cylinder Caterpillar Lubrication Test Engine with a

prototype high pressure variable rate shape injection system. It is equipped with a full dilution tunnel. This engine has been modified to accommodate a window/prism access system. Through this access experiments were run in which a large quantity of energy was deposited into the flow via a Nd:Yag laser pulse. After the energy was deposited the local gas temperature was determined by measuring the speed of the shock wave propagating radially away from the point of energy deposition. By using this same deposition scheme but observing the rate at which the high temperature region diffused outward measurements of the turbulent diffusivity were made. On this same engine extensive data on the influence of injection rate shape on soot and NO<sub>x</sub> emissions is in progress.

The least current engine at the ERC on which diesel combustion studies were performed is a Detroit Diesel 53 engine in which two of the three cylinders have been deactivated, leaving only one operational. This engine has three injection systems, one in the intake manifold for fumigation of the fuel, one at the cylinder inlet port for a more stratified injection and an electronic unit injector in the cylinder which is capable of pilot injection. In addition optical access to the combustion chamber is obtained using fiber optics bundles. Experiments are being done in which UV laser light is introduced into the combustion chamber and the resulting predissociative induced laser fluorescence is then imaged outside the engine using a coherent fiber optic bundle. Also, experiments to understand the pre-ignition chemistry are currently in progress on this engine.

A TACOM/LABECO single cylinder engine is the fourth single cylinder diesel engine on which fundamental experiments were performed. Although this is an old engine, it was modified with a wide, shallow bowl piston, a high pressure Bosch injector and quiescent in-cylinder air motion to give it a geometry and operation typical of a more modern engine. Another important aspect of this particular set-up is the special cylinder head that is installed on the engine. We have a large access port which is used to hold a small post-combustion augmented mixing chamber or a total cylinder sampling system. Both offer unique opportunities for fundamental studies in emissions. This engine also has a mini-dilution tunnel as part of its exhaust system so particulate mass and SOF can be determined. This engine has been used extensively in studies of fuel compositional and distillation curve shape effects.

In addition to the engine facilities a number of off-engine experimental set-ups have been used to isolate specific combustion phenomena for closer examination. Experiments were conducted on jet mixing and soot formation in a pressurized flow tube and in a jet stirred combustor (JSC). A special engine fed combustion bomb was constructed to more closely observe early spray and ignition phenomena. A shock tube was constructed in which the reflected shock region reproduces the diesel engine

environment for up to three milliseconds. [ $T < 4000$  K,  $P < 14,500$  KPa have been attained so far]. Initial experiments in the shock tube attempted to assess if oil film vaporization could be a significant source of hydrocarbon emissions the oil derived SOF.

Experiments done on a modified CFR engine to investigate heat transfer [see Section 7.3] also supplied fundamental data for combustion modeling. In this work well mixed charges of air and fuel were auto-ignited during compression without using a spark plug. The data recorded has been used for comparison with our ignition modeling efforts. Similarly, a see-through engine was used in a spark ignited mode of operation as we developed an air fuel ratio measurement technique using Rayleigh scattering. Both of these projects are peripheral to diesel combustion and emissions but have improved the understanding of combustion or supplied fundamental data for comparison to models [see Section 7.1].

#### DIAGNOSTICS DEVELOPED

Maintaining realistic engines in the experimental work has often required the development of new diagnostic systems to make the desired measurements. To make two color optical pyrometry measurements in an engine required a special design of the two color probe. Yan and Borman (1988) designed a probe in which a sapphire rod, mounted like a fin in a recessed cavity acted as a window into the engine. After the radiant emission passed through the window it entered a fiber optic bundle which routed it from the engine to the wave length separation system. The entrance to the cavity from the engine was an orifice. The combination of the fin heating of the rod (window) and the phased flow of the combustion chamber gases into and out of the cavity through the orifice kept the window clean. (A figure showing the schematic of the two color probe and a description of the experimental results are given below in the In-Cylinder Particulates Studies section.) This basic design enabled acquisition of data over a wide range of engine operating conditions. This design strategy also served as the basis of the miniaturized radiation probes which Mohammad and Borman (1991) used to measure soot and flame temperature along three different directions. The experience with this instrument led to additional diagnostics. Modifying the existing probe with the addition of a fiber optic to focus a laser into the chamber in front of the window allowed measurement of soot size, number density, temperature and volume fraction measurements via scattering and extinction and via scattering and radiant emission (Tree, 1992).

A probe was designed by Suhre and Foster (1992) in which a clear sapphire rod mounted flush with the head surface was surrounded by cooling passages. Measurements of the rate of obscuration of the window at different temperatures were then interpreted as the deposition rates of soot on the wall. The soot wall deposition rates were measured as a function of window temperature.

Other diagnostics that were developed were laser based. Ashikari and Foster (1992) developed a laser sheet extinction-LDV measurement system to measure the cycle resolved soot mass and volume flux from a single cylinder engine. By modeling the exiting exhaust flow at the cylinder head as a gaseous jet with an assumed velocity and concentration profiles it was possible to calculate the soot mass flux from the

cylinder from the total extinction of the laser sheet and a centerline velocity measurement.

Leschiutta, Eng and Martin (1990) developed a laser range finder system [see Fig 7.2.1] to accurately measure the dynamic piston position while the engine was running. Such information is critical to the researcher to verify the accuracy of their shaft encoder position. Once data is obtained and heat release and IMEP calculation are performed even an error of one degree results in IMEP errors of eight percent for direct injection diesels (24% for indirect injection diesels). The laser ranger-finder system was capable of measuring both piston position and piston tilt. As a result of this system the dynamics of piston motion are now more accurately known. [See also pp 142-144]

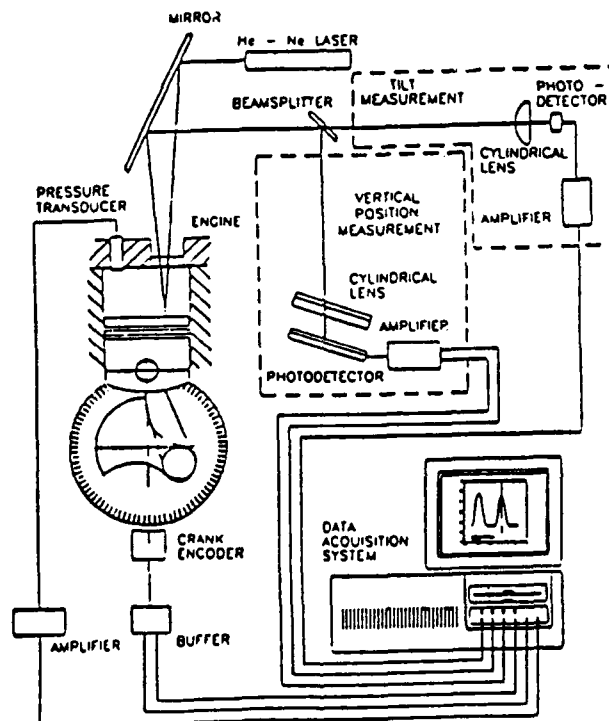


Fig. 7.2.1. Schematic of laser range finding system.

Giangregorio and Reitz (1993) developed two measurement systems using a Nd:Yag laser. The laser was pulsed to deposit energy into a designated region in the flow within 10 nano-seconds. They determined that by observing the initial shock wave as it propagated away from the initial deposition spot (on a time scale of micro-seconds) the temperature could be calculated. Furthermore, information on the turbulent diffusivity was obtained by observing the rate of growth of the thermal region resulting from the energy deposition (using Schlieren imaging).

Shakal (1993) and Martin developed a predissociative laser induced fluorescence system (PLIF) to measure species during the ignition period of the diesel engine. The UV light from the Excimer laser is routed into the engine using a fiber optic cable and the fluorescence from the in-cylinder species is taken from the engine and imaged onto

a CCD camera using a coherent fiber optic bundle. These experiments are being done in the Detroit Diesel 53 engine.

## EXPERIMENTS AND RESULTS

For the purpose of discussion it is convenient to divide the experiments into topic areas. The results and highlights will then be given relative to these categories. The projects will be discussed as they relate to: *Fuel composition effects, Fundamental aspects of particulate formation, In-cylinder particulate formation and, Basic engine combustion studies.*

### Fuel Composition Effects

The research into fuel compositional effects ranged from a study focused on physical effects such as whether the chemical composition of the volatile fraction affected the ignition, combustion and emissions of the engine, to actually examining the effect specific composition changes in the fuel have on the engine combustion and emissions.

The work on fuel distillation effects done under ARO funding was a continuation of work started under DOE funding. The DOE work was carried out in close cooperation with researchers at Southwest Research Institute and the US DOE Synthetic Fuel Center. In this project a set of four fuel blends had been supplied to the ERC. These blends are shown as fuel blends A through D in Table 7.2.1. The cetane number ranged from 31.5 to 49.3, the distillation curves were similar, however Blends C and D had final boiling points approximately 60 °C higher than Blends A and B respectively. Within each blend was a different distribution of hydrocarbon types and in terms of the aromatic content, different distributions of monocyclic, dicyclic and tricyclic compounds. By combining the different blends and Phillips D-2 six fuels were formed, each with similar viscosity, heating value, aromatic content and overall boiling curve. However, the distribution of the aromatic components and the portion of the boiling curve in which they resided differed. The properties of these six test fuels are shown in Table 7.2.2. These six test fuels were then subjected to extensive testing.

In the DOE funded work Bair et al. (1986) found no observable differences in the ignition delay, heat release and emission data for the six special test fuels when run in a high swirl, low injection pressure version of the TACOM/LABECO engine. The behavior of the engine was consistent with the inference that portions of the fuel spray vaporized completely and then ignited. That is the premixed burn portion of the heat release was not from the high volatility portion of the fuel (fractional distillation) but from complete vaporization of that fraction of the fuel which was injected. This observation was reinforced by studies in which a homogeneous fuel vapor and air mixture for each fuel was inducted into a CFR engine and ignited via compression (no spark plug or other ignition source). The ignition trends of the six fuels were the same as those observed in the direct injection engine even though the pressures were lower and the resident times were longer. The data indicate that fuel chemistry dominates the ignition delay and that fractional distillation was not a factor in the combustion and emission characteristics of the engine.

Bair (1989) continued to study these fuels under the subject contract. As a first step in his work he "modernized" the TACOM/LABECO engine by installing the shallow bowl piston and high pressure injection system. The intake flow was

Designation Property	Method	Blend A	Blend B	Blend C	Blend D
Density, G/mL	D 1298	0.8310	0.8934	0.9142	0.8484
Specific Gravity, 60°F		0.8314	0.8939	0.9147	0.8488
°API		38.7	26.8	23.2	35.2
Distillation, °F/°C	D 86				
IBP		349/176	349/176	381/194	372/189
5		372/189	381/194	443/228	403/206
10		387/197	401/205	464/240	421/216
15		399/204	414/212	479/248	432/222
20		406/208	428/220	491/255	441/227
30		426/218	461/238	509/265	463/239
40		441/227	486/252	523/273	482/250
50		462/239	507/264	543/284	504/262
60		482/250	525/274	567/297	525/274
70		511/266	545/285	590/310	552/289
80		541/283	574/301	619/326	592/311
90		585/307	612/322	655/346	655/346
95		617/325	637/336	685/363	718/381
FBP		651/344	658/348	721/383	752/400
Recovery, %		99	99	99	95.5
Residue, %		1	1	1	1.5
Loss, %		0	0	0	0
Cetane Number	D 613	48.7	31.5	32.7	49.3
Cetane Index	D 976	46.4	34.3	33.3	45.6
Viscosity, cSt @ 40°C	D 445	2.01	2.25	3.48	2.84
Pour Point, °C	D 97	-26	-17	-11	-20
Hydrocarbon Type, V%	D 1319				
Saturates		69.8	31.5	15.4	59.1
Olefins		0	0	0	0
Aromatics		30.2	68.5	84.6	40.9
Aromatic Carbon, M%	UV				
Monocyclic		4.35	12.00	10.12	8.13
Dicyclic		3.06	16.05	22.16	5.96
Tricyclic		0.40	2.88	4.40	0.84
Elemental Analysis, M%					
Carbon	D 3178 (Mod) <sup>a</sup>	85.75	88.26	88.49	86.25
Hydrogen		13.18	11.12	11.03	12.95
Sulfur	D 2622	0.27	0.39	0.52	0.33
Heat of Combustion, MJ/KG/BTU/lb	D 240				
Gross		45.434/19533	43.895/18872	43.647/18765	45.350/19497
Net		42.637/18331	41.539/17858	41.307/17759	42.602/18316
Existent Gum, MG/100 mL	D 381	4.4	11.4	323.5	14.9
Flash Point, °C/°F	D 93	62/144	66/151	80/176	74/165
Reid Vapor Pressure, PSI	D 323	0.5	0.5	0.5	0.5
Calculated Vapor Pressure, PSI	D 2889				
500°		40	32	21	28
Surface Tension, dyne/cm	D 971 Mod #	26.84	28.43	28.86	27.74

<sup>a</sup> Modified for liquids  
# Air/sample interface

Table 7.2.1 Fuel Blends

<u>Property</u>	<u>Method</u>	<u>Test Fuel 1</u>	<u>Test Fuel 2</u>	<u>Test Fuel 3</u>	<u>Test Fuel 4</u>	<u>Test Fuel 5</u>	<u>Test Fuel 6</u>
<b>Component, V%</b>							
Blend A		70	50	30	70	50	30
Blend B							
Blend C		30	50	70	30	50	70
Blend D							
Cetane Number	D 613	43.3	40.5	37.5	38.1	41.1	44.5
Specific Gravity	D 1298	0.8576	0.8735	0.8922	0.8800	0.8713	0.8623
<b>Distillation, °F/°C</b>							
IBP	D 86	358/181	360/182	359/182	356/180	356/180	371/188
5		387/197	392/200	404/207	392/200	393/201	401/205
10		402/206	409/209	424/218	410/210	411/211	419/215
15		412/211	422/217	440/227	425/218	424/218	431/222
20		423/217	436/224	457/236	438/226	436/224	443/228
30		444/229	461/238	481/249	463/239	462/239	464/240
40		467/242	485/252	503/262	487/253	485/252	485/252
50		489/254	505/263	523/273	508/264	505/263	506/263
60		515/268	530/277	545/285	528/276	527/275	528/276
70		541/283	555/291	569/298	550/288	551/288	553/289
80		572/300	585/307	599/315	578/303	583/306	583/306
90		611/322	623/328	635/335	616/324	623/328	629/332
95		643/339	653/345	662/350	647/342	661/349	673/356
FBP		674/357	687/364	698/370	690/366	711/377	727/386
Recovery		99	99	99	99	99	99
Residue		1	1	1	1	1	1
Loss		0	0	0	0	0	0
Aromatic Carbon, M%		17.06	22.93	28.59	26.3	23.14	19.91
Sulfur, M%		0.35	0.40	0.45	0.37	0.36	0.35

Table 7.2.2 Test Fuel Properties and Composition

configured to yield as quiescent a chamber flow as possible. He ran tests of longer duration with both a high swirl and a low swirl engine configuration for which he made smoke and NO<sub>x</sub> comparative measurements. The conclusions of his work were the same. However he observed differences in the smoke level with fuels with different sulfur content. These differences lead to further work in which the effect of the sulfur volatility, that is the point in the distillation curve at which the sulfur became gaseous, was varied. In this work Eric Mueller (1990) concluded that the volatility of the sulfur had no effect on the resulting particulate emissions. This conclusion was determined by running mini-dilution tunnel tests. It was further determined that the differences observed by Bair were the result of different reflectivities of the soot and its attendant effect of the smoke filter measurement. It is now understood that smoke readings can be a valuable comparative tests for assessing the sooting trends for changes in engine operating conditions but they can be misleading when changing fuels, especially sulfur content.

Recently the EPA has issued regulations on the chemical composition of diesel fuels to be sold after 1993. The sulfur content is not to exceed 0.05 percent by weight. It has also been proposed to limit the aromatic content of the fuels to below 27% percent. How these changes in fuel composition will affect combustion and emission is not clear. As the chemical composition is changed physical properties of the fuel may also be changed. For example aromatics have a low cetane number. By removing the aromatic component of the fuel the cetane number is also likely to be changed. As the cetane number changes the ignition delay and then the combustion itself changes. It is not clear whether the aromatic component of the fuel or the above differences in combustion are responsible for the differences in combustion observed with lower aromatic fuels. Visiting Faculty Researcher Masanori Fukuda from Tsuyama College of Technology along with Army Fellow Dale Tree and graduate student Blake Suhre investigated this problem. Fuel blends with tetralin (1-2-3-4 tetrahydronaphthalene), a single ring aromatic compound, and naphtalene, a double ring aromatic compound, were prepared for comparison with straight diesel fuel. The additive compounds were chosen so that differences in the boiling points and cetane numbers were minimized. With the addition of the aromatic compounds the aromatic composition was changed from 21% for the base fuel to 28.9% for the additized fuels. Measurements of the total hydrocarbon, NO/NO<sub>x</sub>, CO<sub>2</sub>, O<sub>2</sub>, exhaust particulates, the soluble organic fraction (SOF) of the particulates, two color radiation and cylinder pressure were made.

The results indicated that there was fuel dependence in the combustion and emission data. However these differences depended on both the fuel composition and the combustion characteristics such as ignition delay and premixed burn fraction. Differences in fuel composition can result in differences in fuel properties such as viscosity and cetane number. These in turn will effect combustion ignition delay and premixed and diffusion burned fractions. The ignition delay and premixed burned fraction correlate with engine out emissions, most notably soot and NO<sub>x</sub>.

It is difficult to separate the effect of differences in combustion from differences in chemical composition when evaluating emissions from different fuels. For example in our data at an operating condition with an elevated intake temperature and pressure ( $P_{\text{intake}}=27$  psia and  $T_{\text{intake}}=336$  K) there were no differences in the combustion (heat

release) or emissions between the three fuels for equivalence ratios of 0.3 and 0.5 ( $\Phi=0.3$  and  $\Phi=0.5$ ). However when the operating condition was changed to that of a lower intake temperature and pressure ( $P_{\text{intake}}=116.8$  kPa and  $T_{\text{intake}}=307$  K) differences were observed in the ignition delay, premixed burned fraction and engine out emissions. At the operating condition of  $P_{\text{intake}}=116.8$  kPa,  $T_{\text{intake}}=336$  K and  $\Phi=0.5$  combustion characteristics were identical between the three fuels (same heat release characteristics) yet the emissions were different. Figure 7.2.2 shows these results. In the figure the abscissa lists the three fuels as standard diesel (STD), single ring aromatic tetralin (SAT) and the double ring aromatic naphthalene (DAN). The results indicate that the total unburned hydrocarbon and  $\text{NO}_x$  were slightly higher for the aromatic containing fuels. It was also observed that the single ring aromatic tetralin (SAT) had a higher tendency to produce particulates than did the STD or DAN fuels (a 9% increase in particulates). Finally, it was observed that there was a slight tendency for lower SOF and higher solid fractions with the aromatic containing fuels.

The tendency of the single ring aromatic compound to produce more soot than the double ring compound seems contradictory to the behavior observed in diffusion flame experiments. Based on diffusion flame data one would expect the molecule with a higher number of carbon to carbon bonds, namely the double ring aromatic compound, to have a higher sooting tendency. The fact that this did not occur, and the observation that the emission characteristics of the engine were more strongly correlated to the combustion characteristics than the chemistry of the fuel, is significant. The high temperatures of the typical diesel engine (temperatures above 2500 K) are in a regime where the structure of the aromatics is unstable. The results of the diffusion flame at a relatively lower temperature might not apply directly to the higher temperatures found in a diesel engine.

### Fundamental Aspects of Particulate Formation

There is a large body of literature on soot. The subject is addressed from the aspects of the fundamental chemical kinetics to basic laminar premixed and diffusion flames. At the ERC we were interested in bridging the gap between these fundamental studies and diesel combustion. The construction of an engineering model for soot formation and destruction in an engine is of particular interest. This model could then be used in conjunction with a diesel engine simulation to analyze trends of engine emissions with operational changes, and to assess the likelihood of success of proposed control strategies

Research on particulate formation at the ERC was conducted in both out-of-engine and in-engine facilities. The out-of-engine experiments, which are discussed in this section, were done on experimental rigs which attempted to get closer to engine conditions while still maintaining a high level of parameter control. Two experimental facilities were used: a jet stirred combustor (JSC) and a pressurized flow tube. The jet stirred combustor was used to make measurements of particulate nucleation and growth rates, and particle size and number density in a highly turbulent environment in which products were mixed back into the reactants. The pressurized flow tube was used to examine soot formation from a gaseous fuel jet burning in cross and co-flow

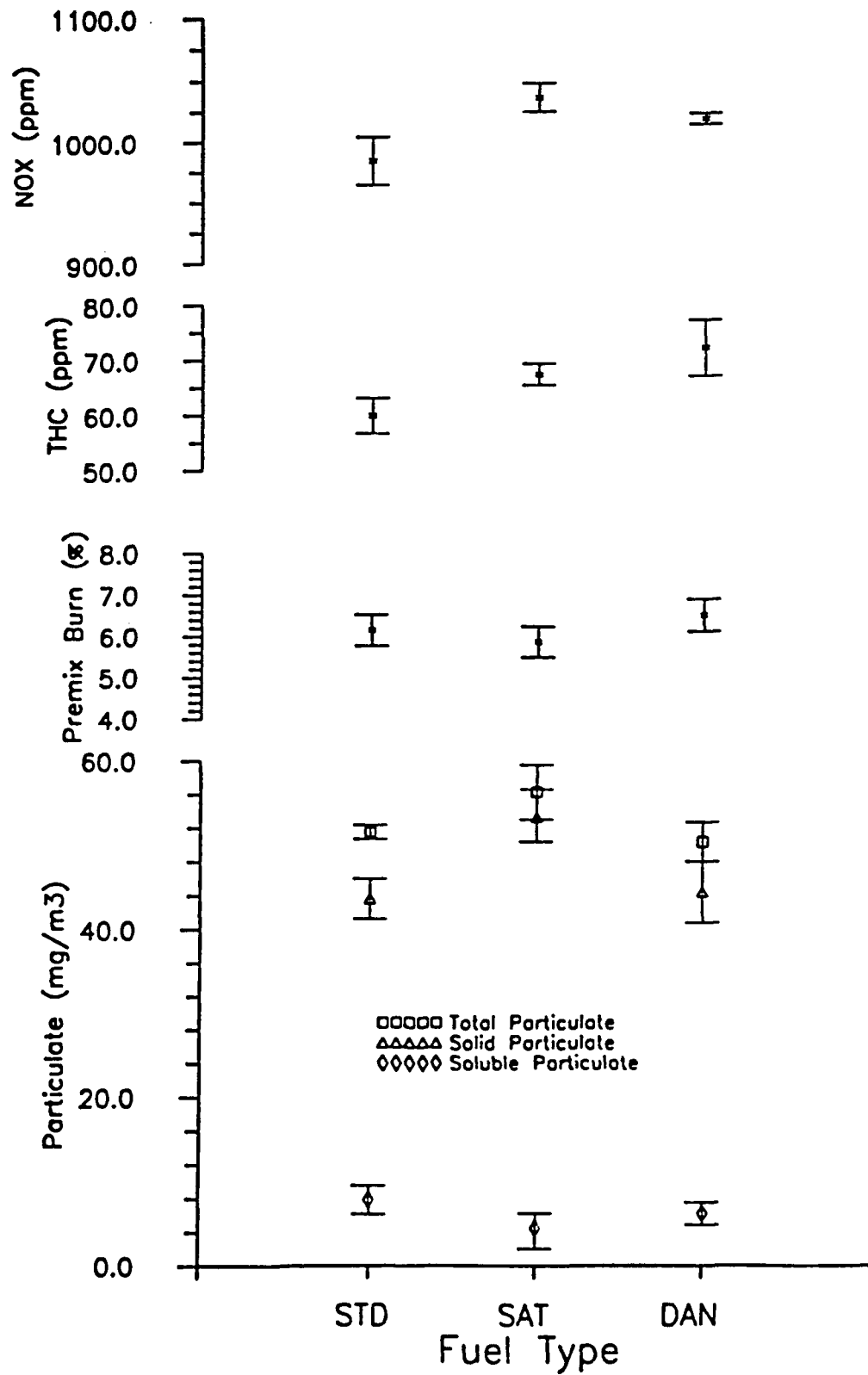


Fig. 7.2.2. Particulate emissions and premix burn for engine condition D, low intake pressure, high intake temperature. Error bars represent one standard deviation.

configurations. The pressure was varied from one to six atmospheres. The soot yield was measured for different flow rates, fuel jet and air flow Reynolds numbers and different fuel jet orientations (cross-flow and co-flow).

The jet stirred combustor was originally designed and built by Hoag (1983) and used to study the effect of fuel and air "premixedness" on sooting tendencies. Hodges (1989) then modified the design and added the measurements of particle size and number density via a combination laser scattering and extinction technique. Hodges (1987) also incorporated a surface growth kinetics model into the dynamic equations of soot particle growth to assess the validity of constant mass coagulation models used to assess the size distribution. If coagulation rates are fast relative to formation rates and surface growth kinetics it will be possible to determine the particle size distribution using aerosol dynamics for constant mass systems. Hodges results indicate that the particle volume distribution functions (PVDF) are sensitive to surface growth and that the self preserving distribution predicted by coagulation theory alone is probably not achieved. The most dominate effect of surface growth on coagulation is seen in the narrowing of the PVDF. Assessing a number density from a volume fraction measurement made using scattering/absorption techniques will require the assumption of a particle volume distribution function. If a two parameter distribution is used, for which Hodges has shown that the two-parameter log normal distribution is a good choice as the form of the unknown distribution of particle sizes, three independent measurements must be made. This will enable the determination of the particle volume fraction, width of the distribution and the number density.

Sato (1989) and Sato et al. (1990) built on the research of Hodges. The JSC modified further to accommodate cooling the sides of the combustor. In this way the effect of temperature on nucleation and surface growth rates was studied. By changing the temperature using heat transfer the ambiguity of species concentration changes which arises when the temperature is controlled via dilution was avoided. Figure 7.2.3 shows a schematic of this final design. As in the work done by Hodges the volume fraction was determined via a well established scattering/absorption technique. From these data a number density and mean particle size was determined by assuming a mono-disperse size distribution.

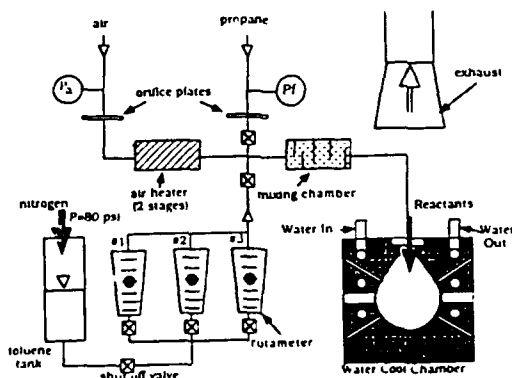


Fig. 7.2.3. Combustion system schematic.

The experiment was very successful. The soot volume fraction and particle number density were measured over a temperature range of 1250 °C to 1430 °C, an equivalence ratio range of  $\Phi= 1.7$  to  $\Phi= 1.8$  and reactor mass flow rates of 1.0 to 1.5 g/s. The particle nucleation rates and the surface growth rates were assessed as a function of equivalence ratio and temperature under the situation of product back-mixing. It was determined that for this system a maximum in soot concentration occurred in the temperature range between 1200 and 1400 °C, the particle size ranged from 7-24 nm and increased with increasing temperature, the majority of the soot mass resulted from surface growth, which increased with temperature, and that nucleation rate changes were responsible for differences in the soot yield at different operating conditions.

Figure 7.2.4 shows the sooting maximum versus temperature for three different equivalence ratios. The mass concentrations at equal equivalence ratios in combustors with different amounts of cooling are connected by dotted lines. The total mass concentration goes through a maximum in the temperature range between 1300-1400 °C. Mass concentration data at flow rates other than 1.25 g/s exhibited the same behavior. Over all of the data the maximum occurred between 1200-1400 °C. These results suggest a trade off between competing processes as temperature is increased. The surface growth rate was assessed to increase with temperature in this temperature range. It seems plausible that the particle inception rate goes through a maximum in this temperature range and therefore controls the soot mass concentration.

What is most significant about these results is that these data are consistent with measurements made in much simpler laminar and turbulent, non-back-mixed laboratory flames. For example, surface oxidation rates that we measured ( $0.3 \times 10^{-4}$  to  $0.7 \times 10^{-4}$  g/cm<sup>2</sup>/s) are consistent with those made by Harris (1989) in laminar flames.

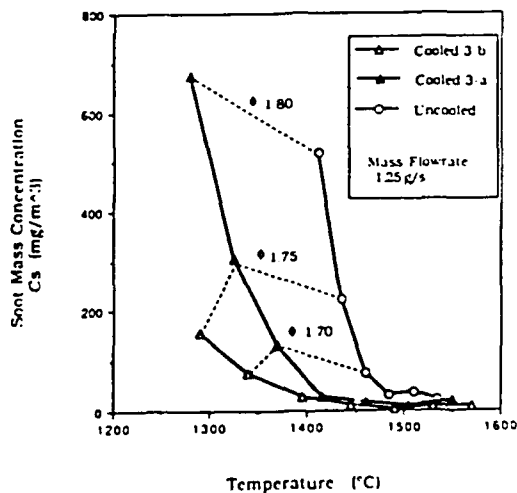


Fig. 7.2.4. Soot mass concentration vs temperature at a mass flow rate of 1.25 g/s.

This supports the use of data on growth and oxidation rates from very fundamental laboratory experiments in engine models.

The jet stirred combustor studies gave insight to the applicability of fundamental data on nucleation rates, surface growth rates, oxidation rates and coagulation rates to more practical combustion systems. It is also important to understand the mixing processes involved and what are the controlling parameters and time scales in the sooting process of a jet diffusion flame. These data were pursued in the pressurized flow tube experiments.

Under the direction of Professor Ellzey and Foster, specialist Berbee and graduate student Tay studied the total soot yield from a propane diffusion flame in cross-flow (Ellzey et. al. 1990). A schematic of the pressurized flow tube is shown in Figure 7.2.5. The main air flow was from the building's air system. Filters were placed in line to remove contaminants. The fuel, propane, was introduced through a fuel tube nozzle which ranged in diameter from 11.9 mm to 24.1 mm. The geometry of the fuel system could be changed from cross-flow, where the fuel tube protruded 25.4 mm vertically from the wall into the test section, to cross-flow, where the fuel tube protruded vertically from the wall 25.4 mm then was bent to flow parallel with the air flow for approximately 10 tube diameters to the exit. Ignition was obtained from a removal set of ignitors. Soot samples were collected on filters downstream of the flame and a window provided optical access.

A series of experiments were conducted in which the flow rates of fuel and air were varied, the diameters of the fuel jets were varied and the pressures of the flow tube were varied. The initial attempts to correlate the data were done by setting the operating parameters of the flow tube to control dimensionless parameters such as the Reynolds numbers of the jet and air stream and the momentum flux ratio between the jet and air streams. These operating conditions were then correlated with the soot yield

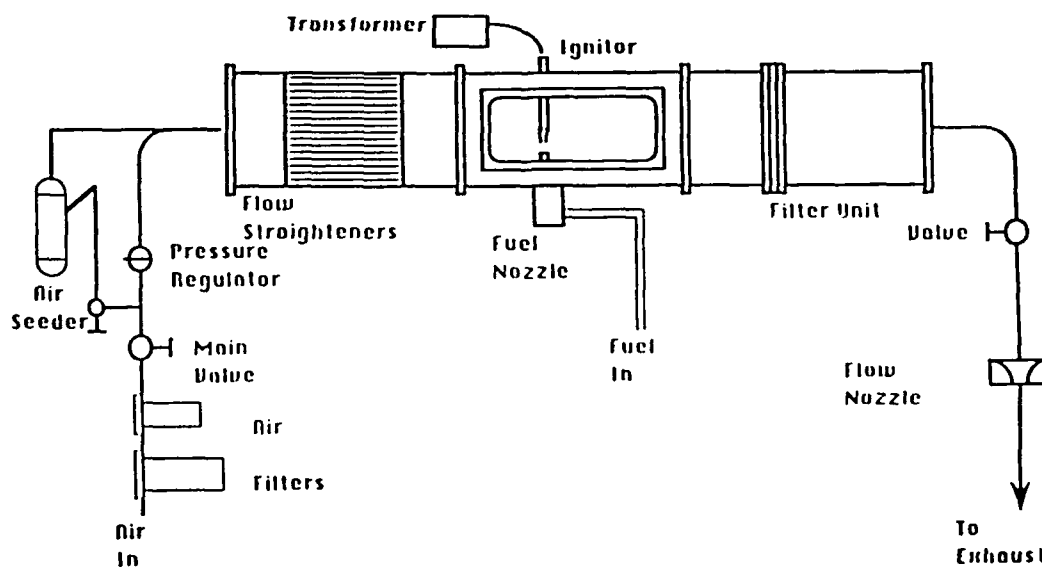


Fig. 7.2.5. Experimental Setup Schematic.

of the experiment (defined as the mass of the soot, captured on the filter, to the mass of fuel burned during the experiment). The soot yield varied tremendously over the operating range of the flow tube.

Figure 7.2.6 shows some of the results. The soot yield did not correlate at all with operating conditions in the co-flow experiments yet showed a strong correlation with the operating parameters in the cross-flow experiments. All attempts to correlate the soot yield with dimensionless parameters, such as Reynolds number or momentum flux ratio, failed. It was interesting, yet not entirely satisfactory, that a successful correlation was obtained when the soot yield was plotted against the product of the air and fuel velocities. Figure 7.2.7 is a plot of that correlation. The mixing index is defined as the product of the air stream and fuel jet velocities (Mixing Index =  $V_a \times V_j$ ). This parameter is a dimensioned parameter and is specific to the experimental set up, which greatly reduces its utility.

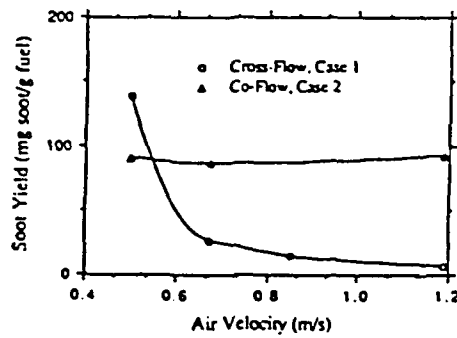


Fig. 7.2.6. Soot yield for cross-flow vs. co-flow geometries.

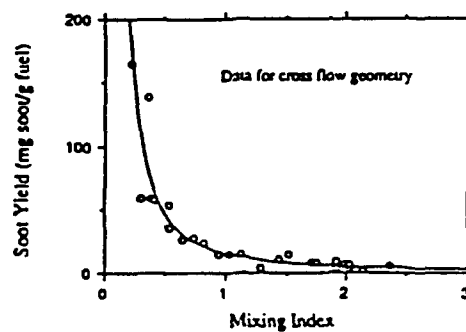


Fig. 7.2.7. Correlation of soot yield to mixing index,  $V_a V_j$ .

Turner (1992) pursued this issue further by following up on the observation that the flames could be classified on the sooting tendency qualitatively by their appearance in short exposure photographs. Turner did extensive LDV probing of the different flames and flow fields. Assessments were made of the velocity and turbulence profiles, calculations were made of the time and length scales of the different operating conditions and finally the power spectra of the different operating conditions were computed. Turner's results indicated that there were common characteristics in the power spectra for all high sooting and all low sooting operating conditions, irrespective of whether the geometry was co-flow or cross-flow. For low sooting operation, it is necessary to have a relatively uniform distribution of flow energy over all frequencies, that is there must be a uniform and continuous cascade of the turbulent eddies over all scales.

### In-Cylinder Particulate Studies

The out-of-engine experiments can lend insight to in-cylinder behavior however it is not possible to reproduce real engine conditions in out-of-engine "bench type" experiments. It is of critical importance to have engine experiments. A series of experiments done during this contract took advantage of the radiant emission and the scattering properties of the in-cylinder particulates to make measurements of in-cylinder temperatures, soot particle loading and mean particle size and number density of operating engines.

In order to make measurements of the radiant emission from in-cylinder particulates it is necessary to have a window into the combustion chamber that remains clean during engine operation. Yan and Borman (1988) were successful in designing a window probe which remained clean over a range of engine operating conditions. Figure 7.2.8 shows a schematic of this two color radiation probe and the fiber optic transmission of the radiant signal to the photo detectors. As described in the previous section on diagnostics developed, the combination of the phased gas exchange into and out of the cavity plus the fin design of the sapphire rod kept the window clean. The probe was located in an instrumentation plug which replaced one of the exhaust valves of our single cylinder Cummins NH engine. Engine data were taken for speeds from 1100 rpm to 1900 rpm, intake temperatures from 305 K to 333 K, intake pressures ranging from 126 to 200 kPa, coolant temperatures ranging from 355 K to 393 K and loads ranging from  $\Phi = 0.3$  to  $\Phi = 0.5$ . The combination of the higher coolant and inlet air temperatures simulated a mini-cooled engine configuration. The data taken included NO<sub>x</sub>, CO, CO<sub>2</sub>, Bosch Smoke and radiant emissions from both on the spray axis and between spray plume axes.

The results of the research indicated that the cycle-by-cycle variation of the flame radiant emissions were very high. The maximum standard deviation of the KL signal was approximately one third of its peak value, while the standard deviation of the flame temperature in the high temperature region was less than 40 °C. It also appears that the soot formed in the early stage of combustion was rapidly oxidized, mainly because of the high temperatures. Exhaust soot seems to be determined by the characteristics of the later portions of combustion. Since the extent of the late burning is determined by the timing of the end of injection, this indicates the potential that rate shaping of the injection may have on engine emissions.

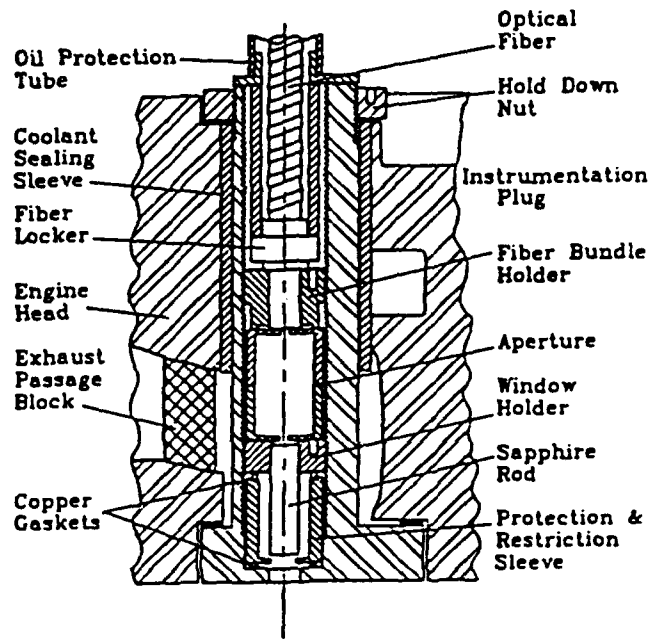


Fig. 7.2.8. Optical Window Cutaway View (part 1 of 2).

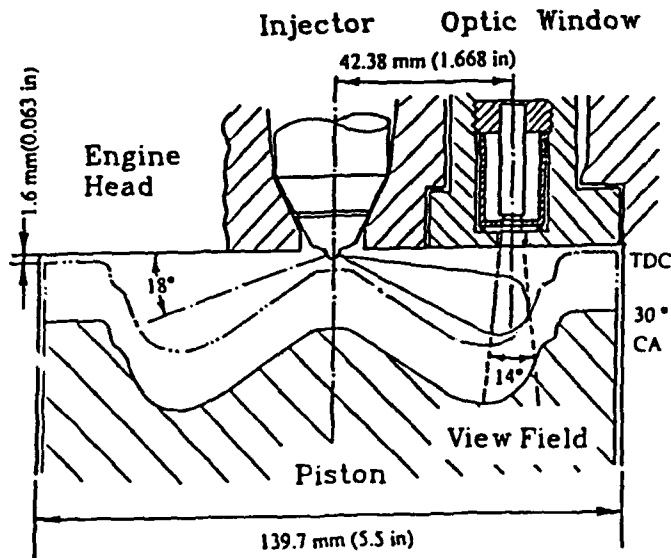


Fig. 7.2.8. Optical window relative position to the combustion chamber (part 2 of 2).

In this work the peak flame temperatures measured were in the range of 2420 to 2500 K. This is approximately 300 K below the calculated adiabatic flame temperatures. The calculated adiabatic flame temperatures and the measured flame temperatures followed the same trend. Furthermore the data were able to explain the trends in engine out emissions with in-cylinder phenomena. For example, the trend of increasing the soot emission that resulted from increased coolant temperature was seen to be caused by the increased late burning occurring at elevated temperatures.

Mohammad (1991) continued the work of Yan by installing three two-color radiation probes into the instrumentation port of the engine. By locating three probes in the engine head the data obtained could be spatially resolved. Figure 7.2.9 shows the engine head with the three two-color radiation probes installed. Indexing the injector lead to nine locations which were studied. One difficulty encountered in this work was that the miniaturized radiation probes did not remain clean like the original design. This limited the operating range and necessitated the use of additional oxygen in the inlet air to ensure clean windows. These data were significant in that now information on the spatial distribution of the soot and its temperature were available. The figures 7.2.10, 7.2.11 and 7.2.12 show the KL and temperature profiles for the three two-color

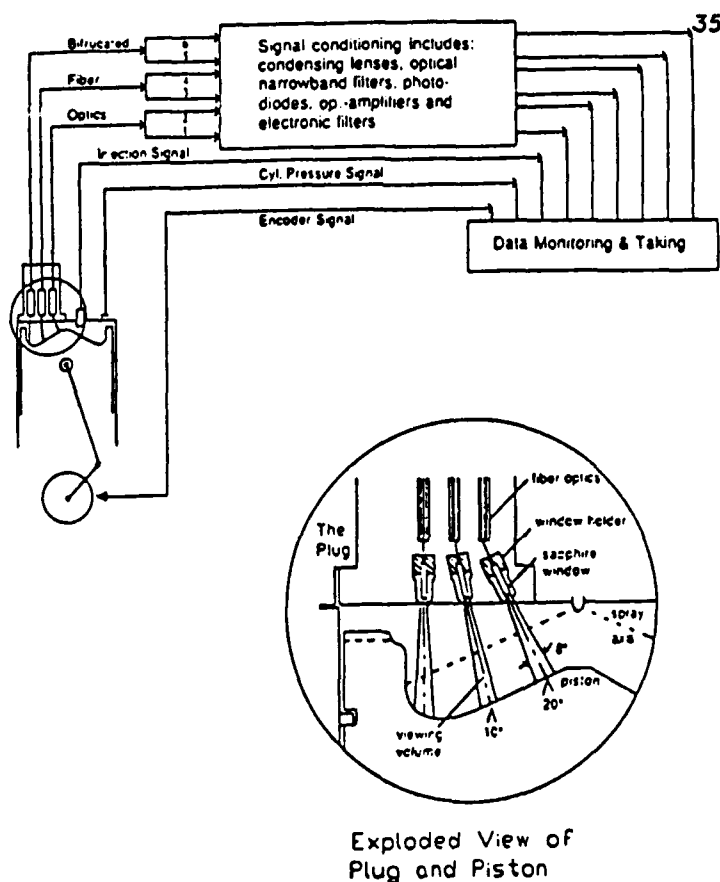


Fig. 7.2.9. The instrumentation system.

probes for locations of on the spray axis, on the spray periphery and in between spray plumes. In these figures one can see the spatial variation of the temperature and soot loading.

Tree (1992), an ARO Fellow, further modified the basic two-color radiation probe design by incorporating laser light transmission into the probe body with a fiber optic cable. The fiber optic cable terminated at a spherical lens near the combustion chamber surface. With this design it was possible to focus the beam of an Argon-ion laser approximately 5 mm from the head surface in front of the sapphire window. In this way a combination of two-color radiation and scattering and extinction data was obtained, yielding the mean particle size and number density as well as the temperature. This is the first such data from an operating engine.

Data were obtained for engine operating conditions of 1000 and 1300 rpm and equivalence ratios of  $\Phi = 0.20, 0.24, 0.30$  and  $0.5$ . Initial particle diameters were measured to be 15 nm and grew to a peak of 35-55 nm. This peak was slightly dependent on equivalence ratio with the higher (richer) equivalence ratios yielding larger diameters.

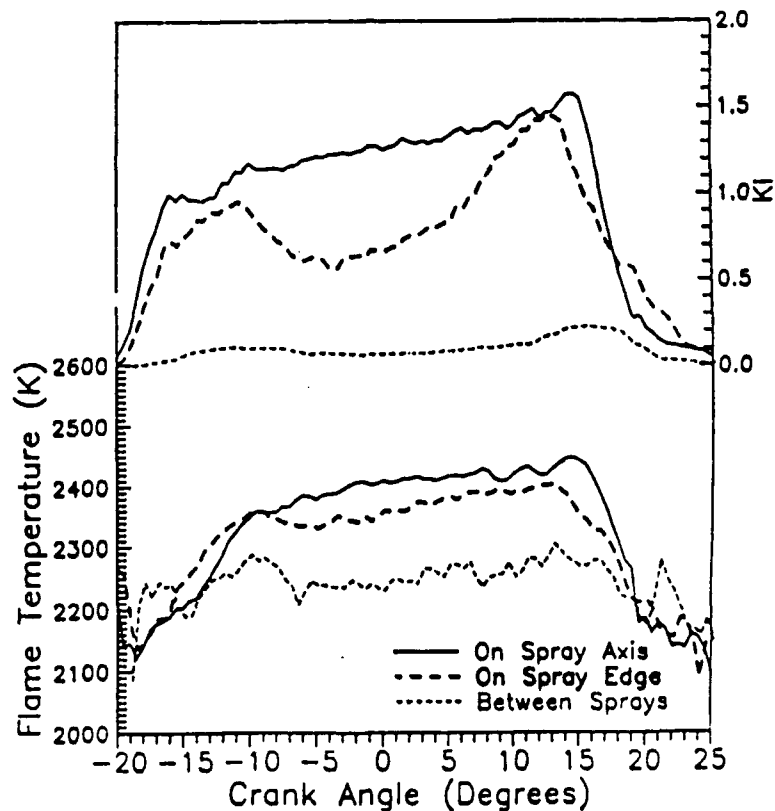


Fig. 7.2.10. Flame temperature and soot concentration factor KL at three angular positions for window A (24, 25, 26-3).

It was observed that the soot particle size changed rapidly with time at the measurement location, experiencing a rapid decrease later on in the cycle while the number density exhibited a corresponding increase. This large change may be the result of tremendous stratification of the soot particles within the combustion chamber as they are formed in different combustion zones at different times with different number densities, or it could be the onset of a very rapid oxidation. This second explanation is preferred because at some time the large particles disappear, no longer scatter, and are not seen by the probe. This means they must be oxidized and it would be difficult to imagine oxidation of so many particles without changing their size. Because of the measurement technique it was not possible to assess the exhaust diameter or number density.

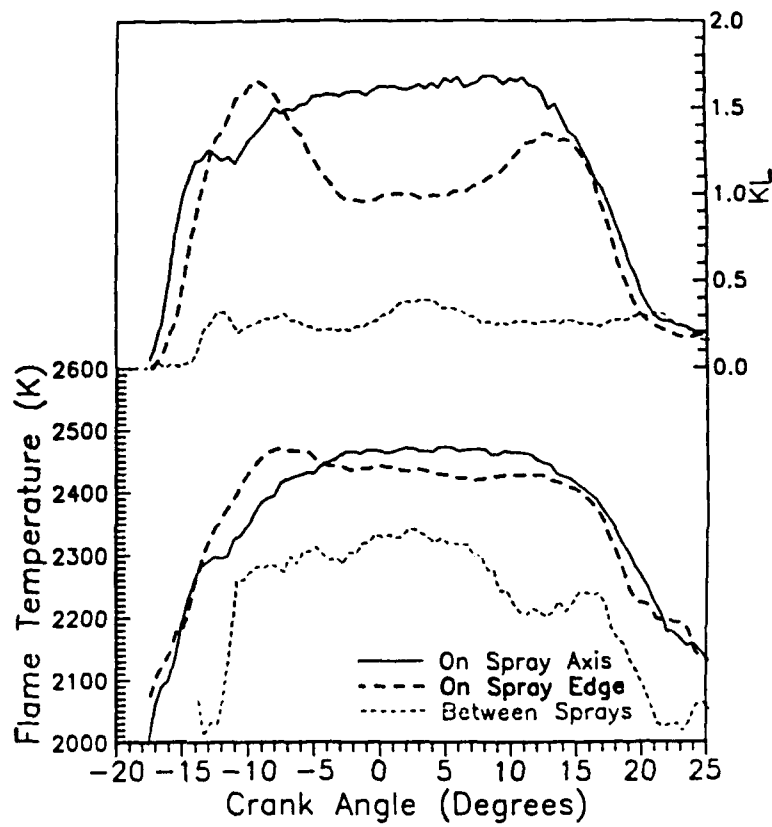


Fig. 7.2.11. Flame temperature and soot concentration factor KL at three angular positions for window B (24, 25, 26-3).

Even though there has been considerable work on understanding the particulate emission from the diesel engine it is still not clear what processes play a dominate role in the final exhaust emissions. For example, do the particulate emissions originate from gas phase processes and somehow escape oxidation, or is the particulate hidden from oxidation by being deposited on the cylinder surfaces and become entrained in the exhaust flow after being sheared off the wall during the blow down and exhaust processes? If this latter scenario were the case it would explain how oil constituents get onto the particulates.

Graduate student Blake Suhre (Suhre 1992 and Suhre and Foster 1992) addressed the question of particulate wall deposit mechanisms. The processes of inertial deposition, electrophoresis, gravitational sedimentation, Brownian diffusion and

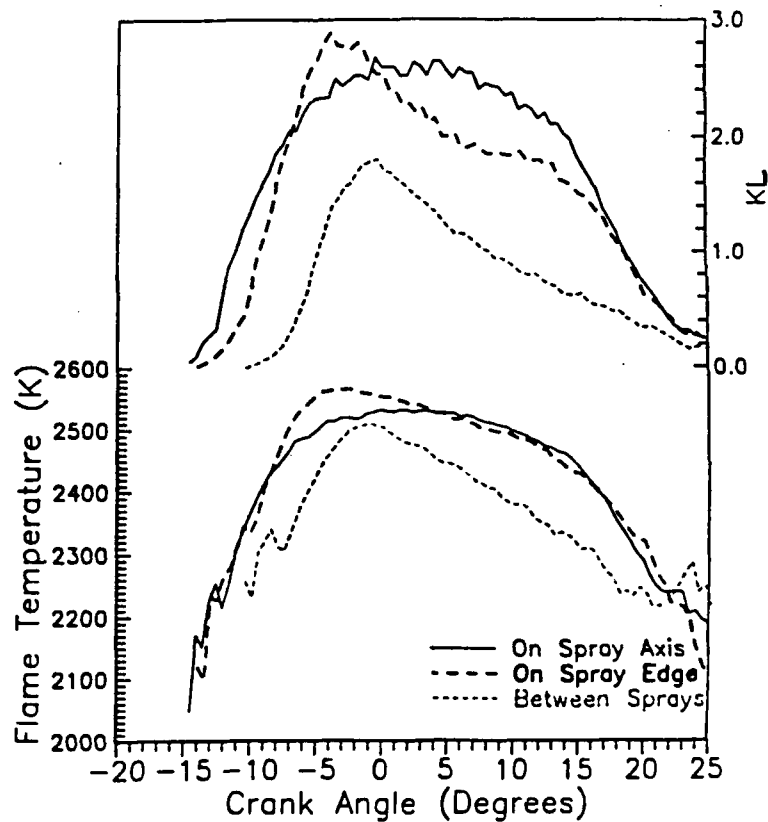


Fig. 7.2.12. Flame temperature and soot concentration factor KL at three angular positions for window C (24, 25, 26-3).

thermophoresis were investigated both analytically and experimentally. The results of this work were consistent with those published by Kittleson et al. (1990). It was found that in order for inertial deposition to be a factor in particulate surface deposition the particle would have to be carried to within a few nanometers of the wall before being "thrown" at the wall by the flow; in other words the particle will decelerate to zero relative velocity within a few nanometers of being thrown out of a turbulent eddie. This would require that the turbulent boundary layers in the engine be extremely thin. [There is some evidence of this however (Pierce et al. 1992 and Boggs and Borman 1991) so inertial deposition cannot be ruled out.] However the largest force acting on the particulates as they get near the wall is the thermophoretic force arising from the temperature gradient between the bulk gas and the wall.

Of particular interest was the prediction of the analytical model of deposition rate changes as the temperature of the engine changed. The inertial deposition rate would change because the viscosity and density of the surrounding gases change with temperature and change the drag on the particle. The thermophoretic force is directly related to the temperature gradient so it has a large temperature dependence. The models predicted very little change in deposition rates from inertial impingement with changes in the temperature gradient. As the wall temperature was increased from 400 K to 800 K the predicted travel distances for thrown particles changed from  $3.2 \times 10^{-8}$  m to  $2.9 \times 10^{-8}$  m. For the case of thermophoresis the model predicted a decrease of the deposition rate on the order of 25%.

Suhre constructed a probe to assess the soot deposition rate by measuring the initial rate of obscuration of a sapphire window mounted in the engine. This probe was mentioned previously and is shown in Figure 7.2.13. Full detail and development of the analysis is given in Suhre and Foster (1992). Figure 7.2.14 shows the measured soot mass plotted against engine cycle number for cases in which the probe was uncooled, Run H3-26, and in which the probe was cooled, C3-26. For the data shown, the difference in the surface temperatures was approximately 125°C; it was assumed that the probe did not affect the combustion. This was verified by comparisons of heat release diagrams for the two operating conditions. Note the large difference in the mass of soot deposited when the temperature gradient is large during cold runs, relative to when the temperature gradient is smaller during hot runs. By taking the slope of these data it is possible to assess the particulate deposition rates at the surface at this location in the combustion chamber for the two different surface temperatures of the probe. For these data there was a 50 percent difference in the surface deposition rates for the uncooled and cooled probe configurations, the hot surface having the lower deposition rate. In comparing the analytical predictions and the experimental results, only the thermophoretic model comes close to accounting for such a large change in deposition rates with temperature.

As an interesting comparison, the data for the soot deposition rate of the probe surface area was used to extrapolate what would be a total deposition rate for the combustion chamber (considering only the piston and head surface areas). If it were then to be assumed that the soot layer reaches a steady state, that is the deposited soot is subsequently sheared off during the exhaust process, one could estimate what portion of the total exhaust particulate emission was from combustion chamber surfaces. When

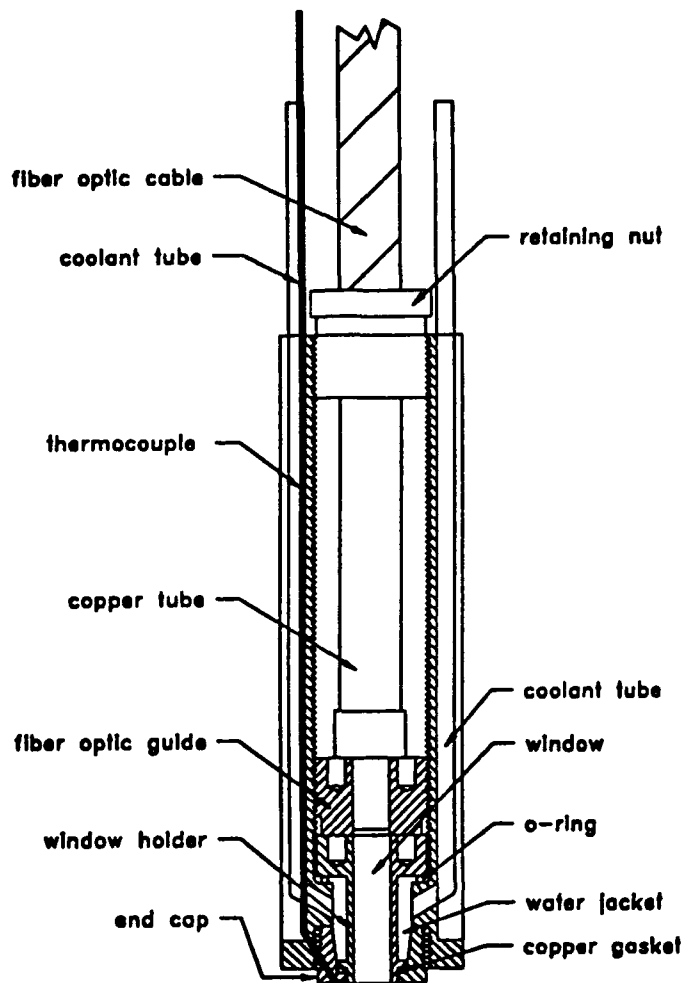


Fig. 7.2.13. Probe

this was done the predicted particulate emission was 83% higher than the measured particulate emission. There are many possible inaccuracies in this extrapolation, however the magnitude of the answer indicates that one cannot neglect this as a particulate emission mechanism and furthermore one must consider the possibility of thermophoresis playing a major role in the surface deposition of particulates.

In some related work done by Visiting Researcher Shinya Ashikari of Komatsu Ltd. the cycle-by-cycle variability of the particulate emission was measured. Mr. Ashikari developed a laser sheet extinction LDV measurement system in which the total mass, or volume, flux could be measured at the exhaust manifold exit. Using this system we were able to measure the cycle-by-cycle variation of the particulate emission. It was found that under conditions where the imep was varying less than 4 percent the cyclic variation in the particulate emission was over 400 percent! These data are shown in Figure 7.2.15. This plot shows the cycle-by-cycle imep and soot volume flux for 500 consecutive cycles. One can easily see the larger variation in the soot volume flux relative to the imep. This confirms what one would initially expect. The particulate

formation and destruction processes are much more sensitive to in-cylinder phenomena than is the cylinder pressure. These data are consistent with the large standard deviation in the KL signal as discussed above.

In the discussion above it was stated that one could not rule out wall deposits and subsequent removal as a source of exhaust particulates. The inverse is also true. If wall depositions with subsequent removal were the main mechanism for the soot emission then steps taken to reduce gas phase soot emissions would be relatively ineffective. Graduate student Larry Golding (1992) completed a study on the TACOM-LABECO engine in which an auxiliary mixing chamber was installed into the head. The 5.5 cm<sup>3</sup> chamber burned a premixed methane charge and exhausted the products into the engine after peak cylinder pressure. Operating the engine at an equivalence ratio of 0.5, the effects of the mixing was a fifty percent reduction in particulate emissions. Operating the mixing chamber and retarding the injection timing to 3 degrees before TDC resulted in a simultaneous reduction of particulates and NO<sub>x</sub>. Ignition of the mixing chamber was difficult to control so it does not represent a viable emission control technique in its current form. However this work clearly demonstrates that reduction of particulate through the control of gas phase phenomena is possible.

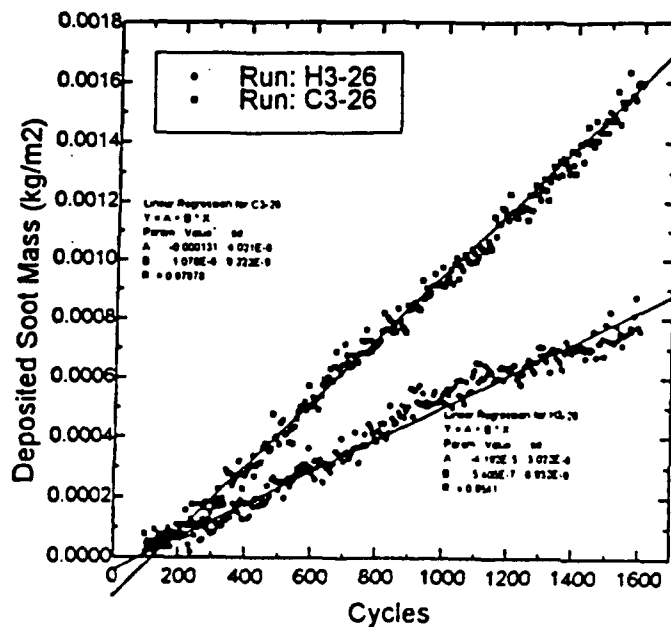


Fig. 7.2.14. Mass deposition for runs 3-6.

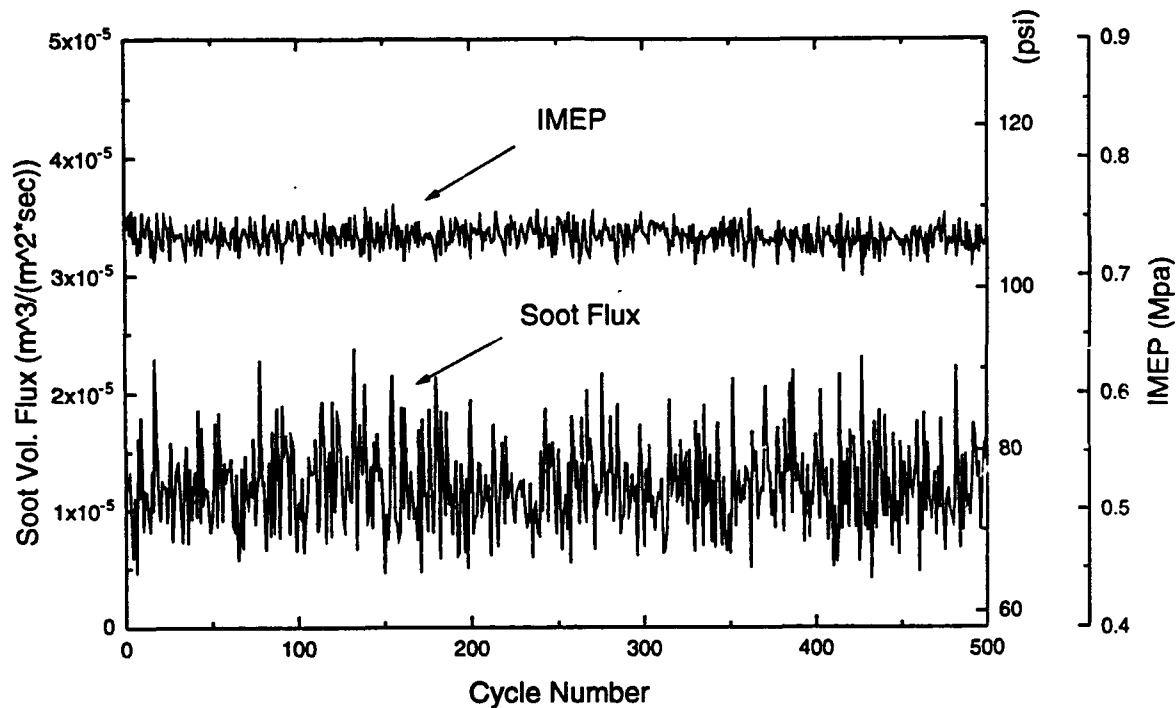


Fig. 7.2.15. Cyclic variation of soot volume fraction in the exhaust stream.

As a result of the ERC research discussed in this section it is now known that the fundamental processes of particulate formation observed in basic laboratory type premixed and diffusion flames are also the fundamental processes that are of importance in the diesel engine. Data on the temperatures, number density, particle sizes and volume fraction in an operating production diesel engine are now available. These data have shown the heterogeneity of the temperature and soot field, given an indication of the magnitude of the heat transfer in a modern engine that can be attributed to the radiation from particulates and given an assessment of the large extent of cyclic variability of the particulate emission. All of these data are important pieces of the puzzle and are currently being incorporated into a phenomenological model of soot formation to be used as a submodel in KIVA.

### Basic Combustion Studies

In addition to the research discussed above there were other studies that more correctly fit under the general description of basic combustion studies rather than one of the above topics. These include energy balances on an insulated engine, an experimental and theoretical evaluation of a toroidal combustion chamber and work on the computation of mass rate of emissions from exhaust gas composition measurements.

One issue that is not well understood is the effect insulating the combustion chamber has on heat transfer. There is data in the literature which suggests contradictory results. Huang and Borman (1987), Yang and Martin (1990) and Morel et

al. (1988) have data and or calculations which suggest that insulated engine components decrease the heat transfer from the combustion chamber, while the data of Woshni et al. (1987), Alkidas (1989) and Gatowski (1990) indicate that insulating the combustion chamber results in higher levels of heat transfer. Graduate student Mark Mueller (1990), initially under TACOM funding and then under ARO funding, ran a series of experiments on the Cummins single cylinder NH engines that were both insulated and non-insulated in an attempt to understand these apparent contradictions. This work was done at both our laboratory and at the Purdue School of Mechanical Engineering, in a special cooperative working agreement in which we rented their facilities and brought our instrumentation and personnel to their engine lab for the data acquisition. In the work done at the ERC [under ARO funding] we included the additional effect of an air gap piston as a means of insulation.

Furthermore, we attempted to optimize the engine injection timing to reach the minimum smoke- $\text{NO}_x$  trade-off for each operating condition for both insulated and non-insulated conditions. Once we had the engine operation optimized we took data for both a complete heat release analysis and for a First Law energy balance on the closed portion of the engine cycle. This enabled analysis of both the global heat transfer and the combustion parameters of ignition delay, premixed and diffusion burn fractions. The combustion characteristics of the insulated engine is what is emphasized in this section.

Some of the results are summarized in Table 7.2.3. From these data it is apparent that the insulated engine did indeed have higher levels of heat transfer relative to the normal non-insulated engine. The heat release analysis indicated a significant difference in the combustion characteristics of the two engine builds. Figure 7.2.16 shows just how different the combustion can be for the two different cases. Notice the tremendous difference between the premixed burn fractions. These differences will lead to differences in the diffusion burn, in the overall temperature and pressure histories and in the particulate formation and oxidation. By merely insulating an existing engine the combustion characteristics are changed. This will have a corresponding effect on the heat transfer as it is the combustion which drives the heat transfer and not the other way around. Theoretically one can show the advantages of insulating an engine however to put this idea into application will require a total engine design optimization and not merely insulating an existing engine.

In an effort to understand the in-cylinder flow, and then use it to the engine's advantage, Quiros et al. (1990) experimented with a toroidal combustion chamber. This work, like that of Mueller started out with TACOM funding and finished with ARO support. The working hypothesis of the design was to establish a controlled air circulation into which the fuel was injected, which in turn used the injected fuel momentum to increase the circulation rate. At full load it would be desired to have one complete rotation of the gas in the toroidal chamber in the time allocated for combustion. Theoretical calculations indicated the momentum of the fuel spray was not sufficient to induce the required fluid motion; some initial velocity is required. It was concluded that such a chamber shape has many advantages and warrants further study. It achieves stratification by geometry, it does not require special treatment of the intake system to achieve the air motion in the combustion chamber, fresh air is continuously being fed into the fuel spray and if a glow plug is used the engine will be insensitive to

Table 7.2.3. Summary of the Heat Transfer and Indicated Specific Fuel Consumption of the Ceramic Coated and Base Engine

Speed, Load	Percent Cycle Energy Input as Heat Transfer		ISFC (kg/hp-hr)	
	ceramic	metal	ceramic	metal
1300, 25%	0.208	0.145	0.138	0.135
1300, 50%	0.152	0.100	0.133	0.130
2100, 25%	0.198	0.136	0.136	0.137
2100, 75%	0.135	0.082	0.135	0.138

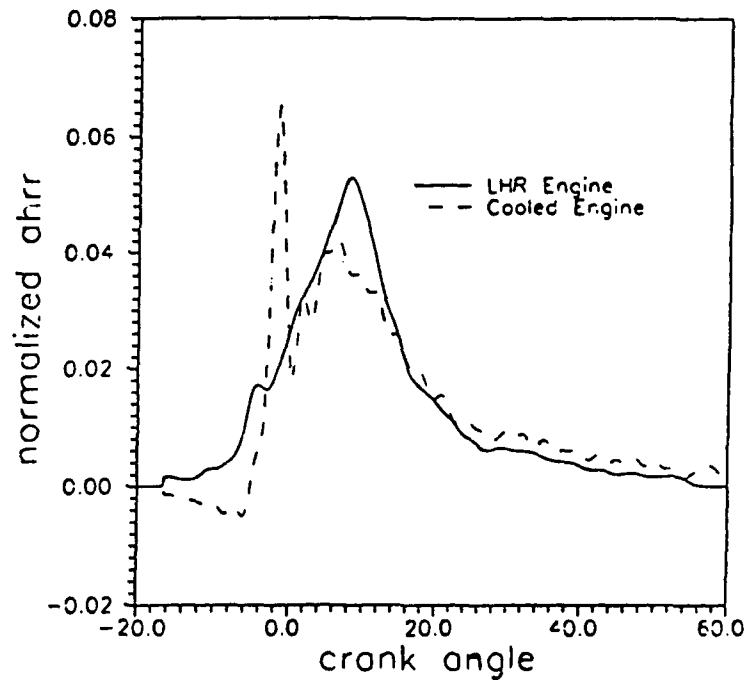


Fig. 7.2.16. LHR and Baseline AHRR (1300 rpm, 25% Load).

the fuels ignition characteristics. The work did not progress to the point of being able to do emission studies so this represents an uncertainty at this time.

One inconvenience that impedes the comparison of research laboratory emission results with those made in the field or on emissions test stands is the methods in which the data are reported. Exhaust emissions are typically measured as a volume fraction of the exhaust stream where as government regulations are expressed as mass per unit quantity such as fuel or energy. Myers, Myers and Myers (1988), motivated by the Diesel Engine Manufacturers Association, offered a suggested computation technique and a computer program to convert the measured exhaust gas composition and fuel flow rate to mass emission rates. The program uses input data from a user supplied fuel data file with data such as heating values of the components of the fuel and the mass fractions of C, H and S. The program then computes the wet moles of exhaust per mole of  $CH_n$ , how many moles of  $CH_n$  there are per mole of fuel and a moisture correction factor to account for wet or dry exhaust emission measurements. With these the mass emission measurements are calculable. It is felt that this program, if used, would standardize the reporting procedure and minimize differences in reporting measurements from different laboratories.

## SUMMARY OF IMPACT

It is felt that significant increases in the fundamental understanding of diesel combustion have occurred during the tenure of this contract. It has been determined that the fuels distillation characteristics are not important in the ignition processes of the diesel. The chemical effects dominate and fractional distillation does not seem to be important. It has also been determined that when combustion is the same fuel effects can be observed but they are not primary effects. Furthermore it was demonstrated that the single ring aromatic compounds had a higher tendency to yield higher soot emissions than comparable amounts of double ring aromatic compounds. In making assessments of the soot emissions, smoke readings can be beneficial as long as the fuel is not changed. Any engine combustion change which results in different reflectivity of the soot can yield misleading smoke comparisons.

The work on the fundamentals of soot formation at the ERC indicated that the data from laboratory "bench type" flames can yield useful results for diesel engine data interpretation, even in light of the very different environments present in the compared systems. The primary reason for differences in soot yield from different combustion systems is due to differences in the nucleation rates for the two systems. Researchers at the ERC successfully measured the particulate temperatures, the variation of the temperature within the combustion chamber, the mean particle size, number density and volume fraction within the combustion chamber during combustion and the cycle-by-cycle variation of the soot emissions. Data on the rate of soot deposition onto the combustion chamber walls was obtained and it was demonstrated that soot-wall interactions cannot be ruled out as a significant source of particulate emission. However it was also demonstrated that enhanced gas phase mixing also has a significant impact on the particulate emission, so enhanced oxidation schemes should also be considered as a means of particulate control. Prior to this contract these data were simply not available. These data are being used for the development and assessment of engineering soot models to be incorporated into KIVA. Such an advancement, when perfected, will enable much more rapid assessment of the impact of possible design changes on combustion, heat transfer and emissions.

It was confirmed that insulating the engine without attention to the resulting combustion changes can lead to confounding results. The combustion drives the heat transfer. If the combustion is altered to yield much longer diffusion burns because of the added insulating then the total heat transfer will probably increase. The insulated engine will have to be designed from the "clean sheet of paper."

Finally, through ERC efforts a computer program that converts the gaseous emissions typically measured in the laboratory to mass based emissions. If adopted this would yield a uniformity between the many research facilities doing combustion and emission research.

### 7.3 Heat Transfer

Almost all aspects of engine design are influenced by heat transfer, but typically in a secondary role. Thus for a typical liquid cooled diesel the combustion aspects are affected by the way heat transfer influences volumetric efficiency, ignition delay, peak pressure, efficiency, emissions, and starting. In each case, however, the effect is not the primary governing parameter, except for cold starting (Gonzalez, et al. 1991), where heat transfer plays a primary role. The mechanical aspects of the engine are more directly affected by heat transfer; the thermal stress, strength of parts, oil and water coolant loads, and friction all are directly influenced. It is thus not surprising that engine heat transfer has been studied extensively (Borman and Nishiwaki, 1987) and that it has been an important topic of ERC research.

In particular, the Army has a great deal to gain from heat transfer reduction, since the volume of the coolant systems and the size of the total vehicular intake air flow are both vital to improvement of combat vehicle performance. This also explains the importance of low heat rejection (LHR) engine technology to the Army (Woods, et al. 1992, Zucchetto et al., 1988, Myers, 1989).

Research on engine heat transfer has had a long history at U.W., starting with the work of Overbye et al. (1961) and Ebersole et al. (1963). At the start of the period covered by this report several projects sponsored by the Army had just ended (Van Gerpen et al., 1985) and (Huang and Borman, 1987). In progress during the reporting period was a parallel contract sponsored by TACOM, (contract DAAE07-84-CR063). The final report for this TACOM contract (Borman et al., 1991) overlaps portions of this report, and may be referenced for more detail of work which is more briefly mentioned here.

In order to put the work reported here in perspective it is important to understand the status of research needs, particularly for application to Army problems. Thus these needs are reviewed prior to discussing the research itself.

#### Research Needs

For diesel engines both convection and radiation play a role during the combustion and expansion period. The total heat transfer flux varies tremendously both in time and space. While global models and to some extent zonal models can be useful in predicting thermal loading only fully three dimensional CFD codes have the potential to predict the spatial distribution and to properly tie the heat flux to the combustion and fluid parameters in the cylinder. However, the gridding required to encompass the boundary layers, which are very thin, (less than 0.5 mm) would exceed current computer capabilities. Thus a subgrid model for the boundary elements is required. This model should use the local velocity, turbulence composition and temperature information generated by the CFD code and should incorporate the correct physical phenomena of the engine boundary layer. As will be explained later, it is unlikely that a single subgrid model will be able to predict the convective flux for all parts of the chamber, and thus several submodels are needed. The radiation flux could be computed if the soot concentration distribution and temperature were predicted by the CFD model. However, this requires both a soot and detailed combustion model which are currently under development. Direct measurement of radiation, flame

temperature and soot concentration in modern engines can however give an improved understanding of the importance of radiation. It should be noted that while improvements in combustion are expected to reduce the radiation flux, it is difficult to significantly reduce the radiant component of wall heat transfer by insulation, because the flame temperature (~2700K) remains much higher than the insulated wall temperature (~1000K) and because it is difficult to lower surface absorptivity. The best hope for radiation reduction is thus to find ways to lower soot concentration through combustion modifications.

The influence of insulated (high temperature) surfaces typical of low heat rejection (LHR) engines has remained unsolved, because it is not possible to duplicate LHR engine conditions except in an LHR engine. Recent results (Beardsley and Larson, 1992) with thick (2.5 - 3.5 mm) thermal barrier coatings have shown that LHR is possible if the coating is not porous. Results in an uncooled silicon nitride engine (Kawamura et al., 1992) have continued to show undesirable combustion effects similar to those experienced with porous coatings. The important Army need, to better understand heat transfer in LHR engines, has thus continued throughout the reporting period.

Because of the unique fluid mechanics and transient pressure in engines the boundary layer structure is not understood to the extent that it is for other interior flow convection applications. Such an understanding was not required for empirical global correlations, but is necessary for models to be used in CFD codes. To gain such an understanding is thus an important need which requires the application of new methods of measurement to the engine problem.

While many of the needs outlined above still remain, much progress was made on these needs by the ERC. This progress is given below and includes: new measurement methods for both total and radiation heat flux in engines; the application of optical measurements to exploring the boundary layers in engines; measurements of heat flux in engines, including LHR engines; new subgrid models formulated and incorporated in the CFD code KIVA; the validation of CFD models for predicting engine heat transfer; and the application of the CFD code to issues where heat transfer plays an important role.

### Diagnostic Methods

The diagnostic methods discussed here can be divided into three broad categories. First, are measurements of the total and radiation fluxes at the solid surface. Second, are measurements of the gas boundary layer characteristics for convection. Third, are the measurements of flame temperature and soot concentration for understanding the radiation source. The first two will be discussed in this section, the third is discussed in the section on combustion.

### Surface Flux Measurements

Conventional measurements of total surface flux carried out prior to 1985 are covered in the review by Borman and Nishiwaki (1987). Most of the prior work utilized thin film coaxial thermocouples. These conventional coaxial surface thermocouple when used with an outer material matching the engine wall (iron), a very small inner wire, and a very thin (1  $\mu\text{m}$ ) film matching the inner wire composition can give excellent results. [Reversing the film composition can, however, cause significant errors

(Assanis, 1989)]. However, the problems with such probes are; (1) application to ceramic surfaces, (2) computation of the steady state flux, (3) the large amount of noise caused by the large signal amplification required, and (4) the effects of surface deposits. The first problem can be overcome by application of an overlapping thermocouple film design (Huang and Borman, 1987), but this does not solve the other problems.

Application of a very thin platinum resistance film (RTD) with silver leads has been shown to work well for ceramic surfaces in engines (Boggs and Borman, 1991); (Reid and Martin, 1991). The use of the resistance measurement and a bridge allows very accurate signal recording, free of noise problems. The signal can be brought out by use of wires attached to the silver leads and led out through holes in the engine surface or for measurements on the head or liner the silver leads can go out through the head gasket. The application to metal parts requires an electrically insulating layer to be applied between the metal surface and the transducer films. To obtain an acceptable resistance the platinum film surface must have an aspect ratio of at least two. This places some restrictions on minification, but nevertheless allowed Boggs to produce sensors of 0.4 by 0.8 mm with seven such sensors placed in a line of 7 mm overall length. It is interesting to note that with small spacing between two sensors they may also be used as an ionization gap for sensing of the flame (Reid and Martin, 1991).

While use of the RTD sensor gives good transient temperature values it does not solve the problem of determining the steady state flux. Application of a single second sensor, a small distance behind the surface sensor, is known to be inaccurate. If the two sensors are very close, the effects of three dimensional conduction are small, but the relative measurement error becomes a problem, because the temperature difference between sensors is very small. If they are a large distance apart, the one dimensional approximation is not valid for engine applications. This problem can be solved by application of multiple sensors applied to the surface. Using an array of five surface sensors plus one internal sensor greatly reduces the error. Application of this concept by Lin and Foster (1989) showed that the steady state flux error could be greatly reduced at high loads, where three dimensional conduction effects became important causing errors of about 70% when using only two sensors.

Combustion chamber deposits which cover the sensor surface can cause a amplitude and phase difference which confounds measurement of the gas-side flux. However the effects of head deposits in clean burning (low emissions) diesel engines was found to be small (Lin and Foster, 1989) and negligible for high temperature ceramic surfaces (Huang and Borman, 1987). The effect for the piston surface is not established. It is interesting to note that the combination of infrared sensing, as discussed below, and surface sensors could answer this question directly (Anderson et al. 1980).

Measurement of the surface temperature from its infrared radiation emission is possible if the surface can be viewed through a clean window, if the intervening gas is transparent, and if radiation coming from other surfaces directly or by reflection can be neglected. To obtain time resolved engine data the detector system must have fast response. Use of a video system allows collection of a 2-D image, however it is necessary to use a method of ensemble averaging, a collection of rapid scans to build up the image. A system of this sort was made available through TACOM (Shepard and Sass, 1990). To utilize the TACOM/Shepard system a small spark ignited side-valve

Briggs and Stratton utility engine was modified to allow viewing of the piston top through a window in the head (Moore, 1990). Because of the long wave lengths of the IR the window was made of zinc sulfide with a yttrium oxide coating on each side. Samples of various materials could be placed on the piston for testing. Tests with premixed methane and air combustion showed that the system could give spatially resolved data, but only when a flame was not present. During combustion the hot product gas radiation (from CO<sub>2</sub> and H<sub>2</sub>O) blocked the view of the piston. The result did however give an ensemble averaged history of the flame front passage. In order to bypass this problem a second experiment was conducted in which the window contained parallel stripes of platinum films on the cylinder side surface. Because the films were very thin (less than 1 μm) the recorded temperature of the film backs could be taken the same as that of the gas side window surface. In addition, identifying stripes were put on the piston to determine if it could be detected during combustion.

The instruments discussed thus far enable measurement of the surface temperature. Conduction calculations then allow prediction of the unsteady component of the surface flux. A portion of this flux is due to convection and during diesel combustion a portion is due to radiation. Only a few measurements of the radiation flux are available and prior to the work of Yan and Borman (1989) all had been taken by measuring the flux on a surface behind a window. In addition, the data were taken for older engine designs with high particulate levels. The instrument fabricated by Yan uses a Lucalox tip with a geometric design that collects the radiation over a full hemisphere. Thus the full hemisphere of radiation flux could be obtained. The modification to the engine was minimal, as shown in Fig. 7.3.1. A fault of the

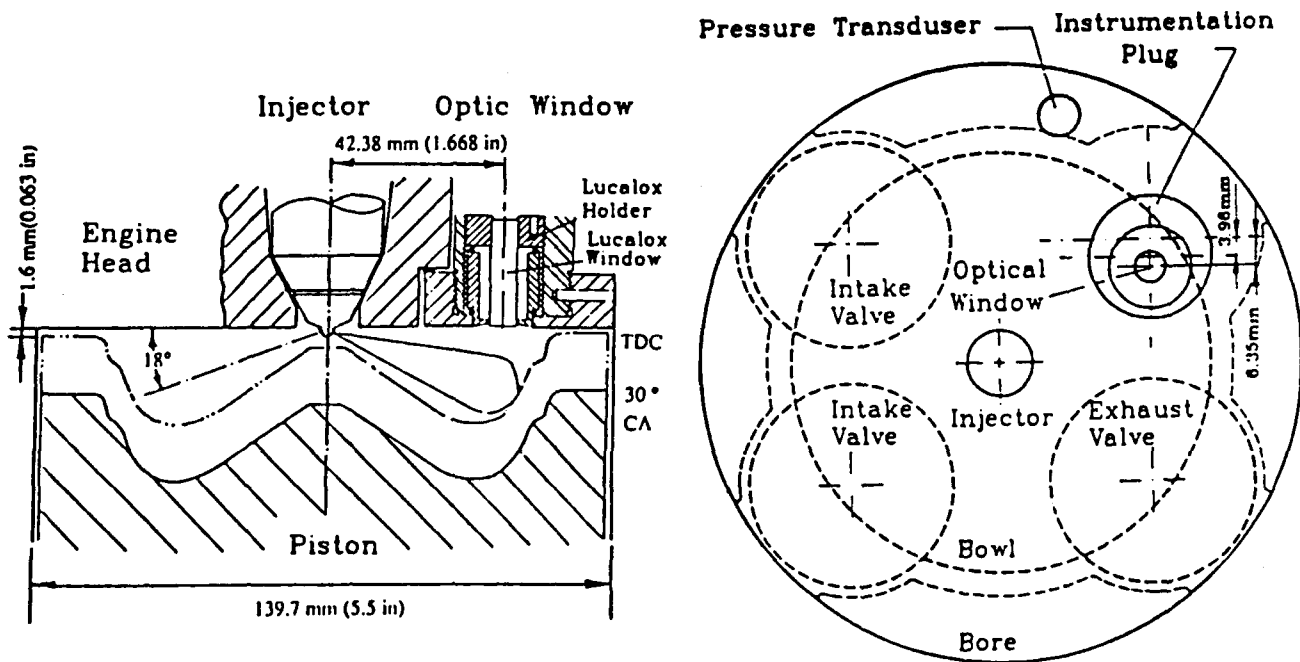


Fig. 7.3.1. Cross-Section Instrument Position in Head and Its Position in Relation to the Piston.

Location of the Radiation Instrument in the Modified Head (Top View).

instrument was that it ran too cool to prevent some deposit formation. Thus the instrument required calibration. This might have been avoided if a small tip of Lucalox had been attached to a sapphire rod or sapphire fiber bundle thus allowing the tip to run hot while still providing a sufficient signal. Because such a method of attachment was not achieved, the entire rod was made of Lucalox. The internal reflections within the Lucalox which allow the instrument to work properly then also cause most of the signal to be lost through the sides thus requiring a higher diameter to length ratio rod than desirable for maintaining a hot tip. Despite the need for calibration, the instrument was successfully used to obtain radiation flux histories which are discussed later.

### Overall Balances

Because of the large spatial variation of heat flux it has been difficult to obtain enough surface measurements to characterize the total cylinder heat transfer. Infrared imaging is not always possible due to lack of windows. Measurements of pressure, however, allow calculation of the molar-averaged-temperature by use of the ideal gas equation, provided that the mixture molecular weight can be estimated. Using the molar-average-temperature, the internal energy can be estimated. The work term can be calculated directly from the pressure and cylinder volume. An energy balance then gives an approximation to the heat transfer for the entire system. Because of the heterogeneous nature of the combustion, it is difficult to estimate the composition during combustion, but the balance can be made between the time prior to injection and the time after the end of combustion. Even then, many factors such as the estimated trapped mass, the inaccuracy of the pressure measurement and its phasing, and mass loss due to blowby, and incomplete combustion, make the calculated global heat transfer inaccurate. It does, however, provide a means for establishing trends with engine parameters and comparing various LHR constructions Mueller et al. (1990).

### Results From Experiments

In the following sections results are given for measurements of motored engine convective heat transfer and fired engine convection and radiation heat transfer. These results come from applications of the various measurement methods described above.

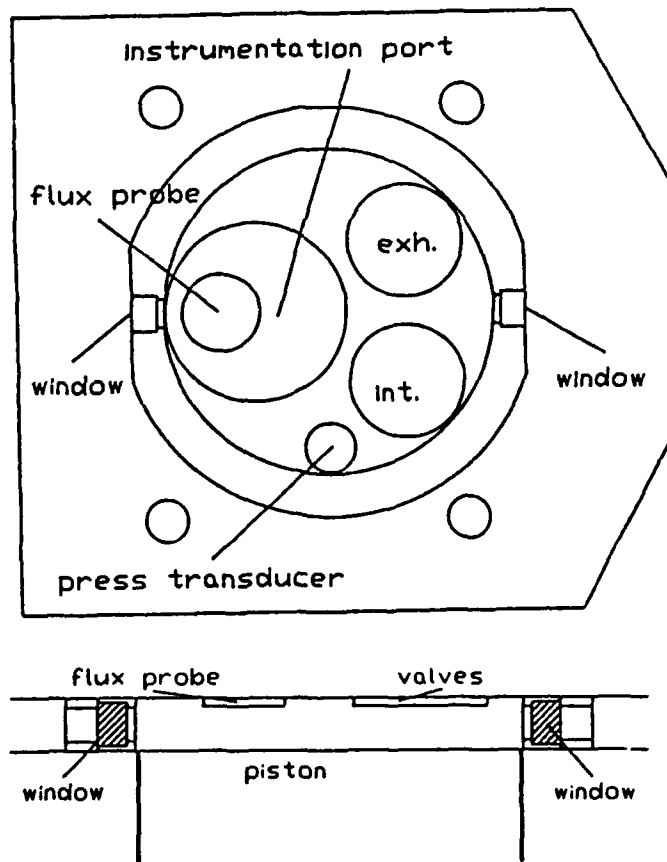
### Motored Engine Results

Two different engines were used to generate the data reported here. The first engine is designated as the "GM Triptane Engine" and has considerable optical access. Table 7.3.1 gives the engine specifications and Fig. 7.3.2 and 7.3.3 show the head and clearance volume, respectively. The engine also has a Bowditch-type see-through piston. The instrumentation port was used to measure surface temperature from which the instantaneous heat flux was calculated using a one-dimensional conduction model. The surface transducer used was a J-type thin-film surface thermocouple. The probe surface protruded down 2 mm below the head surface to allow use of line-of-sight speckle interferometry measurements of the near-wall gas temperature gradient.

Table 7.3.1 Engine Specifications

Engine Specifications

Engine:	GM Triptane
Bore (mm)	91.9
Stroke (mm)	76.2
Displacement (cc)	505
Clearance volume (cc)	63.8
Compression ratio	8.92
Swirl ratio	variable with intake valve position
Valve Timing:	
Intake opens	40 deg BTDC
Intake closes	100 deg BTDC
Exhaust opens	60 deg ATDC
Exhaust closes	80 deg ATDC



Side view of clearance volume

Fig. 7.3.2. Layout of cylinder head bottom view.

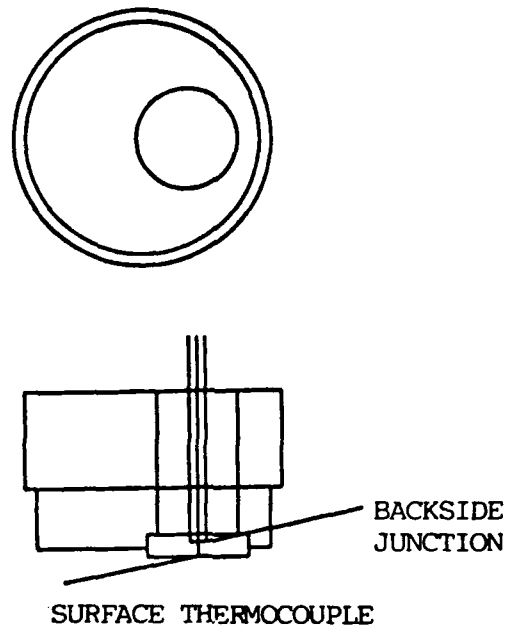


Fig. 7.3.3. Instrumentation plug with heat flux probe.

The objectives of the experiments using the Triptane engine were to generate information for the motoring case which could guide the modeling effort, supply data similar to what KIVA would supply to the subgrid near-wall model and provide validation for the subgrid model evaluation.

It was hoped to obtain data on the velocity and temperature behavior within the boundary layer to guide the modeling effort. Regarding such measurements, it must be recognized that the flow is very complex (being highly turbulent and never fully developed), that it has significant cycle-by-cycle variations, and that the boundary layer is very thin, especially for the important region near TDC. As a result, accurate measurements of the steep gradient region near the wall could not be obtained. Speckle data did give temperature profiles at the lower speeds (300, 750 rpm), which combined with an estimate of the viscous sublayer thickness,  $y_w$ , from

$$y^+ \cong 10 = y_w u^* / \nu$$

and data for the shear (friction) velocity  $u^*$  based on LDV data generated by Pierce (1991), gave reasonable agreement with experimental heat flux values. Figure 7.3.4 shows some of the profiles for the case of 750 rpm and high swirl [a swirl ratio of 2.6 at TDC, based on the velocity measure below the probe]. The LDV data of Pierce et al. (1992) could not resolve the velocity boundary layer for this case, but estimated that it would be 0.1 mm or less based on a boundary layer growing from the edge of the protruding plug. The LDV data indicate that for higher speed engine flows the turbulent structure persists very close to the wall surface, causing fluctuations in whatever viscous layer exists near the surface (Dao, et al., 1973). The measured relative

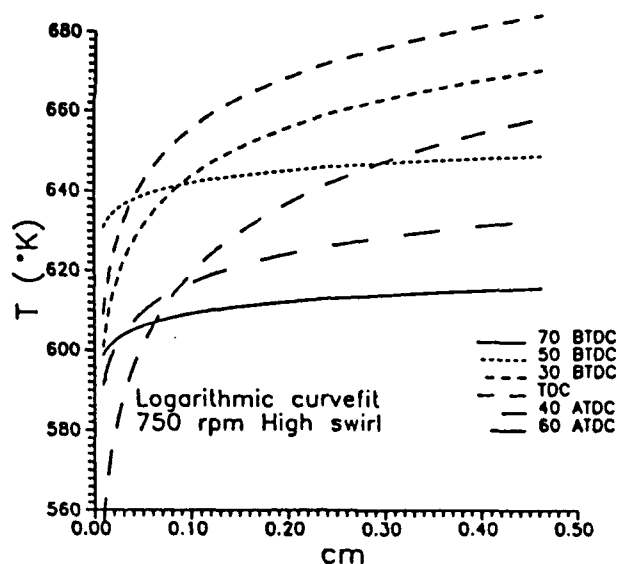


Fig. 7.3.4. (Yamada et al. 1989). Logarithmic fit to temperature data obtained by speckle method.

turbulence intensity at 4 mm below the plug surface was about 0.2 at TDC of compression. This value is more characteristic of an entrance or developing region than a fully established region, but that is to be expected given the unsteady nature of the outer flow. The structure of the near wall layer consists, in conventional theory, of much smaller scale disturbances than the outer layer where the eddies are thought to be elongated in the direction parallel to the wall surface. Given the difficulty of determining the nature for the boundary layer from direct measurement, a more detailed analysis of the wall flux itself was thought to be appropriate. Such a study was carried out by Boggs (1990) using a CFR engine. The study was motivated by the observations of Dao et al. (1973) in a motored engine, Boggs (1990) in both a spark ignited, and Lin (1988) in a fired open chamber diesel engine. They all found large rapid fluctuations of heat flux, during a single cycle which disappear when the data are ensemble averaged. Both Dao and Boggs showed that these fluctuations are connected to the turbulence level in the cylinder.

The head of the CFR engine used by Boggs was modified as shown in Fig. 7.3.5. The engine has the specifications listed in Table 7.3.2. The center of the instrument plug was at a radius of 28.6 mm. The engine could be run with a normal or shrouded intake valve. With the shroud, the maximum induced swirl is about 3 at TDC (Lancaster, 1976).

The plug contained seven  $0.2 \mu\text{m}$  thick platinum film sensors each  $0.4 \times 0.8 \text{ mm}$  and mounted 1 mm apart from center-to-center on a Macor substrate. The objective was to characterize the spatial variations of the observed fluctuations in heat flux during a given cycle.

Table 7.3.2 Engine Specifications

Engine specifications.

Bore	83 mm
Stroke	114 mm
Displacement	$0.62 \times 10^{-3} \text{ m}^3$ (0.62 L)
Compression ratio	Variable
Valve timing	Uses supercharge method cam
Intake	Opens 15° BTDC, Closes 50° ABDC
Exhaust	Opens 50° BBDC, Closes 15° ATDC

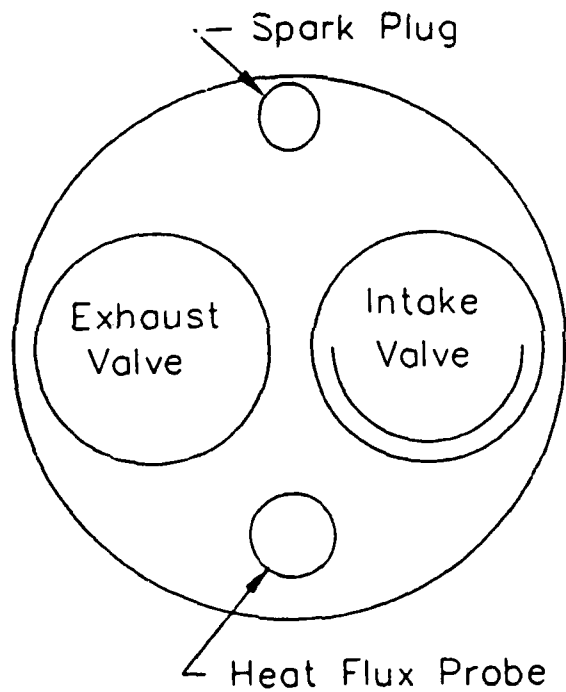


Fig. 7.3.5. Cylinder schematic - top view.

The ensemble averaged data are of interest because ensemble averaged equations are used in both thermodynamic modeling and in CFD models such as KIVA. As mentioned previously it is necessary to remember that the large scale (bulk) motions vary from cycle-to-cycle thus giving a bias which is difficult to sort out. Motoring data taken with an iron thermocouple plug consisting of five surface thermocouples in a cross configuration and 2.4 mm spacing showed no significant differences between the

ensemble averaged heat flux from couple to couple. This indicated no significant change in the boundary layer along the flow direction over a 5 mm distance. Flux data taken under spark ignited homogeneous mixture combustion with the seven RTD sensors or Macor also showed no significant amplitude difference for the ensemble averaged values over the 7 mm distance between sensors. [A small phasing difference was observed due to flame arrival time.] As might be anticipated, the Macor plug showed differences in the ensemble averaged peak flux from sensor-to-sensor during motoring when the temperature difference between the Macor plug and iron head was significant compared to the gas to head surface temperature difference. The sensor at the upwind location gave a 30% higher peak than the furthest downwind sensor, with a linear decrease over the seven sensors.

The single cycle data for each sensor contained significant higher frequency components similar to those noted by Dao et al. (1973). The heat flux signal for a given motored cycle at 1200 rpm with swirl are shown in Fig. 7.3.6. Note that sensors 1-4 correlate while the correlation between 1 and 5, 6, 7 is not as good. If there were no cycle-by-cycle variations in the bulk flow then the difference between  $q_i$ , the heat flux for sensor  $i$  on a given cycle, and the ensemble average value of  $q_i$  would define the

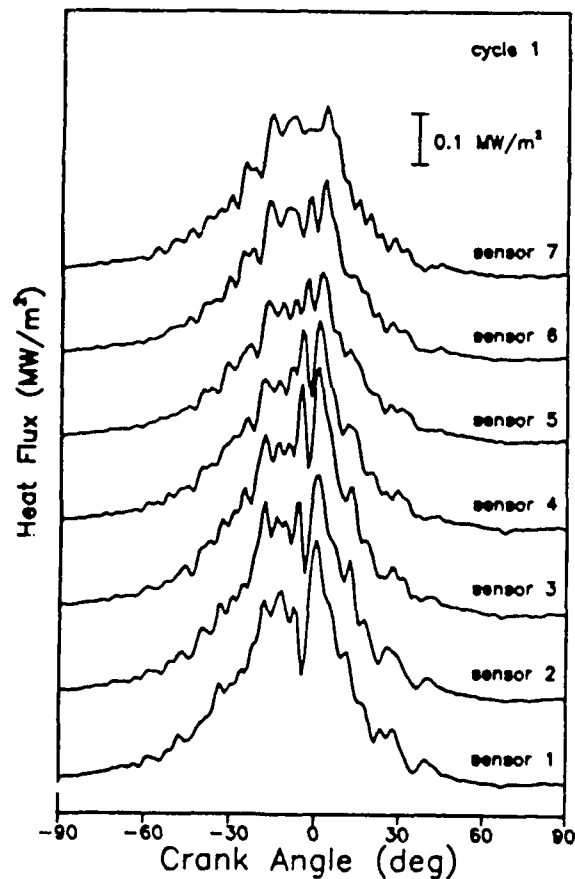


Fig. 7.3.6. Variation of the instantaneous heat flux for the seven RTD sensors.

intensity, the flux variation due to turbulent driven variations, as  $q_i' = q_i - \bar{q}_i$ . However, cyclic variations cannot be ignored. The best procedure might be to use conditional sampling if the outer flow velocity could be measured simultaneously with  $q_i$ . [Note that use of LDV or PIV would require seeding which would affect the heat transfer, and thus this was not done.] The method of low-pass filtering (at 300 Hz) of each record was thus used to define  $\bar{q}_i$  despite the problems associated with this method (Boggs and Borman, 1992). The resulting  $q_i'$  values were then used to define a cross-correlation coefficient with distance  $x$ ,  $R(x_i, x_j)$  and then a lateral heat flux integral length scale,  $L_q$ . Typically 1000 cycles of data were used to obtain  $L_q$  for a given condition.

A comparison of swirl and tumble flow data created by turning the shrouded valve is given in Figs. 7.3.7, 7.3.8 and 7.3.9. As seen from Fig. 7.3.9 the ensemble average heat flux swing is higher for the swirl flow as would be expected. However, the intensity is higher for the tumble flow. The much higher tumble flow intensity obtained by using the ensemble averaged value for  $\bar{q}$  can be explained by the fact that cyclic variations in the bulk flow which bias the result are much higher for tumble than for swirl flow. The filtered analysis gives a less biased comparison. The higher value of intensity for tumble flow versus swirl flow may be the result of early breakdown of tumble kinetic energy into turbulence. This breakdown is caused by the piston motion and peaks at TDC. Note that the tumble flow heat flux intensity peaks near TDC while the swirl flow heat flux intensity peaks about  $10^\circ$  before TDC, similar to the ensemble averaged heat flux values. The intensity values are only ten to twenty percent of the average values, which may indicate that fluctuations of the inner (viscous) layer are not a dominating feature, although they could play an important role in comparisons between various bulk flow effects on heat transfer. It should be noted that such

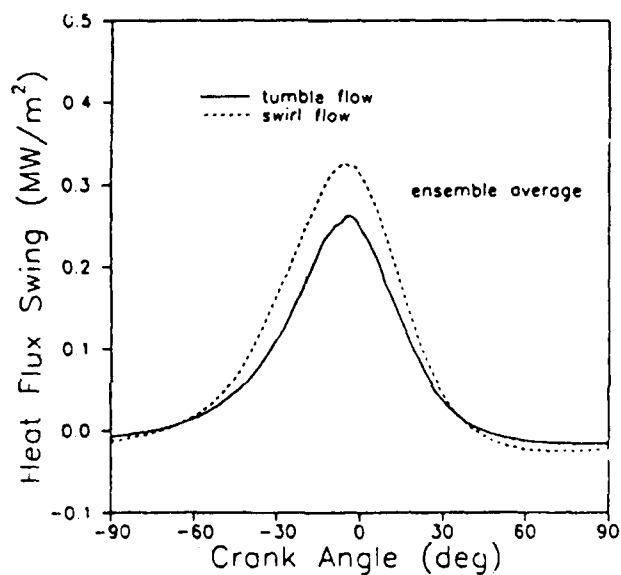


Fig. 7.3.7. Comparison of ensemble average heat flux for the shrouded valve producing tumble flow and swirl flow.

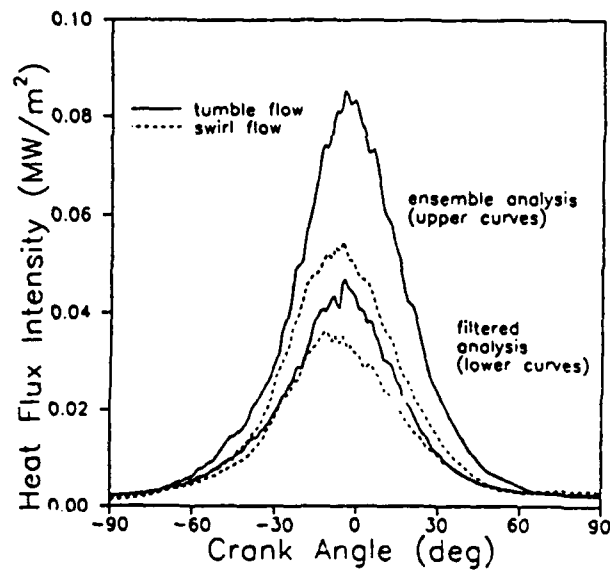


Fig. 7.3.8. Comparison of the heat flux intensities for the shrouded valve producing tumble flow and swirl flow.

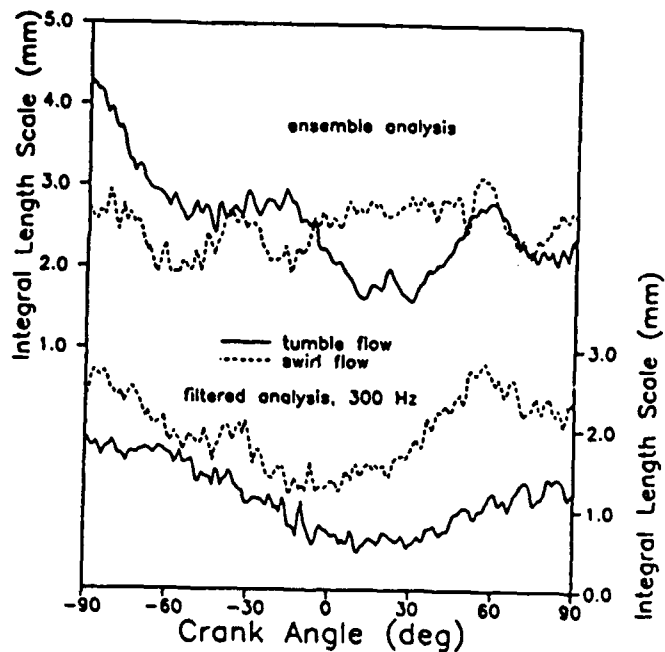


Fig. 7.3.9. Comparison of integral length scales for the shrouded valve producing tumble flow and swirl flow.

fluctuations have also been observed in turbulent steady flows (Armistead and Keyes 1988), and are thus not unique to engines. However, in engines the time scales of these fluctuations are less than an order of magnitude shorter than the significant engine time scale while they are much too high a frequency to be of interest in other practical problems.

Figure 7.3.9 shows the calculated integral length scales are of the order of 1 to 3 mm, very similar to the size as the integral length scales of turbulence in the bulk flow. The scale,  $L_q$ , was found to be insensitive to changes in compression ratio; a similar observation applies to the turbulent length scale of the bulk flow.

The observations from motoring data thus indicate a very thin velocity boundary layer which is stretched as in the case of favorable pressure gradients. These observations also indicate that further study of the engine boundary layer is needed to clarify its structure, but that new experimental methods may be needed which can be carried out simultaneously with heat flux measurements.

### Fired Engine Results

Total engine heat transfer was measured for the fired case in a CFR engine with homogeneous charge (HC) combustion for both spark ignition and compression ignition (CI), (Boggs, 1990); in a Cummins single cylinder NH engine (Lin, 1988) for both steady and transient fueling rates; and in a Ford ceramic diesel engine (Reid, 1991). The NH engine was also used to study the effects of plasma sprayed coatings by use of the energy balance method (Mueller, 1990) and for measurement of radiation heat flux (Yan, 1989). The work of Lin and Mueller was supported by the previously mentioned TACOM contract although some of the instrumentation and supporting staff time was supported by the subject contract. It should also be noted that both the Cummins and Ford engines were provided by the respective companies. The summary here will emphasize the work of Boggs, Reid and Yan. The works of Lin and Mueller are reported in the TACOM final report Borman et al. (1991) and are only briefly mentioned here.

The measurements of Boggs started by using homogeneous charge compression ignition (HCCI) combustion using the CFR engine described earlier (see Fig. 7.3.5 and Table 7.3.2). The concept of these first experiments was to ignite a hot, lean homogeneous charge by compression. Such combustion had been previously shown (Bair, et al. 1986) to be relatively free of cyclic variability and not to be dependent on turbulent flame propagation (so called "flameless" combustion). It was thought that such combustion would provide a decoupling of the fluid motions which influence heat transfer and the rate of combustion. Boggs thus carried out a series of experiments using an ethylene-air mixture and five surface thermocouples located in the instrument plug in the head. For this study the plug material was iron, to match the engine head. It was found that the original objective could not be achieved, because the heat transfer coupled to the combustion rate through the influence of the heat transfer on the mixture temperature level. Thus the decoupling of the combustion rate from the fluid motion was not achieved. Later analysis by Kong et al. (1992) indicates turbulence may also directly influence the rate. Thus the data could not by themselves be used to sort out the effects, but formed a bank of data useful for modeling validation. Such model

validation was in fact later carried out at the ERC by Kong et al. (1992) under a DOE/NASA contract.

The thermocouple array data showed that both motoring and HCCI combustion gave significant variations between closely spaced sensors. As discussed previously, this led to development of an array of RTD sensors on a Macor plug. This instrument was then used to measure heat flux and flux length scale,  $L_q$ , under HCSI conditions. Figure 7.3.10 shows the ensemble averaged heat flux from four of the RTD sensors, using 1000 cycles of data. The small phasing differences are believed to be caused by the differences in flame arrival time at each sensor. Figure 7.3.11 shows the data over a larger crankangle interval and illustrates that such RTD sensors might be used to study details of heat transfer even during gas exchange. The ensemble averaged data show a monotonic decline after the rapid rise due to flame arrival, but the individual cycle data each show large, rather rapid, fluctuations starting about  $5^\circ$ - $10^\circ$  ( $0.7$ - $1.4$  ms) after flame arrival. These fluctuations cause a peak in the intensity that is located at about  $15^\circ$  atdc. Length scale,  $L_q$ , is decreasing in this region, but begins to increase again at about  $30^\circ$  atdc. It is thought that this increase in scale may be due to the high viscosity of the product gas which will rapidly dissipate the smaller scales. Comparisons of hot motored and fired cycles obtained by skip firing show the fired and motored scales are very similar before flame arrival, but that have opposite trends after flame arrival. Note that in both cases temperature and density are dropping due to expansion in the time after peak pressure, tending to increase the scale, but apparently the high product gas viscosity dominates for the fired case. Thus both motored and HCSI combustion show turbulence effects penetrating to the wall, but combustion can induce both additional intensity and changes in scale in the aftermath of the flame.

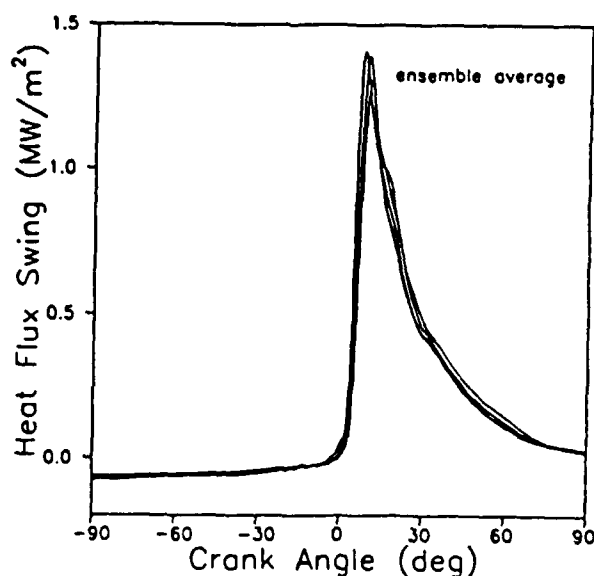


Figure 7.3.10. Ensemble average heat flux from four RTD sensors under SIHC conditions.

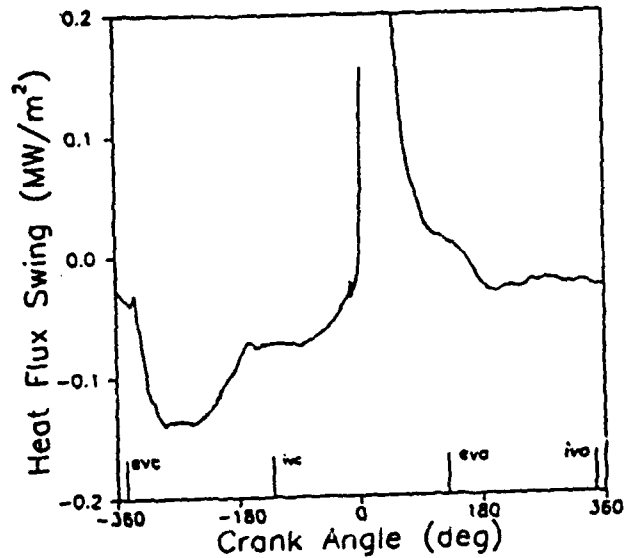


Fig. 7.3.11. 100 cycle ensemble average heat flux trace under SIHC conditions showing details during the gas exchange processes. The peak value of  $1.4 \text{ MW/m}^2$  is not shown on the graph.

In diesel combustion the flame may not always reach the surface because the layer next to the surface may be too lean or too rich to burn. It is also possible that for LHR diesel engines with very high surface temperatures combustion may sometimes originate at the surface. This observation, plus apparent increases of peak heat transfer led Woschni, et al. (1987) to propose that increasing surface temperature above a limit of about 1000 K increases the convection coefficient. This conclusion is confounded however by effects of surface porosity and changes in combustion at high temperature, both of which can also alter the heat flux. The work of Mueller (1990) compared an NH engine with and without a sprayed zirconia surface and showed increases in heat transfer during the combustion period for the coated engine, but the combustion was also significantly different. This led Mueller et al. (1990) to decide that no conclusion could be drawn concerning which effects dominated.

In yet another attempt to look at the LHR question, Reid used a silicon nitride engine head on an 0.4 liter experimental Ford single cylinder diesel. Heat flux was measured at seven head locations by use of platinum film RTD's. Figure 7.3.12 shows the flux at the seven locations indicated on the figure. Reid ran three loads, but even the highest load condition of 0.49 equivalence ratio and 1200 rpm did not give high flux levels, because the engine was naturally aspirated and the peak pressure was at  $12^\circ$  atdc giving an imep of only 0.6 MPa. The surface temperatures ranged from 814 K at position 3 near the intake valve to 573 K at position 4 near the liner and a 4 mm dia. pressure transducer port. Flame arrival measured by use of surface ionization gaps at

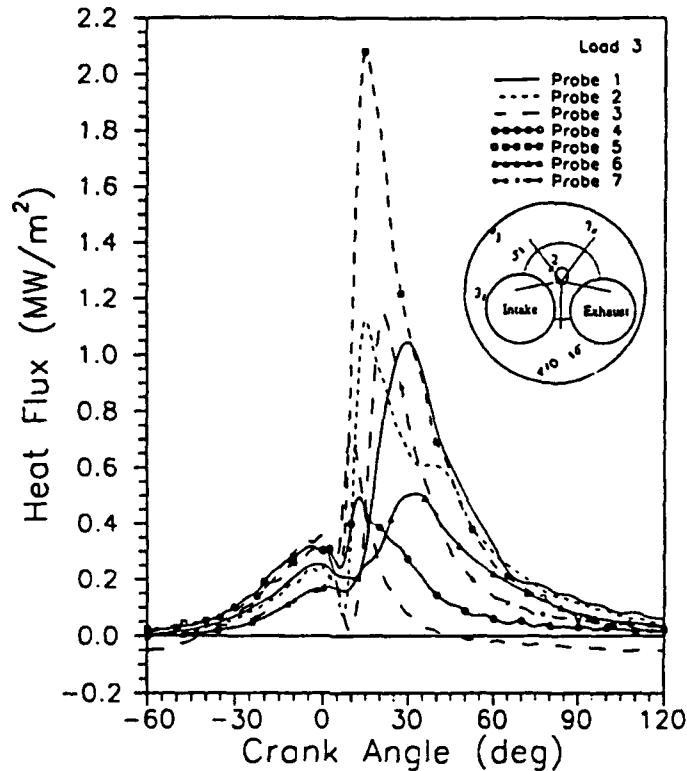


Fig. 7.3.12. Total surface heat flux for all locations at Load 3; equivalence ratio 0.49, imep = 603 kPa, rpm = 1200. (Runs 3, 4, and 7).

locations 5, 6 and 7 was consistently first at 5, then at 6 and last at 7 for all loads. For the highest load the arrival times were 7.25, 7.50 and 8 crank degrees. [Note that position 7 is closer to the piston bowl lip (12.8 mm) than is position 6 (17.9 mm), but 7 is closer to the bowl center than is 6.] In each case the start of the rise in flux about matches the flame arrival, but the peak flux time and magnitude seem to be dominated by fluid mechanical considerations. In particular, position 5 near the bowl lip gives the highest flux peak. The start of the rise for position 4 is early and corresponds to outflow from the pressure transducer port rather than flame arrival. Surface temperature apparently had a minor influence on peak flux as compared to the turbulence and combustion effects, as illustrated by position 3 which had the highest temperature, but a relatively low peak flux. Because of its high temperature this position had a cycle averaged flux of  $-0.082 \text{ MW/m}^2$ , as compared to position 2 which had a temperature of  $187^\circ$  lower and a average flux of  $0.136 \text{ MW/m}^2$ . Unfortunately, the ability to go to higher loads was impaired by concerns for the head strength. The engine has been replaced by a more advanced design, all silicon nitride combustion chamber engine and research is continuing under a contract with Isuzu Ceramics Research Laboratory.

### Radiation Data

The hemispherical radiation instrument previously shown in Fig. 7.3.1 was used by Yan (Yan and Borman, 1989) to obtain radiation data for a range of equivalence ratios at 1500 and 1900 rpm and intake pressures of 130 and 201 KPa. The instrument gathers the incident flux over the whole hemisphere of incident directions. In principle the radiation could be integrated over the range of transmitted by the instrument. A more practical method is to measure the radiation at three wavelengths; 0.55, 0.70 and 0.8  $\mu\text{m}$  were used in this work. These data along with a blackbody calibration of the instrument and the Hottel-Broughton equation to obtain the effective flame temperature ( $T_f$ ), the extinction coefficient ( $K_L$ ) and the total emissivity in ( $\epsilon$ ). The flux was then calculated from

$$q = \epsilon \sigma T_f^4$$

where  $\sigma$  = Stefan-Boltzmann constant.

These four quantities are shown in Figs, 7.3.13, 7.3.14, 7.3.15, and 7.3.16, for the three equivalence ratios shown at 1500 rpm and 201 KPa intake pressure. Part of the change in temperature with load is due to changes in injection timing built into the P-T injection system. Measurements within a 14° cone straight down from instrument and at the piston bowl edge were similar to those shown at the high load and decreased by only 40°C when the load was decreased. This is because there is a hot flame zone below the window for all of the equivalence ratios, but the flame zones fill less and less of the chamber volume as the equivalence ratio is decreased.

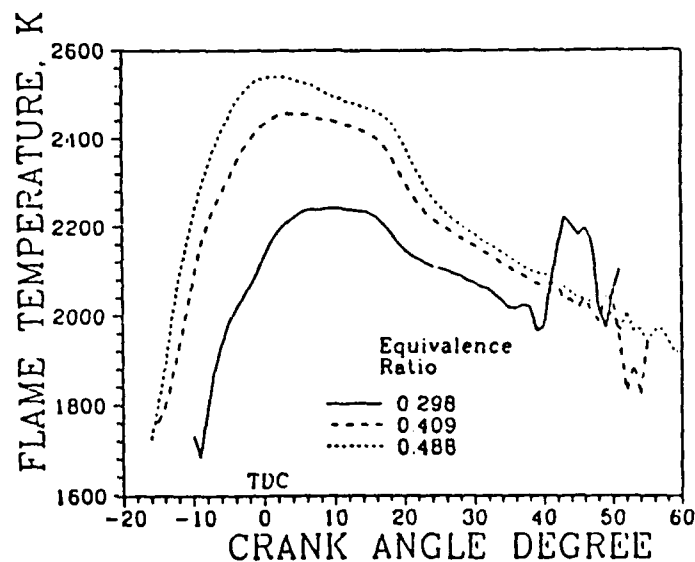


Fig. 7.3.13. Flame temperatures at different equivalence ratios at 1500 rpm (Runs 3, 4, and 7).

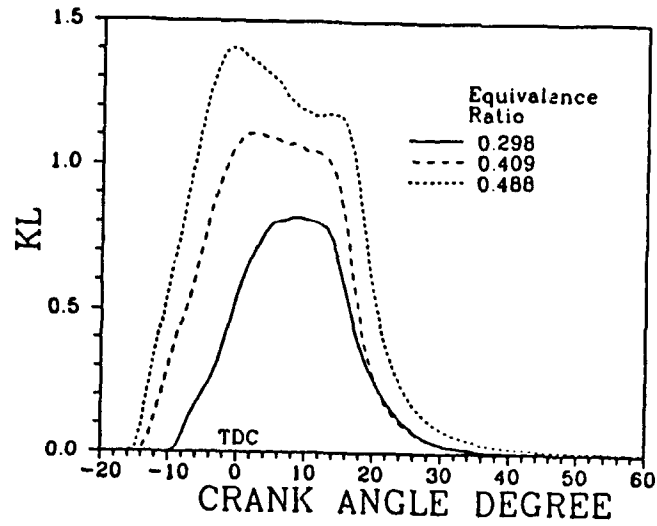


Fig. 7.3.14. Extinction Coefficient, KL, at Different Equivalence Ratios at 1500 rpm (Runs 3, 4 and 7).

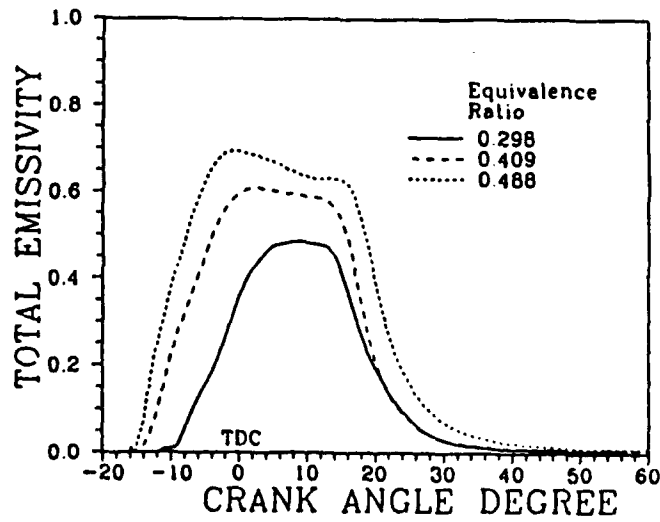


Fig. 7.3.15. Total Emissivities at Different Equivalence Ratios at 1500 rpm (Runs 3, 4, and 7).

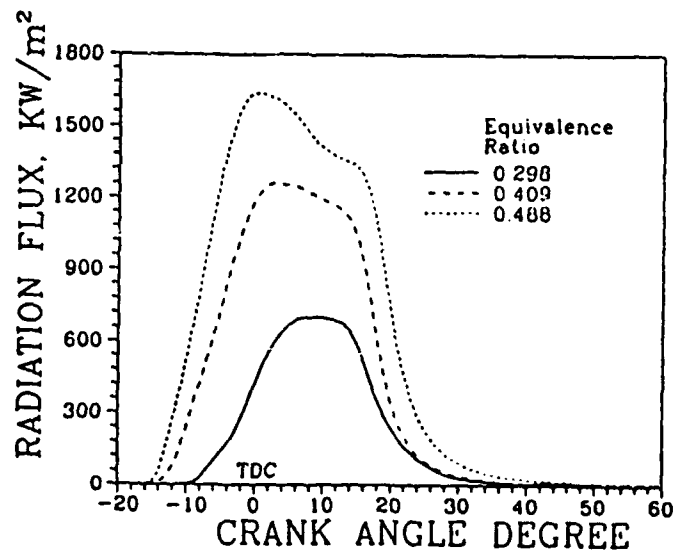


Fig. 7.3.16. Radiation fluxes at different equivalence ratios at 1500 rpm (Runs 3, 4, and 7)

Because of the difficulty of obtaining a hemispherical probe design which will stay clean, it would be desirable to predict the flux from a narrow beam line-of-sight probe which can be designed to stay clean (Yan and Borman, 1988). By using an equivalent mean optical path length for the entire gas volume and the narrow beam data of Yan and Borman (1988) hemispherical flux can be estimated. Figure 7.3.17 shows the measured and estimated flux values for the 0.4 equivalence ratio. Also shown is the total radiation and convection heat transfer at this location. The radiation peak is about one-third of the total flux peak. The time average radiation flux is 5 to 15% of the time average total heat transfer and increases linearly with fuel injected per cycle. The lower relative importance of radiation here as compared to previous data is the result of turbocharging and a low emissions engine design. One expects that for LHR engines the radiation may double while the convection decreases by a similar factor. This would result in radiation being about 40% of the total flux and a net reduction in heat transfer of only 30%. It is thus important that LHR engines are designed to reduce soot formation in order to reduce radiation. Increased soot oxidation during the latter part of expansion, which reduces soot emissions, would be unlikely to reduce radiation.

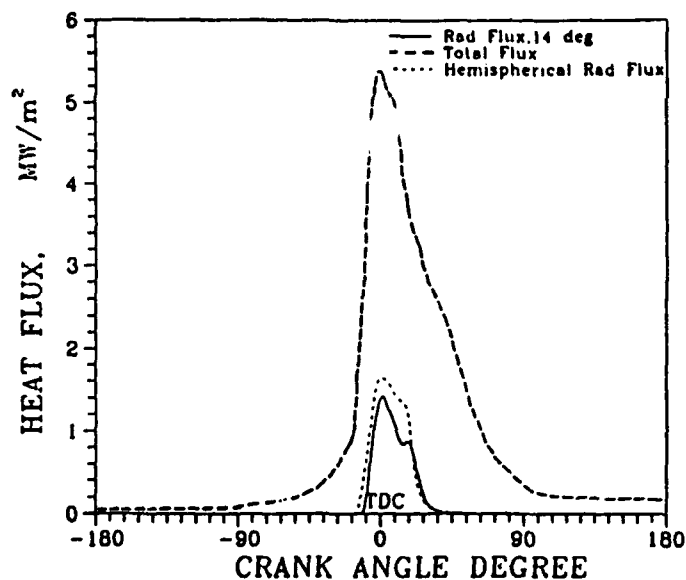


Fig. 7.3.17. Comparison of radiation flux for run 4 with total flux (10).

### Modeling of Engine Heat Transfer

For diesel engine combustion chambers a model is needed for both convection and radiation. As just shown, radiation for normally cooled engines with low soot production has only a small influence on the average heat transfer, but contributes significantly to the peak heat transfer. It is unlikely that models for the radiation will be predictive until better models are available for soot formation. The ERC is currently working on obtaining models for soot which can be incorporated into CFD codes such as KIVA. Thus, during the period covered by this report radiation was measured experimentally, but no detailed models were attempted. The heat transfer modeling efforts were thus directed to convection.

Previous models for engine heat transfer have primarily been empirical correlations which attempt to predict the spatial average flux as a function of mean thermodynamic properties such as pressure and average density. These models tend to work reasonably well in predicting trends of speed and load, but typically are not very accurate unless adjusted by use of data from the specific engine being modeled. To be predictive and to give spatial resolution, it is undoubtedly necessary to have models which can be used in CFD codes. For such models to work well the CFD codes themselves must become most accurate in their representation of intake flows, turbulence and combustion.

To be successful, the heat transfer models must incorporate all the essential physical parameters of the energy transport process. As shown previously, the

boundary layer is very thin, the turbulence is intense and because of the heterogeneity of the flow and combustion, the spatial variation is very significant and complex. Despite this complexity, the model cannot be too expensive to implement if the CFD code is to be used in design practice. This implies that a subgrid model should be used to bridge the boundary layer rather than a full numerical solution of the boundary layer. The model typically used has been the "law-of-the-wall" (LAWAL) model. This model does reasonably well considering its many shortcomings when applied to engine heat transfer. Table 7.3.3 lists these inadequacies which arise from the fact that the LAWAL model is based on steady nonreactive fluid data from simple flows, such as pipe flow. Two approaches to improving the LAWAL model were implemented. In the first method Yang and Martin (1989) solved the one dimensional unsteady energy equation given by

$$\rho C_p \frac{\partial T}{\partial t} + \rho v C_p \frac{\partial T}{\partial y} = \frac{\partial}{\partial y} \left( (k + k_t) \frac{\partial T}{\partial y} \right) + \frac{dp}{dt}$$

with the following assumptions:

- (1) Derivatives parallel to the wall are assumed zero.
- (2) The relationships relating turbulent viscosity to the molecular viscosity for steady-state, turbulent, incompressible flow apply.
- (3) The pressure is uniform, but a function of time.
- (4) The gas thermal conductivity is proportional to gas temperature.
- (5) The gas is ideal.
- (6) No chemical reactions or inhomogeneity.
- (7) The relationship between  $k_t$  and  $\mu_t$ .

$$k_t / k = (Pr / Pr_t) (\mu_t / \mu)$$

where  $Pr_t$  is taken constant; a value of 0.91 is typical.

- (8) An empirical expression obtained from a fit of literature values for turbulent incompressible flow was used to relate  $\mu_t$  to the distance through the boundary layer.

$$\mu_t / \mu = 0.41 y^+ [1 - \exp(-0.0492 y^+)]$$

where

$$y^+ = \left( u^* / \mu_w \right) \int_0^y \rho dy$$

$\mu_w$  = viscosity at  $y=0$

$u^*$  = friction velocity

The friction velocity may be related to the velocity at the edge of the boundary layer through an empirical relationship, for example, by use of the 1/7 power-law model. However, Reitz (1991d) found that for computations with CFD code KIVA the relationship

$$u^{*2} = 0.3 K,$$

where  $K$  is the turbulent kinetic energy at the outer edge of the boundary layer, gave a much better match to heat flux data for an HCSI engine. The model equations were

solved numerically for a step change in pressure and the results curve fit to simple functions. By employing Duhamel's theory, the instantaneous surface heat flux can then be calculated for an arbitrary pressure history

Table 7.3.3

Inadequacy of Law-of-Wall Model

Engine (unknown model)	Tube (law-of-wall)
Nonsteady	Typically steady
Inflection points in temperature gradient	Temperature gradient monotonic
Core flow complicated, 3-D	Flow 2-D, simple
Compressible, $dp/dt$ large	Incompressible
Surface temperature varies with time and position	Surface temperature constant, uniform
Turbulence may penetrate to wall	Laminar sublayer
Pressure Waves	Uniform pressure gradient
Chemical reaction	No reactions
Spray Impingement	No two-phase effects

A modified wall function method (MLAWAL) was used by Huh et al. (1990) to account for compressibility and energy release due to chemical reaction as source terms in the energy equation. For motoring the source term is  $S = -dp/dt$ . This formulation gives modified expressions for the dimensionless temperature profile which collapse to the original log-wall expressions when the source term is neglected. Thus for strong turbulence and small  $dp/dt$  the MLAWAL is the same as LAWAL. In motoring data comparisons where pressure gradients are small, such as in a pancake shaped chamber, the LAWAL underestimated the flux, the MLAWAL peaked too early and the approximate solution of Yang and Martin gave the best result. As expected, for motoring with a deep bowl the LAWAL and MLAWAL gave similar results for low speed data (900 rpm) where  $dp/dt$  is small. However, for this case the approximate solution of Yang and Martin overestimated the peak flux by almost a factor of two. In a later paper Chang and Martin (1991) included the effects of pressure gradient in the MLAWAL approach and found better agreement with the deep bowl data.

It must be recognized that even for the motored case the data currently are inadequate to properly access the models. For the case where velocities were measured (Yang et al., 1988) the agreement between the data and the approximate solution model was excellent. In order to test further, it is suggested that validation of current inflow CFD calculations is vital. Once this is done and the resulting predicted cylinder velocity and turbulence after compression are verified, the heat flux models can then be validated. For the case of combustion, Reitz (1991d) has shown agreement to within 20-

30% for HCSI combustion in a pancake chamber. However the results are still confounded by the flame propagation model and the neglect of chemical reaction in the boundary layer when using the Yang and Martin model.

The case of diesel combustion is difficult to validate because the spray and combustion models are not yet validated. However, it is possible to use the models to help understand some of the effects of interest. This was done by Yang and Martin (1990) using their model, but now including an arbitrarily distributed heat release in the boundary layer. Using this approach they assumed that the boundary layer contains a quench zone with no heat release and that all other cells including the remaining portion of the boundary layer cells have a heat release which is uniform and thus equal to the heat release obtained from a single zone model. This approach spreads the effect of chemical energy release in the boundary layer over time as opposed to a rapid deflagration of the mixture in the boundary layer. Thus the calculation does not give a worst case spike of flux, but does indicate a kind of spatial average case. We have noticed in previous work (Van Gerpen et al., 1985) that if the head receives some liquid fuel from a too wide injector tip hole angle there will be a very narrow and high spike in the heat flux. This was associated with burning of the vapor near or at the surface.

In the calculations of Yang and Martin (1990) the quench distance was taken proportional to  $p^{-0.76} T_w^{-0.85}$  following the formula for lean mixtures of Friedman and Johnson (1950). For the engine conditions modeled, the minimum value was 14.4  $\mu\text{m}$  for  $T_w = 1023 \text{ K}$  (750°C) and about 30  $\mu\text{m}$  for  $T_w = 433 \text{ K}$  (160°C). Figure 7.3.18 shows a comparison for these two wall temperatures and also shows the effect of variation of quench distance ( $y_d$ ) with constant  $T_w = 1023 \text{ K}$ . Note that an increase of peak flux takes place as  $y_d$  decreases, and that the decrease in flux between 750°C and the 160°C wall is minimal. However, the quench distance must be of the order of surface roughness (less than 1  $\mu\text{m}$ ) to cause the higher  $T_w$  to have the higher heat flux. It should be recalled that quench distance increases with increasing turbulence intensity and thus the very small values are unlikely. For very thin quench layers the model predicts that the effect of wall temperature on peak flux is small and the 750°C and 160°C walls have the same peak flux. It must be noted that these comparisons assume the combustion is unaffected by the hot walls, which is not the case. In actual engines the effects of insulation on trapped mass and combustion rate confound the effects of surface temperature on heat transfer.

### Model Validation

None of the models have been sufficiently validated to determine if they are predictive over a wide range of engines and engine conditions. It appears that the model of Yang and Martin (1990) can give very good results when applied to either motored, HCCI, or HCSI engines for cases with small pressure gradients. For cases with large squish flows the model may over predict and a MLAWAL model which incorporates pressure gradients such as that of Chang and Martin (1991) may be needed. It is too early in the modeling of diesel combustion to determine the validity of the heat transfer models.

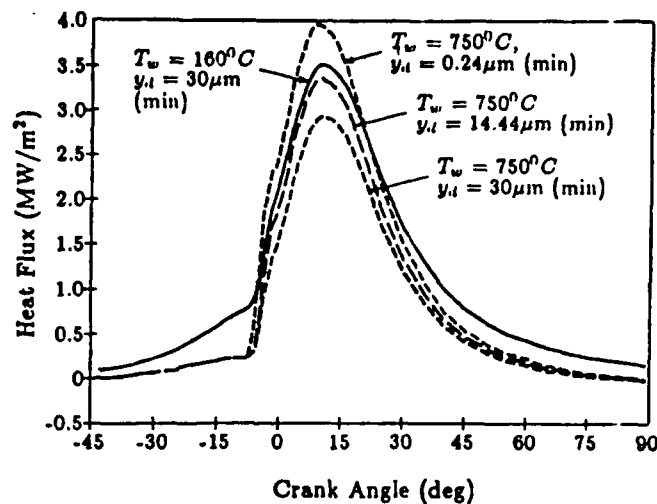


Fig. 7.3.18. Total heat flux at low and high wall temperatures with variations in quenching distances.

#### Impact of ERC Heat Transfer Research

A major impact of the research was the development of new measurement techniques which allow measurement of radiation and total heat transfer. These methods are currently being applied to a ceramic engine at the ERC and should allow gathering of a data base for LHR engines. A second major impact is the development of new models for use in CFD codes which incorporate significant corrections to the currently used law-of-the-wall models. The use of these models is still to be extended to design considerations, however they have a great potential for such use. Meanwhile the CFD codes can be run to try to obtain a better understanding of issues such as cold starting (Gonzalez et al., 1991) and wall temperature effects (Yang and Martin, 1990).

#### Unresolved Issues

Radiation modeling for luminous flames awaits the advent of a suitable spatially resolved soot model. Until this happens measurement techniques need to be used to determine the flux for LHR engines and other important applications. The effects of high surface temperature on heat transfer and combustion are still not sorted out and more experiments are required. The effects of liquid films on surfaces such as the piston under cold starting and the liner are not yet measured or modeled adequately. The piston to liner heat transfer requires additional data which combines oil film measurements and heat transfer (J. Myers et al., 1990). Such work is under way at the ERC using LIF methods for the oil film measurements. The work of Naber (1992) needs to be extended to determine fuel film effects for cold starting and possibly for small bore engines. Current models use ensemble average equations however such averages need to be related to single cycle behavior.

## 7.4 GAS-PHASE FLUID MECHANICS

### INTRODUCTION

The gas-phase fluid mechanics occurring in the gas exchange process and in the cylinder of an engine have a dominant effect on the combustion process and exhaust emissions. Because of this fact, gas-phase fluid mechanics in engines have been studied almost from the inception of the internal combustion engine. However, in spite of decades of research about the gas-phase flows in an engine, there remain many unanswered questions, and areas where there is little in the way of real understanding of the processes that are occurring.

It is appropriate to ask what it is that we need to know to understand the fluid mechanics in an engine, and how this knowledge addresses specific issues important to the Army. To produce a diesel engine that minimizes heat losses through combustion chamber surfaces, it is necessary to understand the mechanisms of transport very near the cylinder walls of an engine. This transport problem will be controlled by the local fluid mechanics. To produce an engine capable of starting at low ambient temperatures, it would be very helpful to understand the incylinder gas-phase fluid mechanics produced during the cranking process, since this will have an effect on the spray, vaporization, and fuel/oxidant mixing during the preignition stage and immediately after ignition occurs. One of the methods currently being considered to produce an engine capable of lower air flow for a given power density is to operate the diesel engine with higher equivalence ratios than is typical. In order to operate at higher equivalence ratios, better air utilization will be necessary, which will require gas-phase fluid mechanics that will assist in producing better air utilization.

The following is a summary of the research on gas-phase fluid mechanics in engines that has been performed at the Engine Research Center during the period of the first ARO Center of Excellence Award. Measurement of the near-wall gas-phase flows have been performed using Laser Doppler Velocimetry (LDV) and Particle Image Velocimetry (PIV). The objective of these measurements was to produce data that would assist in understanding transport that occurs near the wall in an engine. Measurement of the bulk incylinder flow behavior has been studied using the same methods, for the specific purpose of further examining the complex nature of the incylinder bulk flows, for improved understanding of how these flows contribute to mixing and cycle-to-cycle variations. Investigation of the valve jet flow was performed using a special rig and PIV for the purpose of observing how the valve jet flow interacts with the incylinder gas during the intake process. This description begins with a summary of the modifications and improvements made to the diagnostics for their application to engines. This is followed by a summary of research results for the near-wall flows, bulk incylinder flows, and valve jet flows.

### Diagnostic Methods

The behavior of the gas-phase flow near the chamber surfaces controls the engine heat transfer problem, especially in modern diesel and SI engines where radiation heat transfer tends to be small relative to convective heat transfer. Exhaust emissions are also likely to be strongly influenced by this flow. In a diesel where the injected fuel

impacts on the piston surface, such flows will influence the vaporization and/or mixing phenomena.

### LDV Studies

In order to produce accurate velocity measurements near the wall, a number of modifications were made to the LDV system. The measurement volume dimensions were limited to approximately 75 microns in diameter by 58 microns in depth, which was obtained with a combination of spatial filtering in the receiving optics and appropriate optics in the transmitter. To ensure accurate positioning of the measurement volume in the engine, rather than move the probe volume position by translating the transmitter, an extended probe volume was used. Then the receiving optics were translated to cover different parts of the probe volume. This allowed for a small measurement volume, with accurate positioning of the measurement region within the engine.

However, this study also revealed a phenomenon which may be troubling to all optically based measurements made near the wall in an engine. Figure 7.4.1 shows the position of a pin which was projected into the engine 1 mm from the wall. The upper picture was taken at Bottom-Dead-Center (BDC), while the lower picture was obtained at Top-Dead-Center (TDC). Note that for a surface that extends 1 mm into the chamber, there is no apparent movement in the image of the pin. However, when the surface of the pin was positioned within 0.5 mm of the wall, as shown in Fig. 7.4.2, the image translates because of index of refraction gradients near the wall. This was also observed in the LDV measurements, where it appeared that near TDC on compression, the scattered light incident on the detector came from a static surface, rather than the particles in the gas. This phenomenon of image shifting in the engine will likely be a problem for a near-wall measurements in an engine because unless the position of the measurement is measured or established dynamically, the actual region in space being measured will be uncertain. These results also indicate that measurements close to an extended surface will apparently not suffer the same amount of image shift, which should allow for accurate determination of the measurement region relative to the position of the extended surface. Large temperature gradients (and hence, index of refraction gradients) were observed above the protrusion by Yamada et al., 1989. However, the path of the scattered light from the measurement volume to the detector passed through a shorter region of steep gradients, because the large gradients in the path of the scattered light extended only across the surface of the protrusion. Scattered light passing beyond the edge of the protrusion was at least 2 mm above the rest of the cylinder head surface, thus there was little effect from wall-generated temperature gradients.

Finally, for measurements close to a flush surface in the combustion chamber, it was always observed that the image shifted towards the surface, as a result of the effect of the cold walls on the hot gas, which means that the measurements obtained while the engine is being motored are actually closer to the surface than the measurement position determined when the engine is stopped.

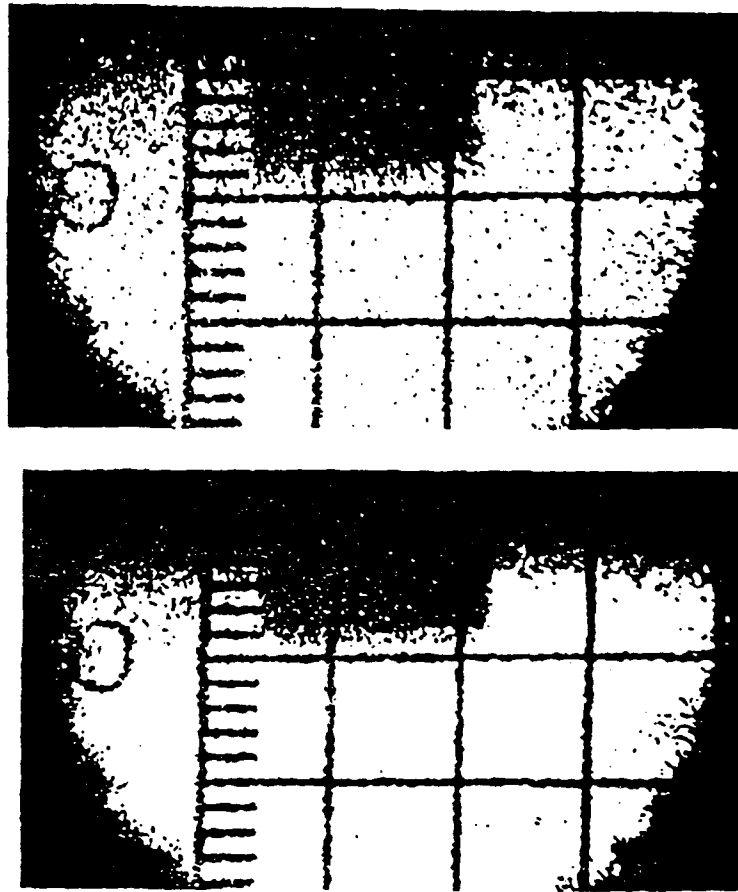


Fig. 7.4.1. Photographs of a pin protruding 1 mm from the cylinder head surface. Top photograph taken at BDC, lower at TDC, engine operated at 750 rpm, low swirl.

#### PIV Studies

Particle Image Velocimetry requires somewhat difficult-to-produce laser characteristics in that it is desirable to have high light power in each laser pulse (typically  $> 10$  mJ) with the capability for large variation in time separation between pulses. For future applications of PIV to engines, it will be necessary to have a laser system to allow for multiple sets of PIV exposures in a single cycle. To date, most PIV results have been obtained with solid-state lasers. Most common is the Nd-YAG laser. However, for several of the studies performed under URI funding, a copper vapor laser was used as the lighting source. Because the power output of the copper-vapor laser is approximately 0.2 mJ, it was necessary to develop methods of film processing that would allow for the acquisition of data with such low light levels. The use of the lower-power, higher repetition rate lasers has been pursued because of the desire to be able to acquire more than one PIV velocity record in a cycle, which is currently not possible with existing solid-state lasers.

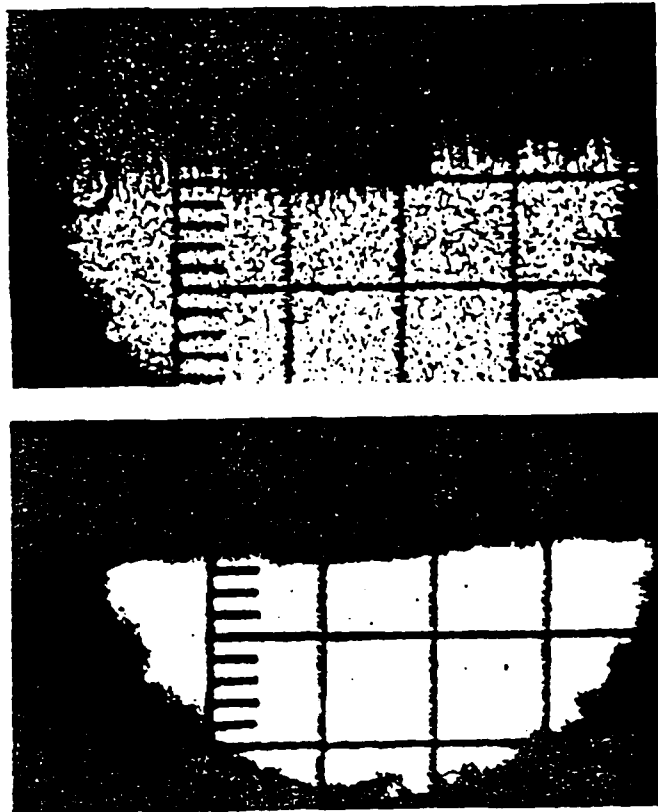


Fig. 7.4.2. Photographs of a pin protruding 0.5 mm from the surface of the cylinder head. Top taken at BDC, lower at TDC, engine operated at 1500 rpm high swirl.

Another method for PIV image acquisition has been under study at the ERC. In this method, rather than collecting light from particles at 90 degrees to axis formed by the incident light, the particles are imaged in a near-forward, or near-backward scatter perspective. Several advantages result from this method: Because of the approximately  $10^4$  increase in scattered light intensity, for a typical 35 mm film with unit magnification, this generates about a gain of 100-500 in exposure. This gain allows for the use of lower power lasers with the objective of producing cycle-resolved PIV results. The near-axis methods will not have as difficult requirements for optical access as the side-scatter or conventional PIV measurements, because only optical access is necessary only in one direction, rather than two.

The major issue with the near-axis scatter techniques is the definition of the measurement volume depth. For the side-scatter methods, the measurement volume depth is determined by the incident laser sheet thickness. With the near-axis methods, the measurement volume depth is determined by the optics of the collection system (typical a camera and lens) and the film processing methods.

The accuracy of the near axis methods are affected by out-of-focus particles which scatter light and distort the image of in focus particles. Work is currently

underway to quantify and establish criteria for particle number density effects on the accuracy of the near-axis methods. Results from one test which compared the results of LDV measurements, and side-scatter and near-forward scatter PIV results are shown in Fig. 7.4.3 (Martin, 1990). As illustrated, the results for laminar flow at the exit to a pipe were the same for all three methods.

Conventional methods of particle tracking identify individual particle trajectories as means of identifying the gas-phase fluid mechanics. In contrast, with PIV, a region in space is identified, and the average particle displacement within this volume is determined. Statistical procedures are used in the determination of the particle displacement. Either autocorrelation or crosscorrelation methods are used (Adrian, 1986).

There are at least three methods of performing the autocorrelation or the crosscorrelation. A method commonly being used is numerical evaluation of the autocorrelation function. A problem with this technique is the amount of computations that must be performed in the analysis, which means that the process is time

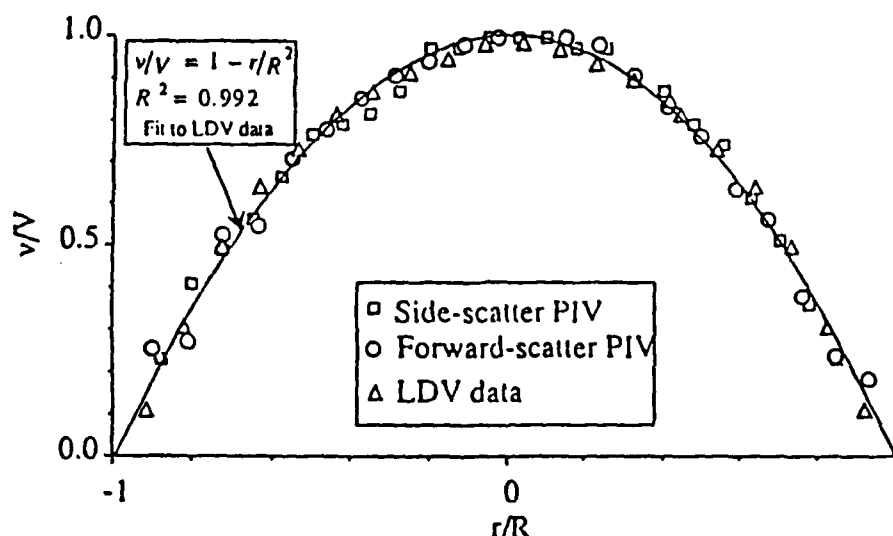


Fig. 7.4.3. Comparison of side-scatter -PIV, near-forward scatter PIV and LDV results for a laminar pipe flow.

consuming. A second method is called "opto-numerical analysis", where one Fourier Transform is produced optically, here termed OFT, producing Young's fringe pattern, and then a second Fourier Transform is performed numerically (an FFT) to produce the autocorrelation function. A third method, which has been developed under funding for the ERC, is the full optical interrogation of the particle images. In this method, shown in Fig. 7.4.4, the Young's fringe pattern is imaged onto a TV camera, and then displayed on a Liquid Crystal Television (LCTV). The image displayed on the LCTV is then transformed optically to produce the autocorrelation function, which can be captured

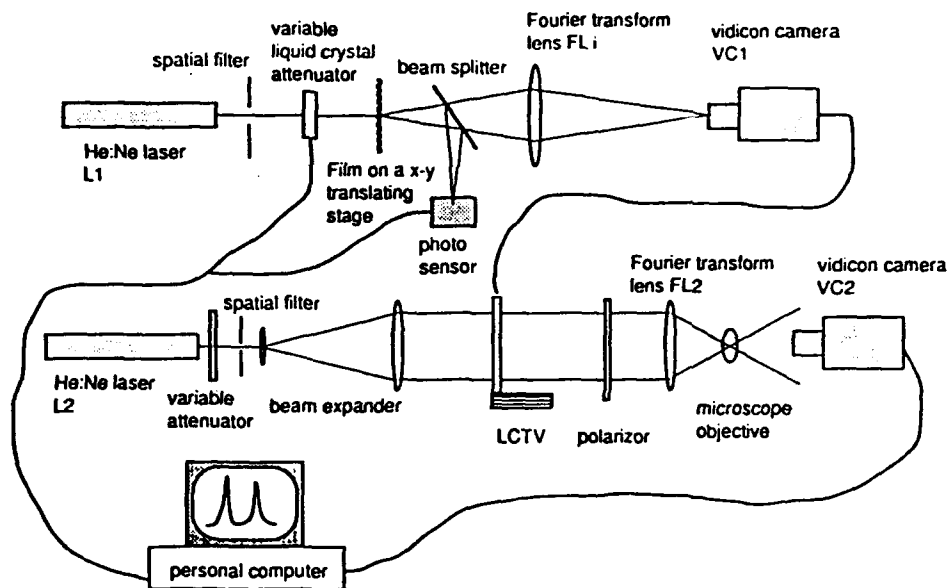


Fig. 7.4.4. PIV optical image processing system incorporating LCTV as a spatial light modulator.

on a video camera. This image is then analyzed after digitization to find the location of the correlation peaks using simple peak finding routines (Farrell and Goetsch, 1989).

The principle advantage of this system is the speed with which the autocorrelation is performed. Because both Fourier Transforms are performed optically, the computational requirements are minimized, and a relatively simple system can do the PIV interrogation at a rate that can exceed the fastest numerically-based interrogation systems. A second potential advantage may accrue because the accuracy of the optical transforms is not limited by finite bit numbers or discretization errors and the resolution of the OFT can be adjusted by optimizing the region of the autocorrelation that is captured by the second video camera. For example, Fig. 7.4.5 is a comparison of the results of an OFT and an FFT from a Young's fringe pattern produced with a double-exposed speckle image with 120 micron displacement between exposures. There are a number of differences between the results. The DC peak of the OFT is blunt or flat-topped, compared to the FFT, which produces a sharp DC peak. This blunt profile probable in the OFT probably occurs from spherical aberration of the transform lens, and the finite size of the laser beam at the focal point of the lens. A similar effect does not occur in the displacement peak, as the OFT and FFT produce the same shape for the displacement peak, but the ratio of the magnitude of the displacement peak to the magnitude of the DC peak is about twice as high for the OFT. Also the magnitude of the background frequency components is much smaller with the OFT, which increases the detectability of the displacement peak.

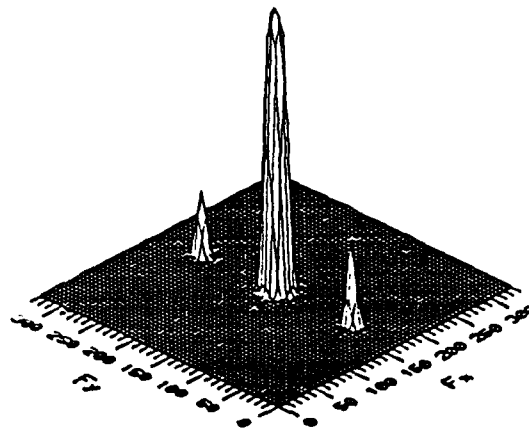


Fig. 7.4.5a. Surface plot of the OFT of a Young's fringe pattern shown.

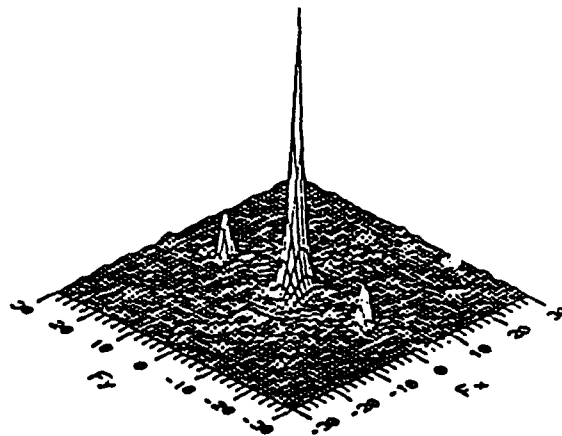


Fig. 7.4.5b. Surface plot of the FFT of a Young's fringe pattern.

#### Measurement Results

To study the near-wall velocity characteristics, measurements were made near the cylinder head of a motored four-stroke engine using LDV (Pierce, 1991, and Pierce et al., 1992). In addition the near-wall velocity characteristics in three different two-stroke geometries were observed, again under motored conditions, but in this case the measurement technique was particle photographs and PIV (Gandhi, 1991, and Gandhi and Martin, 1992).

There have been only a few measurements of the near-wall velocity behavior in engines. Foster and Witze, 1987, observed a distinct region of low momentum fluid extending for 1-2 mm from the wall in the Sandia research engine. Hall and Bracco, 1986, measured similar behavior in their research engine. In contrast, the results

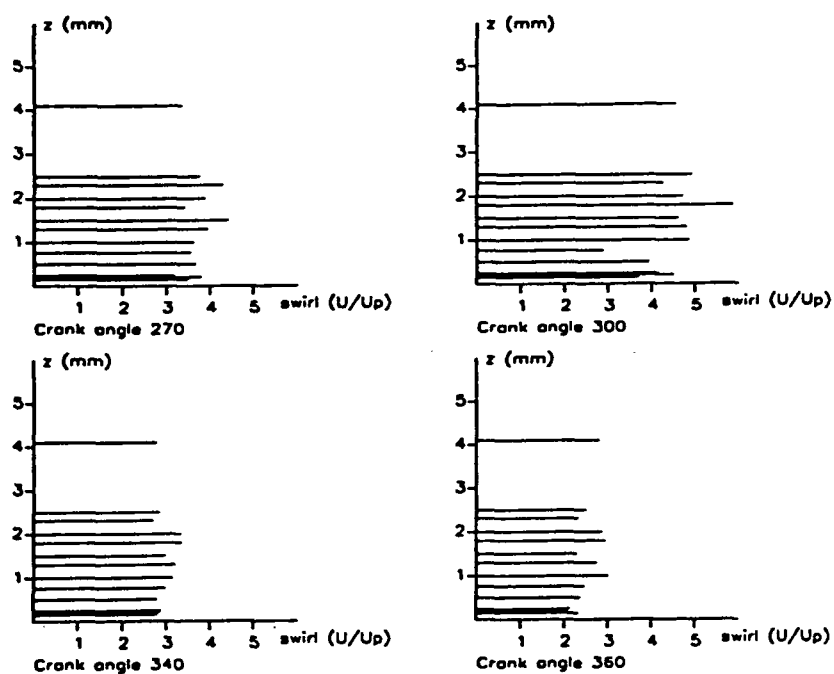


Fig. 7.4.6. Velocity vectors scales by mean piston speed ( $U_p$ ) from the 1500 rpm case.

obtained in the research engine used here showed little evidence of a region of low momentum fluid near the wall. This is demonstrated in Fig. 7.4.6, where the swirl velocity profile was measured to a distance within 0.050 mm of a 2mm in depth cylindrical extension from the cylinder head. In this case, as indicated in the discussion above, the measurement location was accurately known relative to the position of the cylindrical extension.

Figure 7.4.7 is an example of results obtained near a flush surface in the cylinder head. In this case, both the swirl and radial components of velocity were measured. Because these measurements were affected by the image shifting effect described above, it was not possible to acquire measurements at TDC on compression with the measurement volume positioned while the engine was stopped closer than approximately 400 microns from the surface. However, similar to the results obtained close to the protruding surface, the measurements from the flush surface showed little change in mean velocity with distance from the surface.

Measurements of the near-wall velocity characteristics were also obtained for three different two-stroke engine geometries. In all cases, the engines were motored. As represented in Fig. 7.4.8, the PIV results for a two stroke geometry with boost ports and/or squish flows did not show the existence of regions of low momentum fluid near the wall.

As has been described, the near-wall velocity characteristics obtained in the four-stroke engine studied and in the two-stroke engines with modern porting and cylinder geometry showed little evidence of regions of low momentum fluid near the walls. In fact, it appears that the idea of a "classical" turbulent boundary layer for an engine flow is not correct. First, for a conventional flat-plate type boundary layer to exist in an

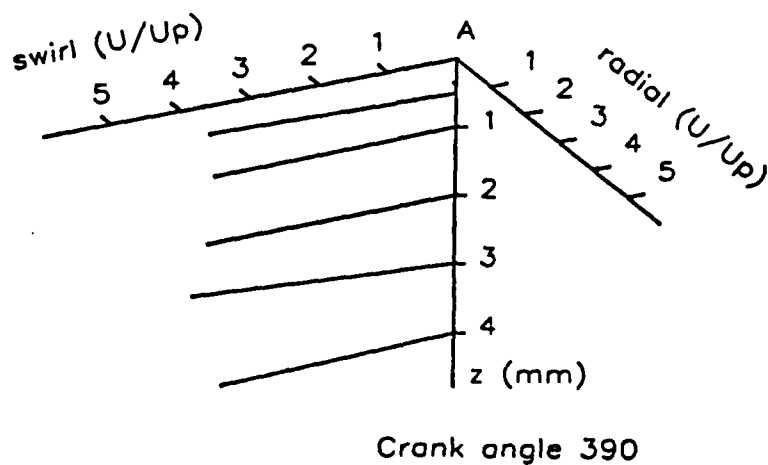
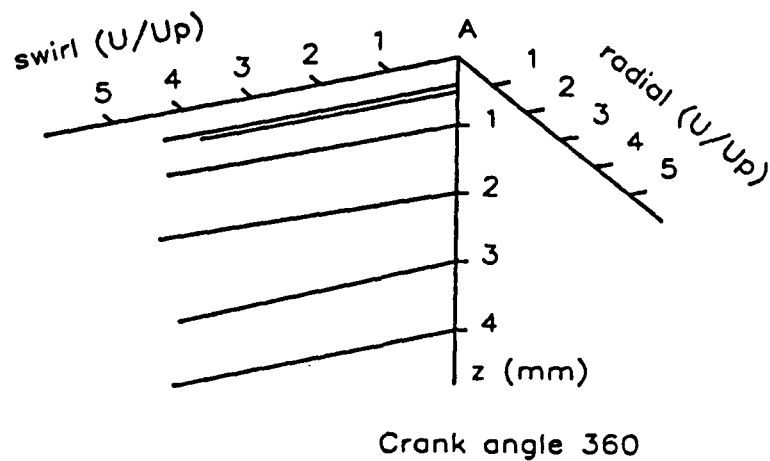


Fig. 7.4.7. Velocity vectors for the 1500 rpm high swirl case at 360 degrees, and 390 degrees.

engine, it would be necessary for there to be sufficient time for the establishment of the boundary layer between times that the boundary layer is scrubbed from the wall by the valve jet flow and other scrubbing mechanisms, such as squish flows. For a modern overhead valve engine, the amount of time between intake valve events is not necessarily too short for the establishment of a boundary layer, but because the flow changes so often and rapidly throughout the cycle, is not the appropriate time to use when estimating the boundary layer growth rate. Second, the relative turbulence levels in an engine can range from being similar to that observed in windtunnels (up to 10 % percent of the kinetic energy of the mean flow) to the unusual case of a flow with no apparent mean motion, with all of the fluid momentum contained in three-dimensional rotating structures. This type of flow is observed in the PIV velocity plot shown in Fig. 7.4.8. Because the relative turbulence levels in an engine can be so large, it is much

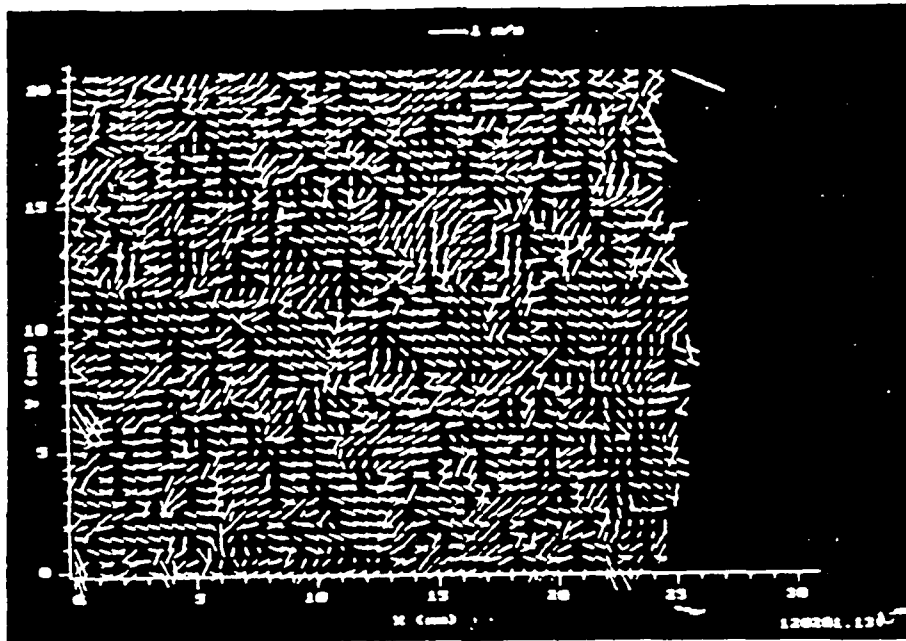


Fig. 7.4.8. PIC vector plot at TDC produced by pancake shape cylinder geometry. Engine crankcase has a boost port. Engine speed: 500 rpm.

more difficult for a region of low momentum fluid to be sustained. Apparently, even though the no-slip condition applies, low momentum fluid at the walls is rapidly remixed with higher momentum fluid contained in turbulent structures that exist at or near the walls.

Finally, the stroke-to-bore ratios of modern engines force the intake flows, whether valve jets or port flows, to become rotational in the engine cylinder. This rotation may take the form of the well-known swirl or tumble, but also may include multiple rotating structures which conform to the cylinder geometry. In the case of a well-established swirl flow or tumble flow, regions of low-momentum fluid tend to be forced to the center of rotation as a result of unbalanced radial pressure gradients (Greenspan, 1969), which further enhances the mixing of the low momentum fluid with the higher momentum fluid found outside of the boundary layer.

These measurement results seem to show near-wall behavior that conflicts with the results of Foster and Witze, and Hall and Bracco, which were described earlier. However, both of those studies used engine intake geometries that are not like modern four-stroke overhead valve engines, or modern ported two-stroke engines. These engines have intake systems which generate strong swirl motion without the same kind of valve jet or port flow found in modern engines, and which do not disturb the flow near the wall.

#### In-cylinder and Valve Jet Flow Results

Shown in Fig. 7.4.9 are representative results of the crank angle dependent characteristics of the in-cylinder swirl component of velocity in the overhead valve see-

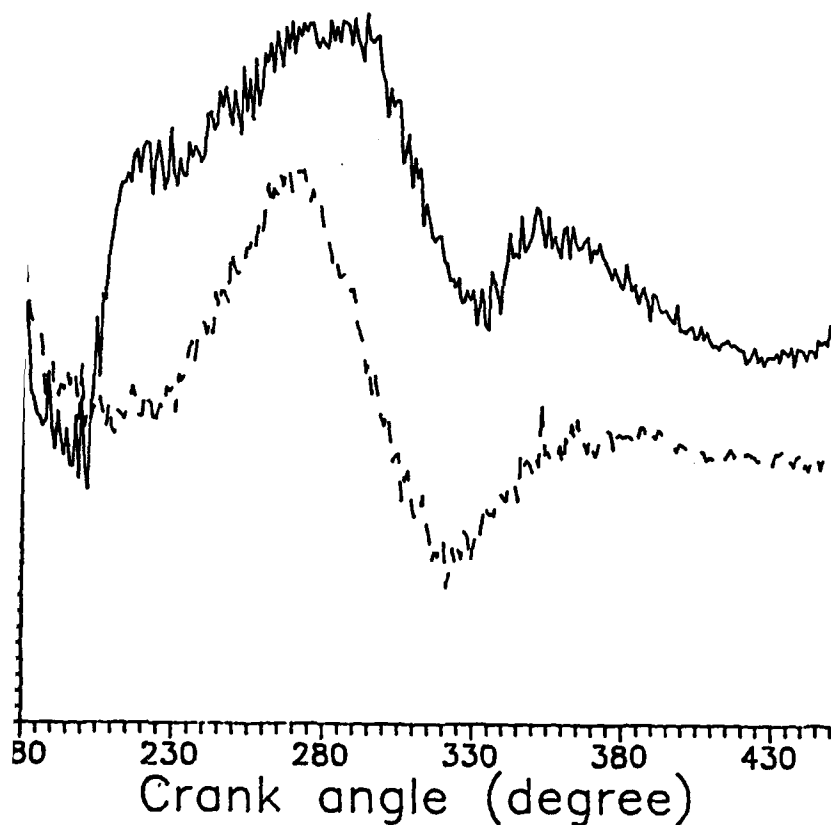


Figure 7.4.9: Swirl component of velocity for the high swirl case at 1500 rpm (solid line) and the low swirl case at 1500 rpm (dashed line). BDC of compression is  $180^\circ$ ,  $360^\circ$  is TDC.

Figure 7.4.9 shows the swirl component of velocity for the high swirl and low swirl case. These data are for an engine speed of 1500 rpm. Two cases are shown, high and low swirl case. For the high swirl case, the swirl velocity component is about 4.6 midstroke on compression at a value for the swirl ratio of about 4.6, which decreases to about 3.1 at TDC on compression. As shown in the figure, the swirl in this engine was effective at changing the swirl level. With the valve timing adjusted to limit the swirl, the swirl ratio decreased to about 3.7 midstroke on compression and quickly decreased to about 1.7 at TDC on compression. The trends for the two swirl cases are similar.

For the low swirl case, the radial velocity components tended to be nearly zero for the high swirl case, at some times in the cycle, substantial radial velocities were observed.

Measurements were also made of the axial component of velocity. A typical result is shown in Fig. 7.4.10. Note that the magnitude of the axial velocity is much less than the swirl component, and that the position of the swirl-control valve has a significant effect on the flow magnitude only just after the intake stroke. Also in

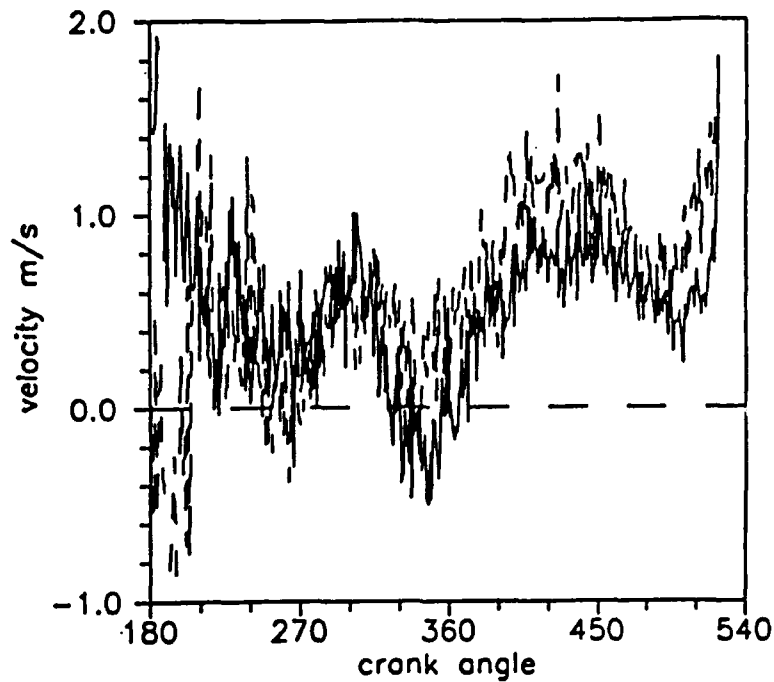


Fig. 7.4.10. Axial component of velocity for both swirl levels measured 2 mm from the at 1500 rpm. Positive velocity is in a direction away from the surface. The solid line represents the low swirl case, and the interrupted line high swirl. BDC of compression is 180 degrees, 360 is TDC.

contrast to what might be expected from piston motion, the flow between midstroke and TDC on compression is towards the piston, instead of towards the cylinder head. However, after TDC, the flow reverts to what you would expect, moving in the direction of piston motion.

For the turbulence intensity behavior, a representative result is presented in Fig. 7.4.11. Here, it is apparent that the position of the swirl-control shroud had little effect on the swirl component of turbulence intensity seen at TDC, in contrast to what was observed in the mean swirl velocity component. As was noted above, the relative turbulence intensities for this component are very high. A representative result for the axial component of turbulence intensity is shown in Fig. 7.4.12. Again the effect of the swirl-control shroud is small, and very high levels of relative turbulence intensities are observed. However, it is also important to note that the magnitude of the axial component of turbulence is approximately 1/3 of that measured in the swirl direction, demonstrating the anisotropic nature of the flow in this engine.

PIV was used to study the velocity field characteristics of motored two-stroke ported engines. In particular, the objective of these studies was to observe the effect of the combustion chamber and porting geometry on the two-dimensional flow field at TDC.

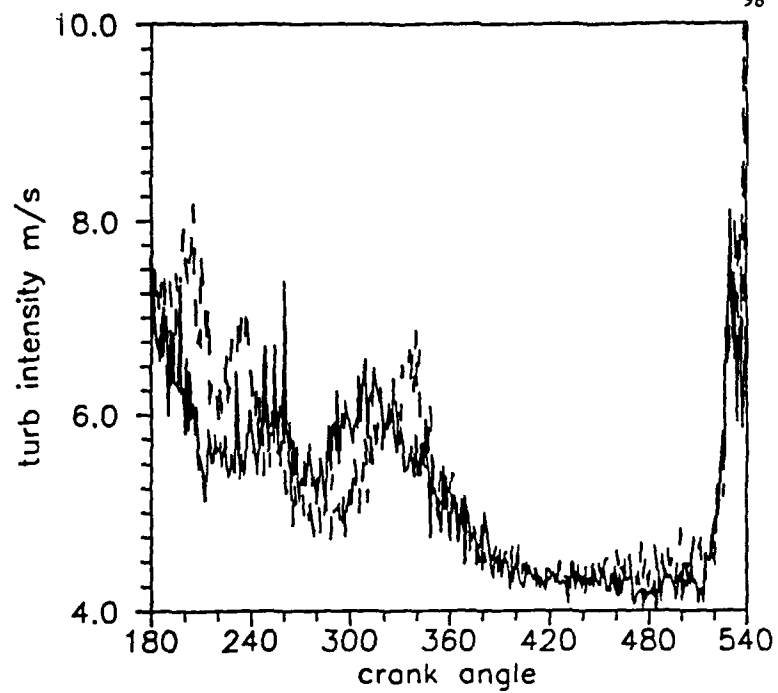


Fig. 7.4.11. Swirl component of turbulence intensity 4 mm from the cylinder head. Solid line represents data from 1500 rpm high swirl, dashed line represents 1500 rpm low swirl case. BDC of compression is at 180 degrees, 360 is TDC.

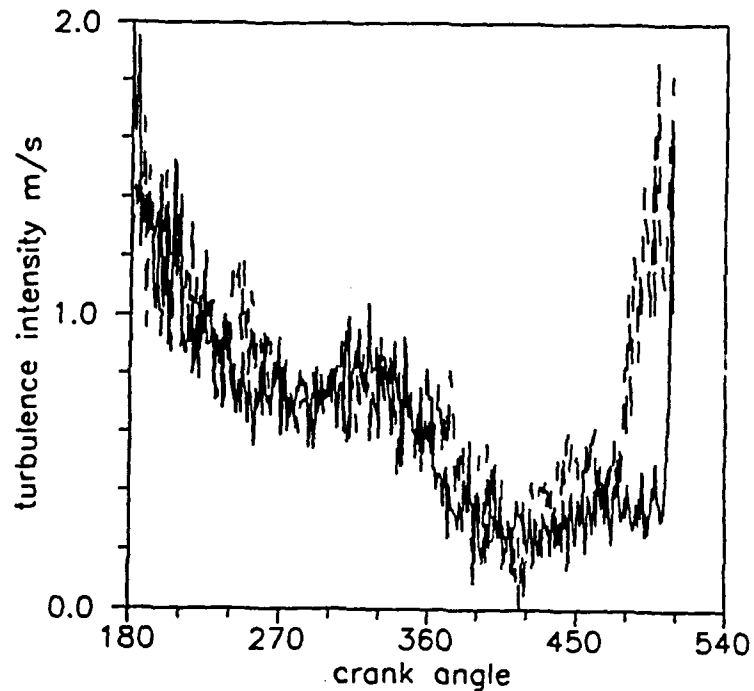


Fig. 7.4.12. Axial component of turbulence intensity measured 2 mm from surface for 750 rpm cases. Solid line represents high swirl data, interrupted line represents low swirl data. BDC of compression is at 180 degrees, 360 is TDC.

To study the effect of induction system geometry on the flow field at TDC, a pancake-shaped combustion chamber was fitted to distinctly different two-stroke induction systems. One of the induction systems was a conventional loop-scavenged arrangement with two induction ports located on opposite sides of the chamber from each other. The other induction system had, in addition, a boost port, opposite the exhaust port.

Comparing Figs. 7.4.8 and 7.4.13, the addition of the boost port dramatically changes the flow field observed at TDC. Without the boost port, the flow is characterized by large-scale swirl structures, which are of the order of the chamber diameter in dimension. However, the introduction of the boost port seems to eliminate these large scale motions, producing a field that is characterized by many small-scale rotational structures.

For comparison of the TDC flow fields for two different combustion chamber geometries with the same induction system, the two-stroke crankcase with the boost port was fitted with a bowl-in-head combustion chamber geometry, to compare with the pancake-shaped combustion chamber geometry. Both geometries had the same compression ratio.

For the bowl-in-head case, the piston comes within 1 mm of the annular shelf on the cylinder head, which generates a squish flow. This is shown in Fig. 7.4.14. In

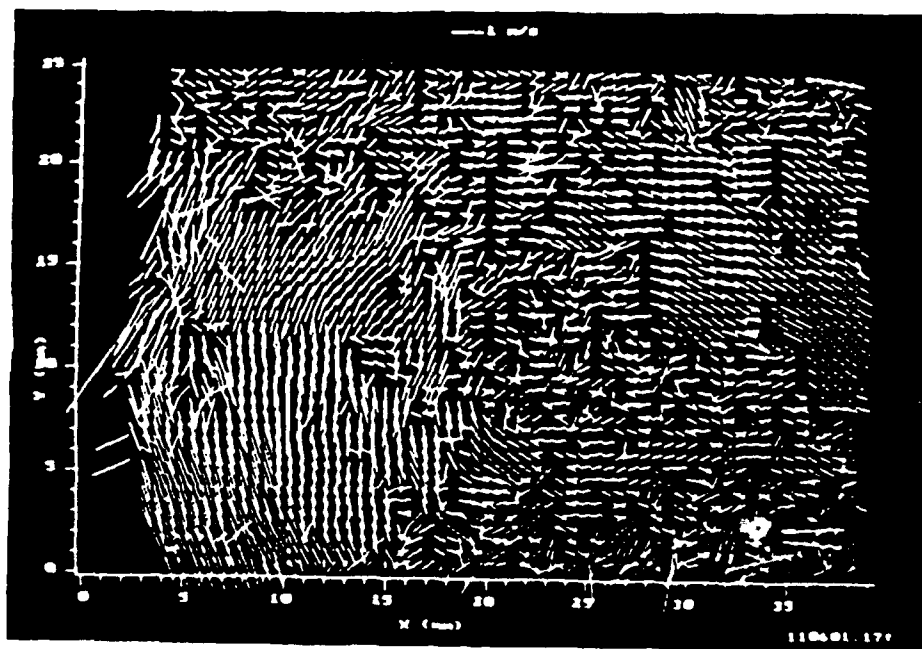


Fig. 7.4.13. PIV vector plot at TDC produced by pancake-shaped cylinder geometry. Engine crankcase does not have a boost port. Engine speed: 500 rpm.

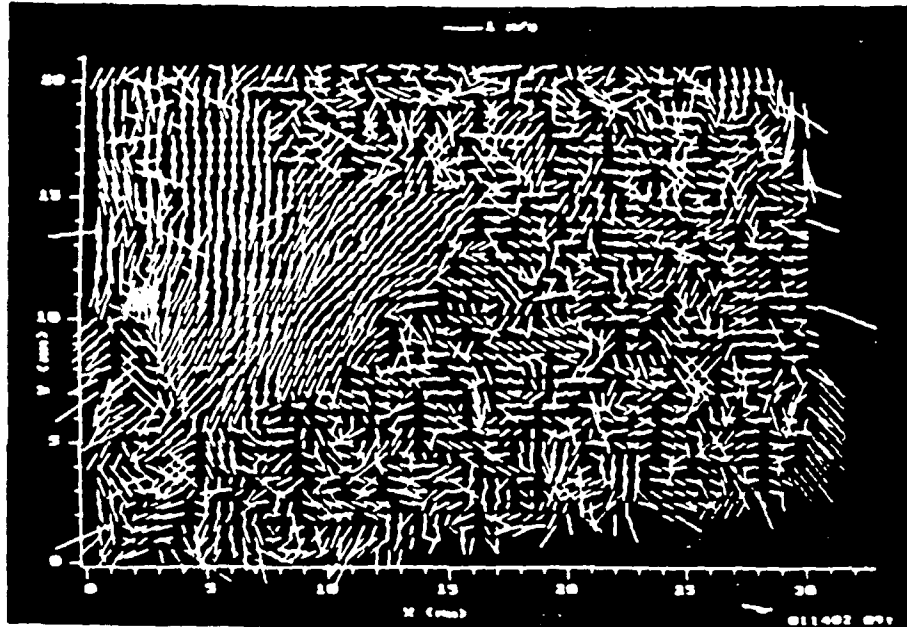


Fig. 7.4.14. PIV vector plot at TDC produced by bomb-in-head engine geometry. Engine crankcase has a boost port. Engine speed: 500 rpm

contrast to Fig. 7.4.8, there is a large area of uniform flow near the center of the chamber, which appeared as a result of the squish flow. From these results it is not possible to determine if this flow is, in fact, the squish flow, as observed by Fansler et al., 1988, or whether the squish flow changes the position of a large rotating structure, which was observed in the calculations performed by Epstein, 1990.

The causes of cycle-to-cycle variation have been intensively debated and studied. The results obtained here, and later by Martin at a study at the Nissan Research Center, indicate the presence of both large-scale and small-scale variations in the gas-phase fluid mechanics. For example, it is possible to observe features of the jet structure described above in photographs taken at identical times in different cycles. However, the apparent strength and position of this jet flow seems to vary from cycle to cycle. Such variation would change the way combustion progressed from one cycle to the next.

The instantaneous, two-dimensional velocity fields occurring in the valve jet flow were measured (Lee, 1992 and Lee and Farrell, 1992) to observe the details of the interaction between the valve jet flow and the incylinder gas. These measurements were obtained in an experiment designed to simulate engine conditions, while allowing better access to the valve jet flow than is obtainable in an ordinary engine. The simulated engine setup consisted of a Cummins NH-250 4-valve cylinder head, which was attached to an acrylic cylinder. The gas flow through the head and cylinder was generated by a standard flow bench. However, the flow itself was not constant because the intake valves were actuated by an electric motor driven cam.

Shown in Fig. 7.4.15 is the plane in which the two-dimensional velocity vectors were determined, which extends through the axis of one of the intake valves through

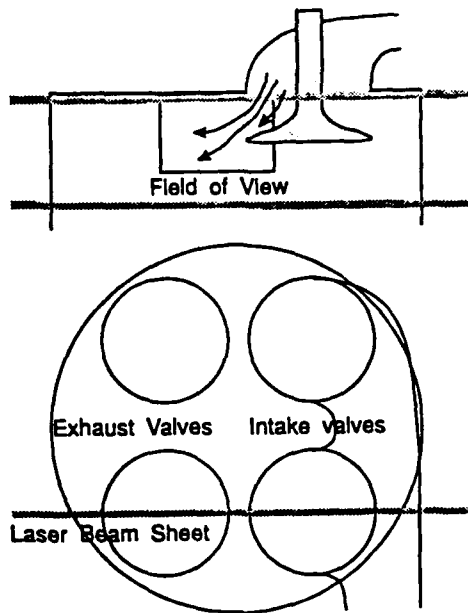


Fig. 7.4.15. Field of view of the measurement plane.

the axis of one of the exhaust valves. The field of view was between the intake and exhaust valve, as shown.

The developed film of the particle motions in this plane were analyzed using the optical processor described earlier. In this case, the interrogating grid step size was 0.5 mm, with an interrogating laser beam diameter of 0.8 mm. As in all PIV measurements, there were regions in the picture where it was not possible to obtain velocity vectors at every position within the flow. This occurs typically because of the low velocities occurring in that region. To produce a complete vector field, a nearest-neighbor interpolation scheme was used to estimate the velocity vector in regions where they could not be determined from the PIV image interrogation. For the results to be shown here, approximately 10 % of the vectors in the field were produced by interpolation.

PIV methods which utilize autocorrelation methods to produce the velocity information do not produce the sign or sense of the velocity vector unless there has been some method employed to shift the particle field image relative to the film plane between exposures. In this set of results, the valve jet direction is known, therefore, the sign of all other vectors within the field was determined relative to the jet direction. At each vector outside of the jet, the sign was chosen that gave the smoothest change in direction from vector to vector, which minimizes the local convective acceleration.

Shown in Fig. 7.4.17 are PIV results for the valve jet flow. These results are for a cam speed of 300 rpm, which would represent a typical 4-stroke heavy duty diesel idle condition. The valve is located in the region to the upper right where there are no velocity vectors. Figure 7.4.16 is the valve lift versus cam profile. The valve jet exits between the valve seat and valve face, with a decrease in jet thickness with distance from the jet axis because of the conical shape of the jet. Early in the intake process there is a vortex between the head and valve jet which tends to cause the jet to bend towards the head. However, as the valve lift increases, and the jet momentum increases, this

effect is reduced and the jet exits without much change in direction. There are intense regions of mixing in the shear layer that exists between the jet and the ambient gas in the chamber. As the valve closes, a vortex reforms between the head and valve jet, which again bends the jet towards the head. After the valve has closed, the intake jet is not identifiable in the field of view, and the flow appears to be dominated by large scale rotational structures.

As shown in Fig. 7.4.18, which was obtained at the same conditions as for Fig. 7.4.17, but for a different cycle, there are substantial differences in the interactions of the valve jet flow and the ambient gas from cycle-to-cycle, even just after the valve jet flow has begun. Variations in the combustion behavior of an engine, which influence performance and emissions characteristics of an engine, occur, at least in part, because of these variations. These results demonstrate that there is variation in the introduction of the valve jet flow and the formation of large structures that provide (later on in the cycle) the turbulent energy that aids transport in the combustion and mixing processes.

### Impact of Research on Technology

The type of research performed by the ERC on the gas-phase fluid mechanics in engines tends to provide results that are useful in understanding and observation of flows that are occurring in engines. To be most useful and to have the largest impact on engine technology, these results should be incorporated into conceptual and/or analytically or numerically based models of engines. Such incorporation is occurring with the efforts in adapting and improving KIVA for use in engine design, but also in generating concepts for engines that, for example, show improvements in air utilization, or cold starting capabilities. Direct use of this research in engine design will increase as more is known about the incylinder gas-phase fluid mechanics, and as tools such as KIVA become more widely used in the design and evaluation process.

Specific achievements and results from this set of investigations:

- 1) Methods were developed that allowed for accurate positioning and spatial resolution for LDV measurements near the wall in an engine.
- 2) The phenomena of image shifting from index of refraction gradients near the wall was identified and photographs showed the magnitude of this shift.
- 3) PIV measurements in engines were obtained using a copper vapor laser for the light source.
- 4) A near-axis scatter method for decreasing the light power necessary for PIV was developed and tested.
- 5) A method for full optical interrogation of particle pictures was developed.
- 6) Near-wall velocity measurements showed little evidence of regions of low momentum flow for engines incorporating overhead valves in a four-stroke engine, or current porting arrangements in two-stroke engines.
- 7) Bulk flow measurements showed the complex nature of the flow in these engines, which ranged from swirl dominated flows at TDC to flows that were characterized by little mean motion, and were primarily decaying turbulent flows.
- 8) Measurements of the valve jet flow characteristics showed the interactions of the jet flow with the incylinder gas, and the existence of differences in the interaction early in the intake process.

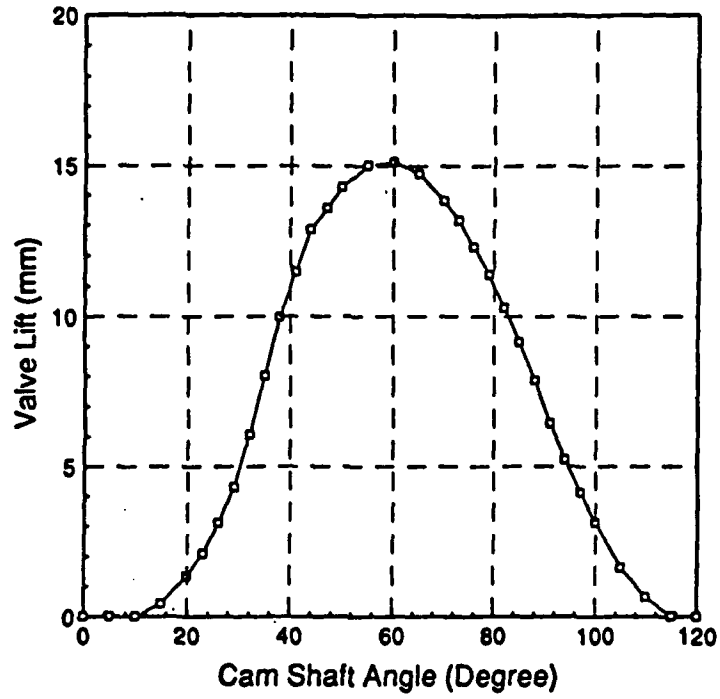


Fig. 7.4.16. Valve lift versus cam shaft angle profile.

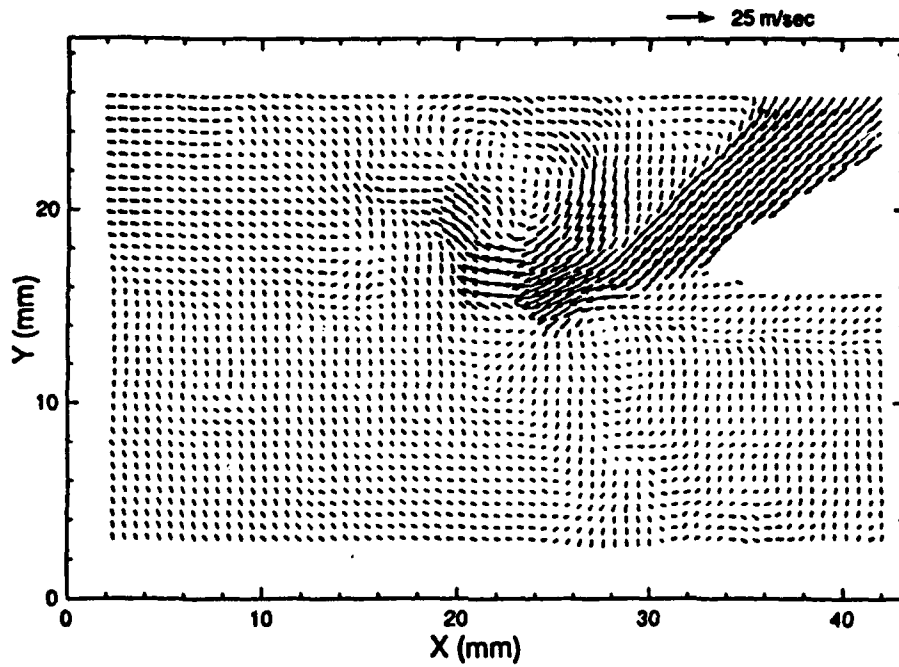


Fig. 7.4.17a. Instantaneous velocity; dynamic intake valve flow, 300 rpm cam speed, 35° cam angle (valve opening, 7.6 mm)

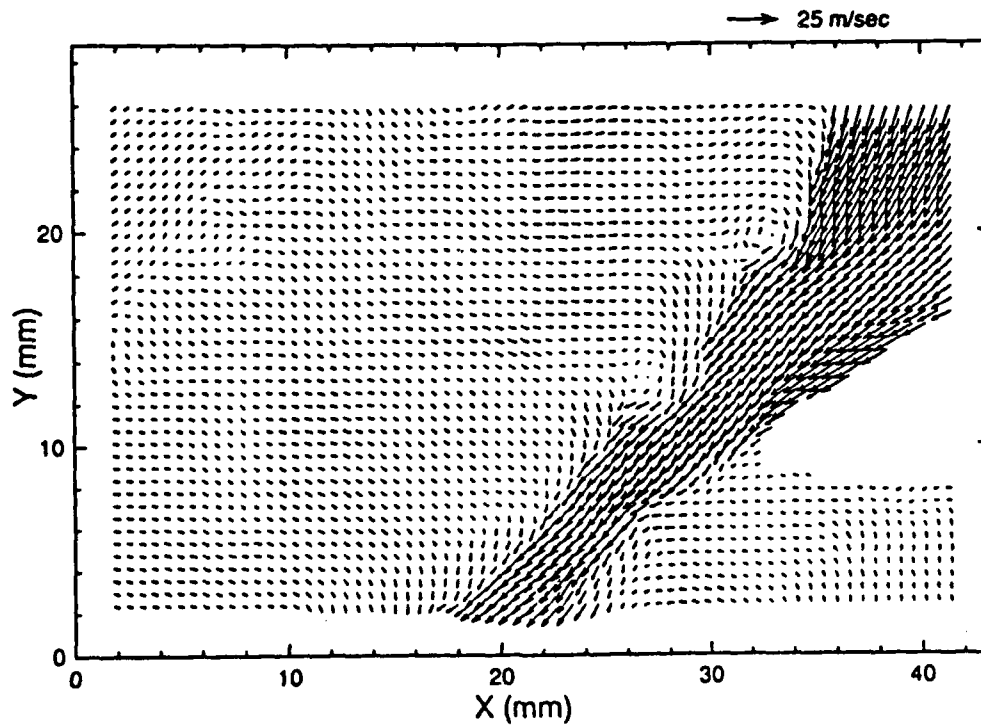


Fig. 7.4.17b. Instantaneous velocity; dynamic intake valve flow, 300 rpm cam speed, 60° cam angle (valve at maximum lift, 15.2 mm).

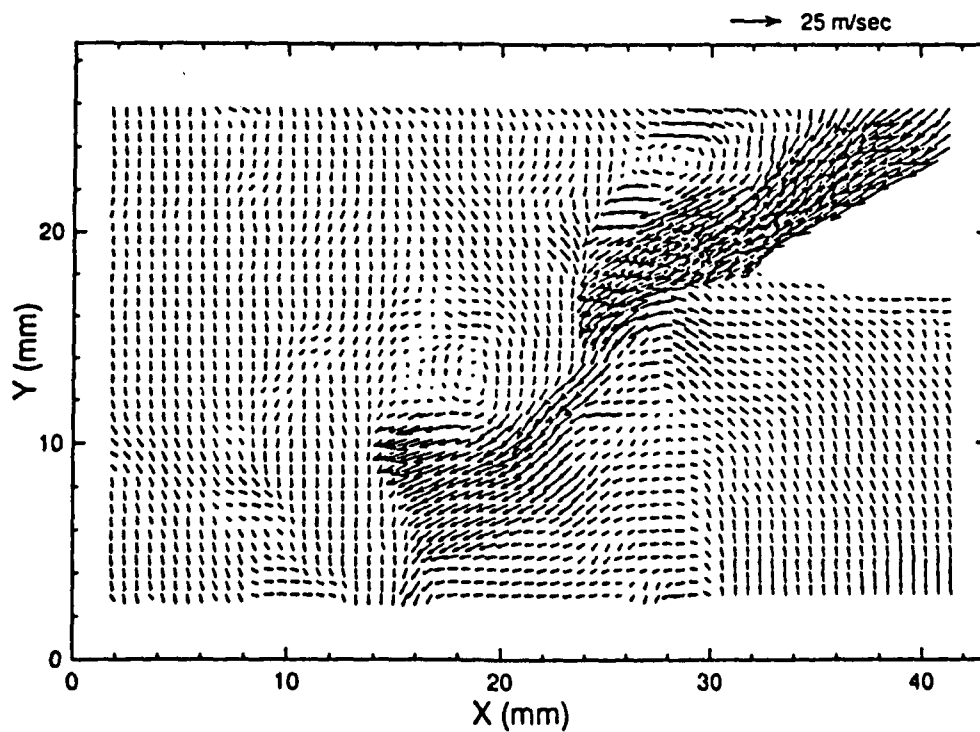


Fig. 7.4.17c. Instantaneous velocity; dynamic intake valve flow, 300 rpm cam speed, 88° cam angle (valve closing 7.6 mm).

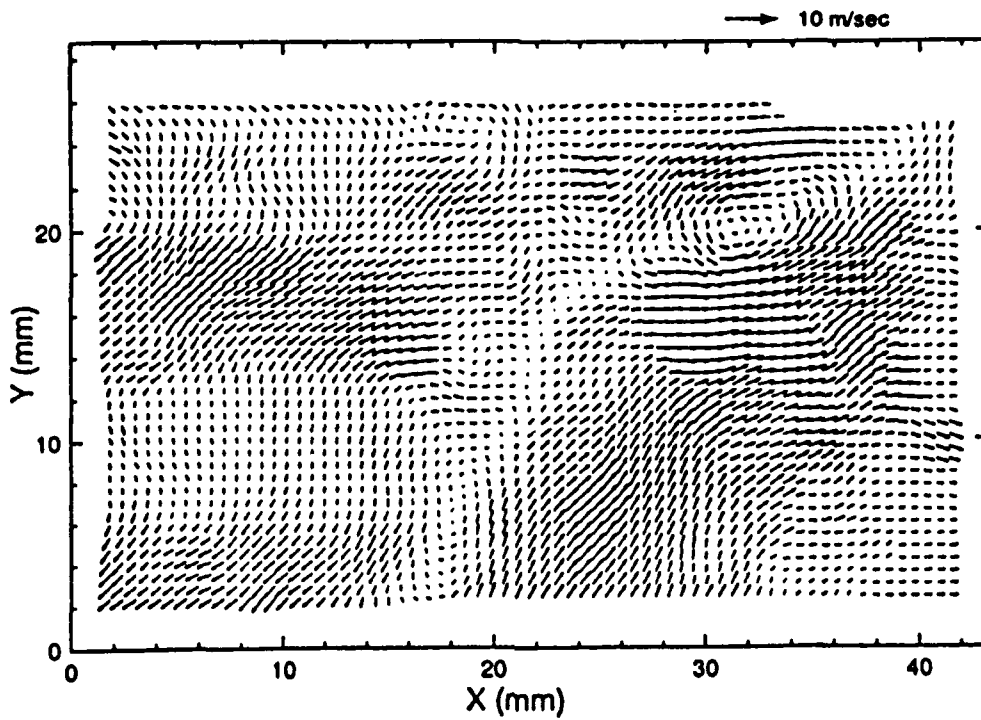


Fig. 7.4.17d. Instantaneous velocity; dynamic intake valve flow, 300 rpm cam speed, 130° cam angle (valve closed).

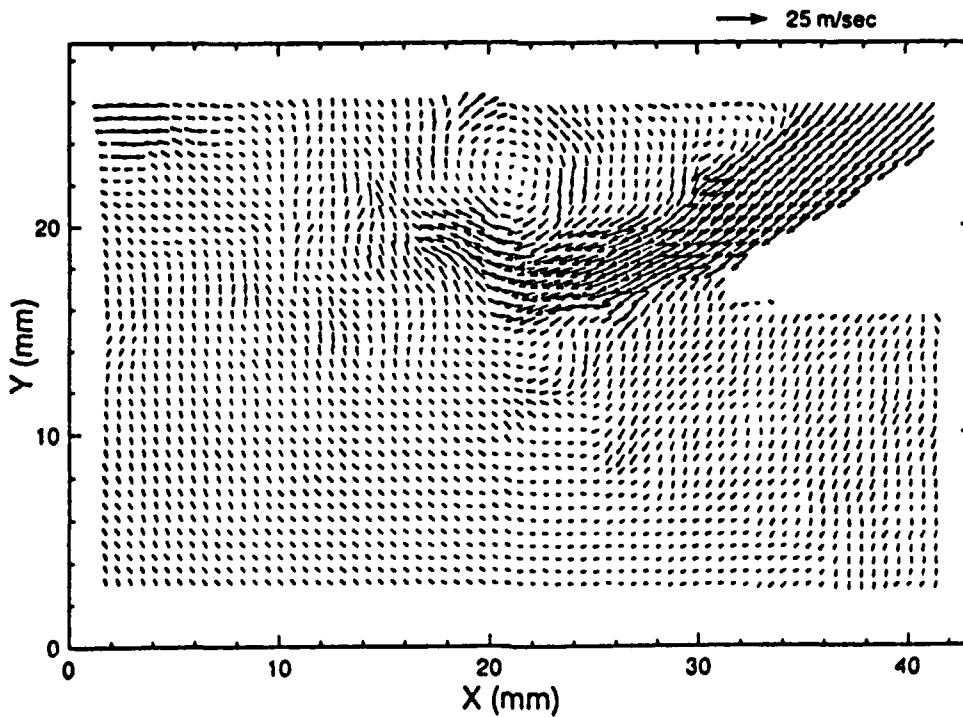


Fig. 7.4.18. Instantaneous velocity; dynamic intake valve flow, 300 rpm cam speed, 35° cam angle (valve opening, 7.6 mm), case 2.

## 7.5 Diesel Sprays

### Introduction

High pressure fuel injection studies have made up a significant portion of the research effort in the Center. The primary motivation for studies of high pressure fuel sprays is the recognition that fuel delivery and the physics that is entailed in the process has a significant impact on subsequent combustion. For some cases, such as cold starting situations, the fuel spray behavior seems to dominate the combustion process. For other situations, fuel mixing and air utilization is expected to significantly affect engine fuel consumption and reduce exhaust signature and emission problems arising from particulate emission.

The specific research goals of the spray studies undertaken in this work were:

- to develop experimental methods which can measure droplet size and velocity throughout a transient, inhomogeneous spray;
- to measure and model the effects of varying injector parameters on injection characteristics and emissions in engine experiments;
- to measure and model details of spray breakup and vaporization relevant to high pressure sprays;
- to use experimental results to develop detailed models capable of reproducing measured spray results and predicting as yet unmeasured spray conditions.

### Experimental Development

The efforts undertaken to advance the current capabilities of spray measurements are presented in this section. These developments were driven by needs within the spray group for detailed measurements under realistic injection conditions. These needs included improved spatial and temporal resolution, as well as the ability to apply more realistic measurement conditions, such as injection into a high pressure gas. The work discussed in this section includes construction and comparisons for commercially available rate of injection meters (Bower and Foster, 1991), applications of commercial measurement devices under adverse conditions (Koo and Martin, 1990b), and development of multidimensional measurement methods (El-Beshbeeshy et al, 1992, Farrell, 1991, Farrell, 1992, and Albert and Farrell, 1992).

A basic and essential piece of information regarding any fuel injector is the time variation of the rate of injection of fuel. Since most high pressure diesel injectors deliver the required amount of fuel in a few milliseconds, the flow from the injector has a significant transient component. Measuring the rate of injection from the injector, or some related parameter, as a function of time has generally been done using a Bosch type injection meter, or by a Zeuch type meter. Since it is unclear which is superior, a prototype of each system was built, and the two were compared on one particular injector.

The Bosch type meter consists of a long coil of tubing, which is filled with fuel. The injector is mounted at one end, along with a strain gage attached to the tubing. At the other end of the tubing is an orifice plate to control the flow rate out of the test tube into a second tube. This second tube is held at a constant pressure by a check valve. The measurement is made by using the strain gage to estimate the fluid pressure within the tube as the fuel from the injector is injected into the stagnant fluid already in the

tube. The volume flow rate,  $dq/dt$ , as a function of time is calculated from the estimated pressure rise in the tube, as

$$\frac{dq}{dt} = \frac{A}{a\rho} P$$

where  $A$  is the cross-sectional area of the tube,  $P$  is the measured pressure,  $a$  is the speed of sound in the fluid, and  $\rho$  is the fluid density.

The Zeuch type meter records the pressure in a constant volume chamber as the fuel from the injector is put into the volume. Typically, a strain gage was used for the DC value of the pressure, and a piezo type transducer was used for the fluctuating portion of the pressure. The mass flow rate for this meter is calculated as

$$\frac{dm}{dt} = \rho \frac{V}{K} \frac{dP}{dt}$$

where  $V$  is the chamber volume,  $K$  is the bulk modulus of the fluid, and  $P$  is the chamber pressure.

The two systems were compared using a BKM injector (Bower and Foster, 1989), at two different injection pressures (100 and 140 MPa) and two different injection frequencies (500 and 1000 Hz). An example of the rate shape for one of the operating conditions (140 MPa at 500 Hz) is shown in fig. 7.5.1. The results of this study indicated that the two methods were generally similar, although they had slightly different detailed characteristics and analysis methods. Details of this work and the results are given by Bower and Foster (1991).

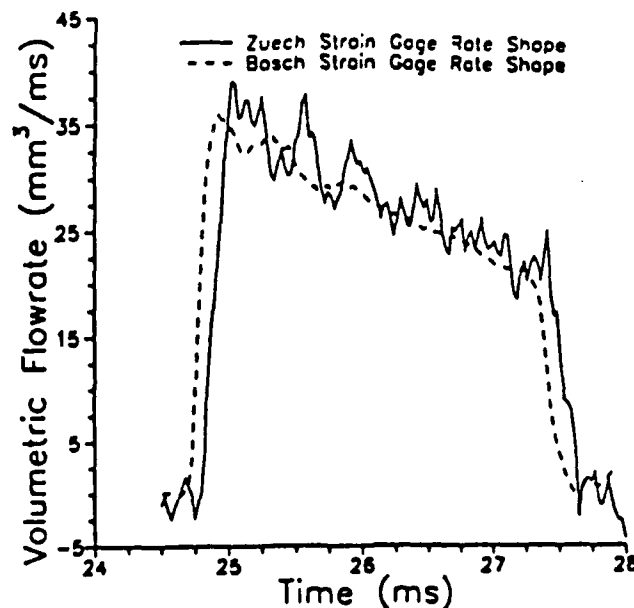


Fig. 7.5.1 A comparison of the strain gage transducer's injection rate shapes from the Bosch and Zeuch rate of injection meters at 140 MPa and 500 Hz.

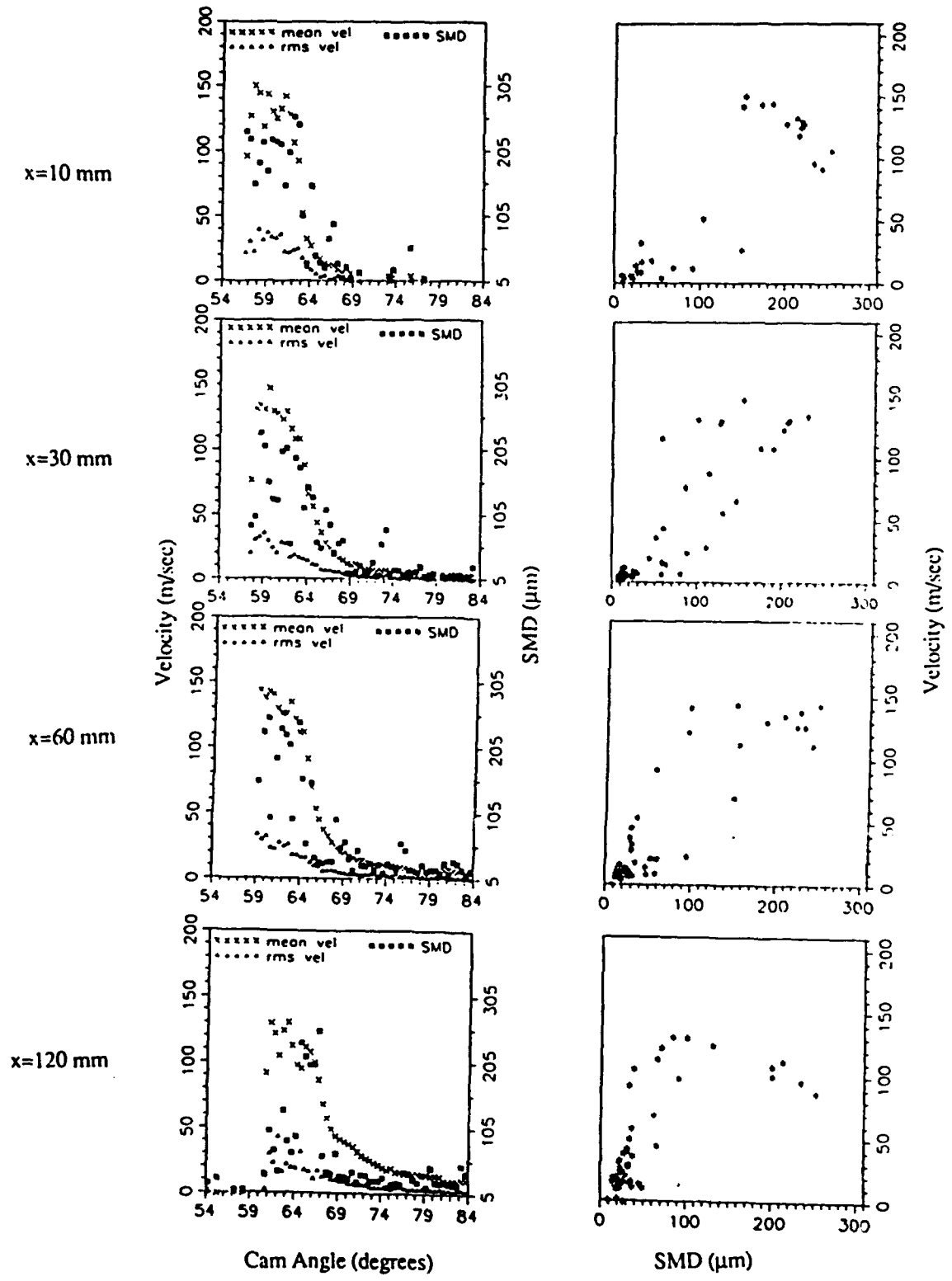


Fig. 7.5.2 Crank angle resolved SMD, mean velocities, RMS velocities, and correlation along spray axis. Each data point was ensemble averaged from 50 injections with 0.5 degree resolution. Injection at 800 rpm, 19.5 mg per injection,  $P_c = 1$  atm.

A detailed look at transient fuel sprays was performed using an Aerometrics Phase Doppler Particle Analyzer (PDPA) by Koo and Martin (1990b). This work reflected the desire for an increased level of spatial and temporal detail in diesel type sprays. The PDPA system had been developed for other spray applications and had shown a remarkable ability to measure droplet sizes and velocities for a variety of sprays. To this point, however, there had been very few applications of the system to transient sprays of as short a duration and as high a particle density as a high pressure diesel spray. In order to obtain a complete picture of the temporal and spatial variation of the spray, a series of "crank angle resolved" ensemble average data were taken. The particle size and associated velocity for a single location in the spray were measured, and each measurement was tagged with the time after the beginning of injection. Subsequent data analysis allowed averaging of size and velocity over some finite time interval ( $\Delta t$ ) of the spray. To make the results consistent with engine type results, time is reported as a crank angle degrees, with the start of injection occurring at about 54 crank angle degrees (CAD). For this set of experiments, a Lucas-CAV injector was used, at three different pump speeds (400, 800, and 1200 RPM) and three different delivery rates. The injector was operated with diesel fuel into atmospheric pressure and temperature air. The resulting data set is extensive, but a sample of these results is shown in fig. 7.5.2.

The results of this detailed examination of the transient spray indicated among other things, that the axial and radial distributions of droplet size and velocity varied considerably with time after injection. The spray shape changed during injection, having a larger cone angle at small injection times, then narrowing. In addition, the data indicated that the first injected droplets are quickly overtaken by subsequent droplets. Photographs of the spray showed apparent overall wave patterns which could affect atomization. The wave pattern frequency had a clear dependence on chamber pressure, although the exact nature of the dependence or the significance of the wave structure is still not clear.

In order to visualize the entire spray and more rapidly evaluate an overall average SMD for a spray, an imaging method based on laser light attenuation was developed (El-Beshbeeshy, et al. 1992). The method was based on high speed photographs made with a high speed movie camera illuminated by a Copper Vapor laser. The 10 ns pulses of the laser were synchronized to the framing rate of the movie camera to produce 5000 fps movies of injection in a pressurized bomb. A calibration step tablet of varying optical density was included in each image. Individual frames of the high speed movie were digitized using a video camera and frame grabber in a microcomputer. From the images, with the calibration step tablets in each image, contours of equal incident laser transmittance were generated. From these attenuation contours, estimates of the Sauter mean diameter (SMD) for the entire spray or for any transverse slice through the spray could be generated. The calculation assumes the spray is axisymmetric and that the droplet size distribution in the spray is known and is constant throughout the spray for these measurements. Calibrations of the entire system were performed to ensure that the intensity measurements made by the video system were accurate representations of the laser light transmitted through the spray.

The basic relation used to estimate SMD was

$$D_{32} = \frac{3 \overline{RQ_{ext}}}{2 \rho_f} \frac{M_f}{a_p \sum_{j=1}^p (-\ln \tau_j)}$$

where  $\overline{R}$  is an optical correction factor,  $\overline{Q_{ext}}$  is a mean extinction coefficient,  $M_f$  is the measured fuel mass flow, and the denominator,  $a_p \sum_{j=1}^p (-\ln \tau_j)$  represents the summation of the laser transmission over all pixels in the spray. A sample of the results for this technique is shown in fig. 7.5.3, along with PDPA measurements made under the same conditions for the same injector. Details of measurement results using this method will be presented in a later section of this report.

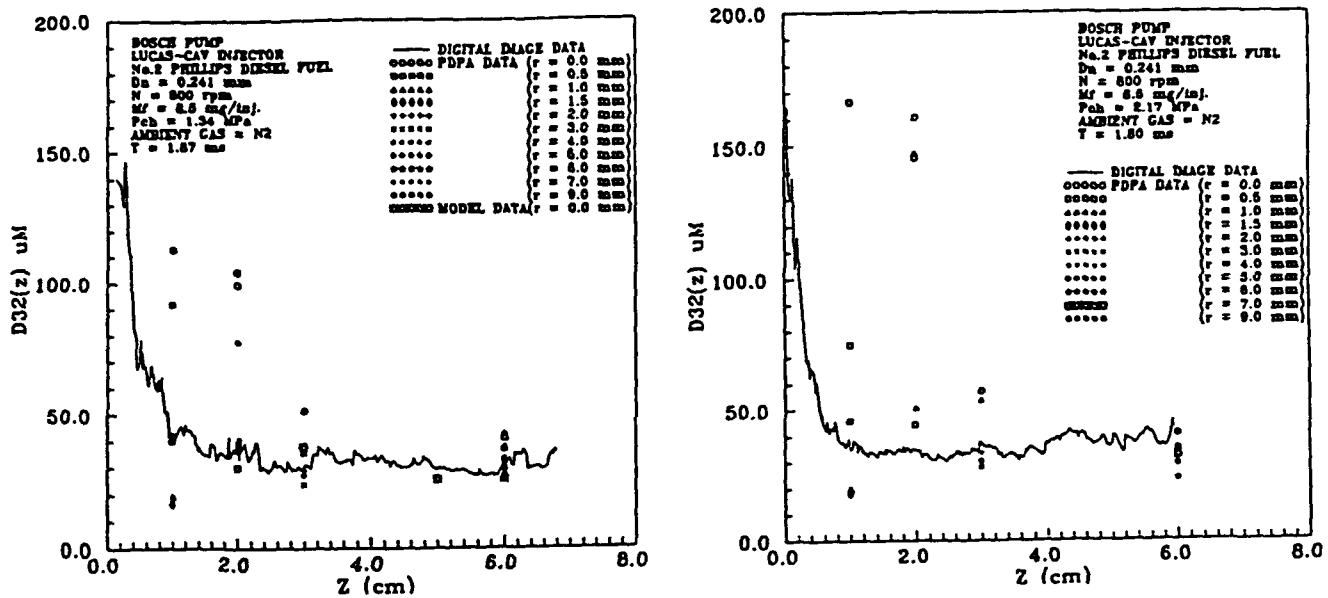


Fig. 7.5.3 Comparison of SMD measured by digital imaging, PDPA, and estimated by breakup model for two chamber pressures.

In an effort to expand the capabilities of currently available single point particle size and velocity measuring devices, a multipoint particle or droplet measuring system is being developed (Farrell, 1991a, Farrell 1991b, Albert and Farrell, 1992). The method is based on particle image velocimetry methods for measuring droplet velocities at many locations in a flow field. In one implementation of this technique a photograph is taken of a region of the particle field of interest. After a short (5-50  $\mu$ s) delay, a second exposure is taken of the same particle field, including the particle displacement between the two exposures. Analysis of the two images or double exposure, can provide the displacement magnitude and direction for the particles captured in the photographs. This is frequently done in a spatial average manner, in which particle displacements in a small region (1 mm diameter) are averaged together to produce an average displacement and direction for the location in the flow field. The particle size distribution for the ensemble of particles in this interrogation spot is also available from

the intensity distribution of the diffraction pattern generated by the particles in this small region. Normally, the diffraction pattern includes a high frequency intensity variation known as Young's fringes which is representative of the average particle displacement and direction, and a lower frequency diffraction halo representative of the particle size distribution.

The particle size information, which is the particle size distribution of the particles in the 1 mm diameter, is available from the diffraction pattern of the particle images. An inversion, producing the size distribution which caused the measured average intensity distribution, provides an estimate of the local particle size distribution. The measured data consists of an intensity distribution  $I(\theta)$  where  $\theta$  is an angle from the center of the diffraction pattern. Theoretically, this kind of distribution should look like

$$I_{\theta} = \frac{1}{k^2 \theta^2 z^2} \int_{x_1}^{x_2} J_1^2(y) x^2 n(x) dx$$

where

$$k = \frac{2\pi}{\lambda} \quad x = \frac{\pi d}{\lambda} \quad y = x\theta$$

and  $J_1$  is a Bessel function of the first kind. The desired information is the  $n(x)$  term, which is the size distribution function. To recover this function from the intensity profile requires an inversion of some sort. One kind of inversion is the Shifrin inversion, which gives

$$n(x) = -\frac{2\pi k^2 z^2}{x^2} \int_0^{\infty} J_1(y) Y_1(y) y \frac{d(\theta^3 I_{\theta})}{d\theta} d\theta$$

where  $Y_1(y)$  is a Bessel function of the second kind of order 1.

The method is generally similar to diffraction methods proposed by Swithenbank (1976) and made commercially by Ma'vern, among others. The major differences are that this system uses a photograph of a plane of the spray, rather than a real-time line of sight average diffraction pattern, and this system uses a video detector rather than the ring detectors of previous diffraction systems. The region sampled with commercial Fraunhofer diffraction systems is usually a 5-10 mm diameter line of sight through the spray. In this method, the sampled region is a 1 mm diameter spot on a plane in the spray. The increased number of data samples from the 512 by 480 video array used here as compared to the 31 ring detector samples used in previous systems allows a wider selection of possible inversion schemes than seems to work for the ring detector geometry.

The method has been demonstrated on single apertures of known size in the 25  $\mu\text{m}$  to 400  $\mu\text{m}$  range (Farrell, 1991a, 1991b). Improvements to the method for smaller particle sizes and some examples of application in a dilute spray are given in Albert and Farrell (1992). The method seems to be promising, but is still in need of development for application in dense sprays typical of diesel engine applications.

### Engine Experiments

A number of experiments related to spray characterization and the effects of aspects of sprays on engine performance have been performed. In this section, the results from experiments which were performed in actual engines are discussed. Out-of-engine spray experiments are discussed in the next section.

The range of effects on engine performance that variations in fuel sprays produce is quite large. Experiments performed under this program included studies on the effects of swirl and injection parameters on heat transfer by Van Gerpen et al. (1985), fuel impingement effects on spray behavior by Naber et al. (1988), auxiliary or piloted injection effects on combustion by Shakal and Martin, (1990), the effects of variable rate shape on spray penetration by Bower and Foster (1990), the effects of split injection on  $\text{NO}_x$  by Bower and Foster (1993), engine modeling of injection and combustion for cold starting by Gonzalez et al. (1991), and the effects of spray models on combustion predictions by Gonzalez and Reitz (1991b) and Gonzalez et al. (1992).

The study of the effects of swirl and injection parameters on engine heat transfer used a TACOM-Labeco single cylinder engine with an electronic fuel injection system capable of injection pressures up to 16,500 psi (Van Gerpen et al. 1985). The engine was equipped with a heat flux gage on the cylinder head, and exhaust analysis equipment ( $\text{CO}_2$ , HC,  $\text{NO}_x$ , Bosch smoke). Particulates were captured in a mini-dilution tunnel on filter paper and weighed after timed operating runs. The fuel injector was operated with a variety of nozzle tips, giving different hole configurations and injection durations for a constant fuel mass supply. Swirl level was varied using a shrouded intake valve.

The results of this study indicated that the  $\text{NO}_x$ -particulate tradeoff is favorably influenced by high pressure injection. It appeared from the heat transfer measurements that the effects of swirl on combustion were much larger than the effects of swirl on convective heat transfer. In summary, this study was able to point out some of the interrelationships between injection and in-cylinder fluid mechanics and emissions, but it also indicated that much more detailed data are needed to completely describe the phenomena.

The series of efforts involving studies of variations in fuel injection rate shape and timing on engine performance and emissions included a study using a Detroit Diesel 3-53 two-stroke diesel engine with a main electronic fuel injector in the cylinder, and two auxiliary air-assist injectors (Shakal and Martin, 1990). One of the auxiliary injectors was mounted in the intake manifold, well upstream of the engine, and the other in the inlet tract just upstream of the inlet to the combustion chamber. These two auxiliary injectors were to provide varying levels of auxiliary injection with different amounts of mixing upstream of the combustion chamber. Two different fuels (Number 2 diesel fuel, CN = 50.4, and a type 1 reference, CN = 20) were used in the study to illustrate chemical effects of piloted injection.

The results of the study were slightly different for the two fuels used. For both fuels, main injection only produced the most rapid pressure rise and heat release. For DF2 fuel, the port and manifold injection produced lower  $\text{NO}_x$  than the main injection alone, and port injection produced the lowest Bosch smoke. For the type 1 fuel, the manifold injection also produced lower  $\text{NO}_x$  than the main injection only, but higher Bosch smoke. These results are summarized in Table 7.5.1, which shows the various test conditions and measured emission results for the experiments. The results indicate

Table 7.5.1 Tabulated Engine Test Results

SPEED (RPM)	FUEL	INJ MODE	EQUIV RATIO	IG DELAY (deg CA)	ISFC (g/kWhr)	MAX PRES (Bar)	MAX dP/dθ (Bar/CA)	BOSCH SMOKE	HC (ppm)	NO <sub>x</sub> (ppm)	NO (ppm)
1800	DF2	MANIFOLD	0.50	-2.9	244	97.8	1.81	2.1	3430	-----	-----
1800	DF2	PORT	0.45	-1.7	224	99.8	2.21	2.9	1070	-----	-----
1500	DF2	PORT	0.46	4.9	240	84.8	2.69	1.8	1450	516	443
1500	DF2	SINGLE	0.45	7.0	222	82.4	3.08	2.7	304	528	450
1500	DF2	PILOT	0.43	-3.9	230	75.8	2.51	2.2	154	459	368
1500	DF2	PORT ONLY	0.08	---	---	58.0	1.83	--	-----	-----	-----
1500	TYPE I	PILOT	0.50	3.6	249	76.0	5.88	6.3	40.2	620	564
1500	TYPE I	PORT	0.56	7.2	245	99.6	7.08	0.4	2500	933	853
1500	TYPE I	SINGLE	0.28	7.1	239	79.8	8.94	0.1	160	755	682
1500	TYPE I	PILOT	0.29	6.5	232	74.0	4.92	0.1	137	556	514

test conditions and measured emission results for the experiments. The results indicate the general trends for manifold and port auxiliary injections, as well as indicating that there are significant fuel or chemical effects in the process.

A further study of pilot injection was undertaken using a single high pressure injector capable of multiple closely spaced injections (Bower and Foster 1990). In this work, some details of the interaction of the pilot injection cloud with the main injection are presented. In addition, some results are presented using different split injection strategies in a combustion bomb. The results of the combustion studies indicated that the proportion of the total fuel charge devoted to the pilot injection and the timing of the pilot injection relative to the main injection is significant in terms of measured NO, NO<sub>x</sub>, and estimates of soot concentration. Consistent with previous work, this study found that pilot injection can reduce NO and NO<sub>x</sub> relative to the no pilot case, without significantly increasing estimated soot concentration. In addition, ignition delay is affected by the amount and timing of the pilot injection.

Continuing this work in a later paper, (Bower and Foster, 1993) in the same combustion bomb, the authors applied Exciplex fluorescence techniques to visualize fuel liquid and fuel vapor in the bomb. It may be noted that this particular combustion bomb has a relatively high swirl level, although the swirl was modulated to a swirl ratio of about 4.5 to 5 for this experiment. The authors used high speed photography to measure liquid fuel penetration as a function of time for a variety of split injection conditions. In addition, vapor phase and liquid phase visualizations were generated using exciplex fluorescence captured with an intensified video camera. A sample of the type of images obtained from the exciplex imaging is shown in fig. 7.5.4.

The results of the visualizations indicated that the tip penetration of the liquid fuel was affected by the amount of pilot injection, apparently due to induced air motion. The split injection appeared to have a significant impact on the rate of pressure rise under combusting conditions, and it appeared that similar rates of pressure rise could

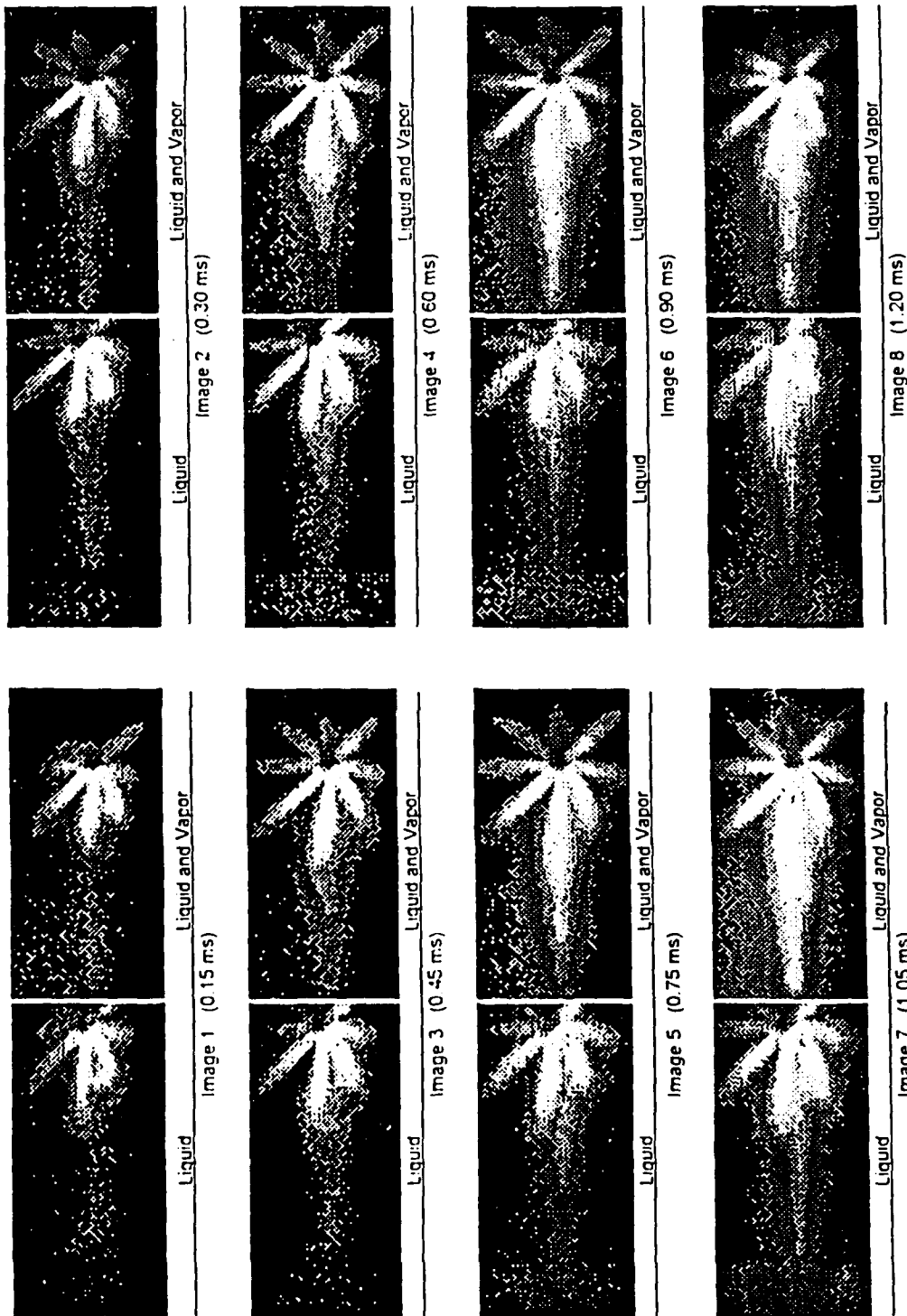


Fig. 7.5.4 Exciplex images for a single main injection. Images are ensemble averaged for 8 individual images. Times are from the start of injection, with swirl clockwise.

be obtained using a variety of different split injection strategies by varying injection timing.

A series of papers have been written concerning numerical work related to the problem of cold starting in diesel engines by Gonzalez et al. (1991) and the effects of variations in spray models on predictions of combustion by Gonzalez and Reitz (1991b), and Gonzalez et al. (1992). The basic model for these studies was KIVA-II, a numerical code developed at Los Alamos National Laboratory, and modified at the University of Wisconsin.

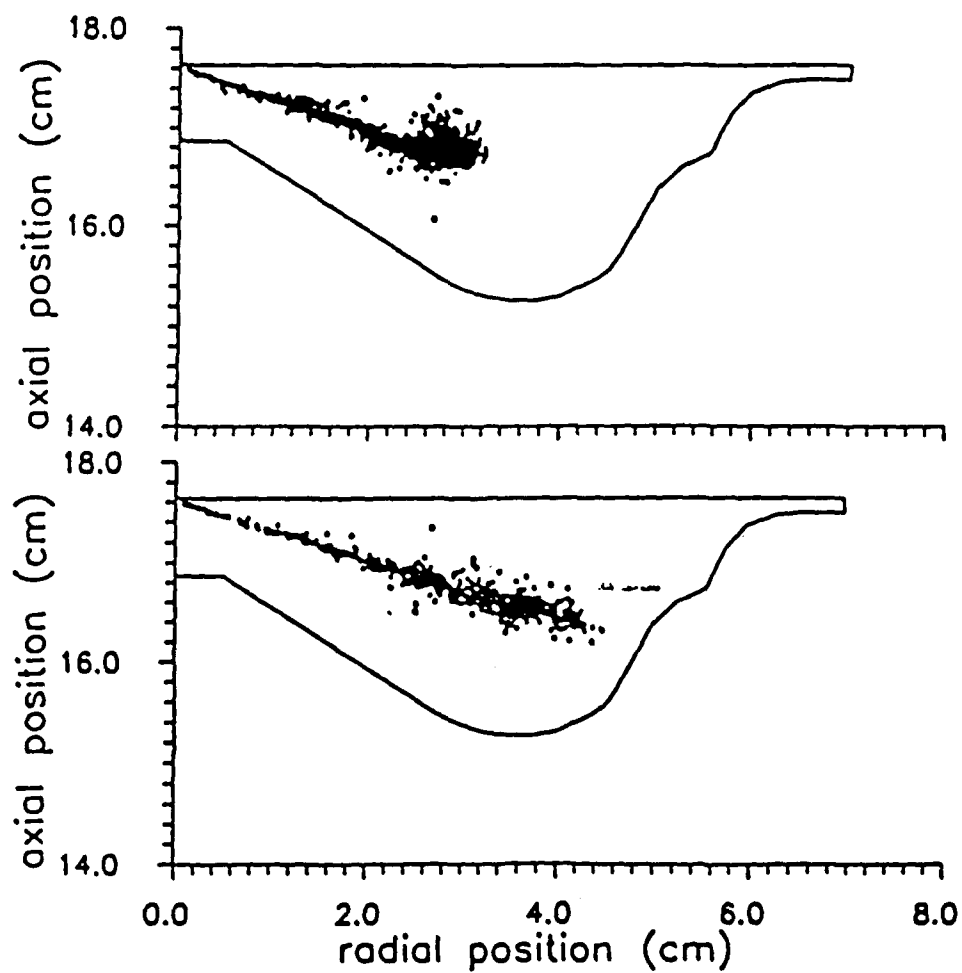
In the first of these papers (Gonzalez et al. 1991b) the geometry used in the model was that of a Cummins NH series heavy duty diesel engine, to be started at ambient temperatures between 241 K and 263 K. In this work, variations in intake temperature, cranking speed, blow-by, and spray characteristics were examined for their effects on cold starting. This type of modeling requires complex interaction of several submodels in the code. Based on results of this work, it appears that some of these sub-models require further work.

The major conclusions of this study were: the spray pattern and timing are important parameters in cold start performance; blow-by is a significant part of the cold start in-cylinder fluid mechanics; higher cranking speeds provide a significant advantage by reducing blow-by and heat transfer; simple reaction kinetics predicts ignition behavior consistent with experiments; and the fuel volatility seems to have a minor effect on vapor distribution.

The second of this series (Gonzalez and Reitz, 1991b) concentrated on evaluating the reasons for the lack of agreement on flame front location predicted by the KIVA II model and experiments in an actual engine. The central issue was the relatively smaller spray penetration predicted by the model compared to estimates based on flame front arrival measurements in the engine (Yan and Borman, 1985). The work focused on effects of fuel vaporization, effects of grid resolution, and effects of the initial drop size used in the calculation. Of these, the vaporization model under-predicted vaporization, if anything over-predicting the penetration length. The grid resolution had a significant effect on the modeled spray plume, in particular the cone angle, but a smaller effect on the penetration. When a sufficiently fine grid spacing was used, good agreement was obtained in comparing predictions for non-vaporizing sprays with measurements. The largest effect seemed to be from the atomization model used in the spray calculation, which predicted a large number of small droplets. These small droplets vaporize quickly with little penetration across the cylinder, and could be the major cause of the difference between the experiments and the predictions. An example of the difference between predictions with the current atomization model and a simpler model using 5 mm diameter droplets without atomization or coalescence is shown in fig. 7.5.5. A major conclusion of this work was that more work needs to be done on the spray atomization models.

The third paper in this series (Gonzalez, et al 1992) discussed the significance of grid resolution, vaporization, and atomization effects in somewhat more detail. In detail, it appears that the need for refined numerical grids in the calculation is most important at high vaporization rates typical of diesel engine operation. The atomization models used in the code were shown to provide good agreement when compared to experiments for non-vaporizing sprays, but under vaporizing conditions, as in an

Fig. 7.5.5 Drop locations in the plane mid-axis of the spray using the atomization model (top) and an initial 5  $\mu\text{m}$  drop radius (bottom) without breakup or coalescence.



engine, the droplet atomization appears to predict small droplets which do not penetrate into the combustion chamber as far as experiments have indicated they would. The conclusions of this work echo the previous one, suggesting additional work on the topic of atomization in vaporizing sprays, in order to improve understanding of the process and application of the models.

### Injector Characterization

Our efforts in this area of research were motivated by a desire to be able to characterize the spray breakup characteristics of injectors. The work centered on developing experimental techniques along with associated analysis that could measure (or calculate) the most relevant parameters for injector operation and determine their interrelationship. As a beginning, the past work in spray breakup processes were reviewed and the most relevant parameters identified for further investigation (Bower, et al. 1988). The research efforts were partitioned into ones involving internal fluid flows within the injector becoming external fluid flows as the fuel enters the combustion chamber, and studies of subsequent jet breakup and atomization. For internal flow characteristics, initial computational results (Huh et al, 1990 and Chang, 1991) indicated that scaled internal flow experiments would prove enlightening and this was the experimental approach taken by Knox-Kelecy and Farrell (1992, 1993). For external injector flows a staged experimental/analytical approach was begun with initial experiments aimed at characterization of the integral injector spray breakup process (Bower, et al, 1988 and 1989) followed by more sophisticated characterization using the Phase Doppler Particle Analyzer (PDPA) technique (Koo and Martin, 1990b and 1991) for local point measurements and direct spray imaging of the jet for radial averaged results (El-Beshbeeshy, et al, 1992) and associated analyses (Chang, 1991). The results of these investigations are summarized below.

The experiments for investigation of internal flows in an injector-like geometry were motivated by initial calculations (Huh et al 1990 and Chang 1991) that simulated the internal flow for a single hole injector and the upstream sac volume. The initial results of these calculations suggested that the turbulence within the sac volume and developed within the injector nozzle hole could have a significant impact on the downstream breakup characteristics by imposing preferred wavelengths and frequencies for aerodynamic wave growth in the spray. These characteristics are influenced by the nozzle length/diameter ratio ( $L/D$ ) and inlet nozzle radius/diameter ratio ( $R/D$ ). The experiments conducted by Knox-Kelecy and Farrell (1992, 1993) investigated the turbulent flow patterns and spectral characteristics for a scaled-up model of a high pressure diesel single-hole fuel injector nozzle. Instantaneous velocity measurements were made in a 50x larger transparent model of an injector nozzle using an Aerometrics PDPA in the velocity mode. Nozzle  $L/D$  values of 1.3, 2.4, 4.9, and 7.7 and inlet nozzle  $R/D$  ratios of approximately 0 and 0.3 were examined under two steady flow average Reynolds numbers (10,500 and 13,300). These conditions were analogous to fuel injection velocities and sac-volume pressures of approximately 320 and 400 m/s and 67 and 107MPa. The results of these measurements were presented as mean and RMS turbulence velocity values at various axial and radial locations. Turbulence spectra were also calculated from the velocity data using the Lomb-Scargle method for irregularly spaced time series data. This produced turbulence frequency

spectra for particular locations in the nozzle. Results indicated that the internal flow turbulence showed a marked dependence on the R/D and a more subtle dependence on L/D for sharp inlet geometry (R/D = 0). Internal flow through rounded inlet shaped nozzles does not produce striking turbulence characteristics. It appears that the rounded holes effectively pass the upstream turbulence through the hole with little alteration in RMS value or spectra until far down the length of the hole. This suggests that the turbulence of the sac volume will still be present at the exit of the hole. The sharp edge nozzle inlets produce high, near-wall, RMS axial velocities which appear to have a minimum at about 4.5 L/D. These sharp inlet holes are more effective in "erasing" upstream turbulence characteristics and generating new local turbulence than the rounded inlet flows. Thus more attention needs to be paid to the effects of the L/D for sharp edge nozzles and on the effect of "aging" or "break-in" of the nozzle as it changes from sharp-edge to more-rounded in character.

External jet spray characterization of injectors was begun (Bower et al, 1988 and 1989, and El-Beshbeeshy and Corradini, 1989) with a focus on the integral effects of spray injection and breakup by measurement of the spray kinematics (tip penetration, spray angle and profile). To demonstrate the technique, a high pressure accumulator-type injector (BKM model up to 155 MPa) was used in a high pressure isothermal quiescent spray chamber of chosen density by selecting pressure and ambient gas. The injector used a standard single orifice nozzle which can produce a single jet or full cone spray. With this apparatus, the injector spray can be examined with variable, but controlled conditions. Experimental data was collected using two photographic techniques with high speed photography and a pulsed laser light source. Direct attenuation allowed for measurement of the tip penetration, spray cone angle and injection duration, while scattering from a laser light sheet was developed to obtain qualitative information on the inner spray cone structure. The controlled variables in these experiments were the injector hole diameter (0.24 - 0.41 mm), the peak accumulator pressure (70 - 140 MPa), the gas density (10 - 15 kg/m<sup>3</sup>) corresponding to a compression ratio of 10-20, as well as the injection frequency. Initial results for variable injection pressures and gas densities indicated that gas density increase had a marked effect on tip penetration and spray profile, causing the spray to spread out radially and reduce axial penetration, independent of the gas pressure or composition. The injection pressure decreased the time scale of the injection and increased the cone angle suggesting better spray breakup. Also no intact liquid core was detected in any of the visual records. Further studies on this injector also measured the accumulator pressure and the injection rate histories and showed that the BKM high pressure injector produces a very fast initial rate of injection which slowly decayed throughout the injection period with a sharp cut-off. This set of experiments also indicated that the spray kinematics were independent of the injection frequency since the peak accumulator pressure determines all the injection characteristics.

Detailed knowledge of the structure of a transient diesel fuel spray (i.e., local measurements of the spray droplet sizes and velocities) is a prerequisite to understanding and eventual prediction of diesel combustion behavior for a particular injector. The primary diagnostic used for this purpose was an Aerometrics PDPA using a Lucas CAV injector to demonstrate the feasibility of the concept (Koo and Martin 1990a, 1990b and 1991). This injector had a single hole of 0.24 mm diameter with a jet

spray discharging into a stagnant isothermal chamber at a variety of gas densities (1-25 kg/m<sup>3</sup>). The PDPA was used to sample the spray droplet diameters and velocities at five different downstream axial positions ( $x/D = 40, 80, 120, 200, \text{ and } 240$ ) and four different radial positions ( $r/D = 0, 2, 4, 6$ ) as a function of time during the jet discharge. This ensemble of raw data was used to determine local Sauter mean diameter and velocity histories and droplet distribution functions in order to compare to droplet breakup/stability criteria and computed distribution functions as well as examine the effect of variable gas densities. Comparison with the stability criteria indicated that the majority of the droplets in the spray at positions near the injector tip are susceptible to aerodynamic breakup, while further downstream the spray droplets appear to stabilize and further redistribution of sizes are probably due to spray droplet collisions. The spray droplet distribution functions were found to exhibit best agreement with multi-parameter-dependent distributions, such as the chi-square or the log-hyperbolic distributions. In addition, these local PDPA measurements supported our past data which indicated that increases in the surrounding gas density greatly decelerated and spread out the fuel sprays. Droplet sizes tended to decrease more rapidly and remain relatively constant at the higher gas densities in contrast to lower densities where spray droplet sizes reductions evolved more slowly.

More recently a different technique was developed (El-Beshbeeshy, et al 1992) to characterize the integral quantities of a non-evaporating, non-burning spray for any particular injector using light attenuation and associated image analysis. This technique was discussed in the section on experimental development. In order to compare the technique to the local PDPA measurements previously obtained, the Lucas CAV injector was also characterized for a range of ambient gas densities (10 - 35 kg/m<sup>3</sup>), injected fuel mass (4.5 - 8.5 mg), pump speeds (400 - 1600 rpm) and nozzle hole diameters (0.24 - 0.41mm at constant nozzle length) which included and extended the range of the PDPA data. The results showed that the SMD decreased as injection proceeded and eventually approached an asymptotic size. Axial variation of the SMD at a specific time indicated that the size reached a minimum in the spray interior. Most importantly, when these results were compared with the data obtained with the PDPA for similar conditions, good agreement was obtained (Figure 7.5.3). To validate our ideas on transient jet breakup (Chang, 1991) a modified jet breakup model for KIVA was compared to this same data set and the predictions were quite consistent with both data sets. This gives us a complete characterization of this injector with local and integral measurements as well as validation for a spray model that could be used to predict injector spray behavior in similar conditions.

#### Alternative Injector Strategies

Traditional methods for fuel spray injection have employed a highly pressurized liquid spray injected into the combustion chamber under a variety of ambient conditions to optimize jet breakup and mixing in droplet form and their eventual vaporization in the combustion chamber. A couple of unique alternative injector strategies have been pursued as part of the ERC efforts (Liu, et al, 1992, ILASS, Rietz, 1990) to examine the possibility of other methods to efficiently break up and mix the fuel with the oxidant. In addition, studies have focused on the interaction of the spray droplets with the combustion chamber walls from a fluid mechanics and heat transfer

perspective (Naber and Reitz, 1988, Naber, et al, 1988, Naber and Farrell 1992, 1993). This interaction is quite important in understanding how the spray breakup is affected by the chamber walls from droplet collisions and possible liquid fuel redistribution.

Air-assisted atomization has the potential of causing efficient jet spray breakup with significantly lower injection pressures. To examine the potential of such a scheme for diesel engines a well controlled experiment (Liu and Rietz, 1992) was designed to study liquid fuel drop atomization. The experiment included a liquid drop generator which sent single liquid droplets through an air jet in a cross-flow pattern near the nozzle exit to minimize shear layer effects; drop diameters were below 0.2 mm and air velocities were up to 250 m/s. Near field and far field photographs were taken to observe the droplets breakup process and their trajectories, as well as PDPA measurements of droplet sizes at two downstream locations. Visual results indicated three distinct droplet breakup regimes in the tests; i.e., bag breakup, boundary layer stripping, and surface wave instability breakup at higher Weber number (250 - 600). The liquid droplet drag coefficient and trajectories were measured and based on this the dimensionless breakup time was found to be near 1.7 with average drag coefficients larger than that for a rigid sphere. This implies that droplet breakup and distortions must be accounted for to accurately predict drop trajectories and diameters.

Another unique approach to augmenting jet spray breakup is to heat the pressurized injector fluid to a temperature at which it would vaporize when depressurized in the combustion chamber; i.e., flash-boiling atomization. This vaporization upon depressurization can aid in the efficiency of jet spray breakup again with significantly lower injection pressures. To demonstrate this idea a heated jet spray experiment was conducted (Rietz, 1990) by injecting a liquid water jet heated by a coflow of air into a quiescent spray tunnel at a specified set of conditions; injection pressure (0.7 MPa), single hole nozzle (0.34 mm,  $L/D = 4$ ) with a variable inlet liquid temperature (300 - 430K). Back-lit spark photographs of flash-boiling sprays indicated the existence of an inner intact liquid core in these jets, whose breakup begins at the nozzle exit and length depends on the degree of liquid heating. More traditional front-lit images did not indicate this intact core and these results cast doubt on previously proposed theories for this process which suggested liquid atomized within the nozzle. A breakup mechanism which considers this two-phase jet breakup outside the nozzle is consistent with the data. As the liquid jet temperature approaches its saturation temperature at the injection pressure the liquid core length decreases and this increases efficient atomization. However, the limit to this is reached at saturation when the channel flow decreases as it experiences two-phase critical flow. This suggests that such a scheme would be difficult to operate near the liquid boiling point for practical intermittent injection systems since the injection pressure usually varies widely with time.

Most studies of injector performance as measured by jet spray breakup consider the spray to issue into a semi-infinite gas field. However, in actual engine conditions the confined space of the combustion chamber causes the spray to impinge on solid surfaces at some location downstream of the injector tip ( $>200D$ , where  $D$  is the injector hole diameter). Some of the initial work on spray/wall interactions (Naber and Rietz, 1988) addressed this issue by examining the problem of a diesel spray impinging on the bowl of a piston in a moderate swirl engine. This work focused on modifying the

models for spray/wall interaction to a more physically based description of spray wetting and liquid film flow in the KIVA spray code (reference for versions 1 and 2) and qualitatively comparing the results to data from an operating engine. The results indicated good agreement for overall far-field spray plume spread and apparent surface wetting.

Some injection strategies have been advanced for relatively novel combustion geometries in which a projection of the piston or the injector protrudes toward the injector tip (Fig. 7.5.6; 15-20D from the tip). The intent is to enhance the fuel injection process by direct impact of the spray on the target surface. Since this is a somewhat different condition from that of the earlier work, a study of this near field interaction was undertaken (Naber, et al, 1988). A series of experiments were performed in a cold, high pressure, constant volume bomb using a single hole fuel injector spray impinging onto a projected surface in the middle of the piston bowl. The overall spray pattern history was recorded photographically and compared with the results of a numerical spray model incorporated into the KIVA code. Good agreement was obtained when the model included estimates of the surface interaction effects on the drop size and normal jet velocity (see Fig. 7.5.7). Standard models of spray/wall interactions did not show satisfactory agreement for the lateral spread of the spray after impact. The assumptions regarding wall interactions which were made in this work in order to allow the numerical model to agree with the experiments were somewhat ad-hoc, suggesting that detailed modeling of this phenomenon required more fundamental data on drop sizes and velocities near solid surfaces.

The detailed study of droplet-wall interactions was the experimental goal of the follow-on work by Naber and Farrell (1992, 1993). The heat transfer and hydrodynamics of a single liquid droplet impinging on a heated surface was investigated and an energy model for the spreading of the resultant liquid film was derived. Individual droplets ( $d = 0.1 - 0.3 \text{ mm}$  @  $v = 2.4 - 7 \text{ m/s}$ ) were produced for a variety of liquids (water, acetone, and n-heptane) and impinged on a heated surface (temp = 56 - 400C). The heat transfer between the droplet and the liquid decreased as the surface temperature increased due to local flow regime changes from droplet wetting and evaporation to film boiling (i.e., beyond Leidenfrost temperature). High speed photography and image analysis were used to quantify droplet atomization observed during impingement; i.e., diameter and velocity distributions of rebounding drops. For the range of droplet sizes and velocities examined, neither atomization nor splashing was observed in the wetting-evaporation regime. In the film boiling regime beyond the Leidenfrost temperature, a larger number of smaller droplets were produced after impact with the surface as the entering Weber number increased. As a way to utilize this data as a spray submodel in injector design and spray-wall interactions an energy model was derived which successfully predicts the hydrodynamics and heat transfer of the droplet as it wets and spreads on the heated surface.

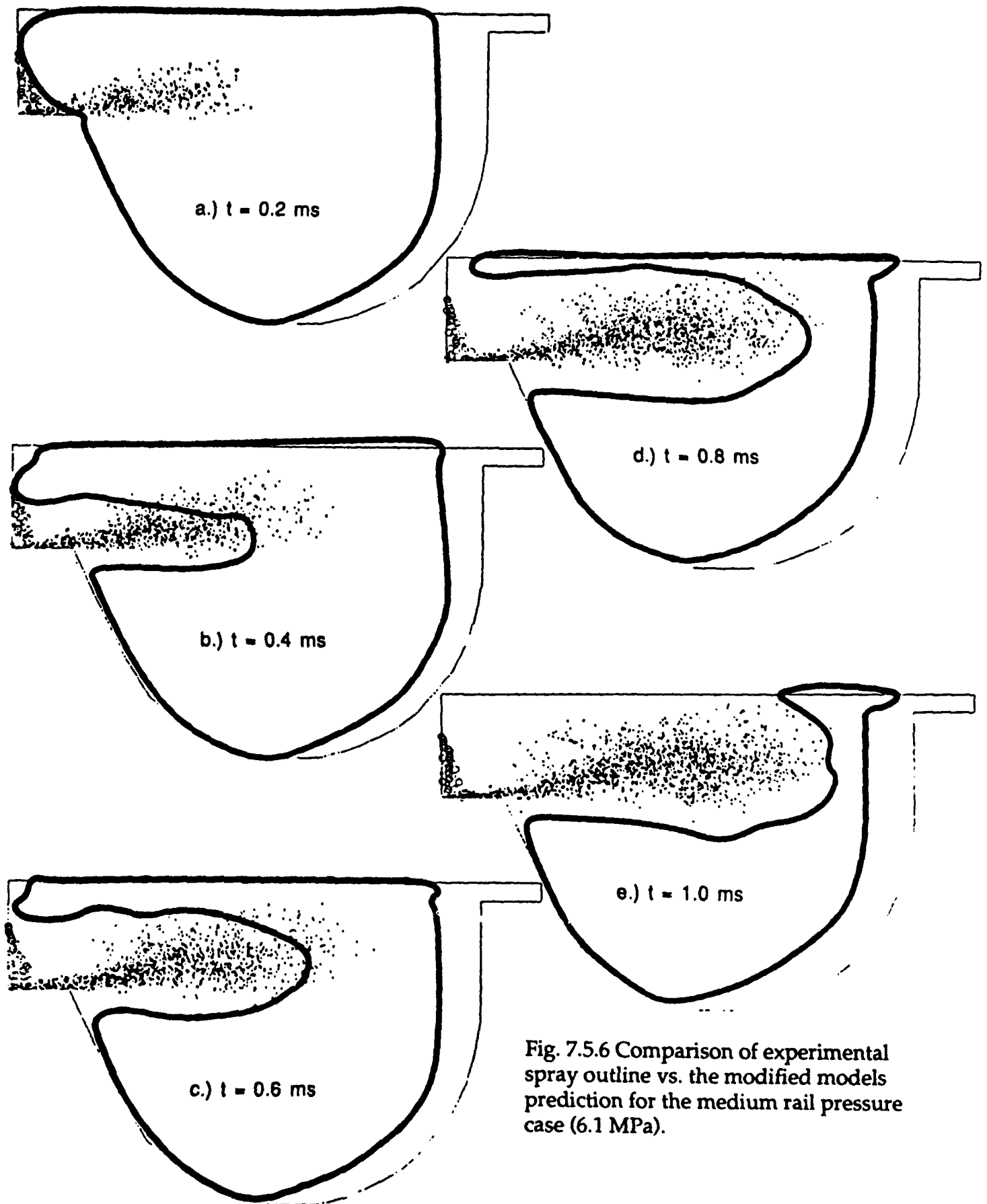


Fig. 7.5.6 Comparison of experimental spray outline vs. the modified models prediction for the medium rail pressure case (6.1 MPa).

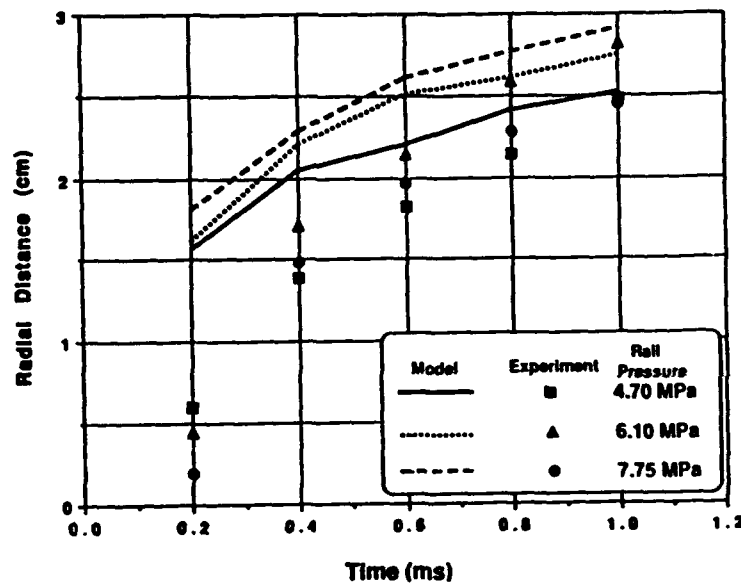


Fig. 7.5.7 Comparisons of the experimental impinged spray penetration vs. the modified models predictions at the three rail pressures as a function of time.

### Spray and Droplet Characterization

Beyond the overall investigation of injector performance and spray characterization, further work is necessary to understand the fundamental processes involved in spray droplet vaporization and kinematics. A number of studies have been carried out in this area as part of the research in the ERC (Curtis and Farrell, 1988, Curtis and Farrell, 1992, Lian and Reitz, 1992, Mather, Liu and Reitz, 1992, and Liu, Mather, and Reitz, 1993).

The evaporation of single, spherical fuel droplets under supercritical conditions was studied numerically in the development of a fully transient droplet vaporization model (Curtis and Farrell, 1988 and Curtis and Farrell, 1992). This model allowed for transport properties which are a function of temperature, pressure and composition along with a Peng-Robinson equation of state and mass diffusion model to account for gas diffusion into the liquid droplet. Data obtained for a variety of liquids were compared to the model and exhibited good agreement in the prediction of the critical mixing state, droplet vaporization rate and the droplet temperature. Transient effects were found to have a large effect in the droplet vaporization process, particularly under very high temperature and pressure conditions where the droplets were found to reach their critical mixing point. Coupled diffusion processes were studied and found to be an important factor in high-pressure droplet vaporization.

In order to better understand the atomization process of high speed liquid sprays in high pressure and high temperature diesel engine environments, a model was developed to include the effect of liquid surface evaporation (Lian and Reitz, 1992c). The results indicated that in the atomization regime, the hydrodynamic instabilities along the jet surface are predicted to be stabilized by the surface evaporation effect. These authors recommended that the analysis be confirmed by experimental evidence. Compressibility effects were also considered and it was found that if the high speed spray enters with a reference Mach number much greater than 1, gas compressibility must be taken into consideration.

In an effort to model the droplet breakup and kinematics that accompany spray breakup, two different droplet breakup models were compared with data on droplet trajectories and spray penetration (Mather et al. 1992, and Liu et al. 1993). Both models indicated acceptable agreement with the data although the proposed wave model for use in KIVA was found to give more consistent drop breakup diameters when compared to the data than the TAB model originally developed for KIVA.

#### Summary of Findings and Impact on Technology

The results of the spray research in this program have included development of new instrumentation techniques for spray measurement, experiments which have provided detailed information on the transient behavior of sprays, modeling efforts which have developed improved methods of modeling spray behavior and breakup phenomena, and some experiments intended to explore new injector concepts and their possible benefits.

In the course of the five years of this program, all questions regarding high pressure fuel injection have not been answered. However, the collection of results has answered some questions, has indicated some questions are not significant, and has indicated those issues which are both important and not yet well understood. These results have been transmitted continuously orally and in written form to interested Army and other government laboratories, industry, and other university laboratories. The primary written record of these results is the record of publications from the program.

Due to the often informal transmission of results from this program and the fundamental nature of the research supported, it is difficult to accurately assess the impact on technology of the spray research performed under this program. An indication of the impact may be inferred from the high level of interest in the program exhibited by colleagues in government, industry and other universities. Some of the experimental techniques developed are under consideration or are being adopted by several industrial engine manufacturers. Interest in the development of suitable spray models is very high, and there are several efforts to transfer the developments of this program to industry.



## 7.6 Lubrication, Mechanical Design and Materials

### INTRODUCTION

The emphasis of the ERC research has been related to thermal science topics as illustrated by combustion and spray processes, heat transfer, etc. However, some additional projects were carried out which relate to the mechanical design of engines. These projects were motivated by a variety of Army needs.

An important need is to produce an engine with low friction that can operate at elevated temperatures. The increase in temperature may be due to low heat rejection design (see Section 7.3) or by unintended loss of coolant. Although development of specific high temperature techniques, such as vapor lubrication is necessary, it is also important to develop the experimental diagnostics and computational models needed in development of such high temperature systems. Thus the ERC has carried out projects which have exercised experimental techniques for oil film measurement on the engine cylinder liner and used these diagnostics for engine measurements and model validation.

The lubrication experiments are important for understanding issues of durability and wear on the gas side of the liner, but conventional heavy duty engines can also suffer problems due to liquid coolant side cavitation caused by liner vibration. The ERC thus undertook a study to improve the methodology for design of liners. This study concentrated on the liner vibration, but clearly the cause of the vibration is contact between the piston and the liner. Thus a design for replacement of the conventional slider-crank mechanism by a new mechanism which greatly reduces vibrations would offer a potential aid to both decreasing wear on the lubricant side and decreasing cavitation on the coolant side. One such mechanism, the hypocycloidal drive, was thus investigated at the ERC to determine if it is appropriate for Army applications.

The motion of the piston for the conventional slider-crank with either a one piece or two piece (articulated) piston is complex and causes difficulty in predicting phasing as well as tipping (sidewise) motions of the piston. These effects may influence combustion, liner vibration, and wear. A laser based technique was thus developed to measure piston position and was applied to a motored diesel engine. The mechanism is described here, but additional applications of the finding are given in Section 7.2.

At the onset of the subject contract it was thought that the ERC should play a role in engine testing of new materials, especially ceramic candidates for LHR application. Clearly the best tests for such materials would be in the actual engine design, however that is a costly procedure in both time and money. Thus a need exists for a rig and instrumentation which can test material samples at engine-like conditions, but with low cost components. Several pathways were followed at the ERC in an attempt to meet this need. First, it was thought that the hypocycloidal drive would offer advantages in creating a diesel test engine in which failure of combustion chamber parts would not destroy the drive mechanism. This would be possible because the rod driving the piston could be easily isolated from the drive. However, it became clear that the drive had to be developed first and that it would not be available as a practical tool for several years. It was thus decided to set up a small conventional S.I. engine for sample testing and diagnostic development. This was done and is described below. The instrumentation utilized the infrared detection system developed by Dr. Shepard at

TACOM. Although both the diagnostics and the loading did not meet all Army needs, the rig was generally successful.

Although development of coatings and monolithic ceramics was being carried out by the Army and DOE at other locations, a small effort on ceramic composites was started at the ERC in conjunction with development of a high temperature rig for tensile testing of samples. The results of these parallel efforts are also described below.

In summary, this section covers the following topics: (1) lubrication measurement techniques, (2) lubrication measurement results for both fired and motored engines, (3) modeling results for both Newtonian and non-Newtonian lubricants, (4) tests of lubricants at high shear rates using a stressmeter, (5) methodology for liner design, (6) design and evaluation of a hypocycloidic drive mechanism, (7) development of a piston position diagnostic system, (8) development of methods for testing material samples under engine conditions, and (9) development and testing of composite materials.

## MEASUREMENT TECHNIQUES FOR ENGINE LUBRICATION

Many issues concerning engine lubrication for both conventional and LHR diesel engines involve needs for new diagnostic methods. Among the measurement needs are; ring to liner distance, liner oil film thickness, liner temperature, ring temperature, gas pressure between rings, piston motions, time resolved lubricant consumption, and insitu physiochemical properties of the oil film. All but the last two have been addressed by the ERC; they are discussed below. While the insitu lubricant properties were not measured, an extensive program was carried out to measure viscosity at conditions typical for engines, i.e. high shear rates and elevated temperatures. These tests have particular relevance to nonNewtonian behavior of the oil, and are discussed below as part of the discussion of engine measurements.

### Insitu Measurement Techniques

Two techniques of liner oil film measurement were developed and used. In the first method capacitance probes were used to measure piston ring to liner distance at the upper ring reversal position. The work is reported in the paper of J. Myers et al. (1990). In this method the capacitance between a small probe mounted flush in the liner and the piston ring is measured as a function of crankangle (time). The resulting signal is interpreted in terms of the ring standoff distance. The probe construction is shown in Fig. 7.6.1. The use of the machinable glass ceramic Macor greatly improved the life of the probe as compared to using a high temperature epoxy as the insulator. At the time of the research a suitable method of calibration was not available and thus the calibration was determined from parallel plate theory. Three gauges were placed 120° apart and at the same height on the liner, just below the reversal point. The top ring covered the gauges over an interval of about  $\pm 6.5$  crank degrees around TDC. In addition, three 0.787 mm O.D. coaxial type surface thermocouples were used to measure the liner surface temperature close to each capacitance probe, as shown in Fig. 7.6.2. A TACOM/LABECO single cylinder research engine was used for the study. Both the capacitance probes and sliver junction thermocouples were durable. The thermocouples gave data for temperature and calculation of instantaneous heat flux, but did not clearly indicate any metal-to-metal contact.

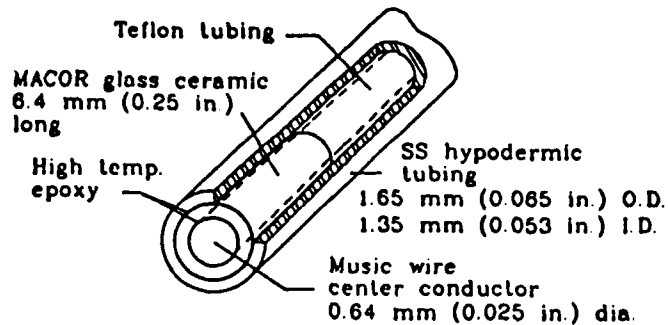


Fig. 7.6.1 Capacitance probe construction.

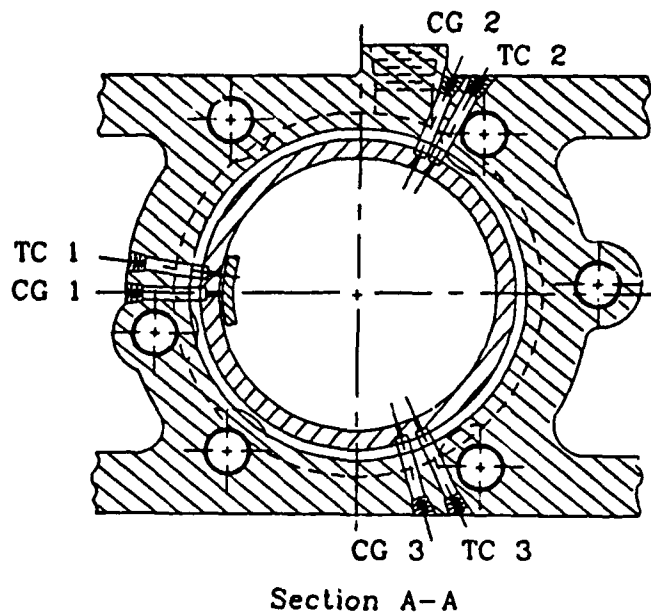


Fig. 7.6.2. Installation of probes, top view.

The use of capacitance probes allows measurement of liner to ring distance, however they do not give a measurement of oil thickness except when the region being measured is fully flooded with oil. Thus a second method of measurement was investigated. In this method laser induced fluorescence (LIF) of the oil was used to indicate the amount of oil being irradiated by the laser. Various methods can be used to bring the laser light to the oil and to sense the fluorescent light. In the ERC version a single fiber optic has been used as shown in Fig. 7.6.3. The laser light (442 nm, blue Helium Cadmium laser) is sent to the oil through a small optical fiber (inner core 50  $\mu\text{m}$ , outer cladding diameter 185  $\mu\text{m}$ ) which is mounted flush in the liner. The greenish fluorescent light (500 nm) returns through the same fiber and is filtered so that the PMT detector measures the fluorescent light. Calibration in a laboratory rig shows the fluorescence level is linear with film thickness for oil layers up to 40  $\mu\text{m}$  in thickness but the slope depends on both oil temperature and composition and can be affected by bleaching if the laser power is too large and/or the exposure is too long. The various additives used in the lubrication package all influence the fluorescence, but in particular, polymers used as viscosity index (VI) improves and dispersant additives greatly increase fluorescence (Richardson and Borman, 1991). Unfortunately both of these additives can break down under engine operation. The addition of a fluorescent dye is also possible, but such dyes also are temperature sensitive and may change oil properties in an unknown way. In addition, the fiber probe can change its transmission quality and ring reflection of both the blue and the green light can cause changes in the calibration. Given these problems it seems necessary to use an in-situ calibration. However, to date, no satisfactory in-situ method other than calibration from known ring shape has been perfected. Unfortunately, ring shape can change due to wear and can be

distorted by ring twist or tilt. This may indicate that a combination of capacitance and LIF methods could give the best results. The capacitance method works best for very thin oil layers while the LIF method works best for thicker layers. However, to compare simultaneously taken data from the two methods it is desirable to design a capacitance probe capable of spatial resolution similar to the 50  $\mu\text{m}$  diameter of the fiber core. It is also desirable to have a method of determining oil property in-situ or by sampling. Both of these objectives are currently being pursued at the ERC along with instrumentation for continuous measurement of gas pressure between the two top rings.

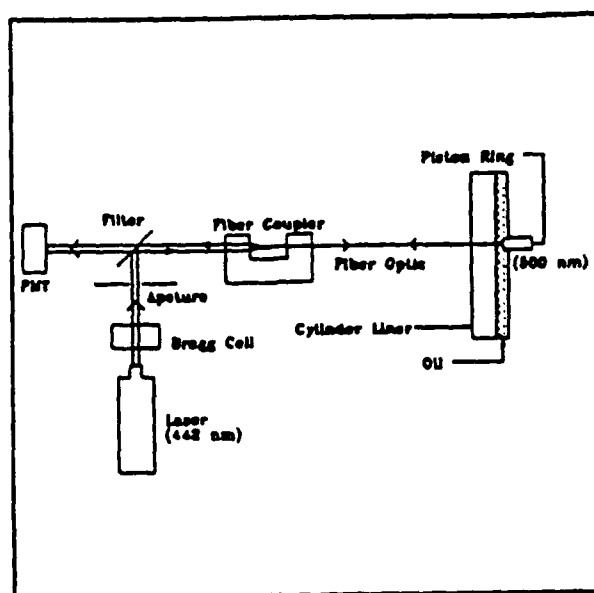


Fig. 7.6.3 Schematic of the laser system for LIF lubrication film measurements.

### Oil Viscosity Measurement Methods

In addition to engine and off-engine measurements of oil films, it is necessary to have accurate data for oil viscosity to use in modeling, particularly for multigrade oils. Thus a companion program was conducted, under the direction of Professor Lodge, to measure lube oil viscosity at shear rates and temperatures typical of engine operation conditions.

Piston-ring/cylinder and journal bearing estimates have shown that oil shear rates can reach values in the  $10^7 \text{ s}^{-1}$  region under typical operating conditions. Most commercial viscometers only reach  $10^6 \text{ s}^{-1}$ ; these are of concentric cylinder rotational type. At these high shear rates, the main practical measurement difficulty is viscous heating; this generates a non-uniform thermal field which has to be dealt with somehow if reliable viscosity data are to be obtained at known shear rates and temperatures.

A more promising instrument is a slit die rheometer in which a short die is used which contains small transverse slots for pressure gradient measurement. Because the

residence time can be reduced to milliseconds (instead of seconds), the temperature rise due to viscous heating can be kept small enough so that the errors arising from the non-uniform thermal field are small and a fairly rough correction method should give adequate accuracy. For degassed decalin (of viscosity 2.5 cP at 20C), shear rates of  $5 \times 10^6 \text{ s}^{-1}$  have been attained with errors of up to about 8% (Lodge, 1987).

It is clearly essential to have an instrument capable of measuring the first normal stress difference,  $N_1$ , up to shear rates of at least  $10^6 \text{ s}^{-1}$  and temperatures up to 150C. The only such instrument at present known is the Lodge Stressmeter for High Shear Rates (Lodge, 1987). This is a small-slit-die rheometer similar to the viscometer mentioned above but with one die wall replaced by a flush-mounted pressure transducer with its effective center opposite the center of one of the two transverse slots in the opposite die wall. The difference of flush- and slot- measured pressures is used to calculate  $N_1$ ; shear rates up to  $3 \times 10^6 \text{ s}^{-1}$  have been attained (Lodge, 1989).

During the contract period, a viscous heating correction procedure was developed for slit die viscometers: for fully developed thermal and flow fields (Lodge and Ko, 1989); for thermally developing fields between isothermal walls (Ko and Lodge, 1991); and, finally, for thermally-developing fields with non-isothermal walls (Ko, 1990). The procedure's validity has been tested by means of a comparison of data obtained with different liquids and different die heights. It is believed that the present procedure is acceptable for viscous heating errors up to about 10% or 20% and for Nahme numbers [The Nahme (or Nahme-Griffith) number is a measure of the ratio, in a flowing liquid, of the heat generated (by work done on the liquid) to the heat conducted to the wall.] up to about 2. The procedure has recently been used elsewhere, with a similar instrument, for a 1 cP liquid at shear rates up to  $10^7 \text{ s}^{-1}$  (Williamson, 1992). It is expected that the desired viscosity range (2 cP - 3 cP) for typical oil applications can be attained when the instrument changes needed for the higher shear stresses are made. Some of the viscosity data obtained using multigrade oils have been used at the ERC by S. Mangkoesobroto in his computations of piston-ring/cylinder lubrication (Johnson and Mangkoesobroto, 1992).

## EXPERIMENTAL RESULTS FOR ENGINE LUBRICATION

The experiments of Myers (1989) and Richardson (1990) were conducted on a TACOM/LABECO, 1173 cc, open chamber single cylinder engine. This engine uses a piston design with oil drain holes behind the oil (scraper) ring and an oil spray for cooling. Both Myers and Richardson found chaotic behavior of the oil film which could not be explained from conventional hydrodynamic theory. This difficulty caused Myers to use a "hopping" technique of data acquisition in which bursts of data are taken at regular intervals, thus allowing a better statistical sampling of events. Richardson, using the LIF technique, and after an extensive analysis of the data, concluded that the combination of the cooling spray and drain holes allows oil to flow back up through the holes during the piston downstroke. This effect was confirmed by Phen (1992) who observed severe oil misting when the engine was motored with the head off. He found use of grooves to drain the oil, instead of holes, greatly reduced oil misting. Because of the oil control problem, the experiments were switched to a single cylinder version of the modern Cummins L-10 engine (donated by the Cummins Engine Company). The

most recent LIF data taken by Phen on this engine show much greater stability and very little chaotic behavior.

Despite the problems of instability some of the data taken on the TACOM/LABECO engine proved informative and useful for comparison with modeling results. These data are briefly reviewed here. For a discussion of the irregularities the reader is directed to the papers and/or theses.

#### Capacitance Probe Data

The data of Myers which could be characterized as "typical", and perhaps representative of more controlled oil flow, are shown in Figs. 7.6.4 and 7.6.5. The data for the intake valve side gauge as given in 7.6.4, shows a minimum film thickness shortly after TDC. During the compression stroke (shown) the film thickness was always thinner than during the exhaust stroke, as would be expected, given the much higher cylinder pressure during compression. The data for the thrust side gauge shown in Fig. 7.6.5 is more complex and requires explanation. The increase in film thickness before TDC is attributed to piston tilt as measured by Eng et al. (1990) on the same engine using the laser range-finding instrumentation shown schematically in Fig. 7.6.6. The tilt measurements were limited to 750 rpm, but the start of tilt as shown in Fig. 7.6.7 agrees remarkably well with the start of the increase in film thickness. The tilt of the piston crown toward the liner moves the ring away by tilting the ring slightly and/or by moving the ring back into the tapered groove causing a vertical component of ring motion which in turn would increase the film by generation of a hydrodynamic force. It is interesting to note that boosting the motored engine intake pressure caused the start of piston tilt to be advanced and that advancing the peak pressure of the fired engine by  $8^\circ$  caused the maximum of the film thickness to advance  $2^\circ$ .

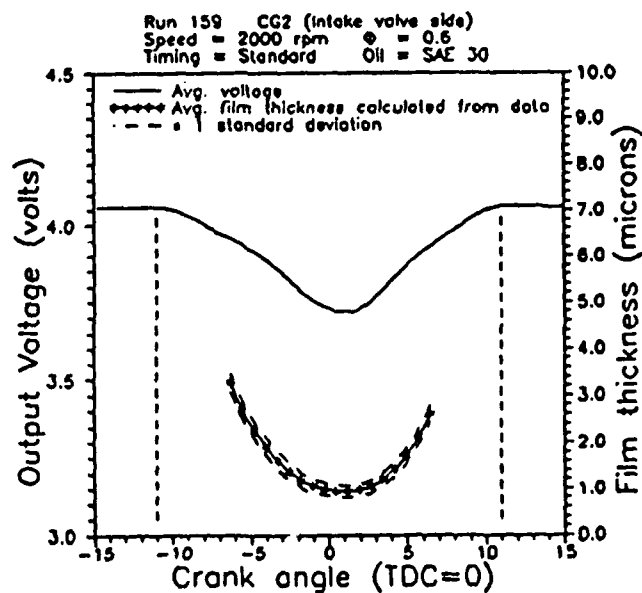


Fig. 7.6.4. Compression stroke oil film thickness, intake valve side.

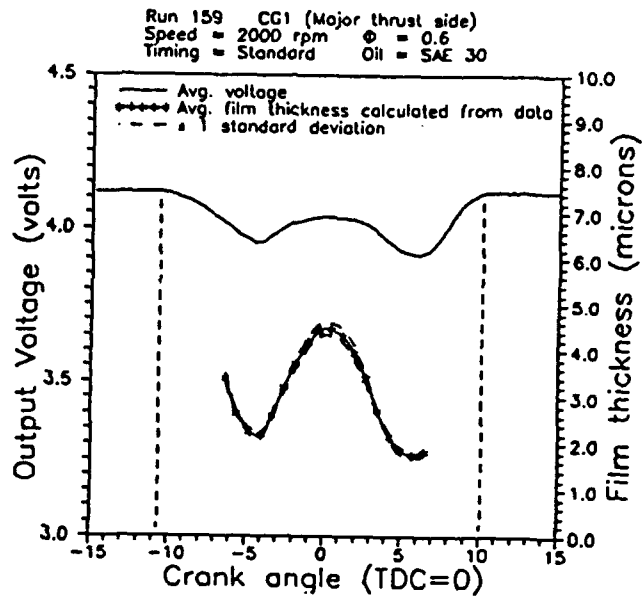


Fig. 7.6.5. Compression stroke oil film thickness, thrust side.

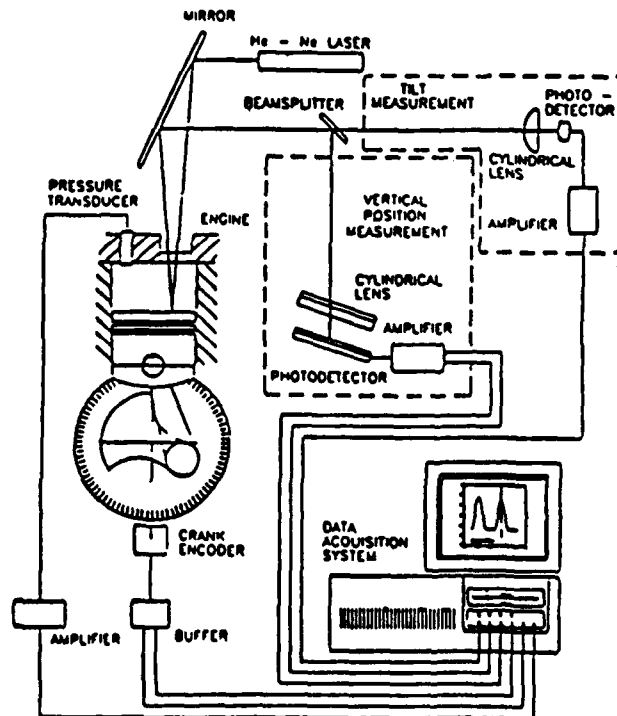


Fig. 7.6.6. Schematic of laser range-finding system.

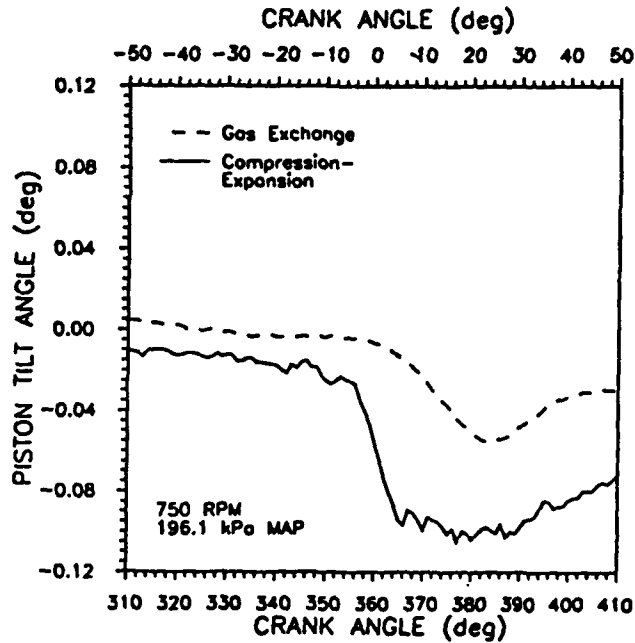


Fig. 7.6.7. Piston-tilt measurements. Conditions 750 rpm, supercharged.

The heat flux history at the thrust side follows as expected from the oil thickness. Figure 7.6.8 shows the heat flux increasing (negatively) until the ring starts to move away from the liner. The flux reaches its smallest negative value at TDC where the oil film is maximum. Note the ring cools the liner indicating the liner at this position is hotter than the ring. [It should be recalled that the liner temperature is typically high near the top and then falls off rapidly (Borman and Nishiwaki 1987) to a region of slower linear decrease with distance]. The fact that the liner is cooled slightly before the ring arrives may be due to a combination of oil pushed up ahead of the ring and the effect of the piston crown crevice. Note the top of the piston starts to shield this position at about  $-38^\circ$ . The heat transfer data corresponding to Fig. 7.6.4 shows a negative flux region from about  $\pm 10^\circ$  CA with a maximum negative value of  $-0.5 \text{ MW/m}^2$  at TDC. Figure 7.6.9 shows an expanded view of this heat flux. Note that after the ring uncovers the thermocouple there is a rapid heating from the crevice gas and then a decrease in flux as gas flows from the crevice until the piston top uncovers the thermocouple at about  $+40^\circ$  CA. It may be expected that the oil film is vaporizing after outward crevice flow begins and that this contributes to the reduced positive heat flow in this region (between  $10^\circ$  and  $40^\circ$ ).

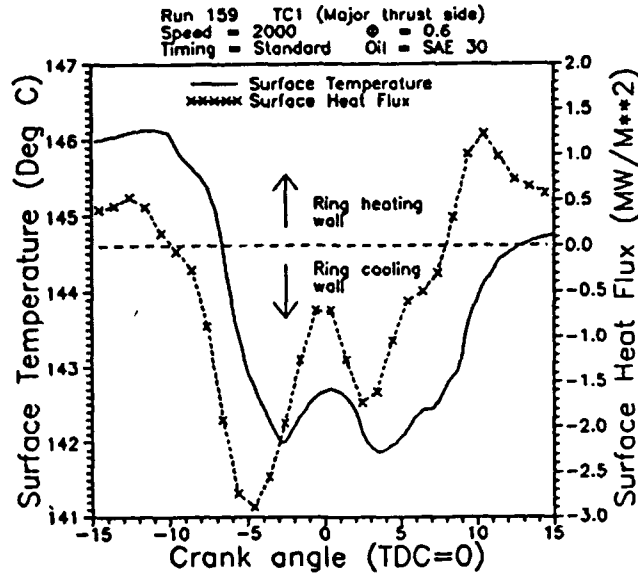


Fig. 7.6.8. Surface temperature and heat flux TC1.

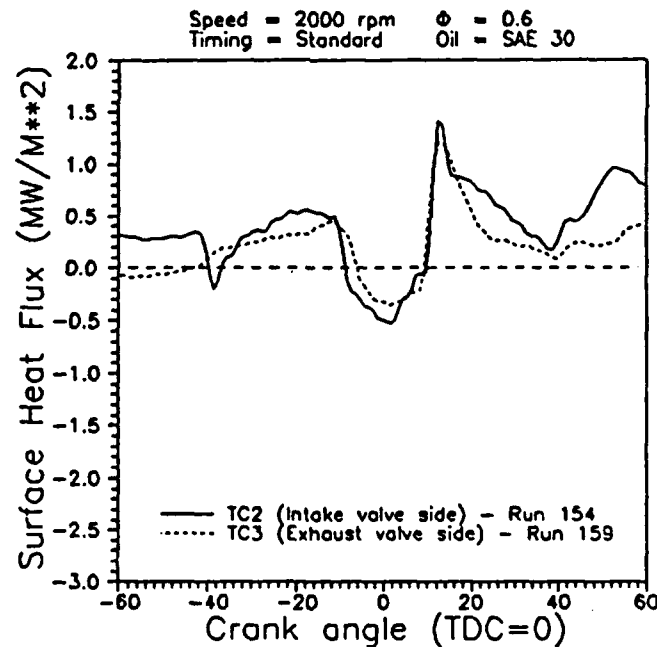


Fig. 7.6.9. Surface heat flux for TC2 and TC3.

Although the variability discussed previously prevented determination of changes due to oil formulation, the effect of fuel on the liner was measurable due to the large difference in viscosity between lube oil and fuel. Tests with about 100 motoring cycles from start up followed by sudden overfueling showed a very rapid decrease in

film thickness at all gauges. This appearance of fuel on the liner is consistent with cold starting computations (Gonzalez et al. 1991c) which show fuel droplet transport into the crevice due to blowby. The capacitance data indicate metal-to-metal contact which would result in high wear conditions, but only about 100 cycles are affected before the oil film is established again. Note that under the conditions studied ignition was essentially immediate, and there was no cranking period at low speed such as would occur when using a battery powered starting motor.

#### Data Using LIF Method

Tests were made using the LIF method for both the TACOM/LABECO and L-10 engines and off the engine using a Cameron Plint wear tester located at the Cummins Tech. Center in Columbus, Indiana. Although the wear tester shown schematically in Fig. 7.6.10 does not duplicate engine conditions it does allow simple, less confounded, changes in parameters. However, the maximum speed of the ring in the engine is much higher than in the wear tester and thus the oil films are much thinner in the tester than in an engine. Also, engine ring load varies over a wide range (400-14 N) during a cycle while the tester load is constant with a maximum value of 250 N. The temperature range for the tester is typical of a normally cooled engine (23° C to 200° C).

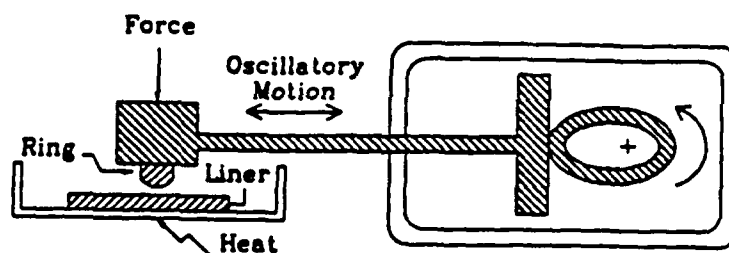


Fig. 7.6.10. Schematic of the Cameron Plint West Tester.

The tester allows mounting of the fiber in the sliding (ring) piece and the static (liner) piece. Measurements of friction and electrical contact resistance were also carried out simultaneously.

Figure 7.6.11 shows the oil film thickness measured by the fiber mounted in the "liner". A portion of the "ring" profile is superimposed. Note the oil does not cover the entire "ring" face (a so-called starved condition) and that the oil film separates behind the "ring" near the minimum film thickness and does not reform. Information of this kind is very important for modeling and cannot be obtained by other measurement methods.

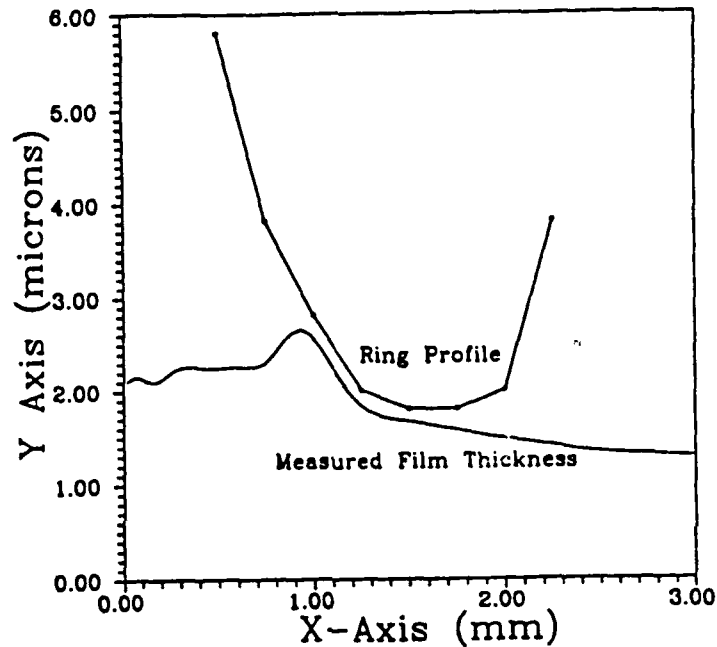


Fig. 7.6.11. Ring profile superimposed on oil film measurement.

When the fiber is mounted in the "ring" the film thickness goes through a minimum at each end (zero velocity) of the stroke and has a maximum at the peak velocity for each direction. This is shown in Fig. 7.6.12 along with the resistance and friction histories. Note that the forward and backward traces are not the same (they should be mirror images of each other) and the minimums are also not the same. Non symmetry of the ring profile and slight misalignment from perpendicular could both contribute to these differences. Note the friction shows no difference in level with direction, but the end-of-stroke resistance values are not the same at each end and correlate with the oil thickness, i.e. thinner films give lower resistance. The flat spots on the film thickness curves occur at the same position on the "liner" piece and may be a liner surface effect.

Figures 7.6.13, 7.6.14 and 7.6.15 show the peak measured oil film thickness obtained from the LIF method for 23° c, 100° c and 200° c respectively. The increase in film thickness with frequency (sliding speed) is predicted by hydrodynamic theory. The behavior at higher temperatures and loads indicate boundary lubrication. The oil

film did not go below  $0.25\ \mu\text{m}$ , indicating that surface asperities were touching. Note that the peak film thickness although relatively constant, does decrease slightly with speed.

Because the tests using the wear tester were run at Columbus, testing time was limited. However, the data show that the LIF method can be used over a wide range of conditions and thus running additional tests (a matrix including oil property variations, different materials, etc.) would appear useful. Such tests should include capacitance probes mounted in the "liner"-piece and fiber LIF probes in the "ring"-piece. Note that

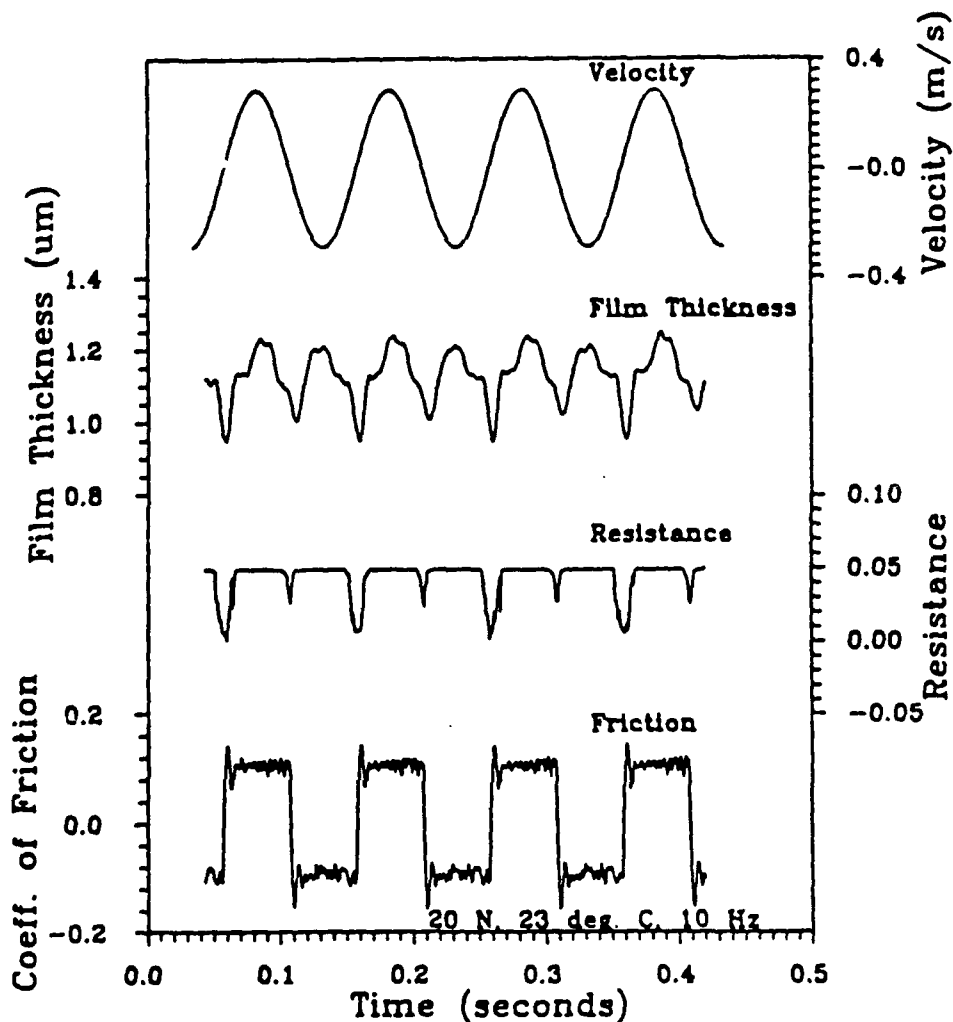


Fig. 7.6.12. Measurements showing hydrodynamic behavior, Cameron-Plint Tester.

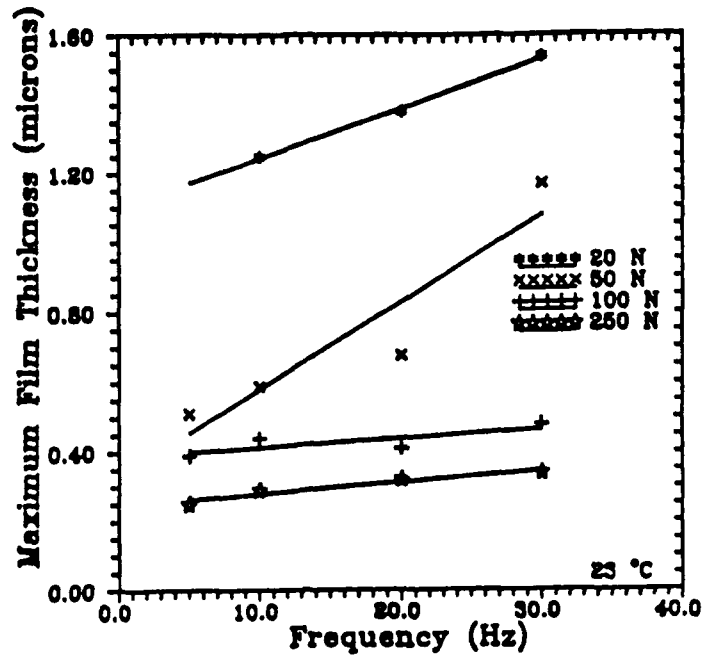


Fig. 7.6.13. Maximum oil film thicknesses at 23°C.

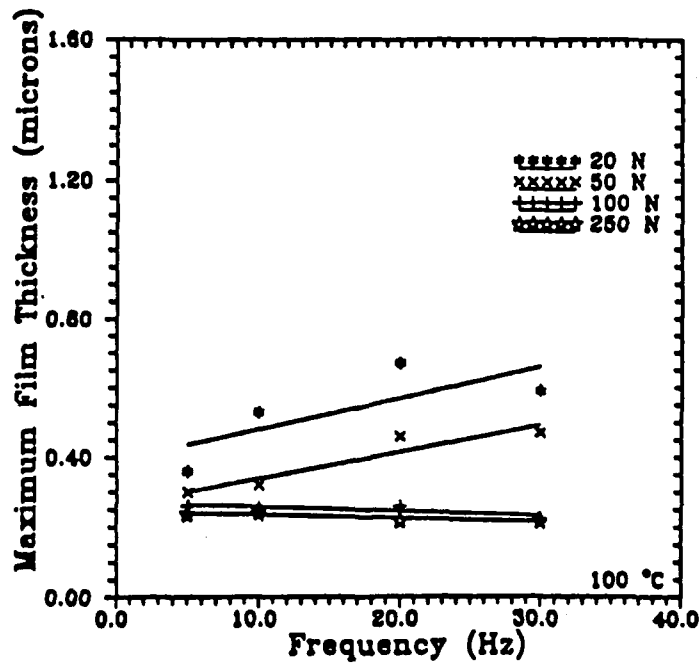


Fig. 7.6.14. Maximum oil film thicknesses at 100°C.

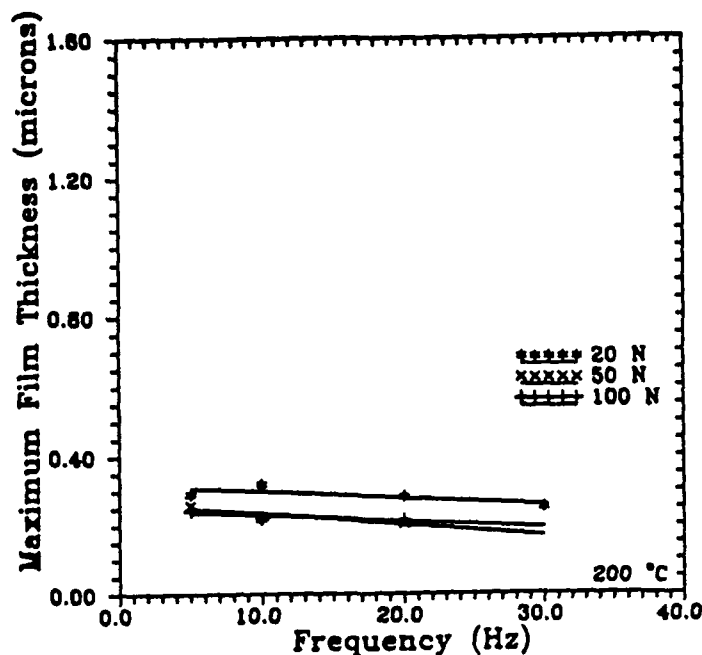


Fig. 7.6.15. Maximum oil film thicknesses at 200°C.

a tester with a longer stroke and much wider "ring" piece would be desirable for such tests. Richardson (1990) [See also Richardson and Borman 1991, 1992] used the TACOM/LABECO engine to obtain LIF Measurements of oil film at four locations on the liner for motoring without head, motoring, and fired conditions. The results proved useful for model validation, as discussed later, and to prove the practicality of the method. The following conclusions were obtained:

1. The method can be used for both motoring and firing without bleaching effects problems. However, the fiber near upper ring reversal broke and some evidence of the effects of deposits were found. The more secure method of fiber mounting used by Phen (1992) and described below should prevent breakage, but dirt on fibers exposed to combustion will likely continue to be a problem.
2. In all the experiments there was no indication of cavitation or ventilation.
3. All the experimental data indicated the ring was starved of oil, with only 33-57% of the face covered by oil.

A single cylinder version of the Cummins L-10, with specifications shown in Table 7.6.1 was used by Phen (1992) to obtain additional data using the same LIF method shown in Fig. 7.6.3. Fibers were fed through a stainless steel tube and then each through a small drilled hole (0.79 mm diam.) in the liner and then for the last 0.8 mm of liner through 200 $\mu$ m diam. holes obtained by use of EDM. The fibers were held in place by epoxy. The thermocouples were not surface type and were thus fed through the same tube and mounted 0.8 mm below the liner surface. It should be noted that with this method several fibers can be mounted in a cluster. However, if the fibers are too close laser light reflections from the ring may overlap with the measurement volume of a nearby fiber. It was also found that ring reflection can also change the calibration of a single fiber by increasing the fluorescence. Thus the calibration test must use a similar

surface finish on the ring as that at the time of measurement. Another effect of similar nature is the signal generated by oil on the piston surface when the fiber is not covered by the ring. This double film effect was suspected by Richardson (1990). Phen (1992) found evidence of signals generated by the grooves on the piston land surface further indicating the effect exists.

Table 7.6.1

**Single Cylinder Cummins L-10 Diesel  
Engine Specifications**

<b>Bore</b>	125 mm
<b>Stroke</b>	136 mm
<b>Connecting Rod Length</b>	218 mm
<b>Crank Radius</b>	68 mm
<b>Displacement</b>	1669 cu cm
<b>Compression Ratio</b>	17.1:1
<b>Peak Cylinder Pressure</b>	15.86 M Pa
<b>Engine Speed at Maximum Output</b>	
Standard Rating	2100 RPM
Formula Rating	1900 RPM

The signals from seven of the fibers in the L-10 liner were very stable. The other three fibers gave instability believed to be caused by improper mounting. New optical methods for in-engine testing of the fibers developed recently by ERC student Dan Ducu show promise as a means of preventing such problems and assuring fiber-to-fiber uniformity.

Unlike the large variations of the TACOM/LABECO data, the L-10 gave a coefficient of variance of 5-20 percent during compression and expansion. The fluctuation of data taken between rings was a major contributor to these cyclic variations.

The following conclusions were obtained from the motored data which were taken over a speed range of 700-1900 rpm, intake pressures of 1-2 atm, and intake temperatures of 50-90° C. The peak cylinder pressure ranged from 4.05 to 8.25 MPa. Liner temperature ranged from 52 to 88° C.

1. Oil film thickness increased with engine speed as anticipated. The upper liner position showed little difference with stroke direction, but the mid-stroke position showed thicker films in expansion than in compression.
2. The effect of intake pressure is small except at low speed. Oil films at 1900 rpm for the top compression ring were almost constant with changing intake pressure. This agrees with the observations of both Myers (1989) and Richardson (1990).
3. The oil film decreased with increasing liner temperature as expected from viscosity variation.

Because these data were taken at the end of the reporting period they are still under analysis by comparison with model results and thus not all conclusions are yet

available. The results are to be given by Phen, Richardson and Borman , at the 1993 SAE Congress.

### Oil Property Data

The viscosity measurement technique described earlier was used to compare new and used oil and to examine multigrade oil behavior. Ryason and Hansen (1991) reported that used engine oil can have a larger viscosity than unused oil when measured at low shear rates. This is surprising because one would expect that the polymer would degrade during engine use and so cause a decrease in viscosity. It is possible that carbon could generate a structure which would increase viscosity at low shear rates, but one would not expect the structure to survive at high shear rates. Using a Stressmeter, Joon-Hyuk Choe has made high-shear-rate measurements of viscosity on an oil supplied by the Caterpillar Tractor Co. who used some of the oil in a fired engine for 250 hours. It was found that used oil has a lower viscosity than unused oil as shown in Fig. 7.6.16.

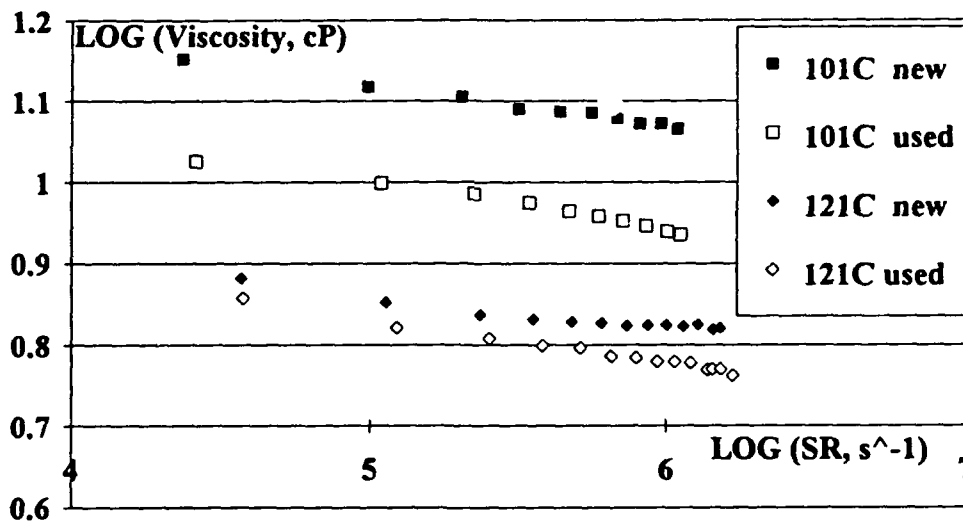


Fig. 7.6.16. Viscosities of new and used oils.

Addition of polymer to an oil gives rise to elastic properties as well as a decrease in the temperature dependence of viscosity. One quantity loosely related to oil elasticity is the first normal stress difference  $N_1$ . At low values of the shear stress,  $N_1$  varies as the square of the shear stress and so can increase rapidly as the shear stress increases. In starting an engine at very low temperatures, the shear stress and hence also  $N_1$  can attain very high values. It is, therefore, important to consider whether oils can be formulated, taking  $N_1$  into account, which could have lower viscosity and hence could

make cold starting easier. The possible effect of  $N_1$  on journal bearing lubrication has been and is being fairly widely studied ever since some early studies of engine wear appeared to show that some oil property in addition to viscosity was involved. In principle,  $N_1$  should increase the minimum oil film thickness in a journal bearing under conditions of full film lubrication and constant load, and hence increasing  $N_1$  should enable one to obtain the same bearing protection with a lower viscosity oil; the main current question is whether the effect is large enough to be of practical value. Investigations have concentrated on journal bearing temperatures in the range 100 C to 150 C; cold start problems have yet to be considered.

Results of the first attempt to correlate measured values of minimum oil film thickness in an instrumented journal bearing in a fired engine with Stressmeter data for  $N_1$  for a set of single- and multi-grade oils suggested that for some oils  $N_1$  could generate as much as 75% of the minimum oil film thickness (Bates et al. 1986). More recent work, involving improved oil film thickness measurements and numerical simulations for isothermal full-film lubrication under static loading, have reduced this percentage to about 30% at most. Model experiments simulating short bearing suggest that  $N_1$  could be more important under dynamic than under static loading (Oliver, 1988).

Joon-Hyuk Choe has used a Stressmeter to measure  $N_1$  and viscosity for dilute solutions of narrow-distribution polystyrene of known molecular weight. Reasonable agreement is obtained when the data are compared with Oettinger's molecular theory (Oettinger, 1990, 1991): as the shear rate is increased, the viscosity first decreases and then increases; the  $N_1$  data are also in agreement with the theory. These investigations offer hope that we can obtain an improved understanding, at the molecular level, of multigrade oil properties. Stressmeter data for the elastic properties of new and used oils Fig. 7.6.17 show a significant reduction in elasticity with use.



*An important aspect of the center research maintaining close contacts with industry. This is exemplified by the many years of close co-operation with Chevron Reserach. Chevron has supplied fuels, lubes and invaluable advice in addition to funds to support a Chevron Scholarship. Shown are Drs. M. Ingham and A. Jessel of Chevron visiting with Chevron Scholar L. Golding.*

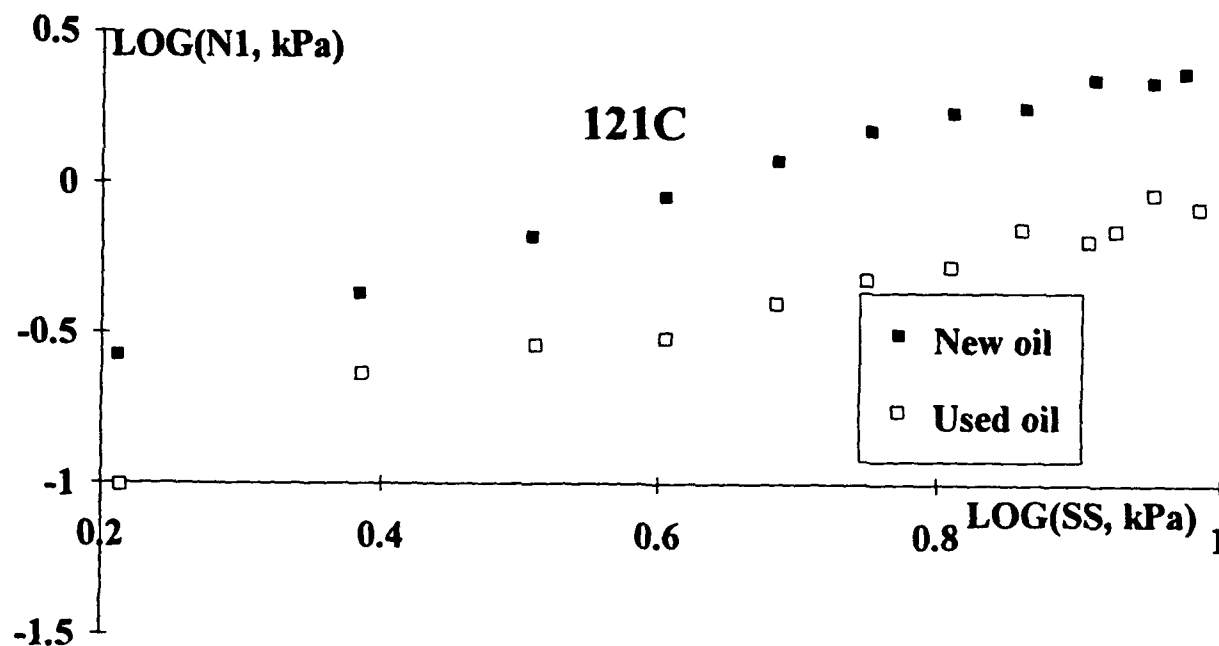


Fig. 7.6.17. Elasticity of new and used oils.

#### RESULTS FROM MODELING

Two lubrication modeling efforts were undertaken during the contract period. In the first, Richardson (1990) used a relatively simple Newtonian model to examine lubrication model assumptions and to compare to his LIF measurements (Richardson and Borman, 1992). In the second, Johnson and his student explored a non-Newtonian (power-law) model (Johnson and Mangkoesobroto 1992a, 1992b).

The data of Phen (1992) discussed above is currently being compared to the more advanced Newtonian model recently made available by Keribar et al. (1991). This analysis will be given at the 1993 SAE Congress Phen et al. (1993).

#### Simple Newtonian Model

The model of Richardson (1990) followed the conventional Reynold's equation model for ring-liner hydrodynamic lubrication, but included temperature variation of viscosity, viscous heating, and a simplified analysis of the effects of liner vibration. Both viscous heating and liner vibrations were shown to be negligible. It was shown that using the local liner temperature to calculate the viscosity is a good approximation.

The boundary conditions for the ring were explored and an approximate technique was devised to include oil starvation effects. The Reynolds and Wada conditions were found to give the best agreement with the model. Oil starvation conditions were required to obtain agreement with the data. While the model agreed reasonably with some of the fired data (5-25% error), the comparisons are not adequate to reach a general conclusion concerning the simple model.

### Power-Law Model

Polymer viscosity improver agents are added to lubricants to improve their viscosity-temperature behavior. As a side effect these multi-grade oils exhibit both shear thinning and moderate elastic effects. An accurate model of shear thinning is provided by the power law fluid which, in simple plane shear, gives the following expression for the viscosity  $\eta$  as a function of shear rate  $\kappa$ .

$$\eta = m \kappa^{n-1}$$

For multigrade lubricants the power-law index  $n$  lies between 0 and 1 which results in a decrease in viscosity with increasing shear rate. For a base oil with no additives,  $n = 1$ , and the behavior is Newtonian with constant viscosity.

The power-law index  $n$  and the consistency index  $m$  are functions of temperature. Figures 7.6.18 and 7.6.19 show their temperature dependence for two multi-grade oils. Note that the variation  $n$  and  $m$  with temperature have counteracting effects on viscosity. The net effect is some shear thinning with temperature increase. Therefore, the use of this model accounts for shear thinning of multi-grade oils with both shear rate and temperature increases.

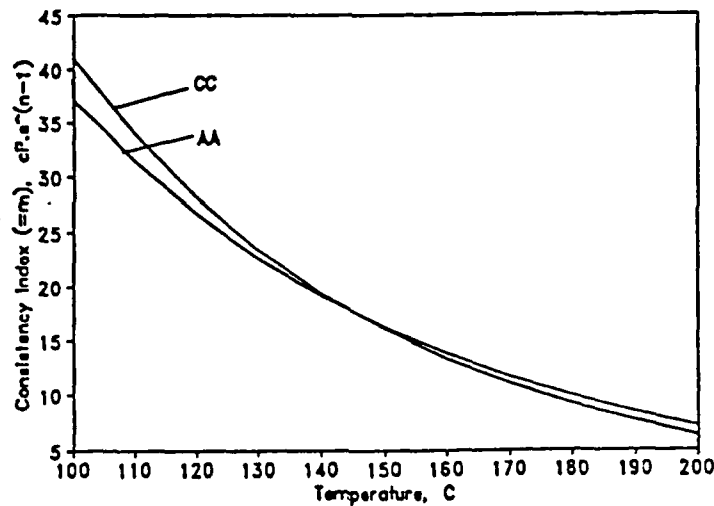


Fig. 7.6.18. Consistency index vs. temperature for two lubricating oils. Data taken from Lee et al. 1988.

Using the power-law model we have developed a lubrication theory which generalizes that of Reynolds for the Newtonian fluid. The equation for the dimensionless pressure gradient is of the form

$$\frac{dp}{dx} = \frac{\gamma}{h} (U/A + Ay) |U/A + Ay|^{n-1}$$

where  $h(x)$  is the film shape,  $U$  is the relative sliding velocity between the surfaces and  $A$  is given by

$$A = -\left(\frac{1}{n} + 1\right)U + \left(\frac{1}{n} + 2\right)\frac{1}{h^2}(Vx + \varphi)$$

where  $V$  is the squeeze velocity between the surfaces and  $\phi$  is a constant. The value of  $y$  is determined by solving numerically a nonlinear algebraic equation (Johnson and Mangkoesobroto 1992a). The pressure is determined by integrating the  $dp/dx$  equation above. For the Newtonian fluid,  $n=1$ , this equation reduces to Reynold's equation, as it should.

$$\frac{dp}{dx} = -6 \frac{U}{h^2} + \frac{Vx + \phi}{h^3}$$

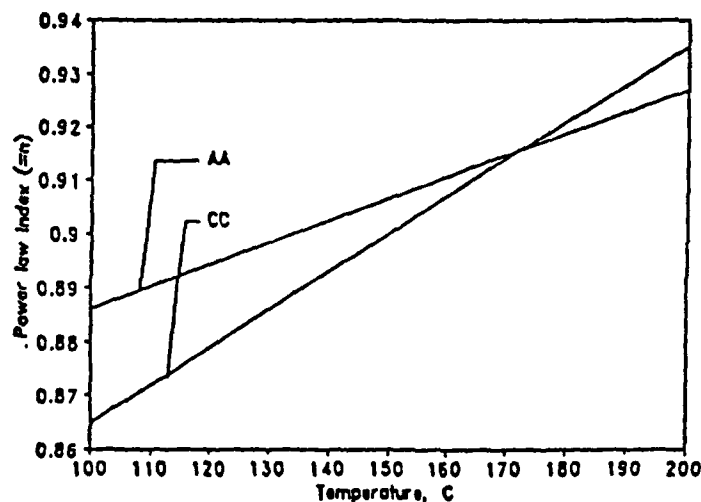


Fig. 7.6.19. Power-law exponent vs. temperature for two lubricating oils. Data taken from Lee et al. 1988.

For a slider bearing of parabolic shape the pressure distribution is shown in Fig. 7.6.20.

The analytical results developed through this research are available for use in any lubrication problem where it is important to account for the dependence of viscosity on shear-rate and temperature. It has been used as part of the theoretical analysis of piston ring lubrication (Johnson and Mangkoesobroto 1992b). One of the results of that analysis is shown in Fig. 7.6.21 where the minimum oil film thickness as a function of crank angle is shown for parameters typical for a diesel engine.

#### Liner Vibration Analysis

The analysis of cylinder liner vibration was conducted by G. Green who obtained his PhD thesis (1992) under the direction of Professor Engelstad and is reported in Green and Engelstad (1993). The procedure developed provides an analysis tool for addressing the cavitation erosion problem that occurs on the outer surface of cylinder liners. The modeling approach is based on the finite element method and includes the cylinder liner and the surrounding coolant using a fluid-structure interface between the

two. The coolant on the outside of the liner has a large effect on the motion of the liner, therefore the structural problem and fluid problem cannot be decoupled.

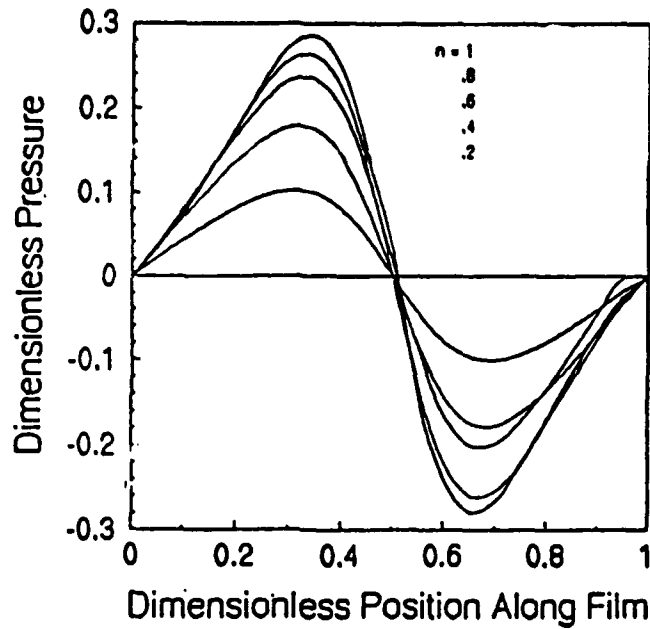


Fig. 7.6.20. Dimensionless pressure vs. dimensionless position along film for a slider bearing with parabolic shape. The pressure is assumed to vanish at the ends of the film.

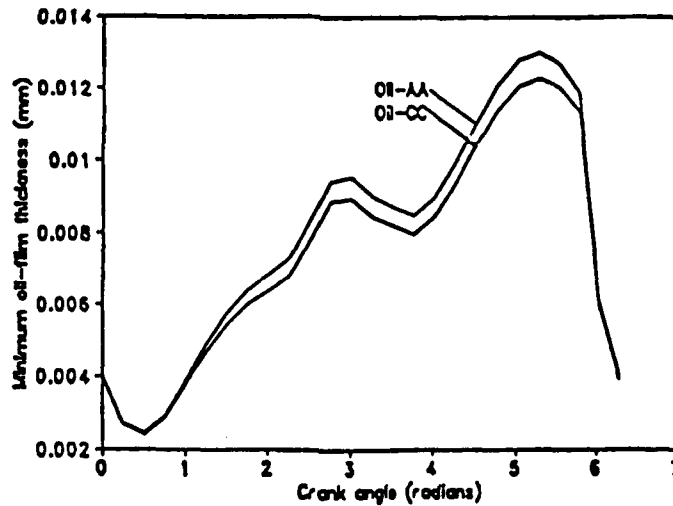


Fig. 7.6.21. Minimum oil film thickness vs. crank angle for two oils.

Experimental studies were carried out in conjunction with the finite element model development to verify the numerical procedure. A modal analysis provides

understanding of cylinder liner vibrations and the effect of the o-ring seals and the surrounding coolant on the liner motion. Data obtained in the time domain were used to determine damping coefficients for the liner, o-rings and water as well as the stiffness coefficients for the O-rings.

Application of the model demonstrates how pressures are generated and propagate through the cooling medium. The studies provide a better understanding of how and where on the liner surface the pressure in the water jacket can drop below the vapor pressure and thus cause cavitation. Parametric studies demonstrate design alternatives for reducing the minimum pressures that cause cavitation.

The following conclusions were obtained from the study. Natural frequencies and mode shapes of the cylinder liner were identified. Characterizing the vibration of the cylinder liner is the first step in understanding cavitation, since it is the liner motion that causes the bubble formation and collapse. The different mode shapes showed two categories identified by the number of nodal circles in the axial direction. Zero order axial modes have no nodal circle occurring in the mid-span of the liner. The modes exhibited maximum displacements at the bottom of the liner and steadily decreasing displacements toward the clamped end. It would be these modes that would create the largest liner movement at the bottom of the water jacket.

The developed finite element model showed excellent correlation with experimental results. Without the water jacket, the experimental and finite element results were virtually equivalent for the first 2.0 msec after impact. Adding water to the model added some variability to the results, however, a good match in displacements and pressures was achieved up to 1.0 msec. The highest oscillations, in both displacement and pressure, occurred in the first 1.0 msec. Consequently, the model would work very well for studying the cavitation problem.

The mechanism creating the pressure fluctuations in the coolant can be attributed to the generation and reflection of acoustic pressure waves. Previous researchers recognized that the velocity of the liner surface generates pressure according to  $vpc$ . These same researchers did not however, account for the acoustic energy already in the fluid. After an impulse load is applied to the inside of the liner, the water pressure at the liner surface is initially equal to  $vpc$ . Soon after the start of the impulse, however, pressure waves generated at other locations on the liner have propagated around the liner and the reflected waves off the block walls create pressures different than  $vpc$ .

#### HYPOCYCLOIDIC DRIVE DEVELOPMENT

A hypocycloid is the path described by a point on the circumference of a circle which rolls on the inside of a larger, fixed circle. Figure 7.6.22 depicts a hypocycloid. The hypocycloid becomes a straight line when the smaller circle shown in Fig. 7.6.22 has a diameter equal to  $1/2$  the diameter of the larger circle. This motion can be achieved with a simple gear set, as shown in Fig. 7.6.23. This gearing arrangement is referred to in this text as *basic hypocycloid gearing*.

In Fig. 7.6.23 the fixed circle of Fig. 7.6.22 is replaced by an internal gear and the rolling circle is replaced by a pinion gear. Bearings located at points C and O allow the pinion gear and crank to rotate freely about these points. As the crank rotates with angular speed  $\omega_C$  in the direction shown, the pinion gear rotates about the crankpin with angular speed  $2\omega_C$  in the opposite direction. As the crank completes one

revolution, point  $D_1$ , located on the pinion gear pitch diameter, executes straight-line motion passing through the crank centerline,  $O$ . The motion of point  $D_1$  is simple

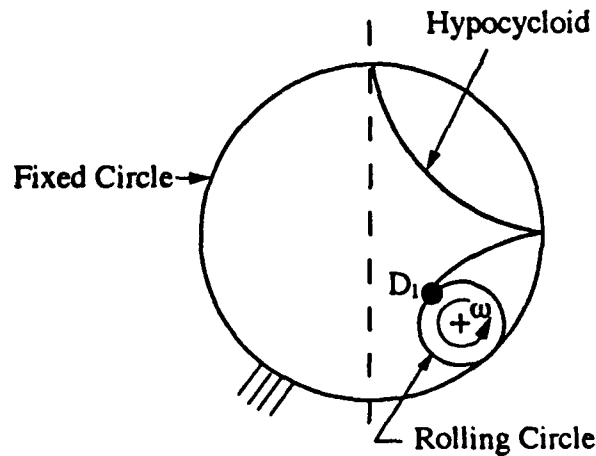


Fig. 7.6.22. Hypocycloid Motion.

harmonic for a constant crank speed. The distance traveled by point  $D_1$  is equal to the internal gear diameter, which is four times the crankthrow  $O-C$  and twice the pinion gear diameter. Point  $D_2$  also performs straight-line, simple harmonic motion, perpendicular to the path of  $D_1$  and through the crank centerline,  $O$ . Any point on the pitch diameter of the pinion gear undergoes this linear, harmonic motion.

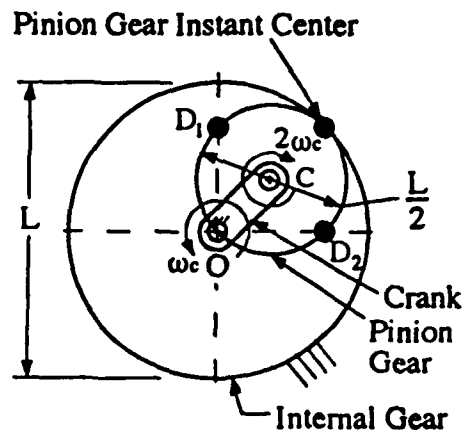


Fig. 7.6.23. Basic Hypocycloid Gearing.

Equivalent motion can be achieved with a gear set that is somewhat more complex, as is illustrated in Fig. 7.6.24. This gearing arrangement is referred to in this text as *modified hypocycloid gearing*. Reasons for considering a more complex configuration will be discussed subsequently.

In Fig. 7.6.24, crankthrow O-C remains the same length as in Fig. 7.6.23, and the crank and pinion gear speeds are unchanged. The pinion gear diameter has increased, however, as has the internal gear diameter. The internal gear is now made to rotate at a particular fraction of the crank speed in the opposite direction. This counter rotation is achieved through a second "stage" of gearing. A sun gear attached rigidly to the crank meshes with a planet gear, which in turn meshes with the internal gear. Gearing sizes are selected so that the instant center of rotation of the modified hypocycloid pinion gear corresponds to that of the basic hypocycloid pinion gear. Straight-line, simple-harmonic motion of point D<sub>1</sub> occurs, as in the basic hypocycloid gearing, but this point is now located inside of the pinion gear pitch diameter. The distance traveled by point D<sub>1</sub> remains equal to L, the diameter of the basic hypocycloid internal gear. Note that point D<sub>2</sub> again performs straight-line, simple harmonic motion, perpendicular to the path of D<sub>1</sub> and through the crank centerline.

#### Advantages of the Modified Hypocycloid Engine

The gearing shown in Fig. 7.6.24 can be applied advantageously in engine design. This can be readily illustrated with the help of Fig. 7.6.25. In Fig. 7.6.25, a piston-rod is shown pivoted about point D<sub>1</sub>, and so undergoes linear, simple harmonic motion, along with point D<sub>1</sub>. This engine is referred to in this text as the *modified hypocycloid engine*. It is so-named because of its use of the two-stage, modified hypocycloid gearing shown in Fig. 7.6.24, rather than the basic hypocycloid gearing shown in Fig. 7.6.23. Although basic hypocycloid gearing could also be applied to engine design, studies have shown that the modified gearing reduces gear tooth loading and crankshaft loading for a fixed engine stroke.

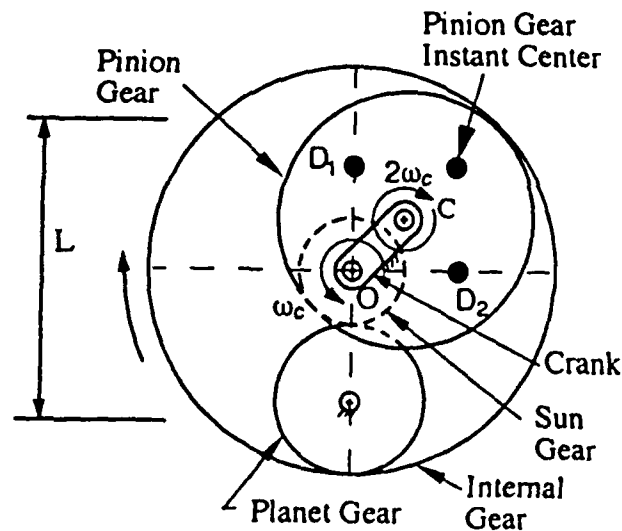


Fig. 7.6.24. Modified Hypocycloid Gearing.

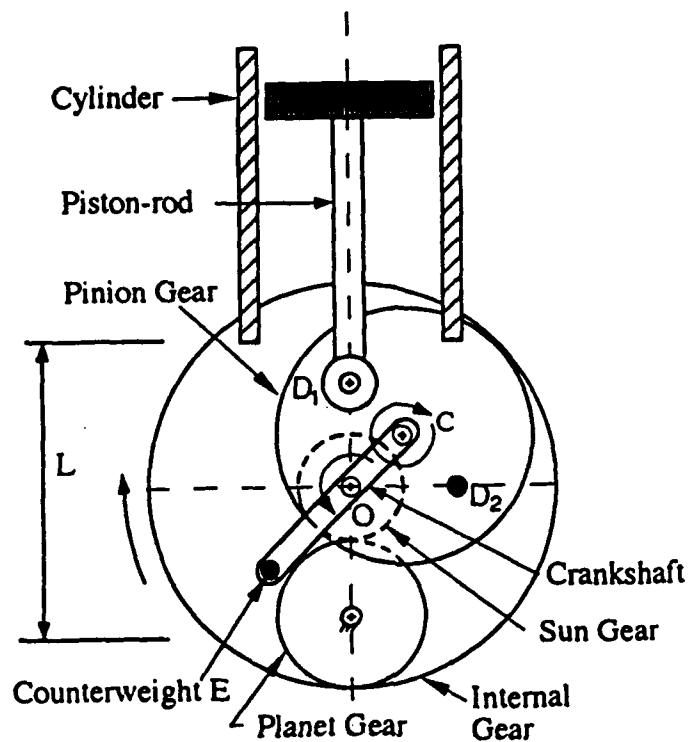


Fig. 7.6.25. Modified Hypocycloid Engine.

Many advantages result from an engine with modified hypocycloid gearing. One of these is perfect balance. The traditional slider-crank mechanism used in engines does not produce linear, simple harmonic motion for a fixed crankshaft speed. As a result, the single-cylinder slider-crank engine cannot be perfectly balanced. In contrast, the single-cylinder modified hypocycloid engine can be perfectly balanced with the use of two sets of counterweights, which should lead to a quieter running engine. Another advantage is the absence of significant side loads on the modified hypocycloid piston, which reduces friction and the possibility of piston slap. The reduction of piston slap should also lead to a quieter engine and to less piston and cylinder wear. A smaller piston skirt is necessary due to the reduced side load, reducing friction and reducing the piston weight. The elimination of the wrist-pin required for the slider-crank piston assembly permits the use of a cylindrical piston and reduces the number of parts required, thus reducing weight and simplifying manufacturing for this assembly.

#### Testing the Drive

An engine was designed and built using modified hypocycloid gearing by modifying a single-cylinder, 4-stroke, spark ignition engine. This was a small gasoline engine with a 2 inch bore and a 1.875 inch stroke, a one-piece piston and rod, and

journal bearings. The major thrust of this work was aimed at demonstrating concept feasibility, developing a workable design, and laying the groundwork for more detailed study.

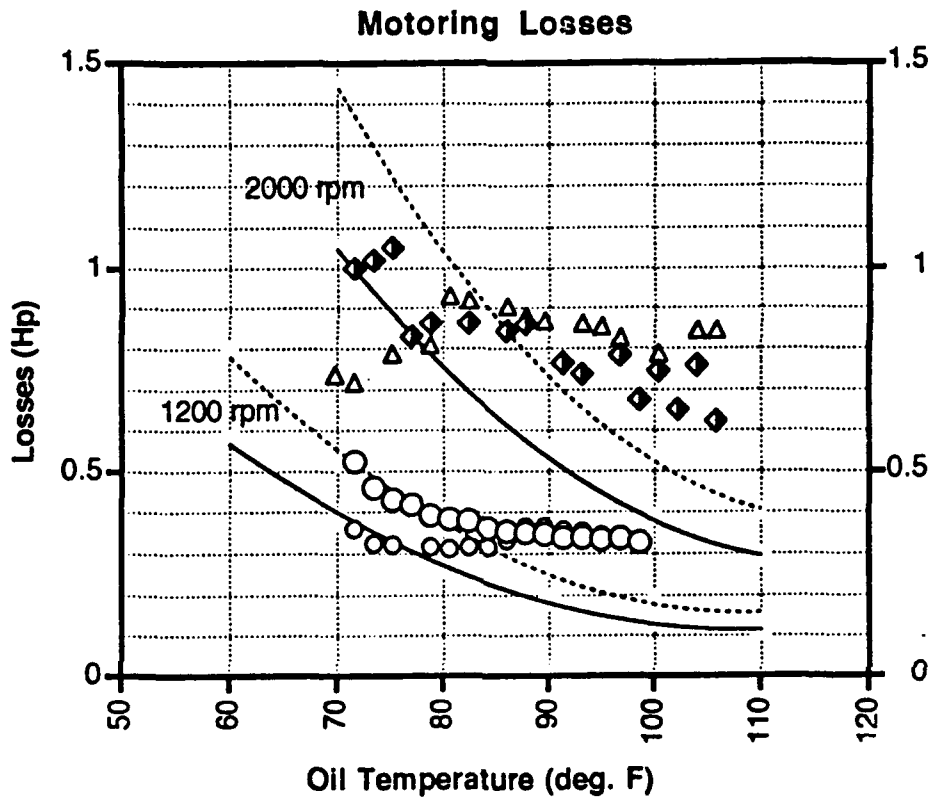
Motoring tests qualitatively indicated low vibration levels, although the engine has not been tested on a vibration table for quantitative results. Data from limited motoring horsepower tests are shown in Fig. 7.6.26, along with theoretical curves. The lack of agreement between the data and theoretical curves is being investigated, although several possible explanations are offered. High oil flow may be contributing to significant windage losses in the engine. Tests in which the lubricant flow was turned off for short periods of time indicated reductions in frictional horsepower losses of 25% at 1200 rpm and 15% at 2000 rpm. The next phase of work will concentrate on optimization of lubricant flow to the engine. It is also suspected that bearing clearances are smaller than intended, leading to higher losses and even the possibility of boundary lubrication. The crankshaft for this engine is assembled in two halves, and eccentricity of one of the halves axis with respect to the other reduced designed clearances for the main bearings. After inspection and some repair work on bearings, the crankshaft has been reassembled with better concentricity results and is being prepared for further testing.

Firing tests for the engine have been very limited to this point. The engine has been run as high as 4500 rpm, with total run time of less than one hour. The one-piece piston and rod appear to be working as expected, and piston cocking due to gear backlash has not caused any apparent problems. Horsepower output has been approximately half of that engine on which the modified hypocycloid engine is based, but timing and other engine parameters have not been optimized. A unique split crankshaft arrangement was developed to maintain compact component size, and functioned well for repeated assembly and disassembly; however, some localized yielding was discovered in the crankpin due to the tapered press fit arrangement used, and is being further investigated. The engine was oversped accidentally at one time, and the crankpin bearing tightened up somewhat subsequently. The engine was torn down, and some wear and minor damage was found in the crankpin bearing. This bearing was the one predicted to be most severely loaded, and so was not completely unexpected. Some minor damage to the ring gear bearing was also found. The crankpin bearing area has been increased, and the ring gear bearing clearance opened slightly to reduce frictional losses, but more testing has not been completed yet.

The results of the first prototype design indicate that the modified hypocycloid engine concept is quite feasible. It seems to be particularly suited for applications that demand low vibration and noise, and the concept can be extended to multiple cylinders. Much work needs to be completed in terms of optimizing component design, but the results of initial prototype construction and tests are very encouraging.

## MATERIALS TESTING

As initially conceived the materials research at the ERC was to concentrate on testing of new materials, particularly ones suitable for LHR engine applications, under engine conditions. A parallel effort was to be conducted by Professor Cooper on laboratory testing of new materials. This later project turned out to concentrate on ceramic composites.



- Head removed, piston installed, some pumping out of crankcase - 1200 rpm
- Head removed, piston removed, big bearing locked - 1200 rpm
- ◆ Head removed, piston installed, some pumping out of crankcase - 2000 rpm
- △ Head removed, piston removed, big bearing locked - 2000 rpm
- Calculated Hp, all bearings except big bearing
- ..... Calculated Hp, all bearings and piston skirt

Fig. 7.6.26. Modified Hypocycloid Engine Motoring Losses.

### Engine Testing of Materials

It is of course almost impossible to duplicate engine conditions except in an engine. Testing of materials by simply exposing them to engine conditions yields some useful information and that approach was followed in the work on coatings (see Section 7.2). In order to test and make significant measurements of temperature or other properties it is either necessary to make actual engine parts, as done in the past work on the Ford ceramic head engine (see Section 7.3), or on an entire ceramic engine as currently underway at the ERC under contract with Isuzu Ceramics Institute, or to especially design the engine to accept a special material test-piece as previously done by Huang (1987) at the ERC under ARO contract. In considering this problem it was decided that the best procedure would incorporate the ability to test simple test shapes, such as a flat disk shape, in an engine and to be able to measure the surface temperature distribution in the test-piece as a function of time or as an ensemble average of time records. It was already known that the spatial variation would be complex so that methods of measurement using discrete point measurements would require an enormous (impractical) number of such measurements. Thus a technique which would give a continuous spatial measurement of test piece surface temperature would be the best solution.

The hypocycloidal drive was evaluated as a potential engine drive for a materials-test-diesel because it would isolate the drive from the cylinder. Because of the higher loads of diesels, durability was questionable. It was decided to develop the drive, as discussed above, but to test the materials in a conventional engine. In an entirely separate program at TACOM, Dr. Steve Shepard had developed an infrared (IR) imaging system. It was decided that use of this instrument to measure test-piece surface temperatures could provide the required data. To use the instrument the test-piece would need to be viewed through a special window. It was decided that by use of a side-valve spark ignition engine a test-piece nearly the size of the piston surface could be viewed through a window in the head. This is because the valves and spark plug are to the side allowing the window to be large. The use of a premixed gaseous fuel was thought to minimize interference from the combustion. It was realized that the choice of H.C.S.I. combustion would limit the thermal loading of the test-piece, but this disadvantage was outweighed by the low cost of the engine compared to a diesel. By use of a low cost engine the expense due to breakage of test-pieces would be minimized. In fact, the engines used were donated by the Briggs and Stratton Company. The engine was set up and redesigned for the testing by ERC graduate student Wayne Moore (1990). The window selected was zinc sulfide (ZnS) coated with a thin layer of Yttria ( $Y_2O_3$ ). The transmission in the 8-12  $\mu\text{m}$  band was 81% and 90% for 1-10  $\mu\text{m}$ . Figure 7.6.27 shows the window design and test-piece mounted on the piston top.

By viewing the test-piece through the window the top surface temperature could be obtained using the IR system of Shepard and Sass (1990). To describe the steady state temperature distribution of the bottom surface a "template" system was devised by Moore (1990). This instrument is a two dimensional version of the Templug (Testing Engineers Inc., 1988), a product which is available commercially and which uses hardened set screws to determine peak temperature at the location of the screw. In the template version a thin plate is substituted for the screws. Hardness testing of this plate allows a two dimensional temperature field to be determined. To test this concept

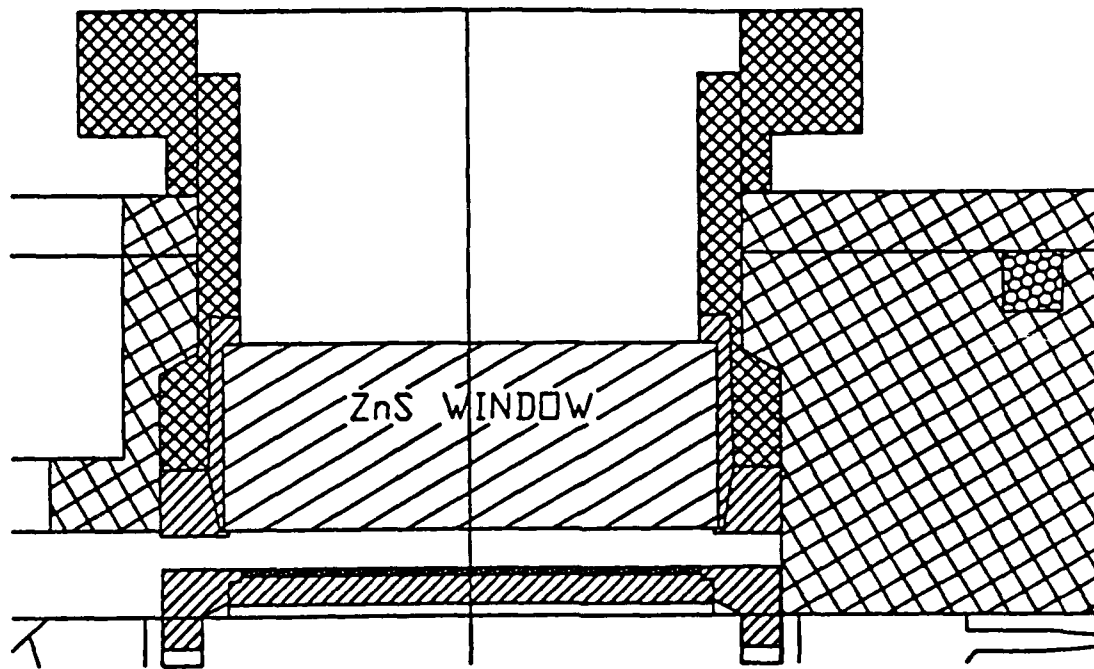


Fig. 7.6.27. Window mounting arrangement in modified head of Briggs and Stratton engine.

Moore mounted the template in the head in place of the window. This allowed use of thermocouples to evaluate the method. The plate used was a heat treated 0-1 tool steel of 0.79 mm thickness. Hardness was measured using the Rockwell C test. Tests were run with the template mounted behind a test-piece mounted in the head and with its front surface exposed to the combustion gases. Figure 7.6.28 shows the result for a test-piece with 0.75 mm  $ZrO_2$  coating. The result on the right shows the effect of insulating the back of the template. The highest temperature is only 475° C, illustrating the limitations of H.C.S.I. combustion. The method worked well, its only limitation being the uniformity of available plate material.

If the back of the template could be totally insulated (perfect insulation) then the front and back surface would have the same temperature and the template method would suffice. However such perfect insulation is not practical because of strength considerations. In addition, the use of plasma sprayed coatings, with possible imperfections, makes it desirable to measure the combustion gas-side-surface temperature. By mounting the flat disk test-piece on the piston with a template behind it and using the window in the head to view the top surface, both top and bottom surface temperature distributions could be obtained. Dr. Shepard provided the IR instrumentation which had been made portable so that it could be thus transported easily. The TACOM team of Shepard and Sass thus brought the instrument to Madison and used it in the ERC lab. The set up was as shown in Fig. 7.6.29. Prior to these engine tests Moore spent time at the TACOM lab calibrating the window, mirror, and test-pieces.

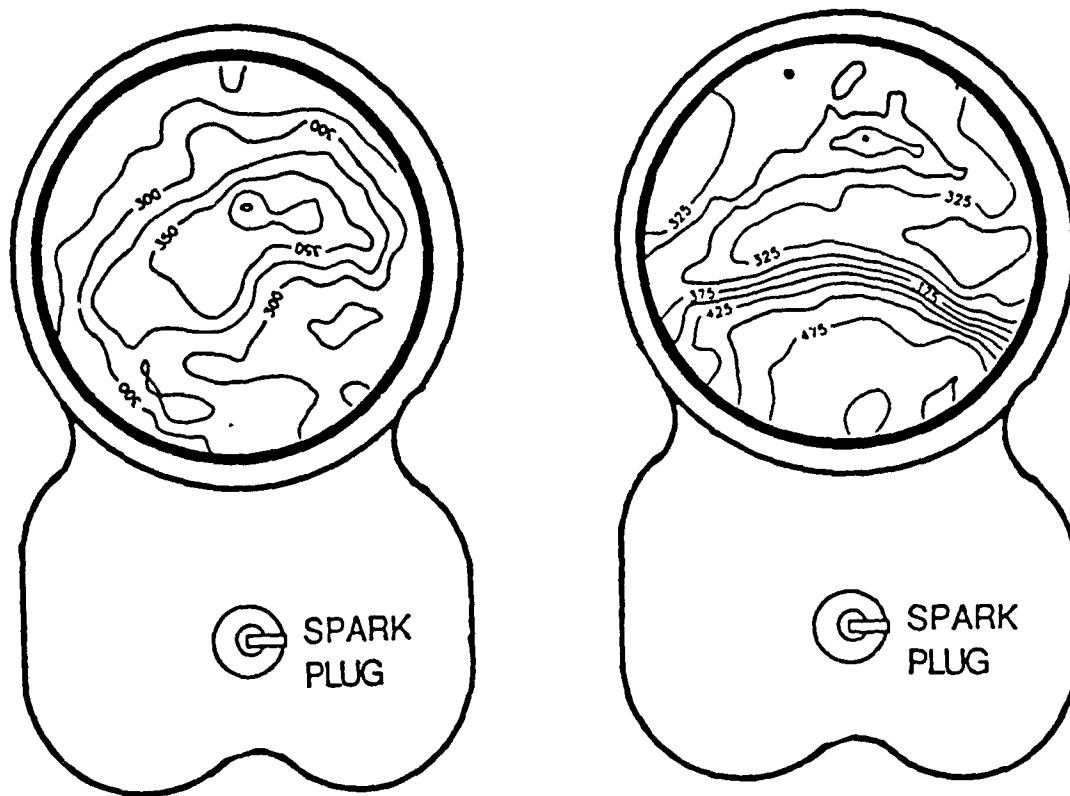


Fig. 7.6.28. At left isotherms for 0.75mm  $ZrO_2$  3000 RPM 0.94 Equivalence ratio, template behind sample. At right, same as left except insulation behind template raises the temperature.

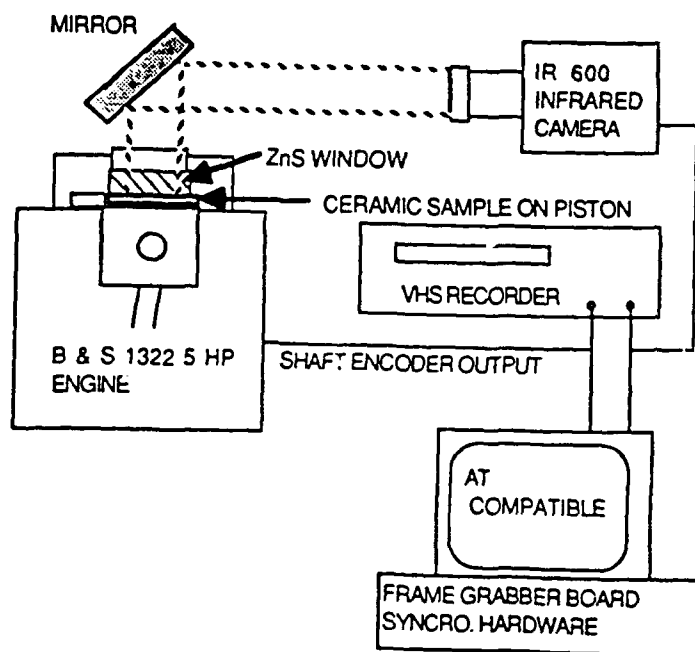


Fig. 7.6.29. Infrared thermal imaging layout.

The IR imaging was saturated at 450° C surface temperature and was saturated by radiation from the hot product gases behind the flame front. Thus the data showed ensemble average flame front motion, but not test-piece temperatures during the combustion period. At other times in the cycle the test-piece could be imaged, but the portions over 400° C were saturated. Although data could be gathered for a single engine condition in about 10 minutes, the analysis of the data to obtain a temperature distribution at a given crankangle is very time consuming. It appears that data analysis is the primary problem for use of the system to determine distributions during the non-combustion portions of the cycle. If one wishes to test materials, especially ceramics, many tests need to be made; thus the speed of data analysis is a major concern. If one wishes to monitor the test-piece for appearance of failure then a faster system of imaging is desired. Currently TACOM is developing a system capable of single cycle resolution. In theory such a system could give heat flux vs. time data if the problems of flame interference and data analysis speed can be overcome.

A second set of experiments was conducted in the spring of 1992 using the same apparatus, but with modifications of the window. In these experiments the TACOM team was helped by ERC staffer David Bidner. The concept of the experiment was to put platinum films on the window in a pattern of stripes with clear window between. Stripes on the two sides of the window were perpendicular to each other. The top side also contained an RTD to act as a calibration for absolute temperature. The data were to give flame position and window temperatures (top and bottom) simultaneously. The piston was polished with diagonal stripes. This was to provide a means of determining if the piston could be imaged during the period of combustion by adjustment of the IR camera. Figure 7.6.30 shows the arrangement. Each individual temperature measurement was an average over 12 adjacent pixels, to reduce noise. The data was taken using the Inframetrics IR 600 camera equipped with a 3x telescope, to increase the spatial resolution. Unfortunately, the transmission of the telescope is quite low (79%). An additional data set was taken without the telescope, which yielded greater contrast, but 1/3 the spatial resolution. Without the telescope, measurement of the window stripes was not reliable, as the stripe width was on the order of the instantaneous field of view of the camera.

In order to avoid saturation of the camera A/D converter in the presence of the flame, the highest dynamic range setting was used to record the data to videotape. Later examination of the data revealed that the lower boundary of the temperature range is uncalibrated at that setting, preventing an accurate determination of the surface and stripe temperatures. Initial data reduction which gave temperature versus crankangle for cell B5 of Fig. 7.6.30 showed an unreasonable variation with crankangle. At this writing additional data analysis is continuing, but it is undoubtedly advisable to repeat the tests, perhaps with a simpler experiment in which two windows are used, one clear for piston measurements and one opaque for window surface measurements.

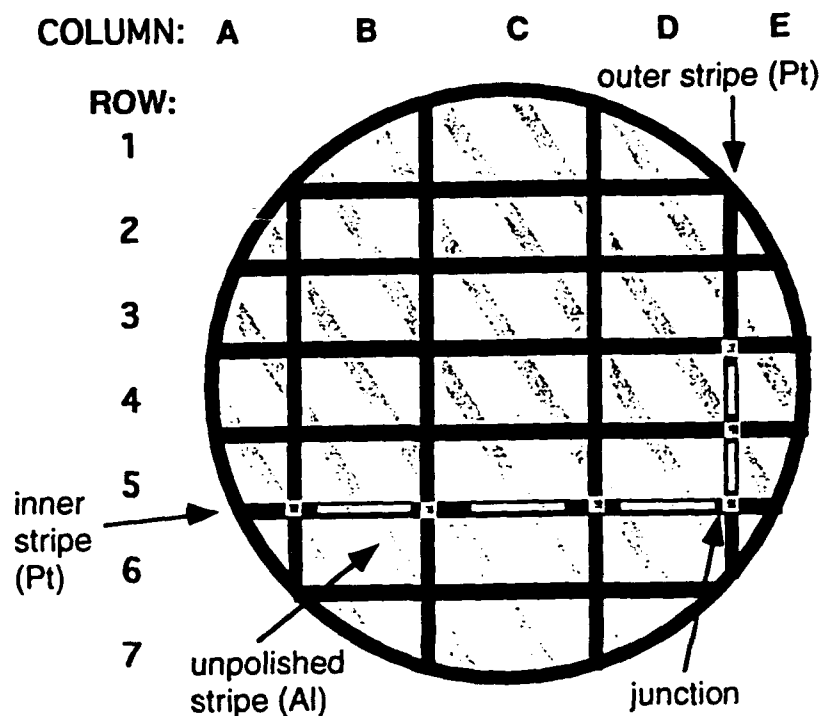


Fig. 7.6.30. Layout of platinum film stripe of window inner (cylinder side) and outer (room side) surfaces. Stripes on aluminum piston were unpolished areas and are shown as shaded diagonals.

#### Ceramic Composite Study

This study was conducted by D. Meyer who received his PhD thesis (1990) under the direction of Professor Cooper and is reported in Meyer et al. (1990), Bidner et al. (1990). The purpose of this research was to evaluate the high-temperature mechanical response of the fiber-matrix interface in ceramic composites. A new technique was introduced for evaluating and quantifying the mechanical response of these interfaces by comparing experiments to analytical simulations of bulk composite rheologic behavior. A decomposition of the displacement and stress fields of a composite specimen subjected to an "off-axis" compressional loading allows the simulation of creep and load relaxation by integrating a generalized two-dimensional boundary value problem in time. The model incorporates nonlinear viscoelasticity in the matrix and a penalized incremental plasticity formulation for contact friction at the fiber-matrix interface. A Newton-Raphson solution scheme and a singular yield surface provision was developed for combining the effects of viscoelasticity and idealized Coulomb friction. The model solution predicts the existence of a steady-state stress field and strain rate for the composite, which is a function of the fiber orientation angle, the viscosity and the stress exponent of the matrix, and the friction coefficient of the fiber-matrix interface. To test the validity and usefulness of the model, an experimental protocol was developed to characterize the creep and load relaxation response of a calcium aluminosilicate (anorthite:  $\text{CaAl}_2\text{Si}_2\text{O}_8$ ) glass-ceramic and the same material

reinforced with 30 vol% SiC fibers. Comparisons between the modeling and experimental results indicate that the interface was debonded with a substantial amount of cavitation. A friction coefficient of 0.4 to 0.7 was predicted for the interface response at 1310° C and 1300° C, respectively. An amorphous SiO<sub>2</sub> layer at the interface was observed to substantially affect the interface response. Comparisons between the model results and experiments were also used to quantify the matrix creep behavior in-situ within the composite: the conclusion is that the creep behavior is strongly influenced by stress with the stress exponent increasing from ~1 to ~3 as the compressive stresses increase from 7 MPa to ~50 MPa. This stress-deformation behavior of the matrix along with several other experimental observations indicate the primary deformation mechanisms of the matrix are diffusion at low stresses and mechanical twinning/dislocation glide at the higher stresses.

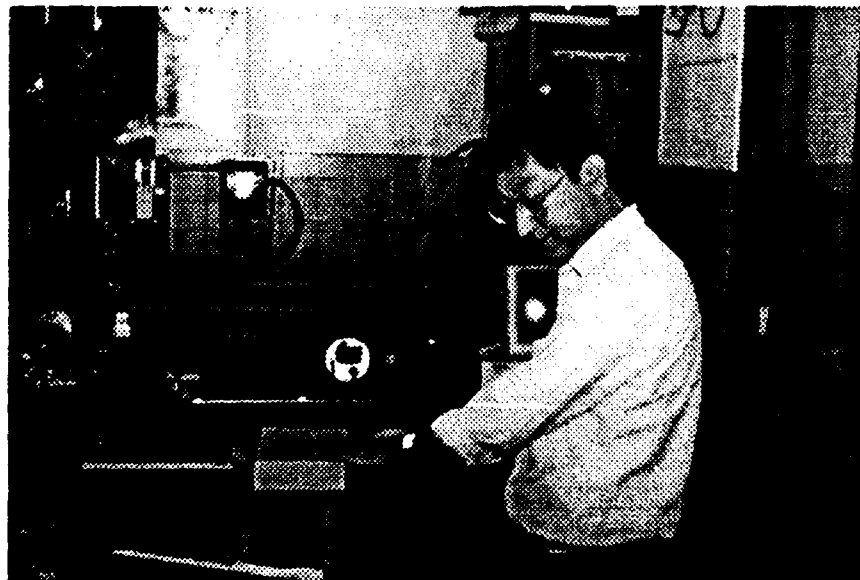
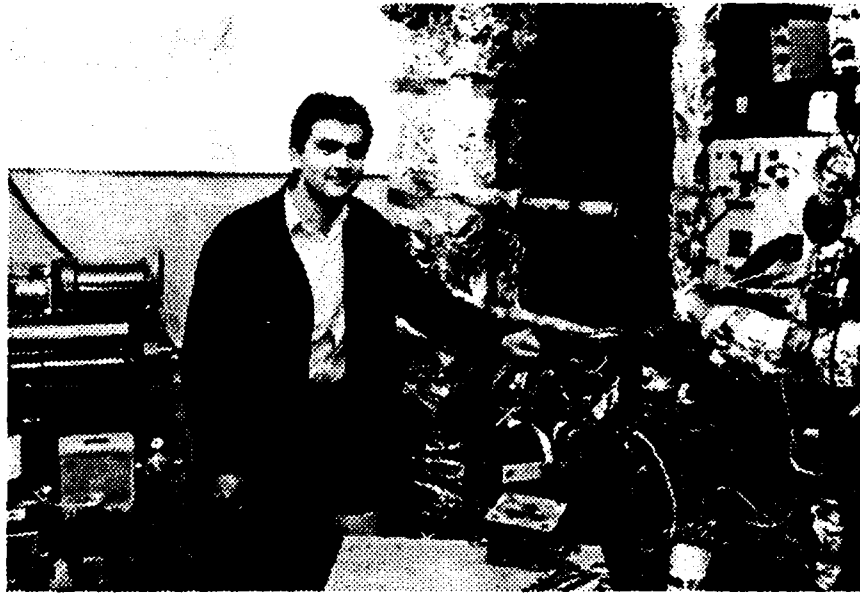
In conclusion, a new approach was introduced for evaluating and quantifying the high-temperature mechanical response of the fiber-matrix interface in brittle-matrix composites by comparing experiments and an analytical simulation of bulk composite behavior. The use of a generalized two-dimensional model incorporating an accurate numerical solution technique has been illustrated to be a very useful method for simulating the time-dependent response of a composite at elevated temperatures. A comparison of the model to the results obtained for a silicate-SiC reinforced composite system illustrates the ability of assessing the interfacial mechanical response based upon the steady-state creep rate of the composite. The goal of developing a fundamentally based micromechanical model and experimental protocol for determining the usefulness of this methodology in evaluating the interface and rheological response has been achieved.

#### IMPACT OF RESEARCH

Much of what was done has yet to have its full impact because the methods developed will be applied in the design process or used to obtain needed new data. The following briefly lists these methods of design and test.

- Development of relatively nonintrusive methods for measurement of oil films and ring standoff distance in running engines.
- Comparisons of data on oil film thickness with models which show the importance of oil starvation on boundary conditions.
- Development of a model for power-law lubricants in piston-liner lubrication.
- Clarification of the effects of viscosity variation, liner vibration and viscous heating in engine lubrication models.
- Measurements of lube oil viscosity at realistic levels of shear and temperature.
- An improved analysis for design of liners with reduced cavitation which includes the effects of coolant on the liner vibration.

- Development of a hypocycloidal drive which shows potential for lower noise and vibration in small engines.
- Development of an engine test system for new ceramic materials which gives complete thermal information for the sample.
- A fundamentally based micromechanical model and experimental protocol for evaluating interface and rheological response of ceramic composites.



## 8.0 REFERENCES

- Abraham, J., Bracco, F.V., and Reitz, R.D. (1985). Comparison of Computed and Measured Premixed Charged Engine Combustion. *Combustion and Flame*, 60.
- Adrian, R.J. (1986), "Multi-point Optical Measurements of Simultaneous Vectors in Unsteady Flow - A Review," *Int. J. Heat and Fluid Flow*, Vol. 7, No. 2, June.
- Albert, R. and Farrell, P.V. (1992). Droplet Sizing Using the Shifrin Inversion. ASME Paper 92-WA/FE-1.
- Alkidas, A.C. (1980). Heat Transfer Characteristics of a Spark-Ignition Engine. *Journal of Heat Transfer*, 102, pp. 189-193, 1980.
- Alkidas, A.C (1989) "Performance and Emission Achievements with an Uncooled, Heavy-Duty, Single Cylinder Diesel Engine," SAE 890144.
- Amsden, A.A., O'Rourke, P.J., Butler, T.D., Meintjes, K. and Fansler, T.D. (1992), "Comparisons of Computed and Measured Three-Dimensional Velocity Fields in a Motored Two-Stroke Engine," SAE Paper 920418, 1992.
- Amsden, A.A., O'Rourke, P.J. and Butler, T.D. (1989), "KIVA-II - A Computer Program for Chemically Reactive Flows with Sprays," Los Alamos National Labs., LA-11560-MS, 1989.
- Anderson, C.L., Uyehara, O.A., and Myers, P.S. (1982), "An In Situ Determination of the Thermal Properties of Combustion Chamber Deposits," SAE paper 820071, SAE Trans. Vol. 91.
- Arcoumanis C. and Enotiadis, A.C. (1991) "In-cylinder Fuel Distribution in a Port-Injected Model Engine Using Rayleigh Scattering," *Experiments in Fluids*, 11, 375-387.
- Armistead, R.A., and Keyes, J.J. (1968), "A Study of Wall-Turbulence Phenomena Using Hot-Film Sensors," *J. of Heat Transfer*, Feb. 1968, pp 13-21.
- Assanis, D.N. and Badillo, E. (1989), "Evaluation of Alternative Thermocouple Designs for Transient Heat Transfer Measurements in Metal and Ceramic Engines," SAE paper 890571, in SP-785.
- Bair, R., Boggs, D., Borman, G., and Foster D. (1986). Diesel Combustion and Ignition Properties of Fuels with Different Volatile Fraction Constituents. SAE Paper No. 861539.
- Bair, R.E., (1989) "Ignition Quality and Composition of Volatile Fraction: Effects on Diesel Combustion," Ph.D Thesis U.W. Madison.
- Bates, B.P., Williamson, B.P., Spearot, J.A., Murphy, C.K. (1986), "A Correlation Between Engine Oil Rheology and Oil Film Thickness in Engine Journal Bearings," SAE Paper No. 860376.
- Beardsley, M.B. and Larson, H.J. (1992), "Thick Thermal Barrier Coatings for Diesel Components," NASA CR-190759, U.S. Dept. Energy.
- Bergeron, C.A. and Hallett, W.L.H. (1989), "Ignition Characteristics of Liquid Hydrocarbon Fuels as Single Droplets," *The Canadian Journal of Chemical Engineering*, Vol 67, 1989.
- Bidner, D., Cooper, R., and Green, D. (1990). Reciprocating Four-Point Flexure Testing at High-Temperature with Application to Attenuation in Partial Melts. In Duba, A., Durham, W., Handin, J., and Wang, H. (Ed.), *The Brittle-Ductile Transition in*

- Rocks: The Heard Volume, Geophys. Monogr. Am. Geophys. Union, Washington, D.C. 56, 201-206.
- Boggs, D.E., (1990), "Spatially-Resolved Measurements of Instantaneous Engine Heat Flux," Ph.D. Thesis, U. W.-Madison.
- Boggs, D., and Borman, G. (1991). Calculation of Heat Flux Integral Length Scales from Spatially-Resolved Surface Temperature Measurements in an Engine. SAE Paper No. 910721.
- Borman, G.L. and Nishiwaki, K. (1987), "Internal-Combustion Engine Heat Transfer," *Prog. Energy Combust Sci.*, 13, pp. 1-46, 1987.
- Borman, G., Farrell, P., Foster, D., Martin, J. and Myers, P. (1991), "Development of a Modular Transient Cycle Analysis Program for the Adiabatic Diesel and Other Compound Engines," Final Report for Contract DAAE07-84-C-R063, U.S. Army TACOM, Warren, MI.
- Bower, G. and Corradini, M.L. (1988), "Physical Mechanisms for Atomization of a Jet Spray: A Comparison of Models and Experiments," SAE Paper 881318, (1988).
- Bower, G.R., Foster, D.E. (1989). "Investigation of the Characteristics of a High Pressure Injector," SAE Paper 892101.
- Bower, G. R. and Foster, D. E. (1990), "Data From a Variable Rate-Shape High Pressure Injection System Operating in an Engine Fed Constant Volume Combustion Chamber", SAE Paper 902082.
- Bower, G. R. and Foster, D.E. (1991), "A Comparison of the Bosch and Zeuch Rate of Injection Meters", SAE Paper 910724.
- Bower, G. R. and Foster, D. E. (1993), "The Effect of Split Injection on Fuel Distribution in an Engine Fed Combustion Chamber", SAE Paper 93xxxx.
- Chang, S.K., Corradini, M.L. (1989), "KIVA Modelling of High Pressure Sprays," Central States SAE Meeting.
- Chang, I.P., (1991), "The Effects of Pressure Gradients on Convective Heat Flux Predictions in Engine Environments", Ph.D. Thesis, U.W.-Madison.
- Chang, I.P., and Martin, J.K. (1991), "Pressure Gradient Effects on Convective Heat Flux Predictions in Engine Environments," in *Fundamentals of Forced Convection Heat Transfer*, edited by M.A. Ebdian and D.A. Daminski, HTD-Vol. 181, ASME, pp. 69-78, 1991.
- Chang, Sang-Ku, (1991), "Hydrodynamics of Liquid Jet Sprays - Physiochemical Analysis and Computer Simulation", Ph.D. Thesis, U.W.-Madison.
- Curtis, E. W. and Farrell, P.V. (1988), "Droplet Vaporization in a Supercritical Microgravity Environment," *ACTA Astronautica* 17, 1189.
- Curtis, E. W. (1992), "A Numerical Study of Spherical Droplet Vaporization in a High Pressure Environment", Ph.D. Thesis, U.W.-Madison.
- Curtis, E. W. and Farrell, P.V. (1992), "A Numerical Study of High Pressure Droplet Vaporization", *Combustion and Flame* 90, p 85-102.
- Dao, K., Uyehara, O. and Myers, P. (1973), "Heat Transfer Rates at Gas-Wall Interface in Motored Piston Engines," SAE paper 730632.
- Ebersole, G.D., Myers, P.S. and Uyehara, O.A. (1963), "The Radiant and Convective Components of Diesel Engine Heat Transfer," SAE paper 701C.
- El-Beshbeeshy, M.S., Corradini, M.L. (1989). "Image Analysis of High Pressure Sprays," Central States Meeting, Combustion Institute.

- El-Beshbeeshy, M. S., Hodges, J. and Corradini, M.L. (1992), "Image Analysis of Diesel Sprays", SAE Paper 921628.
- Ellzey, J.L., Berbee, J.G., Tay, Z.F. and Foster, D.E. (1990), "Total Soot Yield from a Propane Diffusion Flame in Cross-Flow," *Combustion Science and Technology*, 1990, Vol. 71, pp41-52.
- Eng, J., Leschiutta, M., and Martin, J. (1990). Dynamic Piston Position Measurements Using a Laser Range-Finding Technique. SAE Paper No. 900482.
- Epstein, P. (1990), *A Computer Simulation of the Scavenging Flow in a Two-Stroke Engine.*, MS Thesis U.W. Madison.
- Epstein, P.H., Reitz, R.D. and Foster, D.E. (1991), "Computations of a Two-Stroke Engine Cylinder and Port Scavenging Flows," SAE paper 910672.
- Fansler, T.D. and French, D.T. (1988), "Cycle-Resolved Laser-Velocimetry Measurements in a Reentrant-Bowl-In-Piston Engine," SAE Paper 880377.
- Farrell, P., and Goetsch, D. (1989). Optical Analysis of PIV Data. *Proceedings, Laser Institute of America*. 68, 82.
- Farrell, P. V. (1991a), "Particle Sizing Using a Two Dimensional Image," SAE Paper 910725.
- Farrell, P. V. (1991b). Particle Sizing and Velocity Measurements Using Particle Image Velocimetry. *Flucome '91*, W. C. Yang and R. W. Woods, eds.
- Foster, D., and Witze, P. (1987). Velocity Measurements in the Wall Boundary Layer of a Spark-Ignited Research Engine. SAE Paper No. 872105.
- Friedman, R., and Johnson, W.C. (1950), "The Wall-Quenching of Laminar Propane Flames as a Function of Pressure, Temperature and Air-Fuel Ratio," *J. Appl. Phys.*, Vol. 21, No. 8, Aug. 1950, pp 791-795.
- Fukuda, M., Tree, D.R., Foster, D.E. and Suhre, B. (1992), "The Effect of Fuel Aromatic Structure and Content on Direct Injection Diesel Engine Particulates," SAE 920110.
- Gatowski, J.A. (1990), "Evaluation of a Selectively-Cooled, Single-Cylinder, 0.5-L, Diesel Engine," SAE 900693.
- Gentry, R.A., Daly, B.J. and Amsden, A.A. (1987), "KIVA-COAL: A Modified Version of the KIVA Program for Calculating the Combustion Dynamics of a Coal-Water Slurry in a Diesel Engine Cylinder," Los Alamos National Laboratory Report LA-11045-MS, August 1987.
- Ghandhi, J.B. (1991) *Velocity Field Characteristics of Motored Two-Stroke Ported Engines.*, PhD Thesis U.W. Madison.
- Ghandhi, J., and Martin, J. (1992). Velocity Field Characteristics in Motored Two-Stroke Ported Engines. SAE Paper No. 920419.
- Golding, L.H. (1992), "The Effects of Augmented Mixing on Diesel Combustion," MS Thesis U.W. Madison.
- Gonzalez, M., Borman, G. L., and Reitz, R. D. (1991a), "A Study of Diesel Cold Starting Using Both Cycle Analysis and Multidimensional Calculations", SAE Paper 910180.
- Gonzalez D., M. A. and Reitz, R.D. (1991b), "Modeling Diesel Engine Spray Vaporization and Combustion," *Proceedings of the 1st International KIVA Users Group Meeting, Detroit, MI, February 22, 1991.*
- Gonzalez, M. A. and Reitz, R.D. (1991c), "Modeling Diesel Engine Spray Vaporization and Combustion", ICLASS-91, Gaithersburg, MD, July 1991.

- Gonzalez, M. A., Lian, Z. and Reitz, R.D. (1992), "Modeling Diesel Engine Spray Vaporization and Combustion", SAE Paper 920579.
- Green, G. (1992), "Vibration Analysis of Cylinder Liners in the Consideration of Cavitation," PhD Thesis, U.W. Madison.
- Green, G.W. and Engelstad, R.L. (1993), "A Technique for the Analysis of Cylinder Liner Vibrations and Cavitation," SAE paper #930582.
- Greenspan, H.P. (1969), "The Theory of Rotating Fluids," Cambridge University Press, Cambridge.
- Hall, M.J. and Bracco, F.V., "Cycle-Resolved Velocity and Turbulence Measurements Near the Cylinder Wall of a Firing S.I. Engine," SAE Paper 861530.
- Halstead, M., Kirsh, L. and Quinn, C. (1977), "The Autoignition of Hydrocarbon Fuels at High Temperatures and Pressures - Fitting of a Mathematical Model," *Combustion and Flame*, 30, pp. 45-60, 1977.
- Harris, S. J. and Weiner, A.M. (1989), Twenty Second Symposium (International) on Combustion, 1989, pp333, The Combustion Institute.
- Henein, N. A., and Akram, Z. (1990), "Diesel Cold Starting: Actual Cycle Analysis Under Border-Line Conditions," SAE Paper 900441.
- Heywood, J.B. (1976), "Pollutant Formation and Control in Spark-Ignition Engines," *Progress in Energy and Combustion Science*, Vol. 1, pp. 135-164, 1976.
- Hoag, K. and Foster, D. (1983), "The Effect of Mixing Intensity and Degree of Premix on Soot Formation in a Backmixed Combustor," SAE 831395.
- Hodges, J.,T. and Foster, D.,E. (1987) "Soot Coagulation with Surface Growth Kinetics," *Combustion Science and Technology*, 1987, Vol. 51, pp 235-249.
- Hodges, J.,T. (1989), "Soot Formation in a Jet Stirred Reactor," PhD Thesis U.W. Madison.
- Huang, J., and Borman, G. (1987). Measurements of Instantaneous Heat Flux to Metal and Ceramic Surfaces in a Diesel Engine. SAE Paper No. 870155 in SP 700.
- Huh, K.Y. and Gossman (1990), "Atomization Mechanism for Fuel Injection," *Proceedings of ILASS 1990*.
- Huh, K.Y., Chang, I-P. and Martin, J.K., (1990), "A Comparison of Boundary Layer Treatments for Heat Transfer in IC Engines," SAE Paper 900252.
- Jin, J. D., and Borman, G. L., (1985), "A Model for Multicomponent Droplet Vaporization at High Ambient Pressures", SAE paper 850264.
- Johnson, M., and Mangkoesobroto, S. (1992a). Analysis of Lubrication Theory for the Power-law Fluid. To appear in the *Journal of Tribology*.
- Johnson, M., and Mangkoesobroto, S. (1992b). Thin Film Theory for the Power Law Fluid with Application to Piston Ring Lubrication. SAE Paper No. 922285.
- Kadota, T., Zhao, F. and Miyoshi, K. (1990), "Rayleigh Scattering Measurements of Transient Fuel Vapor Concentration in a Motored Spark Ignition Engine," SAE 900481.
- Kamimoto, T., Yokota, H., and Kobayashi, H. (1987), "Effect of High Pressure Injection on Soot Formation Processes in a Rapid Compression Machine to Simulate Diesel Flames," SAE Paper 871610.
- Kawamura, H., Sekiyama, S., and Sasaki, H. (1992), "Observation of Combustion Process of Diesel Fuel Spray in High Temperature Air," SAE paper 922207.

- Keribar, R., Dursunkaya, Z.; and Flemming, M. (1991), "An Integrated Model of Ring Pack Performance," *Trans. ASME, J. Engr. for Gas Turbine and Power* Vol. 113, July 1991, pp. 382-389.
- Kikuta, K., Cary, B., Chikahisa, T. and Martin, J.K., (1992), "Grid Size Effects on the Accuracy of Estimating Diffusion and Convection in KIVA-II," *Proceedings of 2nd International KIVA Users Meeting, Detroit, MI, February 23, 1992.*
- Kittelsohn, D.B., Ambs, J.L. and Hadjicacem, H. (1990), "Particulate Emissions from Diesel Engines: Influence of In-cylinder Surfaces," SAE 900645.
- Kong, S.C., Ayoub, N. and Reitz, R.D., (1992a) "Modeling Combustion in Compression Ignition Homogeneous Charge Engines," SAE paper 920512.
- Kong, S.C. (1992b), "Modeling Ignition and Combustion Processes in Compression Ignited Engines," MS Thesis, U.W.-Madison.
- Kong, S.-C., and Reitz, R.D. (1993), "Multidimensional Modeling of Diesel Ignition and Combustion Using A Multistep Kinetics Models," Submitted to ASME Internal Combustion Engine Symposium, Energy-sources Technology Conference and Exhibition, January 31-February 4, 1993, Houston, TX.
- Ko, Y.S., (1990), "A Study of the Effect of Viscous Heating in High Shear Rate Slit Die Viscometry," PhD Thesis, U.W.-Madison.
- Ko, Y.S. and Lodge, A.S. (1991), "Viscous Heating Correction for Thermally Developing Flows in Slit Die Viscometry," *Rheol. Acta, Vol. 30*, 357-368.
- Koo, J. and Martin, J.K. (1990a), "Ambient Gas Density Effects on Droplet Diameter and Velocity in a Transient Diesel Fuel Spray." *Int'l. Symp. COMODIA, Kyoto, Japan.*
- Koo, J. and Martin, J.K. (1990b), "Droplet Sizes and Velocities in a Transient Diesel Fuel Spray", SAE 900397.
- Koo, J. and Martin, J.K. (1991). Comparison of Measured Drop Sizes and Velocities in a Transient Fuel Spray with Stability Criteria and Computed PDF's. SAE Paper 910179.
- Kuo, T.-W. and Reitz, R.D. (1989), "Computations of Premixed-Charge Combustion in Pancake and Pent-Roof Engines," SAE Paper 890670.
- Kuo, T.-W. and Reitz, R.D., (1992) "Three-Dimensional Computations of Combustion in Premixed-Charge and Fuel-Injected Two-Stroke Engines," SAE Paper 920425.
- Lancaster, D.L. (1976), "Effects of Engine Variables on Turbulence in a Spark Ignition Engine," SAE paper 760195, SAE Trans. Vol. 85.
- Lee, F.L., Klaus, E.E. and Duda, J.L. (1988). "Measurement and Analysis of High-Shear Viscosities of Polymer Containing Lubricants," SAE Paper No. 881663.
- Lee, J. (1992), *Intake Valve Flow in an Internal Combustion Engine*, PhD Thesis U.W. Madison.
- Lee, J., and Farrell, P. (1992). Particle Image Velocimetry Measurements of IC Engine Valve Flows. Sixth International Symposium on Applications of Laser Techniques to Fluid Mechanics, Lisbon, Portugal July 20-23, 1992.
- Leschiutta, M.C., Eng, J.A. and Martin, J.K. (1990), "Dynamic Piston Position measurement Using a Laser Range-Finding Technique," SAE 900482.
- Lian, Z. W. and Reitz, R.D. (1992a), "The Effect of Vaporization and Gas Compressibility on Liquid Jet Atomization", submitted to *Atomization and Sprays*, July 1992.

- Lian, Z.W., and Reitz, R.D. (1992b), "The Effect of Vaporization and Gas Compressibility on Liquid Jet Atomization," Proceedings of ILASS-92, pp. 45-58, San Ramon, CA, May 21-23, 1992. (Submitted to Atomization and Sprays, July, 1992).
- Lian, Z.W., and Reitz, R.D., (1992c) "Influence of Grid Resolution on Diesel Engine Combustion Predictions," Proceedings of the 2nd International KIVA Users Group Meeting, Detroit, MI, February 23, 1992.
- Lin, C.-S. (1988.), *Experimental Study of Combustion and Heat Transfer of a Diesel Engine Under Dynamic Operating Conditions*. PhD Thesis, U.W. Madison.
- Lin, C.S. and Foster, D.E. (1989), "Analysis of Ignition Delay, Heat Transfer and Combustion During Dynamic Load Changes in a Diesel Engine," SAE paper 892054.
- Liu, A.B, and Reitz, R.D., (1992a), "Mechanisms of Air-Assisted Liquid Atomization," Proceedings of ILASS-92, pp. 59-63, San Ramon, CA May 21-23, 1992.
- Liu, A.B, and Reitz, R.D., (1992b), "Mechanisms of Air-Assisted Liquid Atomization," Accepted for publication in Atomization and Sprays, 1992.
- Liu, A. B., Mather, D. and Reitz, R.D. (1993), "Modeling the Effects of Drop Drag and Breakup on Fuel Sprays", accepted for presentation at SAE International Congress, March 1993, Detroit, MI.
- Lodge, A.S., (1987), "A New Method of Measuring Multigrade Oil Shear Elasticity and Viscosity at High Shear Rates," SAE Paper No. 872043.
- Lodge, A.S. and Ko, Y.S., (1989), "Slit Die Viscometry at Shear Rates up to  $5,000,000 \text{ s}^{-1}$ : An Analytical Correction for Small Viscous Heating Errors," *J. Rheol. Acta*, Vol. 28, 464-472.
- Lodge, A.S., (1989), "An Attempt to Measure the First Normal Stress Difference in Shear Flow for a Polyisobutylene/Decalin Solution 'D2b' at Shear Rates up to  $1,000,000 \text{ s}^{-1}$ ", *J.Rheology*, Vol. 33, 821-841.
- Martin, J. (1990). Application of Near-Forward Scatter Particle-Image Velocimetry to I.C. Engines. Presented at the Conference on Mechanisms of Non-Uniform Combustion, Tokyo, Japan, September 10-11.
- Mather, D., Liu, A.B. and Reitz, R.D. (1992), "Effect of Drop Breakup and Drop Drag Coefficient on Spray Penetration", Proceedings of ILASS-92, pp 142-146, San Ramon, CA May 21-23, 1992.
- McDonald, J. (1984), "Construction and Testing of Facility for Diesel Engine Heat Transfer and Particulate Researches," MS Thesis U.W. Madison.
- Meyers, D. (1990), "An Analytic and Experimental Investigation of the Rheology and Interfacial Mechanical Behavior of Ceramic Composites," PhD Thesis U.W. Madison.
- Mohammad, I. Samy and Borman, G.L. (1991), "Measurement of Soot and Flame Temperature Along Three Directions in the Cylinder of Direct Injection Diesel," SAE 910728.
- Moore, W. (1990), *Temperature Measurement Technique for Evaluation of Material Specimens in an Engine.*, MS Thesis U.W. Madison.
- Morel, T., Wahiduzzaman, S. and Fort, E.F. (1988), "Heat Transfer Experiments in an Insulated Diesel," SAE 880186.

- Mueller, E. (1990), "The Effects of Fuel Sulfur Volatility Range and Inlet Air O<sub>2</sub> Enrichment on Particulate Emissions in a Diesel Engine," MS Thesis, U.W. Madison.
- Mueller, M. (1990), *In-Cylinder Flame Temperature, Soot Concentration, and Heat Transfer Measurements in a Low-Heat-Rejection Diesel Engine.*, MS Thesis U.W. Madison.
- Mueller, M., Foster, D., and Myers, P. (1990), Energy Balances and Particulate Temperature Measurement in an Insulated Engine. Proceedings of Coatings for Advanced Heat Engine, Castine ME.
- Myers, J., Myers, M. and Myers, P. (1988), "On Computation of Emissions From Exhaust Gas Composition Measurements," ASME ICE - Vol. 4, Engine Emission Technologies for the 1990's.
- Myers, J. (1989), "Factors Affecting the Top Ring Oil Film Thickness at Top Center," PhD Thesis, U.W. Madison.
- Myers, J., Borman, G., and Myers, P. (1990). Measurement of Oil Film Thickness and Liner Temperature at Top Ring Reversal in a Diesel Engine. SAE Paper No. 900813.
- Myers, P. (1989). Ceramics for Transportation Engines - Siren or Solution. *American Society of Mechanical Engineers*.
- Naber, J.D. and Reitz, R.D. (1988a), "Modeling Engine Spray/Wall Impingement" SAE Technical Paper 880107.
- Naber, J., Enright, B. and Farrell, P. (1988b), "Fuel Impingement in a Direct Injection Diesel Engine", SAE Paper 881316.
- Naber, J. (1992), *Droplet Impingement on a Heated Surface.*, PhD Thesis U.W. Madison.
- Nagle, J. Stickland-Constable, R.F. (1962), "Oxidation of Carbon between 1000-2000 C," Proc. of the Fifth Carbon Conf., Volume 1, Pergamon Press, p. 154, 1962.
- Namazian, M., and Heywood, J.B. (1982), "Flow in the Piston-Cylinder-Ring Crevices of a Spark-Ignition Engine: Effect on Hydrocarbon Emissions, Efficiency and Power," SAE Paper 820088.
- Oettinger, H.C., (1990), "Renormalization of Various Quantities for Dilute Polymer Solutions Undergoing Shear Flow," *Phys. Rev. Vol. A41*, Issue 8 pp. 4413-4420.
- Oliver, D.R., (1988), "Load Enhancement Effects Due to Polymer Thickening in a Short Model Journal Bearing," *J. Non-Newtonian Fluid Mechanics*, Vol. 30, 185-196, 1988.
- O'Rourke, P.J. and Amsden, A.A. (1987), "The TAB Method for Numerical Calculation of Spray Droplet Breakup," SAE Technical Paper 872089.
- Overbye, V.D., Bennethum, J.E., Uyehara, O.A., and Myers, P. (1961) SAE paper 201C, SAE Trans. 69, 461-494.
- Phen, Robert (1992), "An Experimental Measurement of Oil Film Thickness on the Liner of a Motored Diesel Engine Using a Laser Induced Fluorescence Technique and Fiber Optics," MS Thesis, U.W. Madison.
- Pieper, C. (1992), "Modeling Quasi-Steady Flow Through a Two-Valve Intake Port into an Engine Cylinder," M.S. Thesis, U.W.-Madison.
- Pieper, C., Rutland, C.J. and Hessel, R. (1993), "Intake and Cylinder Flow Modeling with a Dual-Valve Port," accepted for SAE Congress and Exposition, March 1-5, 1993, Detroit, MI.
- Pierce, P. (1991), *Near Wall Velocity Measurements in a Motored Four-Stroke Engine.*, PhD Thesis U.W. Madison.
- Pierce, P., Ghandhi, J.B. and Martin, J.K. (1992), "Near-Wall Velocity Characteristics in Valved and Ported Motored Engines," SAE 920152.

- Quiros, E.N., Adams, J.W. Otis, D.R. and Myers, P.S. (1990), "Experimental and Theoretical Evaluation of a Toroidal Combustion Chamber for Stratified Charge Engines," SAE 900606.
- Reid, T., and Martin, J. (1991). Heat Transfer Characteristics of an Uncooled Silicon Nitride Surface in a Naturally-Aspired DI Diesel. SAE Paper No. 912352.
- Reid, T. (1991) *Heat Transfer Characteristics of an Uncooled Silicon Nitride Surface in a Naturally Aspired D.I. Engine*, MS Thesis U.W. Madison.
- Reitz, R.D. (1987), "Modeling Atomization Processes in High-Pressure Vaporizing Sprays," *Atomization and Spray Technology*, Vol 3, pp. 309-337 (1987).
- Reitz, R.D. and Kuo, T.-W. (1989), "Modeling of HC Emissions Due to Crevice Flows in Premixed-Charge Engines," SAE Paper 892085.
- Reitz, R.D. (1990). A Photographic Study of Flash Boiling Atomization. Proc. of ILASS-90, Hartford, CT.
- Reitz, R.D. and Rutland, C.J. (1990), "3-D Modeling of Diesel Engine Intake Flow, Combustion and Emissions," Proceedings of the Annual Automotive Development Contractors' Coordination Meeting, October 22-25, 1990, Dearborn, MI, SAE Publication P-243, pp. 397-404.
- Reitz, R.D. (1991a), "Prospects and Challenges for Fuel Spray Research in the Automotive Industry," *Atomization and Sprays 2000*, NSF Work Proceedings, pp. 89-95, N. Chigier, Ed., Gaithersburg, MD, July 19, 1991.
- Reitz, R.D. (1991b), "Assessment of Wall Heat Transfer Models for Premixed-Charge Engine Combustion Computations," SAE Paper 910267.
- Reitz, R.D. and Rutland, C.J. (1991a), "3-D Modeling of Diesel Engine Intake Flow Combustion and Emissions," SAE Paper 911789
- Reitz, R.D., and Rutland, C.J. (1991b), "Three-dimensional Modeling of Diesel Engine Intake Flow, Combustion and Emissions," Proceedings of the Annual Automotive Development Contractors' Coordination Meeting, October 28-31, 1991, Dearborn, MI, SAE Publication P-256, pp. 725-734.
- Reitz, R.D., Ayoub, N., Gonzalez, M., Hessel, R., Kong, S., Lian, J., Pieper, C., and Rutland, C.J. (1992a), "Improvements in 3-D Modeling of Diesel Engine Intake Flow and Combustion," SAE Paper 920463.
- Reitz, R.D., and Rutland, C.J. (1992b), "Three-dimensional Modeling of Diesel Engine Intake Flow, Combustion and Emissions," DOE/NASA/1087-1, NASA CR-189126 Report, NASA Lewis Research Center, March 1992.
- Richardson, D. (1990), "The Development and Implementation of Theoretical and Experimental Methods for Studying Oil Films in Engine Cylinders," Ph.D. Thesis, U.W.-Madison.
- Richardson D. and Borman, G. (1991). Using Fiber Optics and Laser Fluorescence for Measuring Thin Oil Films with Application to Engines. SAE Paper No. 912388.
- Richardson, D. and Borman, G. (1992). Theoretical and Experimental Investigations of Oil Films for Application to Piston Ring Lubrication. SAE Paper No. 922341.
- Ryason, P.R and Hansen, T.P., (1991), "Voluminosity of Soot Aggregates: a Means of Characterizing Soot-laden Oils," SAE Paper No. 912343.
- Sato, H. (1989), "A Study on the Effect of Temperature on Soot Formantion in a Jet Stirred Combustor," MS Thesis U.W. Madison.

- Sato, H., Tree, D.R., Hodges, J.T. and Foster, D.E. (1990), "A Study of the Effect of Temperature on Soot Formation in a Jet Stirred Combustor," Twenty Third Symposium (International) on Combustion/The Combustion Institute, 1990/pp1469-1475.
- Shakal, J. and Martin, J. K. (1990), "Effects of Auxiliary Injection on Diesel Engine Combustion", SAE Paper 900398.
- Shakal, J. (1993), "Effects of Auxillary Injection on Diesel Engine Combustion," PhD Thesis U.W. Madison.
- Shepard, S.M. and Sass, D.T. (1990), "Thermal Imaging of Repetitive Events at Above-Frame-Rate Frequencies," Optical Engineering, Feb. 1990, Vol. 29, No. 2, 105-109.
- Steinbrenner, J.P., Chawner, J.R. and Fouts, C.L. (1990), "The Gridgen 3D Multiple Block Grid Generation System," Flight Dynamics Laboratory Report, Wright-Patterson Air Force Base, WRDC-TR-90-3022.
- Suhre, B.R. (1992), "In-Cylinder Soot Deposition Rates due to Thermophoresis in a Direct Injection Diesel Engine," MS Thesis U.W. Madison.
- Surovokin, V.F. (1976), "Analytical Description of the Processes of Nucleus-formation and Growth of Particles of Carbon Black in the Thermal Decomposition of Aromatic Hydrocarbons in the Gas Phase," Solid Fuel Chemistry, Vol. 10, pp. 92-101.
- Testing Engineers Inc. (1988), Templog User Information, 2811 Adeline St., P.O. Box 24075, Oakland, CA 94623.
- Tree, D.R. (1992), "Soot Particle Size and Number Density Measurements in a Direct Injection Diesel Engine Using light Scattering, Radiation and Extinction," PhD Thesis U.W. Madison.
- Turner, D.W. and Foster, D.E. (1992), "The Relationship Between Total Soot Yield, Flow Properties and Structure of a Propane Diffusion Flame in Cross-Flow," American Chemical Society, Volume 37, No. 4.
- Van Gerpen, J., Huang, C. and Borman, G.L. (1985), "The Effects of Swirl and Injection Parameters on Diesel Combustion and Heat Transfer", SAE Paper 850265.
- Wachters, L. H. J., and Westerling, N. A. (1966), "The Heat Transfer From a Hot Wall to Impinging Water Drops in the Spheroidal State," Chem. Eng. Sci. 21, 1047-1056.
- Williamson, B.P., (1992), Shell, Thornton Research Center; private communication.
- Woods, M.E., Bryzik, W. and Schwarz, E. (1992) "Heat Rejection form a High Output Adiabatic Diesel Engine," SAE paper 920541.
- Woschni, G., Spindler, W. and Kolesa, K. (1987), "Heat Insulation of Combustion Chamber Walls-A Measure to Decrease the Fuel Consumption of I.C. Engines," SAE paper 870339.
- Yamada, S., Paulsen, H., and Farrell, P. (1989). Heat Transfer Measurements in a Motored Engine. SAE Paper No. 890319.
- Yan, J. and Borman, G.L. (1988), "Analysis and In-Cylinder Measurement of Particulate Radiant Emissions and Temperature in a Direct Injection Diesel Engine," SAE Paper 881315.
- Yan, J. (1988), *Analyses and In-Cylinder Measurements of Local and Hemispherical Particulate Radiant Emissions and Temperatures in a Direct Injection Diesel Engine.*, PhD Thesis U.W. Madison.
- Yan, Y., and Borman, G. (1989). A New Instrument for Radiation Flux Measurement in Diesel Engines. SAE Paper No. 891901.

- Yang, J., Pierce, P., Martin, J., and Foster, D. (1988). Heat Transfer Predictions and Experiments in a Motored Engine. SAE Paper No. 881314.
- Yang, J. and Martin, J.K. (1989), "Approximate Solution - One-Dimensional Energy Equation for Transient, Compressible, Low Mach Number Turbulent Boundary Layer Flows," *Journal of Heat Transfer*, 111, pp. 619-624.
- Yang, J. and Martin, J.K. (1990), "Predictions of the Effects of High Temperature Walls, Combustion, and Knock on Heat Transfer in Engine-Type Flows," SAE Technical Paper 900690.
- Zucchetto, J., Myers, P., Johnson, J., and Miller, D. (1988). An Assessment of the Performance and Requirements for 'Adiabatic' Engines. *Science*. 240, May 27, 1157-1162.
- Zylka, W. (1991), "Gaussian Approximation and Brownian Dynamics Simulations for Rouse Chains with Hydrodynamic Interaction Undergoing Simple Shear Flow," *J. Chem. Phys.* Vol. 94, 4628-4636.



## 9.0 PUBLICATIONS

- Albert, R., and Farrell, P. (1992). Droplet Sizing Using the Shifrin Inversion. ASME.
- Albert, R., and Farrell, P. (1992). Full-field Droplet Sizing in an Air-assisted Atomizer Spray. ASME Paper for WAM.
- Bang, K., and Corradini, M. (1991). Stratified Vapor Explosion Experiments. *Nuclear Science and Engineering*. Vol. 110, No. 2.\*
- Boggs, D., and Borman, G. (1991). Calculation of Heat Flux Integral Length Scales from Spatially-Resolved Surface Temperature Measurements in an Engine. SAE Paper No. 910721.
- Bonney, L., and Cooper, R. (1990). Reaction-Layer Interfaces in SiC-Fiber-Reinforced Glass-Ceramics: A High-Resolution Scanning Transmission Electron Microscopy Analysis. *Journal of the American Ceramic Society*. 73, 2916-2921.
- Borman, G. (1990). A Review of Research Project at the U.W.-Madison Engine Research Center. Invited Keynote Address Paper presented at the Instituto Motori, Engine Workshop. Capri, Italy. May.
- Borman, G. (1990). In-Cylinder Heat Transfer Research at the U.W. Engine Research Center. COMODIA 1990. Kyoto, Japan. Invited Keynote Lecture. September.
- Borman, G. (1990). The Influence of Basic Thermal Sciences Research on Practical Engine Design. Conference on Mechanisms of Non-Uniform Combustion. Tokyo, Japan. Invited Keynote Lecture. September.
- Borman, G., and Brown, W. Jr. (1992). Pathways to Emissions Reduction in Diesel Engines. Keynote address "Second International Conference on Fluid Mechanics, Combustion, Emissions and Reliability in Reciprocating Engines." Capri, Italy. September 14-19.
- Borman, G., and Nishiwaki, K. (1987). Internal-Combustion Engine Heat Transfer. *Prog. Energy Combustion Science*. 13, 1-46.
- Bower, G., and Foster, D. (1989). Investigation of the Characteristics of a High Pressure Injector. SAE Paper No. 892101.
- Bower, G., and Foster, D. (1990). Characteristics of a Variable Rate Shape High Pressure Injection System. ILASS. May 20-23.
- Bower, G., and Foster, D. (1990). Data from a Variable Rate Shape High Pressure Injection System Operating in an Engine Fed Constant Volume Combustion Chamber. SAE Paper No. 902082.

- Bower, G., and Foster, D. (1991). A Comparison of the Bosch and Zuech Rate of Injection Meters. SAE Paper No. 910724.
- Bower, G., and Foster, D. (1993). The Effect of a Split Injection on Spray Development in an Engine-Fed Combustion Chamber. Submitted for 1993 SAE Int'l. Congress.
- Bower, G., Chang, S., Corradini, M., El-Beshbeeshy, M., Martin, J., and Krueger, J. (1988). Physical Mechanisms for Atomization of a Jet Spray: A Comparison of Models and Experiments. *SAE Transactions*. SAE Paper No. 881318.
- Cant, R., Rutland, C., and Trouve, A. (1990). Statistics for Laminar Flamelet Modeling. Studying Turbulence Using Numerical Simulation-III. Center for Turbulence Research, Stanford-NASA Ames Center for Turbulence Research.\*
- Casas, J., and Corradini, M. (1991). A Study of Void Fraction and Mixing of Immiscible Liquids in a Pool Configuration by an Upward Gas Flow. *Journal of Nuclear Technology*. \*
- Chang, I., and Martin, J. (1991). Pressure Gradient Effects on Connective Heat Flux Predictions in Engine Environments. In Daminski, D., and Ebadian, M. (Eds.), *Fundamentals of Forced Convection Heat Transfer*. 181, 69-78.
- Chang, S., and Corradini, M. (1989). KIVA Modeling of High Pressure Sprays. Proceedings of Central States SAE Combustion Meeting. May.
- Chirinos, M., Crain, P., Lodge, A., Schrag, J., and Yaritz, Y. (1990). Measurements of  $N_1$ - $N_2$  and  $h$  in Steady Shear Flow and  $h'$ ,  $h''$ , and Birefringence in Small-Strain Oscillatory Shear for the Polyisobutylene Solution M1. *Journal of Non-Newtonian Fluid Mechanics*. 35, 105-119.\*
- Cooper, R., Green, D., and Bidner, D. (1990). Reciprocating Four-Point Flexure Testing at High-Temperature with Application to Attenuation in Partial Melts. In Duba, A., Durham, W., Handin, J., and Wang, H. (Eds.), *The Brittle-Ductile Transition in Rocks: The Heard Volume*. 56, 201-206.
- Corradini, M. (1991). Vapor Explosion: A Review of Experiments for Accident Analysis. *Journal of Nuclear Safety*. 32-3, 427.\*
- Curtis, E., and Farrell, P. (1988). Droplet Vaporization in a Supercritical Microgravity Environment. *Acta Astronautica*. 17, 1189-1193.
- Curtis, E., and Farrell, P. (1992). A Numerical Study of High Pressure Droplet Vaporization. *Combustion and Flame*. 90, 85-102.
- Curtis, E., Hartfield, J., and Farrell, P. (1988). Microgravity Vaporization of Liquid Droplets under Supercritical Conditions. Proceedings, Third International Colloquium on Drops and Bubbles.

- El Tahry, S., Rutland, C., and Ferziger, J. (1991). Structure and Propagation of Turbulent Premixed Flames--A Numerical Study. *Combustion and Flame*. 83, 146.\*
- El-Beshbeeshy, M., Hodges, J., and Corradini, M. (1992). Image Analysis of Diesel Sprays. SAE Paper No. 921628.
- Ellzey, J., Berbee, J., Tay, Z., and Foster, D. (1990). Total Soot Yield from a Propane Diffusion Flame in a Cross-Flow. *Combustion Science and Technology*. 71, 41-52.
- Enright, B., Myers, P., and Borman, G. (1988). A Critical Review Spark-Ignited Diesel Combustion. SAE Paper No. 881317.
- Epstein, P., Reitz, R., and Foster, D. (1991). Computations of a Two-Stroke Engine Cylinder and Port Scavenging Flows. *SAE Transactions*. SAE Paper No. 910672.
- Fairbanks, J., Sung, R., Foster, D., and Fosenthal, L. (1992). Survey of Emission Reduction Techniques for Heavy Duty Diesel Engines. 1992 Coatings for Advanced Heat Engines Workshop. Monterey, California.\*
- Farrell, P. (1987). Incidental Motion in Interferometry of Phase Objects. *Optics Letters*. 12.
- Farrell, P. (1991). Numerical and Optical Evaluation of Particle Image Velocimetry Images. SPIE Publication 1554B.
- Farrell, P. (1991). Particle Sizing and Velocity Measurements Using Particle Image Velocimetry. In Yang, W. (Ed.), Proceedings of FLUCOME '91, Third International Symposium on Fluid Control, Measurement, and Visualization. San Francisco, CA. August.
- Farrell, P. (1991). Applications of Numerical and Optical Evaluation Schemes for Particle Image Velocimetry. *Experiments in Fluids*. July.
- Farrell, P. (1991). Particle Sizing Using a Two Dimensional Image. SAE Paper No. 910725.
- Farrell, P. (1992). Optical Evaluation of Particle Image Velocimetry Images. *Optics Engineering*. June.
- Farrell, P. (1992). Particle Sizing and Velocity Measurements Using Particle Image Velocimetry. Proceedings of Workshop on PIV. Heriot-Watt University, Edinburgh Scotland. September; revised May.
- Farrell, P., and Goetsch, D. (1989). Optical Analysis of PIV Data. *ICLEO*. 68, 82.
- Farrell, P., and Lee, J. (1993). Measurements of IC Engine Valve Flows Using PIV. Submitted to SAE International Congress, February.

- Farrell, P., and Naber, J. (1993). Spray-wall Interactions. Submitted to SAE International Congress, February.
- Farrell, P., and Verhoeven, D. (1987). Heat Transfer Measurements in a Motored Engine Using Speckle Interferometry. *SAE Transactions*. SAE Paper No. 870456.
- Foster, D., and Witze, P. (1987). Velocity Measurements in the Wall Boundary Layer of a Spark-Ignited Research Engine. *SAE Transactions*. SAE Paper No. 872105.
- Fukuda, M., Tree, D., and Foster, D., and Suhre, B. (1992). The Effect of Fuel Aromatic Structure and Content on Direct Injection Diesel Engine Particulates. SAE Paper No. 920110.
- Ghandhi, J., and Martin, J. (1992). Velocity Field Characteristics in Motored Two-Stroke Ported Engines. SAE Paper No. 920419.
- Giangregorio, R., Zhu, Y., and Reitz, R. (1993). Application of Schlieren Optical Techniques for the Measurement of Gas Temperature and Turbulence Diffusivity in a Diesel Engine. Submitted to SAE Congress and Exposition. Detroit, MI. March 1-5.
- Goetsch, D., and Farrell, P. (1989). Optical LCTV Correlator for Particle Image Velocimetry. *Optics Letters*. 14, 978.
- Gonzalez, M., and Reitz, R. (1991). Modeling Diesel Engine Spray Vaporization and Combustion. In Semerjian, H. (Ed.), Proceedings of the ICLASS-91. *NIST Special Publication 513*. 813, 291-298.
- Gonzalez, M., Borman, G., and Reitz, R. (1991). A Study of Diesel Cold Starting Using Both Cycle Analysis and Multidimensional Calculations. *SAE Transactions*. SAE Paper No. 910180.
- Gonzalez, M., Lian, Z., and Reitz, R. (1992). Modeling Diesel Engine Spray Vaporization and Combustion. SAE Paper No. 920579.
- Hartfield, J., and Farrell, P. (1991). Droplet Vaporization in a Moderate Pressure Gas. In Hoyt, J., and O'Hern, T. (Eds.), *Fluid Dynamics of Sprays*. FED Vol. 131.\*
- Hartfield, J., and Farrell, P. (1991). Experiments in High Pressure Droplet Vaporization. *Journal of Heat Transfer*. November.\*
- Hodges, J., and Foster, D. (1987). Soot Coagulation with Surface Growth Kinetics. *Combustion Science and Technology*. 51, 235-249.
- Huang, J., and Borman, G. (1987). Measurements of Instantaneous Heat Flux to Metal and Ceramic Surfaces in a Diesel Engine. SAE Paper No. 870155.

- Huh, K., Chang, I., and Martin, J. (1990). A Comparison of Boundary Layer Treatments for Heat Transfer in IC Engines. *SAE Transactions*. SAE Paper No. 900252.
- Huhtiniemi, I., Pernsteiner, A., and Corradini, M. (1991). Steam Condensation in the Presence of Noncondensable Gas: Effects of Surface Orientation. In Yilmaz, S. (Ed.), *AIChE Symposium Series*. 87, No. 283.\*
- Johnson, M., and Malkus, D. (1991). Behavior of Non-Affine Viscoelastic Models Under Step Shear Strain. In Massoudi, M., and Rajagopal, K. (Eds.), *Recent Advances in Mechanics of Structured Continua*. 117, 33-41.\*
- Johnson, M., and Mangkoesobroto, S. (1992). Thin Film Theory for the Power Law Fluid with Application to Piston Ring Lubrication. SAE Paper No. 922285.
- Johnson, M., and Mangkoesobroto, S. (1993). Analysis of Lubrication Theory for the Power-law Fluids. To appear in the *Journal of Tribology*.
- Kikuta, K., Cray, B., Chikahisa, T., and Martin, J. (1993). Necessary Grid Size Conditions for Accurate Diffusion and Convection Calculation in KIVA II. Submitted for 1993 SAE Int. Congress and review for SAE Transactions.\*
- Knox-Kelecy, A., and Farrell, P. (1992). Experimental Analysis of Internal Flow in Scaled Fuel Injectors. SAE Paper No. 922308.
- Knox-Kelecy, A., and Farrell, P. (1993). Spectral Characteristics of Turbulent Flow in a Scale Model of a Diesel Fuel Injector Nozzle. SAE Paper No. 930924.
- Kong, S-c., Ayoub, N., and Reitz, R. (1992). Modeling Combustion in Compression Ignition Homogeneous Charge Engines. SAE Paper No. 920512.
- Kong, S-c., and Reitz, R. (1993). Multidimensional Modeling of Diesel Ignition and Combustion Using A Multistep Kinetics Model. Submitted to Internal Combustion Engine Symposium Energy-sources Technology Conference & Exhibition. Houston, Texas. January 31 - February 4.
- Koo, J., and Martin, J. (1990). Ambient Gas Density Effects on Droplet Diameter and Velocity in a Transient Diesel Fuel Spray. COMODIA 90, International Symposium on Diagnostics and Modeling in Internal Combustion Engines. Kyoto, Japan. September 3-5, pp. 225-230.
- Koo, J., and Martin, J. (1990). Droplet Sizes and Velocities in a Transient Diesel Fuel Spray. *SAE Transactions*. SAE Paper No. 900397.
- Koo, J., and Martin, J. (1991). Comparison of Measured Drop Sizes and Velocities in a Transient Diesel Fuel Spray with Stability Criteria and Computed PDF's. *SAE Transactions*. SAE Paper No. 910179.

- Kuo, T-w., and Reitz, R. (1989). Computation of Premixed-Charge Combustion in Pancake and Pentroof Engines. *SAE Transactions*. SAE Paper No. 890670.
- Kuo, T-w., and Reitz, R. (1992). Three-Dimensional Computations of Combustion in Premixed-Charge and Direct-Injected Two-Stroke Engines. SAE Paper No. 920425.
- Lee, J., and Farrell, P. (1992). Particle Image Velocimetry Measurements of IC Engine Valve Flows. Proceedings of Sixth International Symposium on Applications of Laser Techniques to Fluid Mechanics. Lisbon. July, p. 25.4.
- Leschiutta, M., Eng, J., and Martin, J. (1990). Measurements of Dynamic Piston Motion. *SAE Transactions*. SAE Paper No. 900482.
- Lian, Z., and Reitz, R. (1992). Influence of Grid Resolution on Diesel Engine Combustion Predictions. Proceedings of ILASS-92. San Ramon, CA.
- Lian, Z., and Reitz, R. (1992). The Effect of Vaporization and Gas Compressibility on Liquid Jet Atomization. *Atomization & Sprays*. July.
- Lin, C., and Foster, D. (1989). An Analysis of Ignition Delay, Heat Transfer and Combustion During Dynamic Load Changes in a Diesel Engine. SAE Paper No. 892054.
- Liu, A., and Reitz, R. (1992). Mechanisms of Air-Assisted Liquid Atomization. Proceedings of ILASS-92. San Ramon, CA. May 21-23, pp. 59-63.
- Lodge, A. (1987). A New Method of Measuring Multigrade Oil Shear Elasticity and Viscosity at High Shear Rates. SAE Paper No. 872043.
- Lodge, A. (1989). An Attempt to Measure the First Normal-Stress Difference  $N_1$  in Shear Flow for a Polyisobutylene/Decalin Solution "D2b" at Shear Rates up to  $10^6 \text{ s}^{-1}$ . *Journal of Rheology*. 33(6), 821-841.
- Lodge, A. (1989). Elastic Recovery and Polymer-Polymer Interactions. *Rheological Acta*. 28, 351-362.
- Lodge, A., and Ko, Y. (1989). Slit Die Velocimetry at Shear Rates up to  $5 \times 10^6 \text{ s}^{-1}$ : An Analytical Correction for Small Viscous Heating Errors. *Rheological Acta*. November/December, 28, 464-472.
- Lodge, A., Pritchard, W., and Scott, L. (1991). The Hole-Pressure Problem. *IMA Journal of Applied Materials*. 46, 39-66.\*
- Martin, J. (1990). Application of Near-Forward Scatter Particle-Image Velocimetry to I.C. Engines. Presented at the Conference on Mechanisms of Non-Uniform Combustion. Tokyo, Japan. September 10-11, pp. 15-19.

- Martin, J. (1993). Transient Diesel Sprays: Application of Phase/Doppler Particle Analyzer for the Measurement of Droplet Characteristics. To appear in the *Journal of the Japanese Section of the Combustion Institute*.
- Martin, J., Plee, S., and Remboski, D. Jr. (1988). Burn Modes and Prior-Cycle Effects on Cyclic Variations in Lean-Burn Spark-Ignition Engine Combustion. *SAE Transactions*. SAE Paper No. 880201.\*
- Mather, D., Liu, A., and Reitz, R. (1992). Effect of Drop Breakup and Drop Drag Coefficient on Spray Penetration. Proceedings of the Twenty-Second International KIVA Users Group Meeting. Detroit, MI. May 21-23, pp. 142-146.
- Meyer, D., Cooper, R., and Plesha, M. (1990). A Contact Friction Algorithm Including Nonlinear Viscoelasticity and a Singular Yield Surface Provision. Submitted to *Computers and Structures*. December.
- Meyer, D., Cooper, R., and Plesha, M. (1990). An Evaluation of the Interfacial Mechanical and Time-Dependent Responses of a Ceramic Composite at Elevated Temperatures. Submitted to *Acta Metallurgica*. December.
- Meyer, D., Cooper, R., and Plesha, M. (1990). Analytical Rheology Simulation and Interface Mechanisms in Ceramic Composites. Proceedings of the Symposium on Composites, Second International Ceramics Congress. *American Ceramics Society*.
- Meyer, D., Cooper, R., and Plesha, M. (1990). Rheological Modeling of Ceramic Composites: An Indirect Method of Interfacial Mechanical Property Measurements. *International Solids Structures*. December.
- Mohammad, I., and Borman, G. (1991). Measurement of Soot and Flame Temperature Along Three Directions in the Cylinder of a Direct Injection Diesel. SAE Paper No. 910728.
- Mueller, M., Foster, D., and Myers, P. (1990). Energy Balances and Particulate Temperature Measurement in an Insulated Engine. Proceedings of Coatings for Advanced Heat Engine, Castine ME.
- Myers, J., Myers, M., and Myers, P. (1988). On the Computation of Emissions from Exhaust Gas Composition Measurements. *Engine Emission Technology for the 1990's*. ASME ICE, 4.
- Myers, J., Borman, G., and Myers, P. (1990). Measurement of Oil Film Thickness and Liner Temperature at Top Ring Reversal in a Diesel Engine. SAE Paper No. 900813.
- Myers, P. (1989). Ceramics for Transportation Engines - Siren or Solution. *Applied Mechanical Rev.* 42, 53-69.
- Myers, P. (1992). Reducing Transportation Fuel Consumption - How Far Should We Go? SAE Convergence 1992 Meeting.

- Naber, J., Enright, B., and Farrell, P. (1988). Fuel Impingement in a Direct Injection Diesel Engine. *SAE Transactions*. SAE Paper No. 881316.
- Naber, J., and Reitz, R. (1988). Modeling Engine Spray/Wall Impingement. *SAE Transactions*. SAE Paper No. 880107.
- Phen, R., Borman, G., and Richardson, D. (1993). Measurements and Modeling of Cylinder Liner Oil Film Thickness in a Motored Engine. Submitted for presentation at the 1993 SAE Congress. Detroit, Michigan.
- Pieper, C., and Rutland, C. (1993). Intake and Cylinder Flow Modeling with a Dual Valve Port. SAE 1993 International Congress.
- Pierce, P., Ghandhi, J., and Martin, J. (1992). Near-Wall Velocity Characteristics in Valved and Ported Motored Engines. SAE Paper No. 920152.
- Plee, S., Remboski, D., and Martin, J. (1987). Application of Conditional Sampling to the Study of Cyclic Variation in a Spark-Ignited Engine. SAE Paper No. 971173.\*
- Quiros, E., Adams, J., Otis, D., and Myers, P. (1990). Experimental and Theoretical Evaluation of a Toroidal Combustion Chamber for Stratified Charge Engines. SAE Paper No. 900606.\*
- Reid, T., and Martin, J. (1991). Heat Transfer Characteristics of an Uncooled Silicon Nitride Surface in a Naturally-Aspired DI Diesel. SAE Paper No. 912352.
- Reitz, R. (1990). A Photographic Study of Flash-Boiling Atomization. *Journal of Aerosol Science*. 12, 561-569.
- Reitz, R. (1990). Effect of Vaporization and Turbulence on Spray Drop Size and Velocity Distributions. In Bachalo, W., and Felton, P. (Eds.), *Liquid Particle Size Measurement Techniques*. 2, 225-237.
- Reitz, R. (1991). Assessment of Wall Heat Transfer Models for Premixed-Charge Engine Combustion Computations. *SAE Transactions*, SAE Paper No. 910267.
- Reitz, R. (1991). Prospects and Challenges for Fuel Spray Research in the Automotive Industry. In Chigier, N. (Ed.), *Atomization and Sprays 2000 NSF Work Proceedings*. Gaithersburg, MD. July 19, pp. 89-95.
- Reitz, R., and Kuo, T-w. (1989). Modeling of HC Emissions Due to Crevice Flows in Premixed-Charge Engines. *SAE Transactions*. SAE Paper No. 892085.
- Reitz, R., and Rutland, C. (1991). 3-D Modeling of Diesel Engine Intake Flow, Combustion and Emissions. *SAE Transactions*. SAE Paper No. 911789.

- Reitz, R., and Rutland, C. (1992). Three-Dimensional Modeling of Diesel Engine Intake Flow, Combustion and Emissions. DOE/NASA/1087- , NASA CR-189126 Report. NASA Lewis Research Center. March.
- Reitz, R., Ayoub, N., Gonzalez, M., Hessel, R., Kong, S., Lian, J., Pieper, C., and Rutland, C. (1992). Improvements in 3-D Modeling of Diesel Engine Intake Flow and Combustion. SAE Paper No. 920463.
- Remboski, D., Plee, S., and Martin, J. (1989). An Optical Sensor for Spark-Ignited Engine Combustion Analysis and Control. *SAE Transactions*. SAE Paper No. 890159.\*
- Richardson, D., and Borman, G. (1991). Using Fiber Optics and Laser Fluorescence for Measuring Thin Oil Films with Application to Engines. SAE Paper No. 912388.
- Richardson, D., and Borman, G. (1992). Theoretical and Experimental Investigations of Oil Films for Application to Piston Ring Lubrication. SAE Paper No. 922341.
- Ruch, D., Fronczak, F., and Beachley, N. (1991). Design of a Modified Hypocycloid Engine. SAE Paper No. 911810.
- Rutland, C., and Ferziger, J. (1990). Unsteady Strained Premixed Laminar Flames. *Combustion Science and Technology*. 73, 305.\*
- Rutland, C., and Ferziger, J. (1991). Simulations of Flame-Vortex Interactions. *Combustion and Flame*. 84, 343.\*
- Rutland, C., and Trouve, A. (1990). Premixed Flame Simulations for Non-unity Lewis Numbers. Studying Turbulence Using Numerical Simulation-III. Center for Turbulence Research, Stanford-NASA Ames Center for Turbulence Research.\*
- Rutland, C., Ferziger, J., and El Tahry, S. (1990). Full Numerical Simulations and Modeling of Turbulent Premixed Flames. *Twenty-third International Combustion Symposium*, The Combustion Institute.\*
- Sato, H., Tree, D., Hodges, J., and Foster, D. (1990). A Study on the Effects of Temperature on Soot Formation in a Jet Stirred Combustor. *Twenty-Third International Symposium on Combustion*. pp. 1469-1475.
- Suhre, B., and Foster, D. (1992). In-cylinder Soot Deposition Rates Due to Thermophoresis in a Direct Injection Diesel Engine. SAE Paper No. 921629.
- Turner, D., and Foster, D. (1992). The Relationship Between Total Soot Yield, Flow Properties and the Structure of a Propane Diffusion Flame in Cross-Flow. *American Chemical Society*. 37, No. 4.
- Witze, P., and Foster, D. (1988). A Comparison of Flame Position Measurement Techniques for Premixed-Charge Combustion in Spark Ignition Engines. *Experiments in Fluids*. 6.

- Witze, P., and Foster, D. (1988). Velocity Measurements in the Wall Boundary Layer of a Spark-Ignited Research Engine. SAE Paper No. 872105.
- Witze, P., and Foster, D. (1988). Two-Component Laser Velocimeter Measurements in a Spark Ignition Engine. *Combustion Science and Technology*. 59, 85-105.
- Witze, P., Foster, D., and Kroeger, H. (1988). Linear Fiber-Optic Array for Measuring the Transient Propagation of a Premixed-Charge Flame. *Twenty-Second International Symposium on Combustion*. pp. 1897-1905.
- Yamada, S., Paulsen, H., and Farrell, P. (1989). Heat Transfer Measurements in a Motored Engine. *SAE Transactions*. SAE Paper No. 890319.
- Yan, J., and Borman, G. (1988). Analysis and In-Cylinder Measurement of Particulate Radiant Emissions and Temperature in a Direct Injection Diesel Engine. SAE Paper No. 881315.
- Yan, J., and Borman, G. (1989). A New Instrument for Radiation Flux Measurement in Diesel Engines. SAE Paper No. 891901.
- Yang, J., and Martin, J. (1989). Approximate Solution - One Dimensional Energy Equation for Transient, Compressible, Low Mach Number Turbulent Boundary Layer Flows. *Journal of Heat Transfer*. 111, 619-624.
- Yang, J., and Martin, J. (1990). Predictions of the Effects of High Temperature Walls, Combustion, and Knock on Heat Transfer in Engine-Type Flows. *SAE Transactions*. SAE Paper No. 900690.
- Yang, J., Pierce, P., Martin, J., and Foster, D. (1988). Heat Transfer Predictions and Experiments in a Motored Engine. *SAE Transactions*. SAE Paper No. 881314.
- Yang, J., Plee, S., Remboski, D., and Martin, J. (1990). Comparison Between Measured Radiance and a Radiation Model in a Spark-Ignition Engine. *ASME Journal of Engineering for Gas Turbines and Power*. 112, 331-335.\*
- Zucchetto, J., Myers, P., Johnson, J., and Jahns, T. (1989). Mobile Electric Power Technologies for the Army of the Future. SAE Paper No. 891876.\*
- Zucchetto, J., Myers, P., Johnson, J., and Miller, D. (1988). An Assessment of the Performance and Requirements for 'Adiabatic' Engines. *Science*. 240, 1157-1162.\*

\*Indicates papers not primarily funded by the ARO grant.

## 10.0 STUDENT THESES

Copies of a thesis can be obtained by requesting an UMI Order Number from the U.W. Memorial Library at (608) 262-3242. This number can then be used to order the thesis from:

University Microfilms International  
300 North Zeeb Road  
Ann Arbor, MI 48106  
1-800-521-0600

Micro-form copies are currently priced at \$31.00 for academics (\$44.00 for non-academics) and paper Xerox copies at \$34.50 for academics (\$55.00 for non-academics).

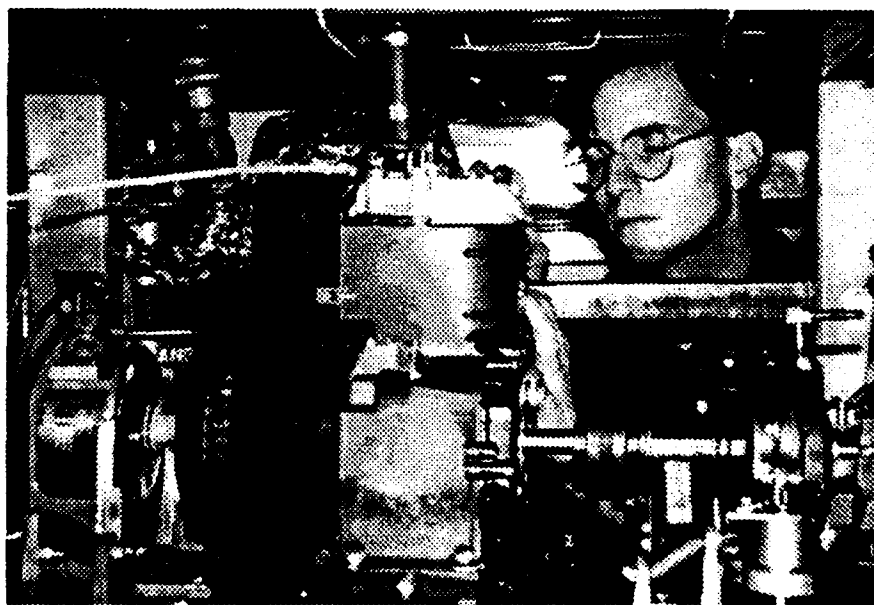
- Albert, Richard. 1992. MS Thesis: *Diffraction-Based Particle Sizing in a Two-Phase Fluid Flow.*
- Angelo, Theodore. 1992. MS Thesis: *Emissions and Performance of a Small L-Head Engine.*
- Bair, Robert. 1989. PhD Thesis: *Ignition Quality and Composition of Fuel Volatile Fraction: Effects on Diesel Combustion.*
- Berbee, James. 1988. MS Thesis: *Aspect Ratio and Reynolds Number Effects on the Flow Behind a Rearward-Facing Step.*
- Boggs, David. 1990. PhD Thesis: *Spatially-Resolved Measurements of Instantaneous Engine Heat Flux.*
- Bower, Glenn. 1992. PhD Thesis: *The Effect of a Split Injection on Early Combustion in an Engine-Fed Combustion Chamber.*
- Chang, I-Ping. 1991. MS Thesis: *The Effects of Pressure Gradients on Convective Heat Flux Predictions in Engine Environments.*
- Chang, Sang-Ku. 1991. PhD Thesis: *Hydrodynamics of Liquid Jet Sprays--Physiochemical Analysis and Computer Simulation.*
- Cook, Donald. 1986. MS Thesis: *Transient Cycle Simulation Program of a Research Diesel Engine.*
- Curtis, Eric. 1991. PhD Thesis: *A Numerical Study of Spherical Droplet Vaporization in a High Pressure Environment.*
- El-Beshbeeshy, Mahmaud. 1992. PhD Thesis: *Image Analysis of Sprays by Light Extinction Technique.*
- Eng, James. 1990. MS Thesis: *Measurements of Dynamic Piston-Position and Effects on Closed-Cycle Thermodynamic Engine Analysis.*

- Enright, Bernard. 1988. MS Thesis: *Low Cetane Fuel Performance in a Direct Injection Spark-Assisted Diesel Engine.*
- Epstein, Peter. 1990. MS Thesis: *A Computer Simulation of the Scavenging Flow in a Two-Stroke Engine.*
- Feiereisen, John. 1989. MS Thesis: *Design, Construction and Testing of an Engine-Fed Spray Chamber with Optical Access.*
- Fieschko, Craig. 1991. MS Thesis: *A Method for Predicting the 100 C and 40 C Kinematic Viscosities and Cold Crank Viscosities of Commercial Lubricant Blends.*
- Gebbeken, Bernhard. 1991. MS Thesis: *Parallelization of KIVA-II Engine Simulations on the Intel iPSC/860.*
- Ghandhi, Jaal. 1988. MS Thesis: *Swirl Center Precession in Spinning Down Flows.*
- Ghandhi, Jamshed. 1991. PhD Thesis: *Velocity Field Characteristics of Motored Two-Stroke Ported Engines.*
- Giangregorio, Roberto. 1992. MS Thesis: *Optoacoustic Temperature and Turbulent Diffusivity Measurements in a Diesel Engine.*
- Golding, Lawrence. 1992. MS Thesis: *The Effects of Augmented Mixing on Diesel Combustion.*
- Gonzalez, Manuel. 1990. MS Thesis: *A Computational Study of In-Cylinder Cold Starting Processes in a Diesel Engine.*
- Green, Gerald. 1992. PhD Thesis: *Vibration Analysis of Cylinder Liners in the Consideration of Cavitation.*
- Hartfield, John. 1991. PhD Thesis: *Droplet Vaporization in a High Pressure Gas.*
- Hodges, Joseph. 1989. PhD Thesis: *Soot Formation in a Jet Stirred Combustor.*
- Knox-Kelecy, Andrea. 1992. PhD Thesis: *Turbulent Flow in a Scale Model of a Diesel Fuel Injector Nozzle Hole.*
- Ko, Young-Soo. 1990. PhD Thesis: *A Study of the Effect of Viscous Heating in High Shear Rate Slit Die Viscometry.*
- Kong, Song-charng. 1992. MS Thesis: *Modeling Ignition and Combustion Processes in Compression Ignited Engines.*
- Koo, Ja-Ye. 1991. PhD Thesis: *Characteristics of a Transient Diesel Fuel Spray.*
- Lee, Janghee. 1992. PhD Thesis: *Intake Valve Flow in an Internal Combustion Engine.*
- Lei, Ning. 1988. MS Thesis: *A Cycle Simulation Program for the Dynamic Operation of a Single Cylinder Direct Injection Diesel.*
- Leschiutta, Maurizio. 1988. MS Thesis: *Piston-Position Measurements in an IC-Engine Using a Laser Range-Finding Technique.*

- Lin, Chieh-Shen. 1988. PhD Thesis: *Experimental Study of Combustion and Heat Transfer of a Diesel Engine Under Dynamic Operating Conditions.*
- Liu, Alex. 1992. MS Thesis: *Mechanisms of Air-Assisted Liquid Atomization.*
- Malone, Ronald. 1990. MS Thesis: *Air Side Heat Transfer Enhancement for an Engine Cooling System.*
- Mangkoesebroto, Sindur. 1992. PhD Thesis: *Analysis of Piston Ring Lubrication with the Power-Law Lubricant.*
- Meyers, Dallas. 1990. PhD Thesis: *An Analytic and Experimental Investigation of the Rheology and Interfacial Mechanical Behavior of Ceramic Composites.*
- Miller, Daniel. 1989. MS Thesis: *A Study of Reed Valve Performance on an Engine Simulator Using Dimensional Analysis.*
- Mohammad, I. Samy. 1990. PhD Thesis: *Simultaneous Pyrometer Measurements Along Three Path Directions in an Open Chamber Diesel.*
- Moore, Wayne. 1990. MS Thesis: *Temperature Measurement Technique for Evaluation of Material Specimens in an Engine.*
- Mueller, Eric. 1990. MS Thesis: *The Effects of Fuel Sulfur Volatility Range and Inlet Air O<sub>2</sub> Enrichment on Particulate Emissions in a Diesel Engine.*
- Mueller, Mark. 1990. MS Thesis: *In-Cylinder Flame Temperature, Soot Concentration, and Heat Transfer Measurements in a Low-Heat-Rejection Diesel Engine.*
- Myers, John. 1989. PhD Thesis: *Factors Affecting the Top Ring Oil Film Thickness at Top Center.*
- Naber, Jeffrey. 1992. PhD Thesis: *Droplet Impingement on a Heated Surface.*
- Neely, Michael. 1938. MS Thesis: *A Numerical Model of a Turbulent Jet in a Cross-Flow.*
- Patrie, Bryan. 1987. MS Thesis: *Computer Imaging of Rotating Flows.*
- Phen, Robert. 1992. MS Thesis: *An Experimental Measurement of Oil Film Thickness on the Liner of a Motored Diesel Engine Using a Laser Induced Fluorescence Technique and Fiber Optics.*
- Pieper, Christopher. 1992. MS Thesis: *Modeling Quasi-Stream Flow Through a Two Valve Intake Port into an Engine Cylinder.*
- Pierce, Philip. 1991. PhD Thesis: *Near Wall Velocity Measurements in a Motored Four-Stroke Engine.*
- \*Quiros, Edwin. 1989. PhD Thesis: *Control of Fresh Fuel-Fresh Air Mixing in a Toroidal Engine Combustion Chamber.*

\*Research done at U.W. degree awarded by U. of Philippines.

- Reid, Timothy. 1991. MS Thesis: *Heat Transfer Characteristics of an Uncooled Silicon Nitride Surface in a Naturally Aspired D.I. Engine.*
- Richardson, Dana. 1990. PhD Thesis: *The Development and Implementation of Theoretical and Experimental Methods for Studying Oil Films in Engine Cylinders.*
- Ruch, David. 1992. PhD Thesis: *An Experimental and Analytical Evaluation of a Single-Cylinder Modified Hypocycloid Engine Design*
- Sato, Hiroki. 1989. MS Thesis: *A Study of the Effect of Temperature on Soot Formation in a Jet Stirred Combustor.*
- Shakal, Joseph. 1993. PhD Thesis: *Effects of Auxillary Injection on Diesel Engine Combustion.*
- Shure, Blake. 1992. MS Thesis: *In-Cylinder Soot Deposition Rates Due to Thermophoresis in a Direct Injection Diesel Engine.*
- Tay, Zhu-Fei. 1988. MS Thesis: *The Study of Soot Production in a Flame in a Cross-Flow.*
- Tree, Dale. 1992. PhD Thesis: *Soot Particle Size and Number Density Measurements in a Direct Injection Diesel Engine Using Light Scattering, Radiation, and Extinction.*
- Turner, David. 1991. MS Thesis: *An Investigation into the Relationship Between the Total Soot Yield, the Flow Properties, and the Structure of a Propane Diffusion Flame in a Cross-Flow.*
- Yan, Jingde. 1988. PhD Thesis: *Analyses and In-Cylinder Measurements of Local and Hemispherical Particulate Radiant Emissions and Temperatures in a Direct Injection Diesel Engine.*
- Yang, Jialin. 1988. PhD Thesis: *Convective Heat Transfer Predictions and Experiments in an I.C. Engine.*



## 11.0 INVENTIONS AND PERSONNEL

### List of Inventions

1991 Patent Number 5,011,278 Issued April 30, 1991

"Optical Correlator Method and Apparatus for Particle Image Velocimetry Processing." P. Farrell.

1992 Currently in patent preparation.

"High Speed Pulse Generator for Q-Switching Pulsed Lasers." P. Farrell with A. Beal and J. Lee.

### List of Participating Scientific Personnel

The students who have received degrees are listed with degree and thesis title in Appendix B. Other participating scientific personnel are listed below.

#### *Students with degrees in process:*

Ayoub, Nabil; Carabell, Kevin; Choe, Joon-Hyuk; Cleary, David; Donahue, Richard; Donahue, Ronald; Douba, Michael; Ducu, Daniel; Lee, Kyung-Hwan; Nehmer, Daniel; Shakal, Joseph; Shamis, Dmitry; and Simescu, Stefan

#### *Faculty:*

Borman, Gary; Cooper, Reid; Corradini, Michael; Farrell, Patrick; Fiedler, Ross (Visiting); Foster, David; Fronczak, Frank; Greiner, Richard; Johnson, Millard; Lodge, Arthur; Martin, Jay; Myers, Phillip; Powell, Hugh; Reitz, Rolf; and Rutland, Christopher

#### *Scientific Staff:*

Bidner, David; Foo, Victor; Horn, Jeffrey; Hutchins, Douglas; Jensen, Peter; Kaufman, Duane; Krueger, Joseph; Moore, Fred; Sehmman, Boleslaw; and Yu, James

#### *Visiting Scientists:*

Ashikari, Shinya (Komatsu Ltd.); Brown, William (Caterpillar Engine Company); El Shenawy, El Hamid (Tanta University, Egypt); Fukuda, Masanori (Japan's Ministry of Education); Fusco, Annunzia (Istituto Motori); Hassaan, Hamdy (Arab Marine Transport Academy); Hayashida, Masaru (Kubota Corporation); Ishida, Masahiro (Nagasaski University); Kim, Sung Soo (Korean Advanced Institute of Science and Technology); Valentino, Gerado (Istituto Motori); and Yukioka, Masahiro (Isuzu Ceramics Research Institute Co., Ltd.)

#### *Post-Doctoral Researchers:*

Hodges, Joseph; Huh, Kang; Lian, Zhi; Zhu, Yuaxian; and Zurlo, James

#### *Intern-Trainees:*

Birch, Anne; Matias, Bruno; Paulsen, Halvard; Quiros, Edwin; Raz, Michael; Sheldon, Timothy; and Smaling, Rudolph